DISCLAIMER NOTICE

THIS DOCUMENT IS BEST QUALITY AVAILABLE. THE COPY FURNISHED TO DTIC CONTAINED A SIGNIFICANT NUMBER OF PAGES WHICH DO NOT REPRODUCE LEGIBLY.

TABLE OF CONTENTS

APPENDIX I

Research Program On Additives For Use
In Ammonia Fuel For Internal Com-
bustion Engines

SUMMARY REPORT

From

RESEARCH AND DEVELOPMENT DEPARTMENT, AMERICAN OIL COMPANY

to

CONTINENTAL AVIATION AND ENGINEERING CORPORATION

on

RESEARCH PROGRAM ON ADDITIVES FOR USE IN
AMMONIA FUEL FOR INTERNAL COMBUSTION ENGINES

By

American's Project Team:

D. S. Gray, leader
C. J. Domke, project automotive engineer
    and principal author of this report
G. H. Meguerian, consultant
R. L. Mieville, project chemist

RESEARCH PROGRAM ON ADDITIVES FOR USE IN
AMMONIA FUEL FOR INTERNAL COMBUSTION ENGINES

ABSTRACT

A project was conducted, for Continental Aviation and Engineering
Corporation, to develop and evaluate additives to improve the performance of
the ammonia-fueled engines which the military proposes to operate in localities
where supply of conventional hydrocarbon fuel is difficult. Technical work on
this project was active from March 15, 1965, to December 17, 1965. This work
mainly comprised preliminary assessment of the performance of candidate
ammonia-additives using a bench reactor to measure tendencies of the additives
to increase the oxidation rate of ammonia and/or cause ignition, followed by
final evaluation of these and other additives using CFR single cylinder engines.
Of the many gaseous, liquid, and solid additives investigated, hydrogen and ace-
tylene were by far the best ammonia-additives in the engines. In the CFR
spark-ignition engine, hydrogen was the best additive in terms of good engine
performance at low additive concentration with normal compression ratios, and
acetylene was the second best additive. In the CFR compression-ignition engine,
acetylene was the best additive in terms of good engine performance at normal
compression ratios, whereas hydrogen performed well at compression ratios
somewhat higher than normal.

- 1 -

RESEARCH PROGRAM ON ADDITIVES FOR USE IN
AMMONIA FUEL FOR INTERNAL COMBUSTION ENGINES

The objective of this project was to develop and evaluate additives
to improve the performance of the ammonia-fueled spark-ignition and compression-
ignition engines which the military proposes to operate in localities where
supply of conventional hydrocarbon fuel is difficult. Additives were developed
via a literature survey to review current technology and secure leads, a study
of the theoretical mechanism by which additives might function, and a selection
of promising-appearing additives to be evaluated. To evaluate candidate
additives, a small bench reactor was used for preliminary screening, and both
spark and compression-ignition CFR single cylinder engines were used to determine
effectiveness of specific additives on improving engine performance. This report
comprises a brief synopsis of the principal project activities, plus appendices
which document the results in greater detail.

DEVELOPMENT OF ADDITIVES

Literature Search

This search relied mainly on the Chemical Abstracts published by
the American Chemical Society. Except for numerous references to the
catalytic oxidation of ammonia to nitrogen oxides, the literature contained
relatively few references to the combustion of ammonia. The references are
listed in Appendix A, and could be grouped into three categories: gas phase
kinetics (6 references), flame properties (6 references), and general
combustion in terms of engineering and rocketry (8 references). The latter
category included some French research on combustion of ammonia in motor
vehicle engines. A resulting U. S. Patent (Frejacques) claimed acetylene
concentrations in ammonia of 3% (w) to 20%, although 10% to 12% evidently
was the preferred concentration. Frejacques noted that the favorable
solubility characteristics of acetylene in liquid ammonia eliminated the
need for auxiliary containers for additives and the need for other devices
such as dissociators. Another U. S. patent (Davis) covered ammonium nitrate
in liquid ammonia as a fuel for internal combustion engines.

Study of Additive Mechanism

The main problem with ammonia combustion was regarded to be
relative inertness to oxidation as compared with hydrocarbons. A successful
ammonia-additive should overcome this inertness by:

    1) initiating the combustion chain at lower temperatures;

    2) sustaining the combustion chain process once initiated.

To provide information on the ammonia combustion process, and thus on the mechanism by which an additive might function, a bench reactor apparatus was devised which would facilitate the measurement of the ignition temperature and level of oxidation of a mixture of ammonia and oxygen, and which subsequently could be used in evaluating ammonia-additives. Gaseous ammonia and oxygen were flowed separately to this reactor, which was installed in a small furnace, and were heated until ignition occurred. Reactor temperature vs. elapsed time were recorded on a strip chart and ignition (sudden temperature rise) was read directly. The consumption of ammonia was measured with an infra-red spectrometer. Flow rates were kept constant for all runs, oxygen at 100 cc/min and ammonia at 56 cc/min. The reactor and its operation are described in greater detail in Appendix B, which also presents a schematic drawing of the reactor and a photograph of the installation.

Preliminary work showed that no ignition could occur up to 700°C at atmospheric pressure with any ratio of ammonia to oxygen; what did occur was considerable oxidation. The oxidation rates expressed in terms of ammonia consumed were determined at three levels of ammonia concentrations and over the temperature range 500-800°C. The results are illustrated by Fig. 1. The rate of oxidation is seen to be inversely proportional to the ammonia concentration. Moreover, at high concentrations, the oxidation goes through a region of negative temperature dependence.

Another experiment was made to determine the role of oxygen in the combustion process. Experiments were performed in the presence and absence of oxygen. It was found that the rate of ammonia consumed in the presence of oxygen was 7 times greater than the rate in the absence of oxygen. This indicated that oxygen does not only react with the hydrogen produced by thermal initiation, but plays an important role in initiating chain reactions of ammonia.

Selection of Additives

In light of the preceeding information, additives were selected according to possible use with ammonia in spark ignition engines and in compression ignition engines. For spark ignition engines, the primary interest was in gaseous additives which could be introduced with gaseous ammonia, although some liquid additives were considered for introduction via the air-ammonia stream. This selection thus mainly comprised gases which could be prepared on-site in any locality, such as hydrogen, and gases which could be prepared on-site in some localities, such as butane.

For compression ignition engines, the primary interest was in
additives that might be effective at low concentrations and that would be
soluble in liquid ammonia, although gaseous additives also were considered
for introduction via the intake air. This selection was mainly based on
providing a good representation from the classes of compounds which had
at some time been claimed as cetane improvers as well as providing repre-
sentation between compound which might be classed as "catalytic oxidizers"
and as "explosives".

EVALUATION OF ADDITIVES IN BENCH REACTOR

Additives For Spark Ignition Engines

Eight gases and two liquids were tested. Two of the gases,
hydrogen and ozone, appeared to have a strong effect on the oxidation of
ammonia, whereas the remainder had either a slight or no effect. Both
liquids, a mixture of iso-octane and n-heptane, and a light lubricating
oil, had strong positive effects on oxidation. Overall, the scope of the
work on additives for spark ignition engines burning ammonia was quite
limited because the favorable performance of hydrogen and acetylene was
well known, whereas emphasis on additives for compression ignition engines
was desired by Continental. Detailed results of the bench reactor work on
additives for spark ignition engines are given in Appendix C.

Additives For Compression Ignition Engines

A total of 45 additives were tested. All were considered to be
soluble in liquid ammonia, and several were tested at several concentrations.
Of this total, one, styphnic acid, was found to induce ignition at concentra-
tions down to 0.05%(w) of ammonia. Six additives at 0.5% substantially
reduced ignition temperature as did 6 additives at 1.0%, 2 at 1.5%, and 4
at 5.0%. Although not inducing ignition, 11 additives at 5.0% or less
significantly increased the oxidation of ammonia. Detailed results of
this work are given in Appendix D.

EVALUATION OF ADDITIVES IN ENGINE

The CFR single-cylinder test engines and installations are described
in Appendix E, along with an account of mechanical problems encountered which
were believed to be peculiar to operation on ammonia and additives. The per-
formance of the various additives in the engine can be summarized as follows:

Spark Ignition

Ten gases and fourteen liquids were tested as ammonia-additives in
the spark ignition CFR engine at 900 and 1800 RPM and 8.0 to 1 compression
ratio, using 35° spark advance and best power air-fuel ratio. The results
are shown in Table I. Engine performance on ammonia only and on hydrogen
only was checked first for reference purposes; combustion was achieved at
900 RPM but not at 1800 RPM. Of the gases, hydrogen was by far the best
additive, permitting fairly good engine operation at 900 and 1800 RPM at

concentrations of less than 1.5%(v). Acetylene was the next best additive, requiring about 6% to give good engine operation at both speeds. Ethylene, ethane, and butane permitted good performance at relatively low concentrations at 900 RPM, but concentration had to be increased substantially to obtain operation at 1800 RPM. The remaining gases, nitrous oxide, nitrogen dioxide, carbon monoxide, Freon-12, and ozone, were ineffective. The liquid additives, although several permitted good engine operation at both 900 and 1800 RPM, all required use at unreasonably high (over 10%) concentrations.

Hydrogen also was checked as an additive at several concentrations at varying spark advance and compression ratio. The results for 900 RPM are shown in Table II, and for 1800 RPM are shown in Table III. Hydrogen was an effective ammonia-additive in this engine at concentrations of less than 1.0%, provided compression ratio was above 12:1 and spark advance was more than $50°$. Checks on carbon monoxide and nitrous oxide were made also; fairly good engine operation could be obtained, even at 1800 RPM, provided additive concentration, compression ratio and spark advance were sufficiently high.

Compression Ignition

This work comprised an evaluation of the performance of gases added to the intake air, and of several liquid-ammonia additives selected from the bench reactor program. The work on the inducted gases was conducted first, to simultaneously evaluate the gases as ammonia additives and pinpoint the best engine operating conditions to use for evaluating the liquid-ammonia additives.

Of gases added to the intake air while ammonia was being injected, hydrogen, normal butane, and acetylene all facilitated combustion at some engine operating condition. The gases generally were tested at 20:1, 25:1 and 30:1 compression ratio, and at 900 and 1800 RPM. The results are summarized in Table IV. Combustion with ammonia and hydrogen was achieved at 25:1 and at 30:1 compression ratio at both 900 and 1800 RPM; performance improved as either compression ratio or speed was increased. Combustion with ammonia and normal butane was achieved at all compression ratios and speeds (not tested at 30:1 CR and 1800 RPM) but butane consumption was excessive at 1800 RPM. Combustion with ammonia and acetylene was achieved at 20:1 and 25:1 CR and 900 and 1800 RPM (not tested at 30:1 CR). Performance improved as either compression ratio or speed was increased.

The additives selected from the bench reactor program were engine tested at 25:1 CR and 900 RPM, the condition where all inducted gases performed most similarly. Of the "non-explosives", ammonium nitrate was tested at concentrations of 1.0 and 5.0% of an additive-liquid ammonia mixture, and ammonium perchlorate was tested at 1.0%. Styphnic acid was selected as the most effective "explosive" and was tested at 0.1%. During the testing of these additives, the engine was closely observed for any evidence of the additive affecting combustion, and was checked for fireability by bracketing runs on the additives with runs using inducted acetylene. All of these liquid-ammonia additives proved to be completely without discernible tendency to initiate combustion of ammonia in this engine.

CONCLUSIONS

1) For a CFR single-cylinder spark ignition engine burning ammonia, hydrogen was the best additive in terms of good engine performance at low additive concentration with normal compression ratios, and acetylene was the second best additive.

2) For a CFR single-cylinder compression ignition engine burning ammonia, acetylene was the best additive in terms of good engine performance at normal compression ratios, whereas hydrogen performed well at compression ratios somewhat higher than normal.

TABLE I

PERFORMANCE OF AMMONIA AND ADDITIVES IN SPARK IGNITION ENGINE AT 35° SPARK ADVANCE, 8:1 COMPRESSION RATIO; AND BEST POWER AIR/FUEL RATIO

	900 RPM				1800 RPM			
	Conc. % (V)	Air/Fuel Ratio	Horse-Power	Combustion ?	Conc. % (V)	Air/Fuel Ratio	Horse-Power	Combustion ?
Ammonia (only)	--	7.4	3.6	erratic	--	--	0	none
Hydrogen (only)	--	60.9	2.4	even	--	--	0	none
Ammonia + Gases:								
Hydrogen	0.6	7.7	4.7	even	0.7	7.9	0	none
"	1.1	7.7	4.6	even	1.3	7.9	6.7	slt. erratic
"	2.3	7.7	4.5	even	2.6	7.9	7.0	very even
"	3.2	7.7	4.4	even	3.8	7.9	7.5	very even
Acetylene	1.0	7.5	2.8	erratic	1.0	--	0	none
"	2.0	7.5	4.6	erratic	--	--	--	--
"	3.0	7.5	5.0	even	3.0	--	0	none
"	4.9	6.8	5.1	even	--	--	--	--
"	5.5	7.8	5.0	even	6.3	8.0	8.0	even
Ethylene	2.4	10.7	3.9	even	13.2	9.0	7.8	even
Ethane	6.4	7.9	5.1	even	21.9	10.9	7.8	even
Butane	4.4	7.0	--	very erratic	20.2	10.9	7.0	erratic
Nitrous Oxide	59.0	5.3	5.1	even	49.0	--	0	none
Nitrogen Dioxide	10.0	4.6	5.0	(rapid plug fouling)	--	--	--	--

TABLE 1 (Cont.)

	900 RPM				1800 RPM			
	Conc. % (V)	Air/Fuel Ratio	Horse-Power	Combustion ?	Conc. % (V)	Air/Fuel Ratio	Horse-Power	Combustion ?
Carbon Monoxide	41.0	7.9	0	even	19.0	--	0	none
Freon -12	to 25.0	--	0	none	to 25.0	--	0	none
Ozone	0.3	--	0	none	0.3	--	0	none
Ammonia + Liquids:								
Hydrazine	4.2	6.7	3.6	erratic	--	--	--	--
"	6.4	6.7	5.1	erratic	--	--	--	--
"	11.0	6.7	5.1	erratic	37.0	7.0	8.0	erratic
Nitromethane	9.2	6.6	4.9	slt. erratic	45.0	7.9	7.6	knocked
Nitroethane	8.0	6.7	4.9	slt. erratic	42.5	8.0	7.9	slt. erratic
1-Nitropropane	8.7	6.7	5.0	slt. erratic	35.0	6.2	5.0	erratic
2-Nitropropane	12.0	7.5	5.	even to slt. erratic	to 50.0	--	0	none
Amyl Nitrate	12.4	6.8	5.0	slt. erratic	20.0	8.0	7.3	knocked
Gasoline	13.5	7.5	5.0	even	13.5	--	0	none
n-Heptane	20.5	7.9	4.8	erratic	?	--	0	none
Methanol	33.7	7.5	5.1	very erratic	33.7	--	0	none
Trimethyl Propylene Oxide	to 50.0	--	0	none	to 50.0	--	0	none
Tertiary Butyl Acetate	to 25.0	--	0	none	to 25.0	--	0	none

TABLE I (Cont'd)

	900 RPM				1800 RPM			
	Conc. % (V)	Air/Fuel Ratio	Horse-Power	Combustion ?	Conc. % (V)	Air/Fuel Ratio	Horse-Power	Combustion ?
Amyl Acetate	to 25.0	--	0	none	to 25.0	--	0	none
Lube Oil	to 25.0	--	0	none	to 25.0	--	0	none
Castor Oil	to 25.0	--	0	none	to 25.0	--	0	none
Ammonia + Ammonium Nitrate in Liquid Ammonia	5.0	--	0	none	5.0	---	0	none

TABLE II

PERFORMANCE OF AMMONIA AND ADDITIVES IN SPARK IGNITION ENGINE AT 900 RPM AT VARYING SPARK ADVANCE AND COMPRESSION RATIO

Horsepower at Best Air/Fuel Ratio[1] for the Following Compression Ratios and Spark Advances

COMPRESSION RATIO						SPARK ADVANCE
4.5:1	6:1	8:1	10:1	12.3:1	16:1	
			Ammonia			
0	0	0	0	0	0	15°
0	2.5	3.6	5.1	4.9	4.9	35°
0	0	0	3.7	4.4	4.0	55°
		Ammonia + 0.6% Hydrogen				
0	0	0	0	0	0	15°
0	3.3	4.7	5.1	4.9	4.8	35°
0	2.4	4.2	4.0	3.7	3.5	55°
		Ammonia + 1.1% Hydrogen				
1.4	1.8	2.6	0	0	0	15°
2.1	4.2	4.6	5.0	4.8	4.7	35°
1.4	3.7	3.9	3.5	3.3	3.2	55°
		Ammonia + 2.3% Hydrogen				
3.4	3.4	4.1	0	0	0	15°
3.0	4.2	4.5	4.9	4.6	4.3	35°
3.4	3.9	3.6	3.3	3.0	2.9	55°
		Ammonia + 3.4% Hydrogen				
3.6	3.8	4.4	4.8	0	0	15°
3.4	4.1	4.4	4.8	4.5	4.2	35°
3.6	3.8	3.5	3.1	2.8	2.6	55°
			Hydrogen			
2.4	2.4	2.4	2.4	2.0	1.9	35°

6:1	7:1	8.5:1	SPARK ADVANCE
	Ammonia + 59% Nitrous Oxide		
--	--	5.1	35°
	Ammonia + 41% Carbon Monoxide		
4.3	4.5	4.7	35°

(1) 7.7:1 for ammonia-hydrogen
    5.3:1 for ammonia-nitrous oxide, and
    7.9:1 for ammonia-carbon monoxide.

CJD:bjb
1/4/66

- 10 -

TABLE III

PERFORMANCE OF AMMONIA AND ADDITIVES IN SPARK IGNITION ENGINE AT 1800 RPM AT VARYING SPARK ADVANCE AND COMPRESSION RATIO

Horsepower At Best Air/Fuel Ratios[2]
For The Following Compression Ratios
And Spark Advances

FUEL	COMPRESSION RATIO					
	4.5:1	6:1	8:1	10:1	12.3:1	16:1
Ammonia +						
.7% H_2	0	0	0	0	7.2 (55)	7.3 (50)
1.3% H_2	0	0	6.7 (50)	6.9 (40)	7.4 (45)	7.6 (40)
2.6% H_2	0	6.4 (60)	7.0 (35)	7.5 (35)	7.7 (30)	8.1 (30)
3.8% H_2	3.4 (45)	6.7 (40)	7.5 (35)	7.8 (30)	8.1 (30)	Very erratic
2.6% H_2	-	6.4 (40)	7.0 (35)	7.5 (35)	0	0
19% CO	0	0	0	6.3 (35)	8.4 (35)	8.3 (35)
15% N_2O	0	0	0	0	4.7 (45)	7.5 (45)
49% N_2O	0	0	0	0	0	6.7 (35)
.3% O_3	0	0	0	0	0	0

Note: Numbers in parenthesis are spark advances in °BTDC.
Unless otherwise indicated, the spark plug gap is .035 inches.

(2) 7.9:1 for ammonia-hydrogen, 7.2:1 for ammonia-carbon monoxide, and
7.6:1 for ammonia-nitrous oxide.

TABLE IV

PERFORMANCE OF GASEOUS AMMONIA ADDITIVES
IN CFR COMPRESSION IGNITION ENGINE
(Ammonia injected, gases added to intake air)

	Reference (Heater Oil)	Ammonia and		
		Hydrogen	n-Butane	Acetylene
20:1 CR & 900 RPM -- 37.5 PPH,Air				
# additive/# Ammonia	-	-	.268	.167
# Ammonia/Hr	-	-	2.8	3.8
Best Power, *HP	4.3	No ignition	5.4	5.2
20:1 CR & 1800 RPM -- 75.7 PPH,Air				
# additive/# Ammonia	-	-	.922	.118
# Ammonia/Hr	-	-	2.6	8.2
Best Power, HP	9.1	No ignition	9.2	10.6
25:1 CR & 900 RPM 00 37.5 PPH,Air				
# additive/# Ammonia	-	.237	.242	.105
# Ammonia/Hr	-	1.9	2.6	3.6
Best Power, HP	4.9	4.8	6.0	6.5
25:1 CR & 1800 RPM -- 78.0 PPH,Air				
# additive/# Ammonia	-	.067	1.50	.088
# Ammonia/Hr	-	6.4	1.2	10.2
Best Power, HP	9.2	11.5	8.4	12.4
30:1 CR & 900 RPM -- 37.5 PPH,Air				
# additive/# Ammonia	-	.105	.105	-
# Ammonia/Hr	-	3.8	3.8	-
Best Power, HP	4.8	5.5	5.8	Not tested
30:1 CR & 1800 RPM -- 78.5 PPH,Air				
# additive/# Ammonia	-	.032	-	-
# Ammonia/Hr	-	8.2	-	-
Best Power, HP	9.7	11.7	Not tested	

*Best Power at 30° BTDC injection advance

FIGURE 1

EFFECT OF TEMPERATURE AND AMMONIA CONCENTRATION
ON NET RATE OF AMMONIA CONSUMED BY OXIDATION

TOTAL FLOW: 150 cc/MIN.
RESIDENCE TIME: 3 MIN.
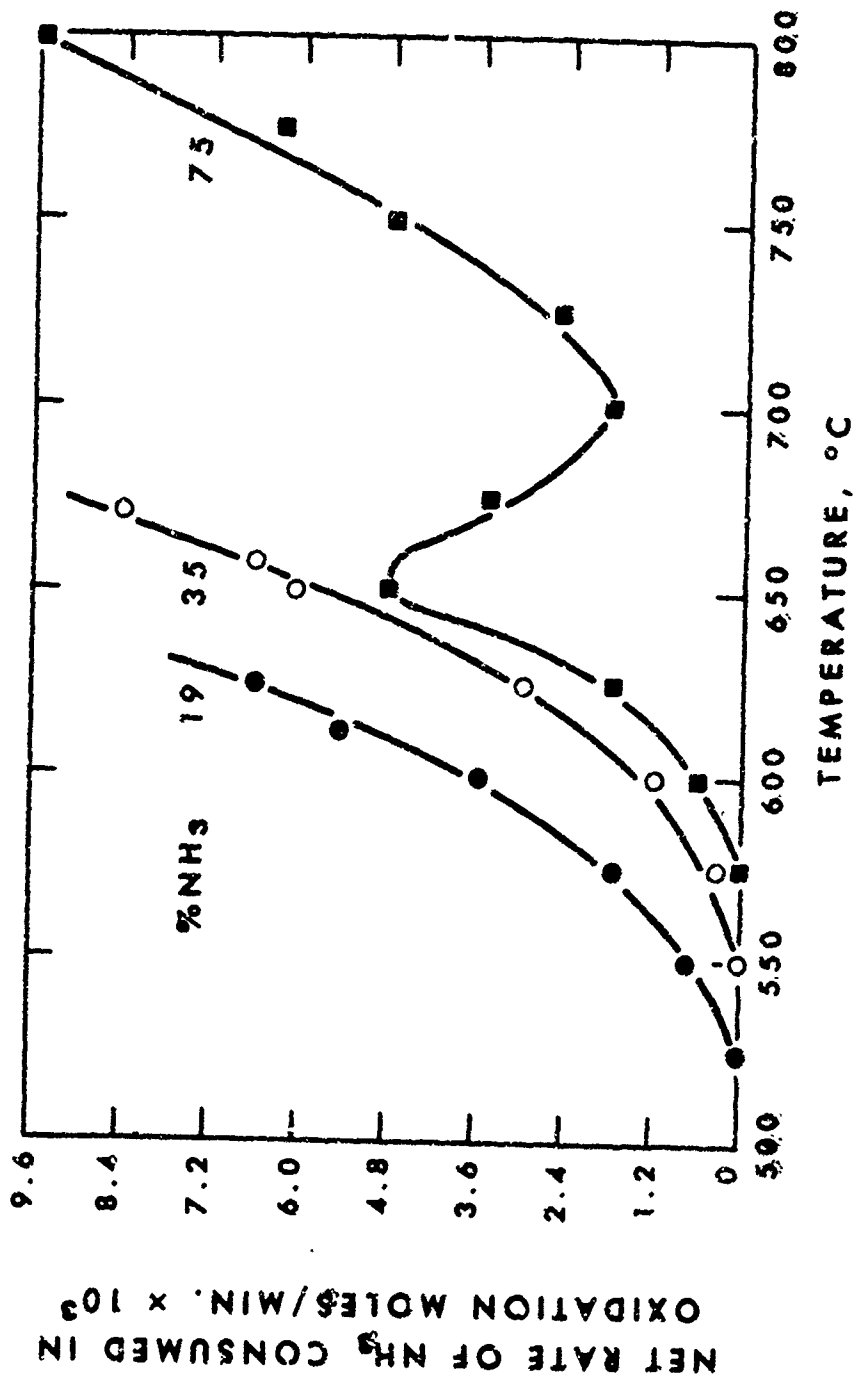
RECORDS

Records for this work are contained in:

1) Laboratory Journal No. J-494, "Ammonia Engine" issued to
   C. J. Domke

2) Laboratory notebook No. 856, issued to R. L. Mieville

3) "Log Sheet File, Project 6114", C. J. Domke

APPENDIX A

LITERATURE SEARCH

Gas Phase Kinetics

1) E. R. Stephens & R. N. Pease: J.A.C.S. _72_ 1188 (1950)
2) E. R. Stephens & R. N. Pease: J.A.C.S. _74_ 3480 (1952)
3) J. Werwimp & A. VanTiggelen: Bull Soc Chim Belg _62_ 205 (1953)
4) Ordogh M. & Szaboz G.: Acta Univ. Szeged. Acta Phys Chem _3_ 78 (1957)
5) M. Destrian & P. Laffitte: Compte Rendu _252_ 4003 (1961)
6) Takeyama T. & Mujama H.: J. Chem Phys _42_ 3737 (1965)

Flame Properties

1) P. Ansloos & A. VanTiggelen: Bull Soc Chim Belg _60_ 433 (1951)
2) R. C. Murray & A. R. Hall: T.F.S. _47_ 743 (1951)
3) H. F. Coward & G. W. Jones: Bull No. 503 Bur Mines (1952)
4) L. Cohen: Fuel London _34_ 123 (1955)
5) E. A. Arden, J. Powling & W. A. Smith: Comb. & Flame _6_ 21 (1962)
6) D. G. R. Andrews & P. Gray: Comb. & Flame _8_ 113 (1964)

Engineering and Rocketry

1) U. S. Patent 2,357,184 (Acetylene--Frejacques)
2) U. S. Patent 2,393,594 (Ammonium Nitrate--Davis)
3) I. Cornet et al Ind Eng Chem. _45_ 1033 (1953)
4) D. I. Baker Jet Propulsion _25_ 217-26, 234 (1955)
5) B. J. Clark, M. Hersch, & R. J. Pren NASA Memor 12-29-58E 31 (1959)
6) C. H. Liebert, R. C. Ehlers NASA Tech Note D-1048,20 (1961)
7) W. L. Bulkley & H. W. Husa Chem. Eng. Prog. _58_ 81 (1962)
8) Ohm J. B. and Sage B. H. Private communication

APPENDIX B

DESCRIPTION OF BENCH REACTOR AND OPERATION

The apparatus shown in Figs. B-1 and B-2 consists of a reactor, a furnace for heating the reactor and preheating the oxygen, and an additive solution atomizer. Ammonia and oxygen entered the apparatus separately. The ammonia entered at the top of the atomizer at a rate of 56 cc/min. After mixing, the oxygen and ammonia and additive, (when used) passed into the furnace which was programmed for a linear temperature increase. The ammonia-oxygen mixture flowing into the reactor was heated progressively to higher temperatures until ignition occurred. The temperature of the oxidation reaction was monitored by a thermocouple placed in the reactor. Temperatures were measured in the reactor (T_R) indicated by a "kick" on the temperature recorder. The effluent gas was passed directly into a Perkin Elmer Model 112 Infra Red Spectrometer which measured the concentration of ammonia.

When testing additives, the additive was fed to the atomizer by a syringe pump, generally at a rate of 0.01 cc/min. The additive solution entered the apparatus through a 1/16" O.D. stainless steel tube with a sharp pointed tip which was maintained at a potential of about 15 KV. The solution was charged as it came to the tip and atomized as it was pulled into the high potential field. Atomization was achieved by charging the additive solution to a high potential and exposing it to a high potential field.

Additive solutions were made up previously, at the required concentrations. In most cases the solvent used was water. Ammonium hydroxide solution was used with hard to dissolve compounds. In the case of insoluble liquids, a detergent was added and an emulsion was used.

With additives which did not induce ignition below 600°C. the programmer was stopped at 600°C and the system allowed to equilibrate. At this temperature, the concentration of ammonia was observed. This was compared with a similar run with no additive present, and the difference was ascribed to the induced oxidation by the additive.

The initial work with gaseous additives was performed by introduction of the gas at top of the reactor without the voltage turned on the atomizer. Measurement of oxidation increase was made by a differential temperature method. The exothermicity of reaction could be measured by the difference in temperature readings between (T_R) and (T_F).

FIGURE B-1

BENCH REACTOR
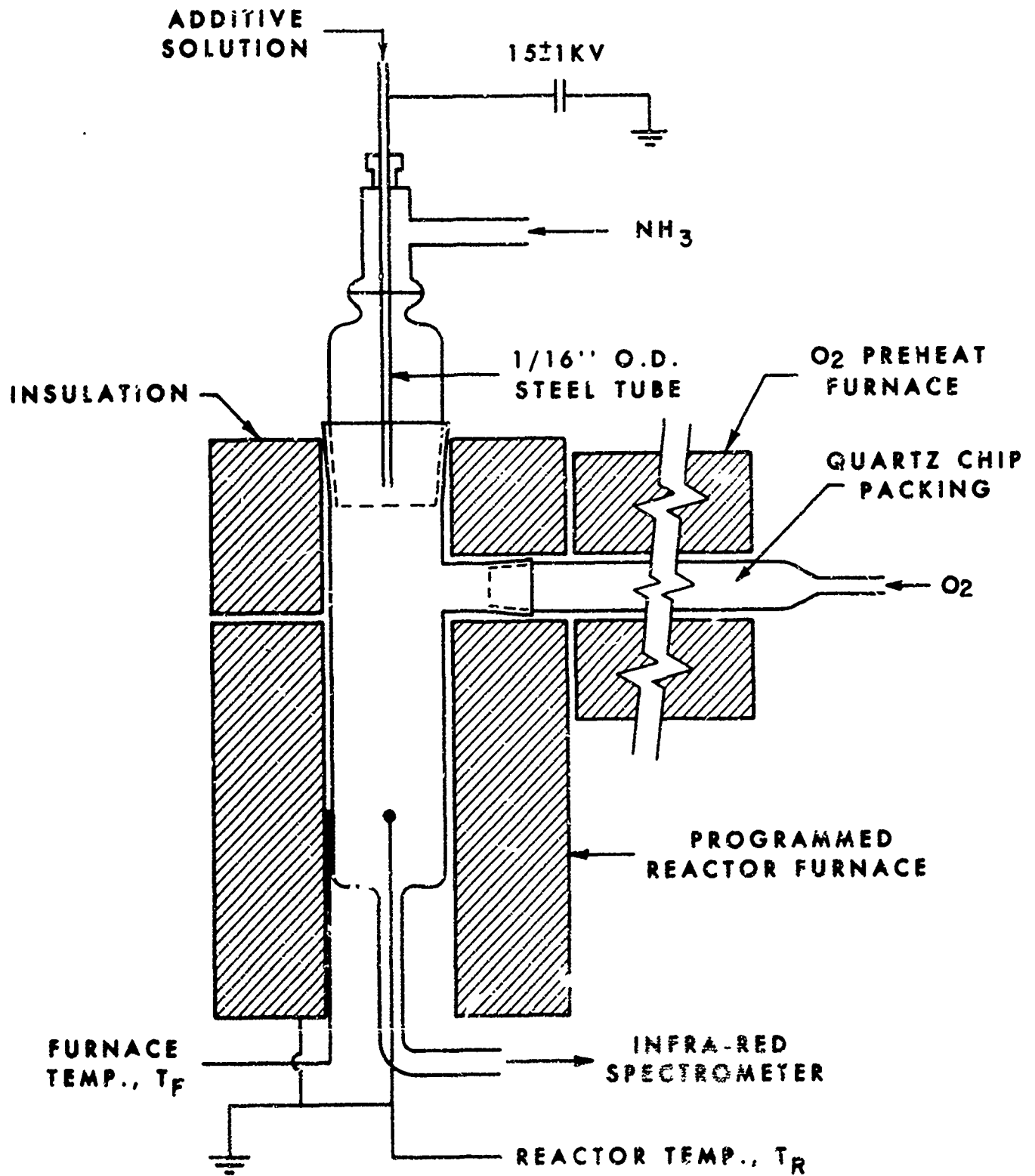
FIGURE B-2

BENCH REACTOR

- 18 -
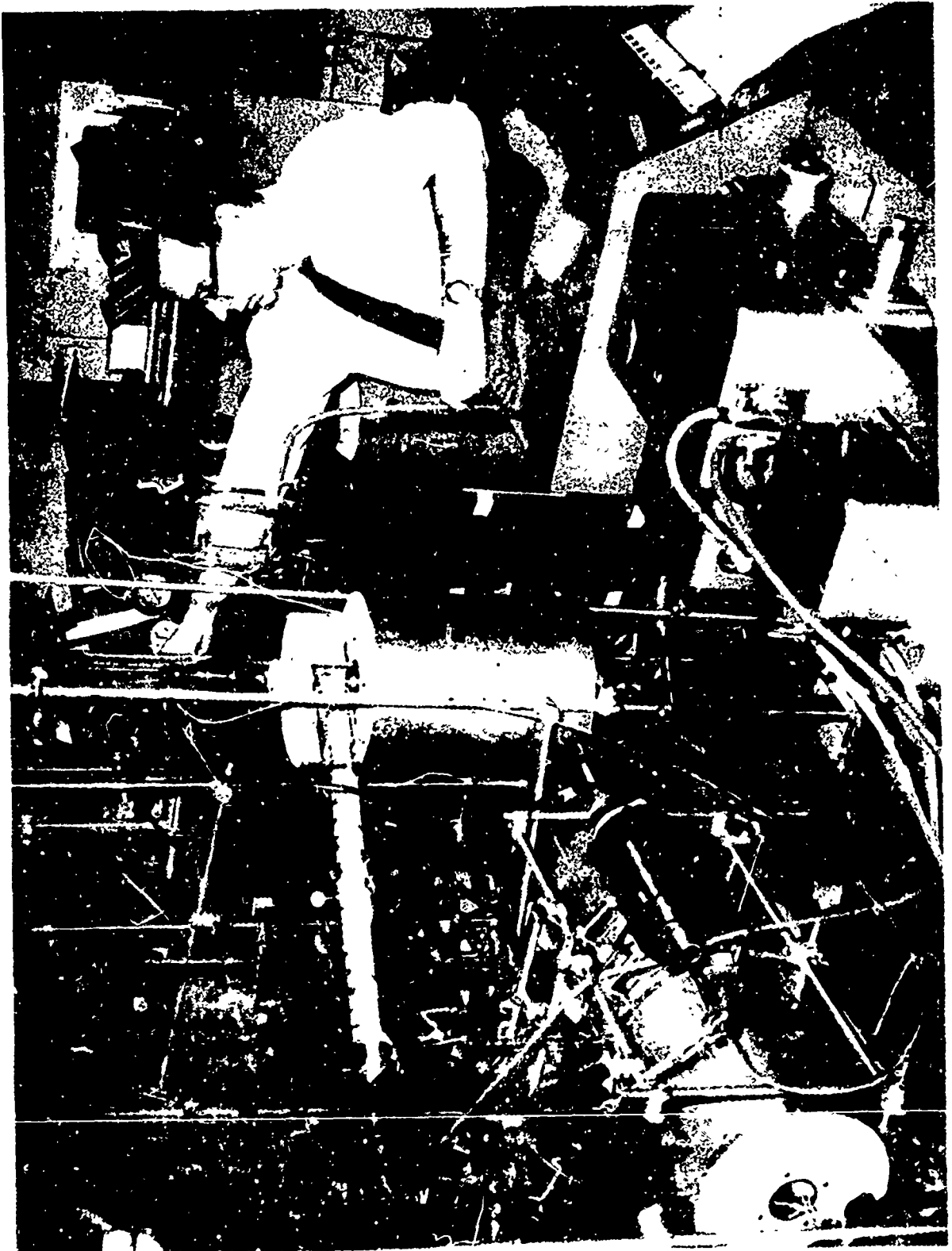
APPENDIX C

BENCH REACTOR RESULTS ON ADDITIVES FOR
SPARK IGNITION ENGINES BURNING AMMONIA

Additive	Concentration, % (v)	Effect on Oxidation of Ammonia
Hydrogen	3- 5	Strong
Ozone	1	"
n-Butane	3	Weak
Butene-1	3	"
Carbon Monoxide	3	"
Chlorine	3	"
Nitrous Oxide	1-10	None
Nitrogen Dioxide	1-10	"
Iso-Octane-n-Heptane, 80/20%	3	Strong
Lube Oil Base, No. 5, Solvent Extracted	5	"

APPENDIX D

TABLE D-I

<u>ADDITIVES FOR LIQUID AMMONIA WHICH INDUCED IGNITION IN THE BENCH REACTOR</u>

	Ignition Temperature, Degrees Centigrade
No Additive	> 700
Additives at < 0.5% (w) of ammonia:	
Styphnic Acid (0.35%)	400
" " (0.25%)	395
" " (0.10%)	520
" " (0.05%)	580
Additives at 0.5% (w) of ammonia:	
Styphnic Acid	395
Trinitrometacresol	410
Nitroguanidine	430
Trinitrotoluene	455
Picric Acid	460
Ammonium Picrate	580
Additives at 1.0% (w) of ammonia:	
Ammonium Perchlorate	480
Sodium Azide	500
Trinitrobenzene	515
Trinitromethane	525
Isoamyl Nitrite	570
Amyl Nitrate	645
Additives at 1.5% (w) of ammonia:	
Ammonium Nitrate	540
Potassium Azide	685
Additives at 5.0% (w) of ammonia:	
Potassium Nitrate	450
Ammonium Perchlorate	460
Ammonium Carbonate	610
Sodium Nitrite	625
Additives at > 5.0% (w) of ammonia:	
Ammonium Nitrate at 7.5%	535
Ammonium Nitrate at 15.0%	420
Hydrazine at 35.0%	510

TABLE D-II

ADDITIVES FOR LIQUID AMMONIA
WHICH INCREASED OXIDATION IN THE BENCH REACTOR

Additives at 1.0% (w) of ammonia
  Potassium Azide
  Ammonium Nitrate

Additives at 2.5% (w) of ammonia
  Potassium Permanganate
  Sodium Dichromate
  Potassium Dichromate
  Triethylamine

Additives at 5 0% (w) of ammonia
  Ammonium Persulfate
  Sucrose
  Hydrogen Peroxide
  Hydrazine
  Urea

- 21 -

TABLE D-III

ADDITIVES FOR LIQUID AMMONIA
WHICH ARE INEFFECTIVE IN THE BENCH REACTOR

Additives at 0.25% (w) of ammonia:
  Trinitrometacresol
  Nitroguanidine

Additives at 0.5% (w) of ammonia:
  Trinitrobenzene
  Tetranitromethane

Additives at 1.0% (w) of ammonia:
  Nitroethane
  Nitropropane
  Potassium Perchlorate
  Sodium Nitrite
  2-Nitro 2 Methyl Propanol
  2-Nitro 2 Methyl Propanol Nitrate

Additives at 2.0% (w) of ammonia:
  Ethyldiazoacetate

Additives at 2.5% (w) of am.   :
  Potassium chlorate
  Ammonium Vanadate
  Tert Butyl Acetate
  Tert Butyl Nitroso Mercaptan
  Butyl Mercaptan
  n-Butyl Ether
  Acetomide
  Acetoxime

Additives at 5.0% (w) of ammonia:
  Ammonium Oxalate
  Ammonium Acetate
  Ammonium Chloride
  Sodium Nitrate
  Sodium Chlorate

APPENDIX E

TEST ENGINES, INSTALLATION, AND MECHANICAL PROBLEMS RELATED TO OPERATION ON AMMONIA AND ADDITIVES

Spark Ignition Engine

A CFR Research method engine was used. The standard CFR fuel system was omitted and the engine was fitted with a manifold that permitted simultaneous independent introduction of ammonia and additive. Air flow measurements were made using a Meriam Laminar Flow Meter. Ammonia flow measurements were made using a Fischer and Porter Variable Area Flowmeter. Average coolant and oil temperatures were about 212°F and 135°F respectively. Mechanical experiences with this engine were:

1) Excessive leakage of ammonia was experienced through the crank-shaft and injection pump drive seals and the distributor shaft. This condition was corrected by fitting lip seals to the crankshaft, an "O-ring" seal to the distributor, and sealed ball bearing sets to replace standard ball bearing sets.

2) Nitrogen dioxide addition resulted in extensive spark plug fouling and substantial combustion chamber deposits. The deposits were identified as ammonium nitrate. These deposits probably contributed to engine wear which required replacement of the cylinder and piston. At the time of replacement, the engine had operated on ammonia and additives for a total of 110 hours.

3) The ignition system consisted of an automotive ignition coil, a 4 mfd. capacitor, UD-16 spark plug gapped at .035", and a primary voltage of 12V. No ignition difficulty was experienced in this system.

To provide some bench-mark information on ignition requirements, oscillograms of voltage traces from the high tension lead wire were taken while the engine was running with ammonia and with ammonia plus hydrogen. The oscillograms showed numerous high voltage spikes following firing, plus much hash on the decay curve, upper traces, Figs. E-1 and E-2. These traces indicate that ionization took place at about 6-7 kilovolts (1 cm $\stackrel{.}{=}$ 2 KV).

Compression Ignition Engine

A CFR Cetane method engine was used for this phase, Figs. E-3 and E-4. Average coolant and oil temperatures were 205-212°F and 130-190°F respectively. Air flow measurements were made using a Meriam Laminar Flow Meter. The injection pump rack was calibrated on heater oil. Ammonia flows were then determined in terms of equivalent flow on heater oil. Mechanical experiences with this engine were:

1) Piston seizure was experienced three times using cast-iron pistons during the shake-down runs. The piston seizures evidently were due to lack of adequate lubrication and cooling, and to difficulty in establishing proper piston-to-cylinder clearances at higher engine speeds, particularly at 2700 RPM. One piston developed a hairline crack from the skirt to the wrist-pin boss. No further difficulty occurred when an aluminum piston was substituted for the cast-iron piston. The advantages of the aluminum piston apparently lay in: 1) greater clearances used in fitting, 2) greater strength of the skirt, 3) better heat conductivity and 4) less risk of damage to the cylinder.

2) Head gasket failure was a continuing problem. Three gaskets failed in rapid succession, Fig. E-5. The failures were thought to result from the high pressures developed at elevated compression ratios. Several attempts to correct this difficulty were made by substituting a homemade copper gasket for the composition gasket which is standard with the CFR engine. The homemade gaskets were not completely successful.

Then the engine was modified in an effort to prevent further head gasket failures. The cylinder was counterbored a short distance down below the valve deck, and an aluminum fire-ring was fitted to the groove. The ring projected above the deck a distance about equal to the crush-thickness of the standard head gasket. The fire ring was cut from a standard gasket to enlarge the hole to accommodate the aluminum ring. Thus, the aluminum ring sealed the combustion chamber and the gasket sealed the water jacket. The aluminum rings were cut from sand-cast aluminum.

This approach was reasonably successful. However, the sand-cast aluminum fire ring eventually failed and had to be replaced. The ring showed heavy ablation (Fig. E-6) in the same relative location where the head gaskets had failed previously. A second ring of the same material was installed. Upon failure, it was found that half of the ring had disappeared, Fig. E-7. Several rings were then fabricated from 2024-T351 aluminum, it being thought that the higher Young's modulus might reduce ablation occurring during periods when the cylinder head might flex away from the seal. However, upon final engine disassembly, a 2024-T351 ring was removed which had a 1-1/2 inch segment missing.

This suggests that the gasket failures are probably not completely attributable to pressure, or to irregularities in the mating surfaces. A possible explanation might be that extremely high flame temperatures exist, compared to normal combustion, during the period of spontaneous ignition of the gaseous additives tested. This theory is supported by the evidences of pilot work conducted earlier (preceeding work under this contract) wherein the engine was operated at elevated compression ratios (37:1) and high jacket (350°F) and inlet air (200°F) temperatures for sustained periods. No gaseous additives were used during this earlier work and no head gasket damage was experienced.

3) Injector nozzle sticking occurred repeatedly during periods of acetylene addition. Microscopic examination revealed varnish-like deposits on the injector pintle. This apparently was due to polymerization of acetylene during periods when pressures in the combustion chamber exceeded the 1500 psi injector nozzle pressure setting. Increasing the injector pressure to 2500 psi reduced the incidence of nozzle sticking. Nozzle sticking also resulted during operation on ammonium nitrate and ammonium perchlorate.

4) Two cylinder heads were cracked during these tests. Each crack occurred in the web between the valves. Detonation was often quite severe, particularly with hydrogen, and undoubtedly caused this damage.

5) Erosion of the piston crown area was observed, plus extensive nibbling of the piston corner in an area adjacent to the point where the charge enters the cylinder. This could be due only to chemical attack by ammonia on the aluminum and/or to preignition.

Examples of dp/dt traces for heater oil and ammonia + various additives are shown in Figs. E-8 to E-15.

The upper trace is injector travel and the left boundary of the oscillogram marks the beginning of injection. Hence, at 900 RPM, we see an ignition delay of $17°$ for heater oil, $37°$ for ammonia + n-Butane, and $37°$ for acetylene. Oscillograms for ammonia + hydrogen, at 900 RPM, are not available due to failure of the pressure pick-up, however, the traces characteristically looked like those for ammonia + n-Butane but with a high spike on the peak.

Combustion chamber resonance is evident with heater oil and ammonia + hydrogen at 1800 RPM. This contrasts with the traces for ammonia + n-Butane or acetylene wherein there is no resonance.
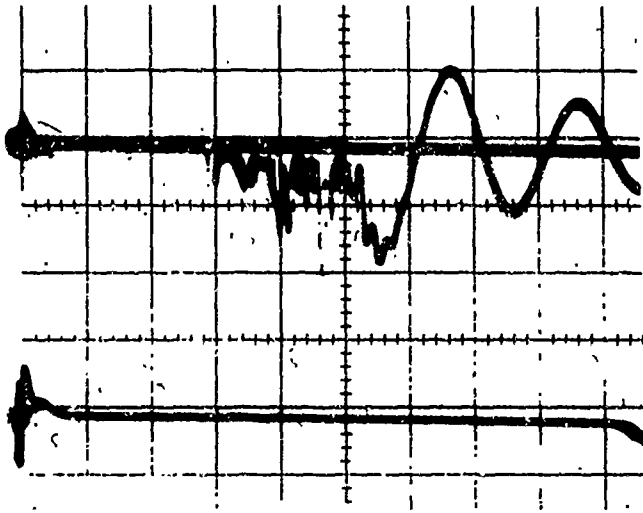
FIGURE E-1

AMMONIA
900 RPM
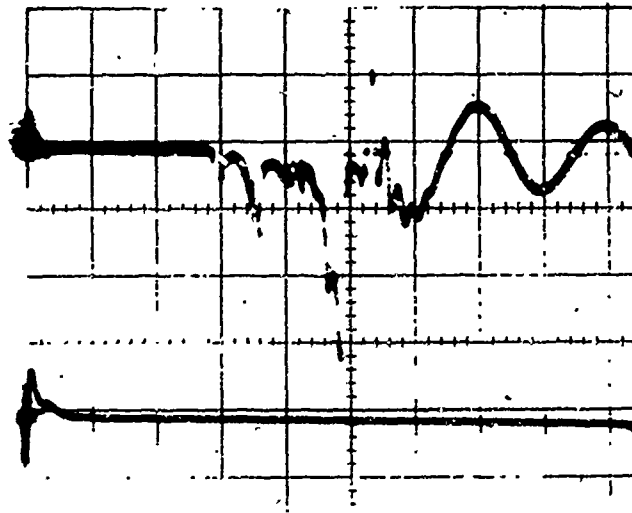
FIGURE E-2

AMMONIA + HYDROGEN
900 RPM

FIGURE E-3

CFR CETANE ENGINE
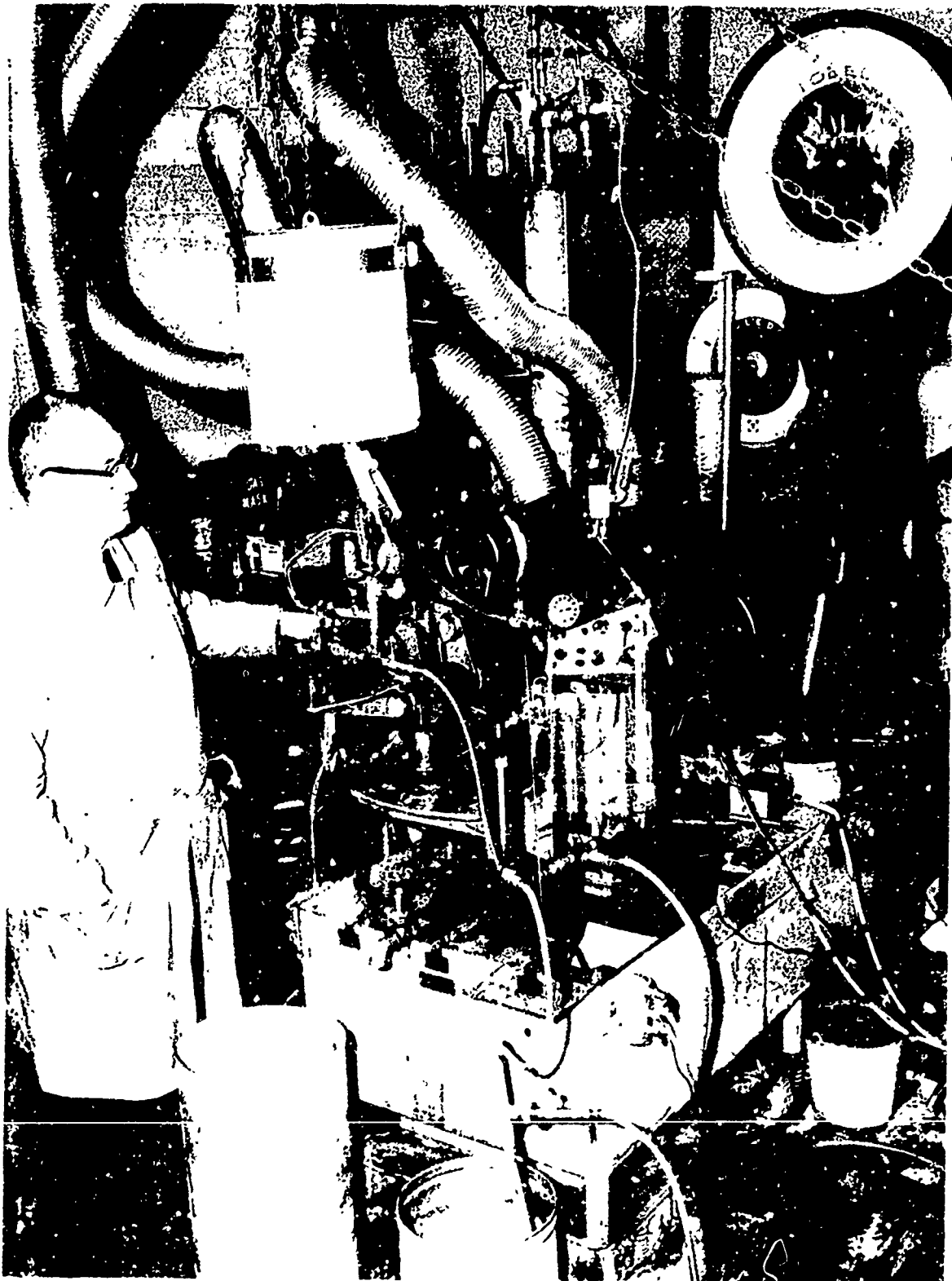
FIGURE E.4

CFR CETANE ENGINE
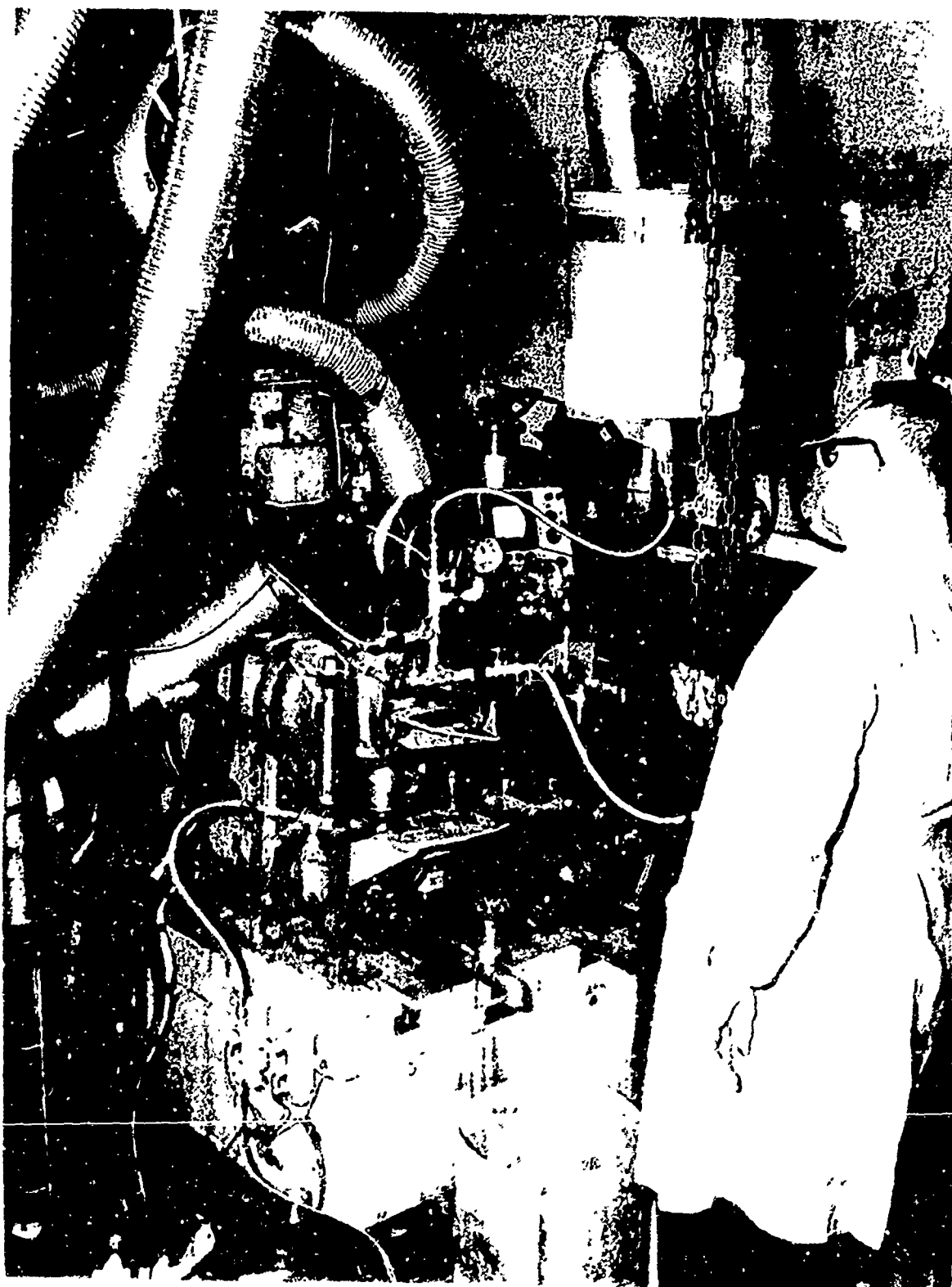
FIGURE E-5
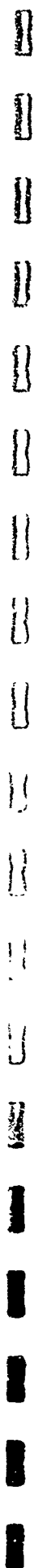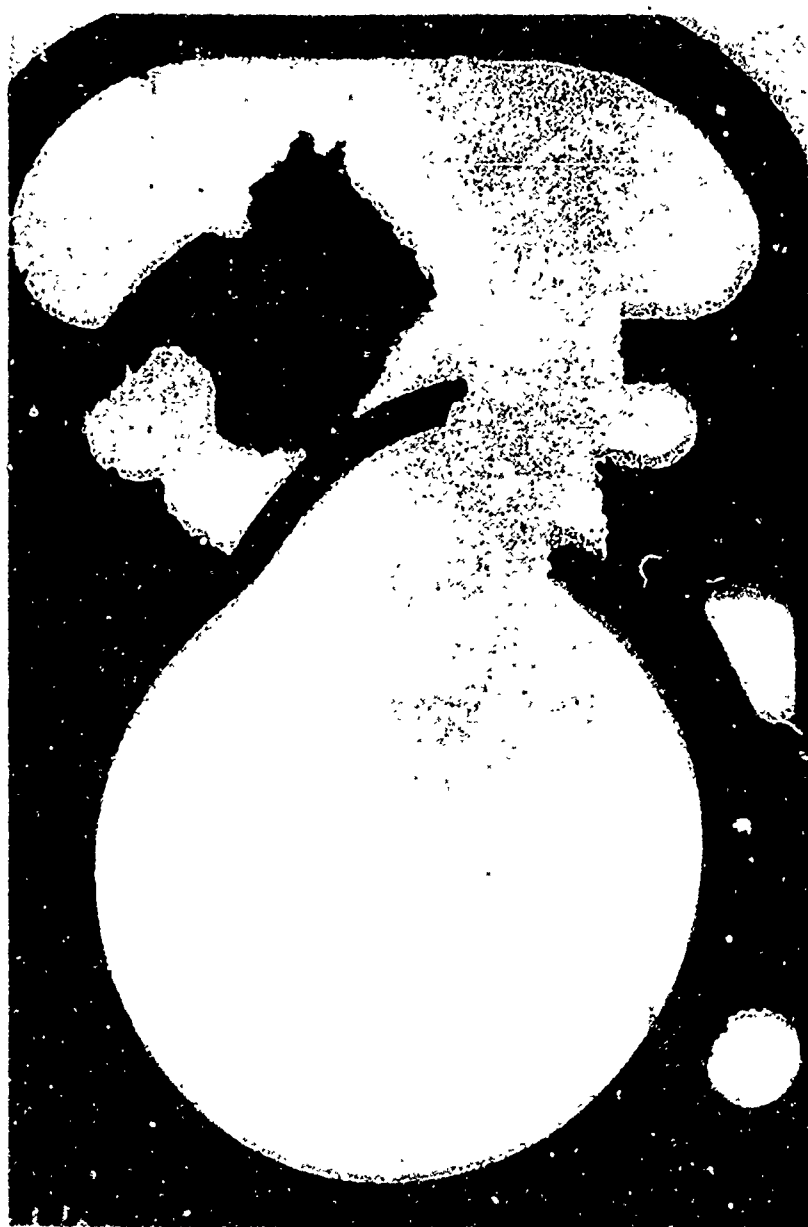
FIGURE E-6
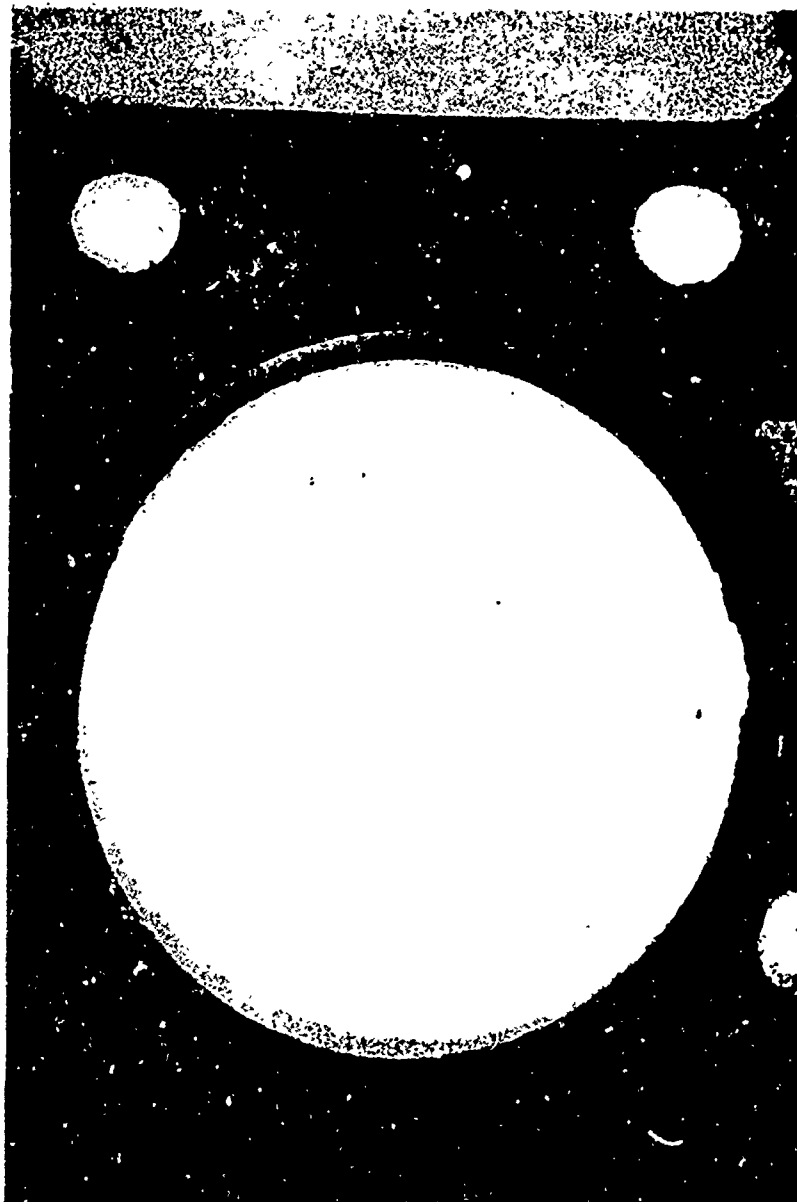
FIGURE E.7
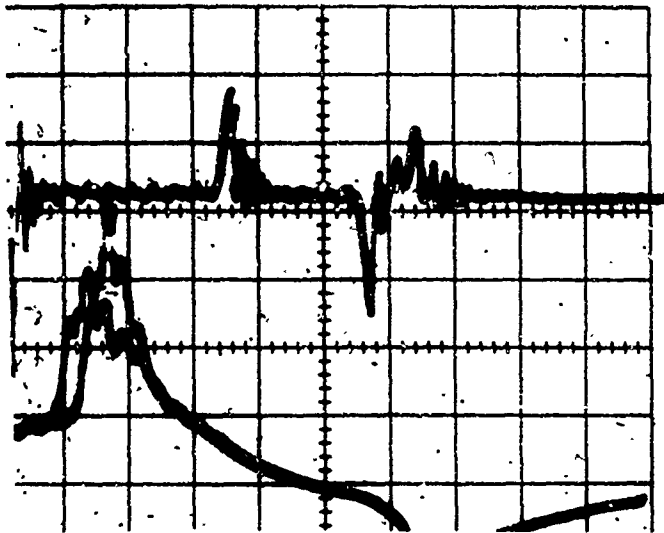
FIGURE E-8

HEATER OIL
900 RPM
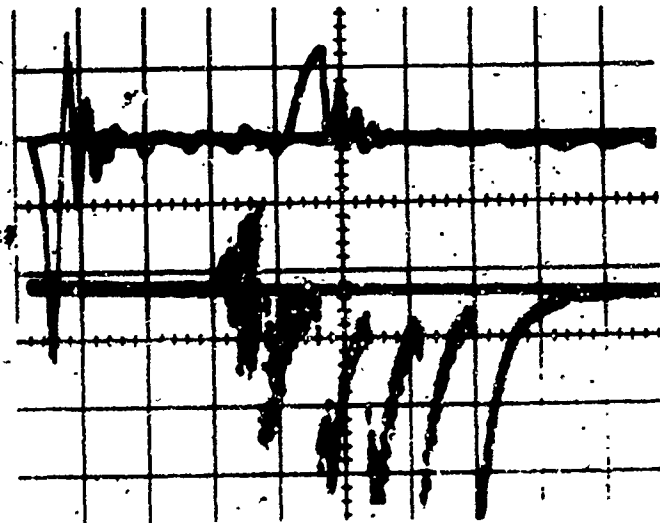
FIGURE E-9

HEATER OIL
1800 RPM
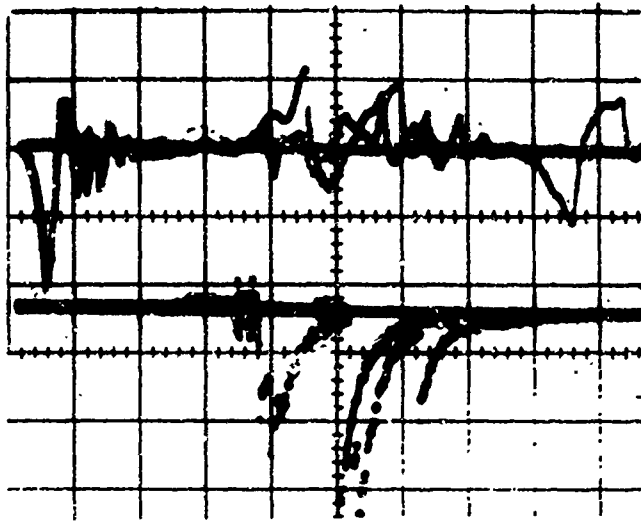
FIGURE E-10

AMMONIA + HYDROGEN
1800 RPM
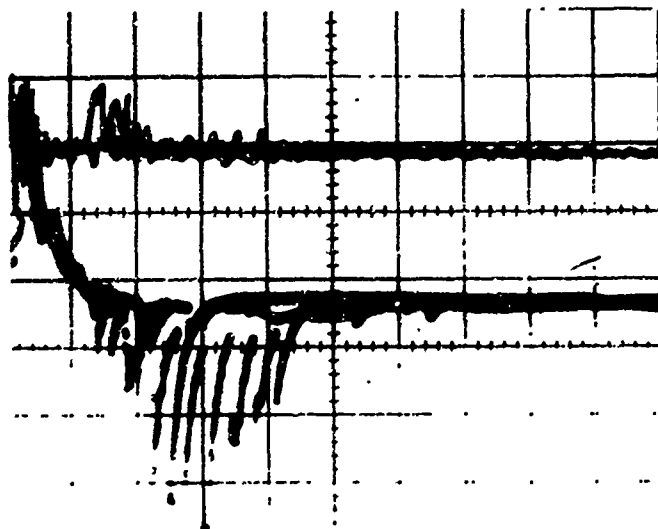
FIGURE E-11

AMMONIA + HYDROGEN
2700 RPM
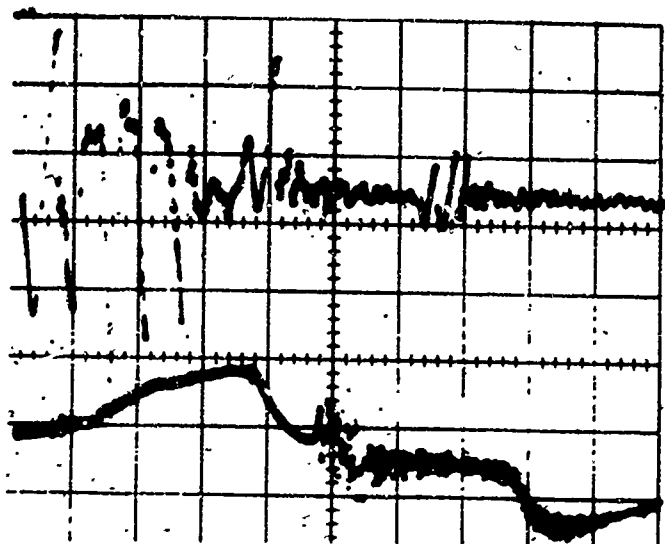
FIGURE E-12

AMMONIA + N-BUTANE
900 RPM
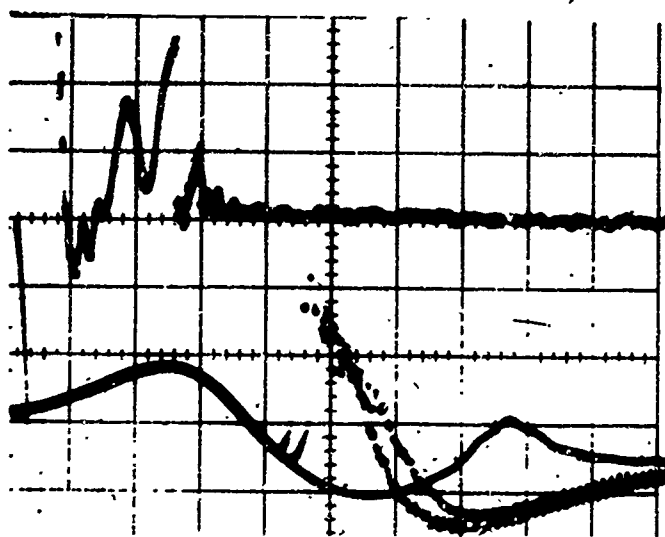
FIGURE E-13

AMMONIA + N-BUTANE
1800 RPM
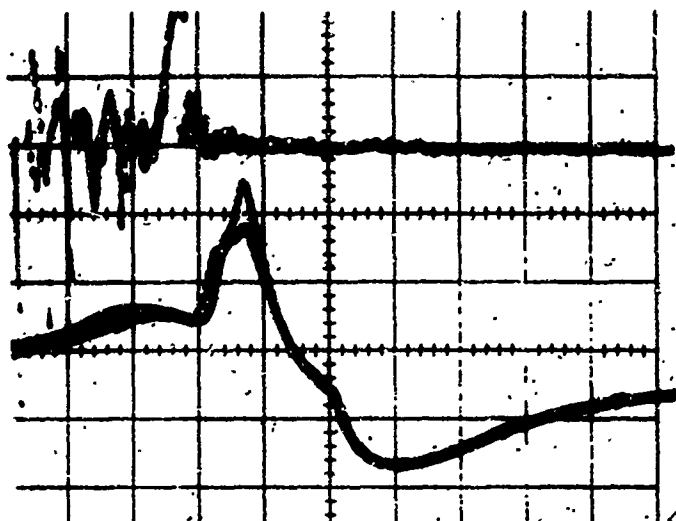
FIGURE E-14

AMMONIA + ACETYLENE
900 RPM
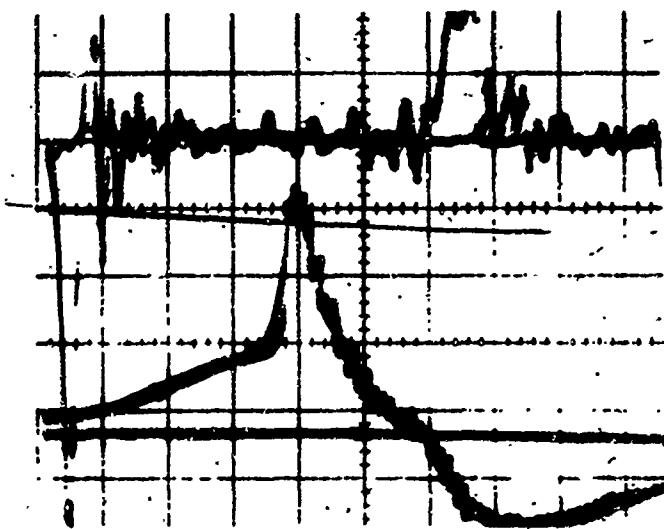
FIGURE E-15

AMMONIA + ACETYLENE
1800 RPM

APPENDIX II

**Effect Of Selected Additives Upon
The Stable Burning Limits Of
Ammonia-Air Flames**

EFFECT OF SELECTED ADDITIVES UPON

THE STABLE BURNING LIMITS OF

AMMONIA-AIR FLAMES

RN 66-9

18 March 1966

J. R. Williams

M. C. Hardin

Allison Division

General Motors Corporation

TECHNICAL DATA REPORT

DIV. **ALLISON** GMC	FDO NO REF	PAGE 1 OF 16	PAGES REPORT NO RN 66-9
TITLE		PREPARED J.R.Williams/M.C. Hardin	DATE
Effect of Selected Additives Upon the Stable Burning Limits of Ammonia-Air Flames		CHECKED	3/18/66
		APPROVED	

INTRODUCTION

This Research Note was prepared by the Allison Division of General Motors to present the technical results of ammonia additive screening tests conducted for Continental Aviation and Engineering Corporation under Purchase Order No. RD 101033. Continental Aviation and Engineering Corporation is investigating ammonia as a fuel for spark and compression ignition engines under Army Contract No. DA-20-113-AMC-05553(T). This activity is under the technical supervision of the U.S. Army Tank Automotive Center.

The additives to be screened in the Allison flame tubes were to be selected by Continental Aviation and Engineering Corporation based on the results of an independent investigation by the American Oil Company, Whiting, Indiana. Prior to the receipt of definitive additive results from the American Oil Company's investigations, Allison recommended and was authorized to conduct screening tests with three oxides of nitrogen and carbon monoxide. In addition, Continental requested that screening tests be conducted on ammonia nitrate and hydrogen peroxide. The nitrogen oxides were of interest due to their apparent activity as a rapid scavenger of the amidogen radical in ammonia oxidation [1], and evidence that NO reacts directly with NH and NH_2 radicals without prior decomposition [2]. Carbon monoxide and ammonium nitrate were included based upon observations from early studies by American Oil [3]. Hydrogen peroxide was of interest due to its exothermic

TECHNICAL DATA REPORT

DIV	**ALLISON**	GMC.	EDO NO REF	PAGE 2 OF *16*	PAGES	REPORT NO
TITLE				PREPARED		DATE
				CHECKED		
				APPROVED		

decomposition characteristics which would liberate both energy and free oxygen during the initial combustion process. All of the materials except carbon monoxide were also potentially producible in the field by the Energy Depot concept.

CONCLUSIONS:

1. In 5% volume, none of the additives tested increased the apparent ammonia-air flame propagation velocity to the degree obtainable by dissociating 28% of the incoming ammonia fuel.

2. The beneficial effect of carbon monoxide and the nitrogen oxides tested are very dependent upon the local fuel-air ratio of the ammonia-air mixture.

3. Nitric oxide appears to offer the most promise as a flame propagation rate improver over the fuel equivalence ratio range of 0.9 to 1.2. However it did not significantly exceed the effects of 5% acetylene additions at any mixture ratio. Also the formation of solid deposits resulting when the additive vapor in air mixed with the ammonia fuel could render its engine application difficult.

4. Carbon monoxide provided significant improvement to the ammonia-air flame propagation rate at fuel lean (0.9 stoichiometric) conditions, but was ineffectual at fuel-rich conditions.

TECHNICAL DATA REPORT

DIV. **ALLISON**	GMC.	EDO NO REF	PAGE	PAGES	REPORT NO
			. 3 OF / :		
TITLE			PREPARED		DATE
			CHECKED		
			APPROVED		

5. Flame stability limits were extended markedly at fuel-rich
   (> 1.2 of stoichiometric) conditions by nitrogen dioxide
   addition, but the benefits were minor in the stoichiometric
   region. Undesirable solid deposits were also experienced
   with this material in the fuel-air mixing region.

6. No conclusive results could be obtained as to the effect of
   ammonium nitrate additions due to injection and mixing pro-
   blems inherent to the test burner system.

7. The burner used in this investigation is useful for screening
   the effects of gaseous or readily vaporizable additives upon
   the propagation rate of ammonia-air flames. However, it is
   not suitable for evaluating non-volatile additives without
   development effort beyond the scope of the present project.

RECOMMENDATION

Further additive screening with the presently developed test
burner is recommended only for readily vaporizable materials.

DISCUSSION:

Test Equipment

The Powling type flat flame burner [4] developed for the previous
ammonia fueled gas turbine burner investigation was used. The
basic configuration is shown in Figure 1. The fuel-air mixture
is admitted through the inlet port at the base of the burner. The
normally gaseous or vaporized additives are admitted to the air

TECHNICAL DATA REPORT

DIV. **ALLISON** GMC.	EDO NO REF	PAGE 4 OF *16*	PAGES	REPORT NO
TITLE		PREPARED		DATE
		CHECKED		
		APPROVED		

stream ahead of the fuel-air mixing point. Mixing of the fuel
and air-additive mixture is completed as the mixture progresses
through the glass bead filled section in the base. After passing
through a sintered stainless steel flame arrestor, the gases flow
through the honeycomb-glass bead-honeycomb section to flatten the
velocity profile of the effluent gases. The burner is enclosed
within a 2.9 in. diameter jacket covered at the top by a screen to
minimize effects of random air currents and convective diffusion
of outside air into the reaction zone. The burner mixing section
and fuel and air inlet lines were wrapped with resistance heating
tape to provide controlled inlet temperatures from ambient to
500°F. The air, fuel, and additive flows were individually con-
trolled and measured, and the temperature and pressure of the
incoming mixture was measured in the burner mixing section. A disc
type flat non-diffusion flame adjacent to the top of the 1/16"
honeycomb surface results at stable burning conditions. When stable
burning limits are approached, the flame normally lifts abruptly
from the surface and blow-out results. This condition is readily
reproducible.

The previously described system was suitable for testing the
normally gaseous or readily vaporizable additives. However, to
evaluate ammonium nitrate, modifications were necessary. Electro-
static atomization and distribution of a 50% by weight of aqueous
ammonium nitrate in the mixing zone below the burner flame-holding
grid was attempted. This approach was selected based upon recent

TECHNICAL DATA REPORT

DIV **ALLISON** GMC.	EDO NO REF	PAGE 5 OF 16	PAGES REPORT NO
TITLE		PREPARED	DATE
		CHECKED	
		APPROVED	

work at California Research Corporation [5,6]. The ammonium
nitrate additive supply and electrostatic atomization system is
schematically shown in Figure 2, and the final burner configuration
is presented in Figure 3. A number of variations in location of
the charged grids and the additive injector were explored with only
limited success in obtaining the desired additive solution dis-
tribution across the reaction zone.

Due to the thermal instability of vaporized hydrogen peroxide, the
electrostatic atomization approach was planned for use in examining
this additive. In addition, passivation of the peroxide inlet
system and minor modifications to avoid trapping hydrogen peroxide
at any point in the system would also be necessary. Due to the
difficulties encountered in effective electrostatic atomization of
the aqueous ammonium nitrate, and the expense required for rig
modifications to test hydrogen peroxide, no attempt was made to
obtain data on this material when information was received that the
project was being terminated due to redirection of the total program.

Experimental Technique

For this screening effort, all gaseous additives were checked at a
concentration of 5% by volume of fuel flow. Stable burning was
established and the fuel a. additive flows adjusted to the desired
test condition. The air-flow rate was then increased or decreased
until blow-out resulted. This point is normally a sharp and
reproducible condition. An attempt was made to run only the number

TECHNICAL DATA REPORT

DIV. **ALLISON** GMC.	EDO NO REF	PAGE 6 OF 16	PAGES	REPORT NO
TITLE		PREPARED		DATE
		CHECKED		
		APPROVED		

of test points necessary for comparison of the additive effects.

Determinations of the effect of CO, N_2O, and NO additives, and a baseline of ammonia-air were run at ambient (77°F) inlet temperatures. The NO_2 (boiling point 70°F) additive supply and inlet line was pre-heated to 125°F to adequately vaporize the material. However, at the 77°F ammonia fuel and air inlet temperature condition, severe deposition of solid nitrate deposits occurred at the fuel-air mixing zone.

Testing at an inlet air temperature of 300°F was found to be necessary to minimize this deposit formation and to obtain reproducible results. An ammonia-air baseline was also obtained at the 300°F air inlet temperature. The limited scope of the program and the indicated additive benefits did not justify the additional determinations of CO, N_2O, and NO effects at 300°F air inlet temperature to provide the same baseline for all evaluations.

In the attempts to evaluate the effects of the ammonium nitrate solution additive, the ammonia-air flame was stabilized and a metered flow of the additive injected with an electric potential of 12,000 to 18,000 volts between the injector and upper honeycomb section. Potentials greater than 18,000 volts resulted in arcing between the fuel injector and the grid. Atomization benefits of the electrostatic field were evident, but an even dispersion across the flame holder area was not obtainable. At additive flow-rates

TECHNICAL DATA REPORT

DIV	**ALLISON**	GMC	FDO NO REF	PAGE 7 OF 16	PAGES	REPORT NO
TITLE				PREPARED		DATE
				CHECKED		
				APPROVED		

greater than 5% by weight, flame quenching or arcing was experienced. Elevation of the inlet air temperature to 500°F and modifications to the injection procedure did not resolve the problem.

Test Results

Flame stability limits obtained in these tests are presented in Figure 4 and Figure 5. The vertical ordinate in both figures is fuel equivalence ratio or the operating fuel-air ratio divided by the stoichiometric fuel-air ratio. In Figure 4, the maximum stable burning limits are plotted in terms of burner air flow velocity at the inlet air temperature. Figure 5 presents the same data on the basis of total gas flow velocity. While the velocity limit values differ in the two figures, the relative ratings of the additive effects are not changed.

Due to the variations in inlet air temperature found necessary for examination of these additives, the influence of the gaseous additives upon the maximum stable burning limits is more easily compared in Figure 6. Here the percentage improvement in blow-out velocity is shown for each additive over that for the ammonia-air flame at the same air inlet temperature and fuel equivalence ratio. The influence of pre-heating the ammonia-air mixture to 300°F is also compared with 77°F ammonia-air limits in this figure. Also plotted in this figure is the improvement in flame stability limits afforded by the additions of 5% by volume of acetylene.[7].

TECHNICAL DATA REPORT

DIV **ALLISON** GMC	E.DO NO REF	PAGE 8 OF 16	PAGES	REPORT NO
TITLE		PREPARED		DATE
		CHECKED		
		APPROVED		

The following observations can be made from the Figure 6 summarizing presentation. In 5% by volume additions to the fuel, none of the additives tested in this project appear as beneficial in improving the ammonia air flame propagation rate as partial pre-cracking (28%) of the ammonia. Acetylene additions at 5% volume are also competitive with the additives investigated herein. The flame propagation effects of the additives varied significantly over a relatively narrow range of fuel-air ratio. The "fuel type" additive (CO) exhibited a marked improvement in the fuel-lean area only, while the nitrogen oxides effects were larger in the fuel-rich region. Of those materials examined, nitric oxide appears most promising as to flame propagation rate improvement.

Quantitative data was not obtained for ammonium nitrate additions due to the atomization and additive distribution difficulties previously described. Qualitatively, it appeared that the ammonium nitrate might be improving the propagation rate of the flame. When the ammonia flame initially separated from the flame holder, a pale green reaction zone, characteristic of ammonium nitrate flames, remained attached to the flame holder. The injection operating difficulties and the transient character of this condition prevented its detailed examination.

Burner system fouling encountered during operation with NO and NO_2 is also of significance to considerations of practical application

DIV	**ALLISON**	GMC.	EDO NO REF		PAGE 2 OF 16	PAGES	REPORT NO
TITLE					PREPARED		DATE
					CHECKED		
					APPROVED		

of these materials in ammonia fueled engines. In our tests, the
nitrogen oxides were admitted to the air stream prior to mixing
with the fuel. Downstream of the air-fuel mixing region is a
sintered stainless steel filter disc. Deposit formation was en-
countered where the fuel and additive containing air flow joined
in sufficient quantity to block the sintered filter. Chemical
analysis indicated these deposits to be ammonium nitrate. Removal
of the sintered filter screen and the $300°F$ inlet air temperature
used for NO_2 testing alleviated the problem in our case, but this
condition could be detrimental in extended engine operations.

While only comparative, the relative values reported herein on
additive effects are believed to provide a valid screening of
gaseous additives based upon previous correlations between this
test and engine performance. However, extensive modifications
to the bench burner approach appear to be necessary before meaningful
data can be obtained on materials such as ammonium nitrate which
cannot be readily vaporized.

TECHNICAL DATA REPORT

DIV **ALLISON** GMC.	EDO NO REF	PAGE 10 OF /6	PAGES	REPORT NO
TITLE		PREPARED		DATE
		CHECKED		
		APPROVED		

REFERENCES

1. "Oxidation of Ammonia in Flames", C. P. Fenimore and G. W. Jones;   Jr. Physical Chemistry, V 65, pp 298-303 (1961)

2. "Spontaneous Ignition Temperatures of Fuel-Nitric Oxide Mixtures", H. G. Wolfhard and A. Strasser; Jr. Chemical Physics, V 28, p. 172 (1958)

3. "Ammonia Application to Reciprocating Engines", Fourth Progress Report for June 1965, T. J. Pearsall; Continental Aviation and Engineering Corp.

4. "A New Burner Method for the Determination of Low Burning Velocities and Limits of Inflammability", J. Powling; Fuel, Vol. XXVIII-2, pp 25-28

5. "Breakup of Small Liquid Volumes by Electrical Charging", P. E. Graf Preprint Paper for Presentation at ASHRAE Semi-annual Meeting, February 1963.

6. "Electrostatic Atomization of No. 2 Heating Oil", F. E. Luther; Preprint Paper for Presentation at ASHRAE Semi-annual Meeting (February 1963)

7. "Experimental Determination of the Flame Stability of Ammonia-air and the Effect of Fuel Additives and Partial Ammonia Dissociation", F. J. Verkamp; Allison RN 64-62 (Dec. 1964)

Screen

Pyrex Glass

Quartz

1/16" Stainless
Steel Honeycomb

1/8" Stainless
Steel Honeycomb

Glass Beads

Sintered Stainless
Steel

Pressure Tap

Temperature Tap

Stainless Steel

Glass Beads

Fuel-Air Inlet
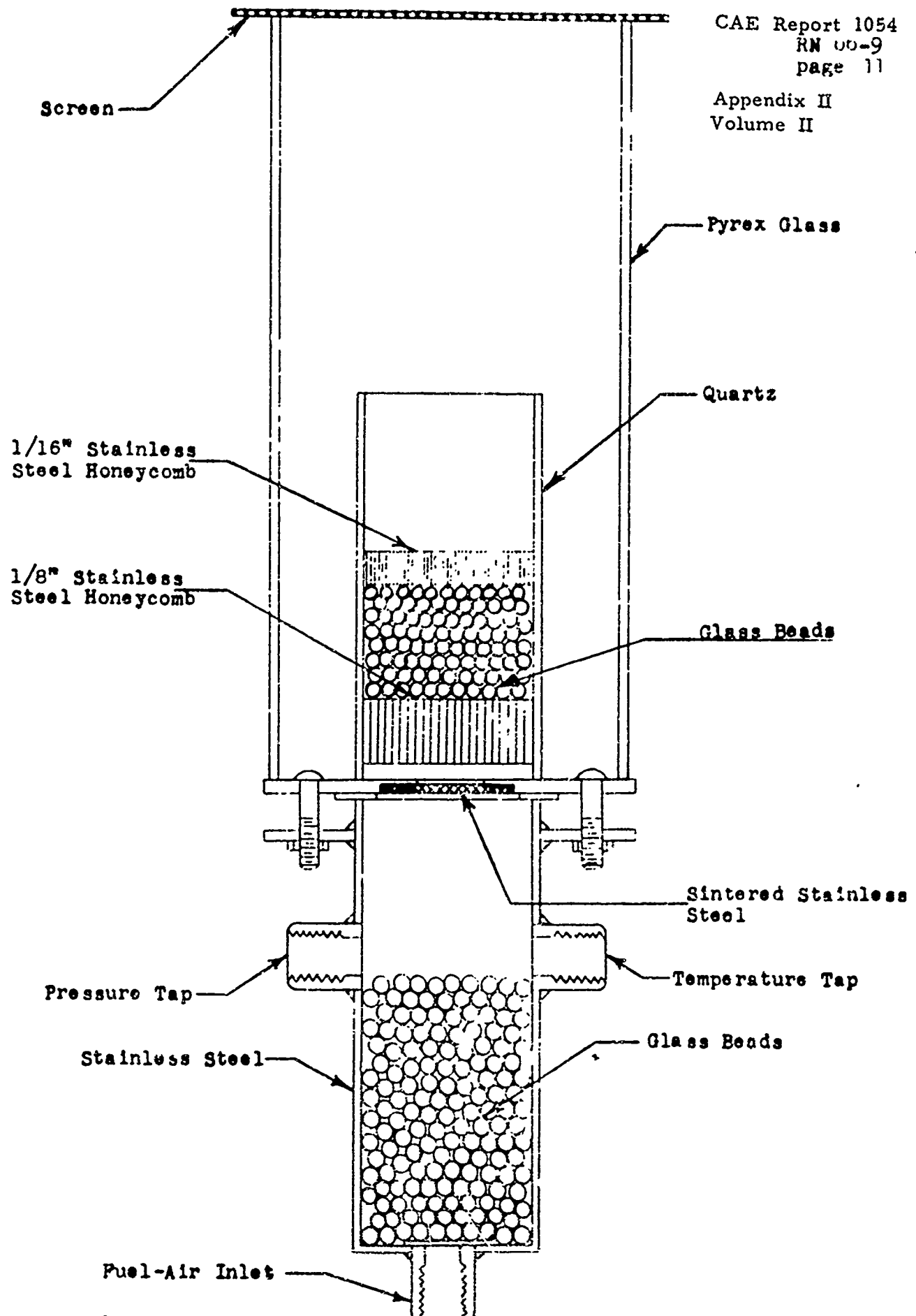
Figure 1 Laboratory Burner for Investigating the Effect of Additives
on the Flame Stability Properties of Ammonia

-11-
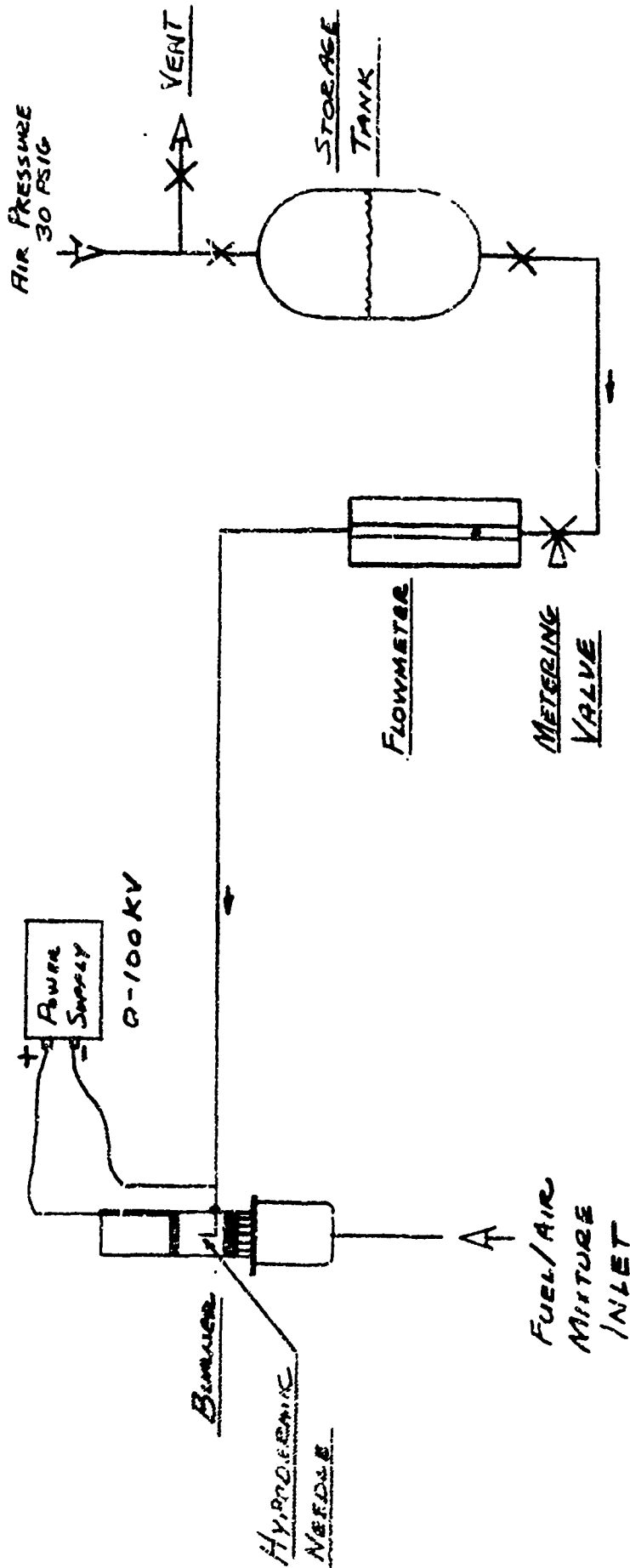
ADDITIVE SUPPLY
SYSTEM SCHEMATIC

FIGURE 2

Quartz Tube

Upper Honeycomb Grid

High Voltage Leads

Hypodermic Needle

Additive Tube

Glass Beads

Lower Honeycomb

Tygon Tubing

Mixing Chamber

Figure 3

Flame Stability Limits
Ammonia & Additives
Equivalence Ratio
vs
Total Velocity
Figure 5

PERCENT IMPROVEMENT FACTOR
vs
EQUIVALENCE RATIO

Figure 6

$$I_{PF} = \frac{B.O.\ Vel.\ with\ Additive - Baseline\ B.O.\ Vel.}{Baseline\ B.O.\ Vel.}$$
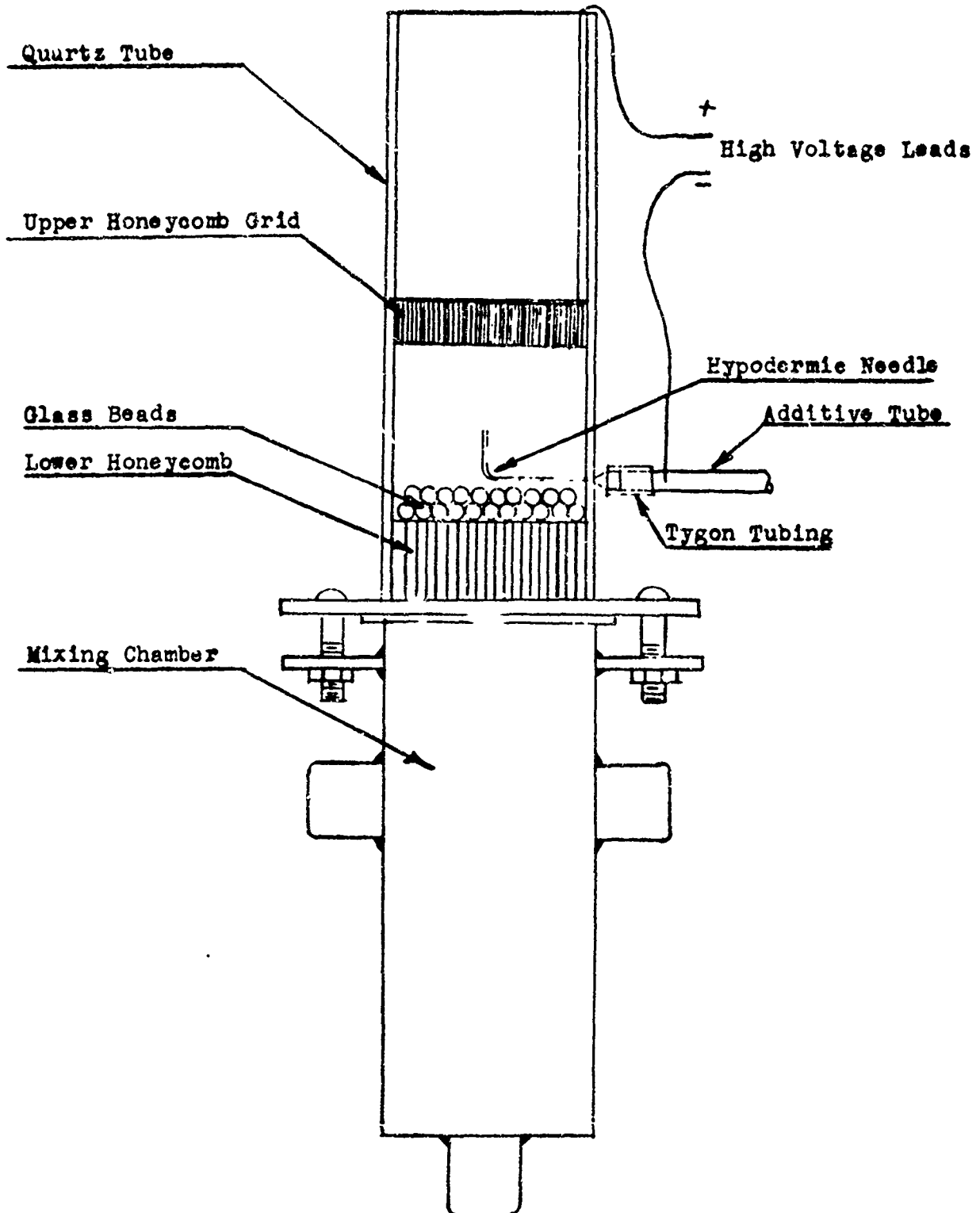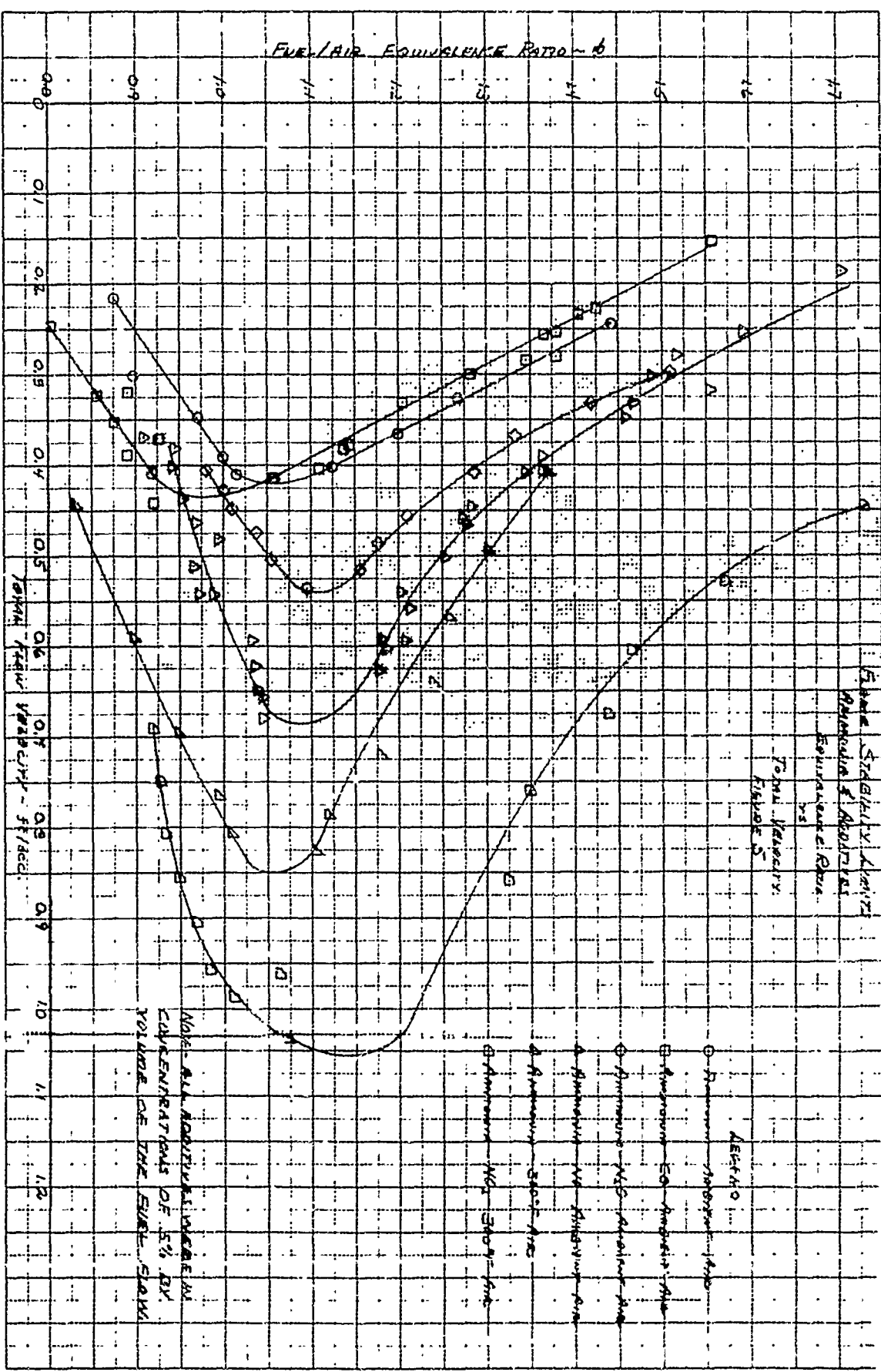
APPENDIX III

Ammonia Fueled Spark Ignition Engine
Dissociator Development

APPENDIX III

AMMONIA FUELED SPARK IGNITION ENGINE
DISSOCIATOR DEVELOPMENT

Allison Division of General Motors Corp.

AMMONIA DISSOCIATION BACKGROUND DATA

Catalytic Material Investigation

Early in 1964, Allison made a survey of the use of catalysts in the ammonia industry. As a result of this survey, the following four catalysts were selected for investigation:

Triply promoted iron (ICI 35-4)

Nickel on alumina

Iron on silica (G-47)

Platinum on alumina

Preliminary tests were run to evaluate the effectiveness of the various catalysts vs. no catalyst at ammonia flow rates of 1.3 lb./hr. and at various temperatures. Results are shown in Figure 1. As indicated, the promoted iron was the only catalytic material showing any measurable increase in dissociation rates. No further tests were made with the other three catalytic materials.

In August 1964, a subscale ammonia dissociator was designed and fabricated to determine the performance of a dissociator under simulated engine operating conditions. Dissociation of the ammonia fuel was achieved by passing superheated ammonia vapor through a bed of triply--promoted iron oxide catalyst which was heated by engine exhaust gases. The effect of exhaust temperature on the dissociation level at various

Operating Conditions
Ammonia flow rate-- 1.3 lb/hr
Catalyst weight-- 0.05-0.06 lb
Catalyst bed temperature
$\approx$100°F below preheater
temperature

△ Triply promoted iron
◇ Nickel on alumina
▽ Iron on silica
□ Platinum on alumina
-O-No catalyst

Percent Ammonia Dissociated

Preheater Temperature (°F)
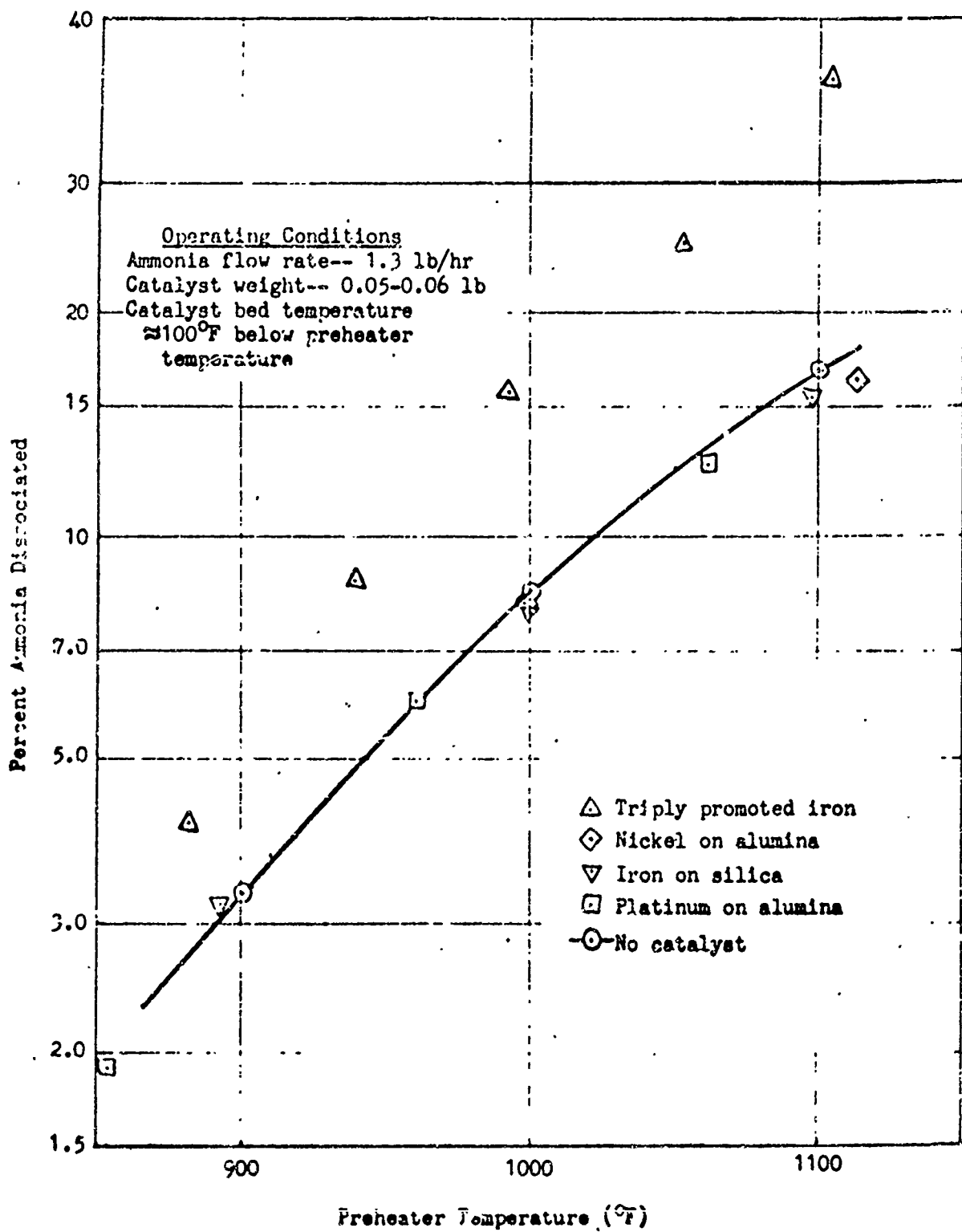
Fig. 1. Performance Comparison of Ammonia Dissociation Catalysts.

ammonia flow rates was determined by operating the dissociator at exhaust gas temperatures above and below the equivalent engine temperatures. Results of this investigation are shown in Figure 2.

L-141 Engine Dissociator System

In the early stages of the present contract, and before actual engine data was available, Allison was given the assignment to design and develop a dissociator for the L-141 engine. The following design criteria were established:

Fuel enrichment - 2.5 percent Hydrogen by weight
$$\%H_2 = \frac{H_2 \times 100}{H_2 + N_2 + NH_3}$$

Fuel temperature - The partially dissociated ammonia fuel to be cooled to a temperature compatible with requirements of the carburetor.

Physical size - To permit installation in the M-151, 1/4 Ton vehicle

Design parameters - Based on 2400 r.p.m. gasoline engine data (See Table I).

Dissociation Products Cooler

The dissociation products cooler - ammonia vaporizer consisted of two helical coils enclosed in a 3-1/2 inch stainless steel shell. The high temperature partially dissociated ammonia from the dissociator was cooled as it passed through the inside of the coiled tube and the heat rejected was used to vaporize the incoming liquid ammonia which passed over the outside of the tubing. Calculations based on tests of the sub-scale dissociator indicated that the dissociation products would be cooled to approximately 80° F. The heat rejected by cooling the dissociation
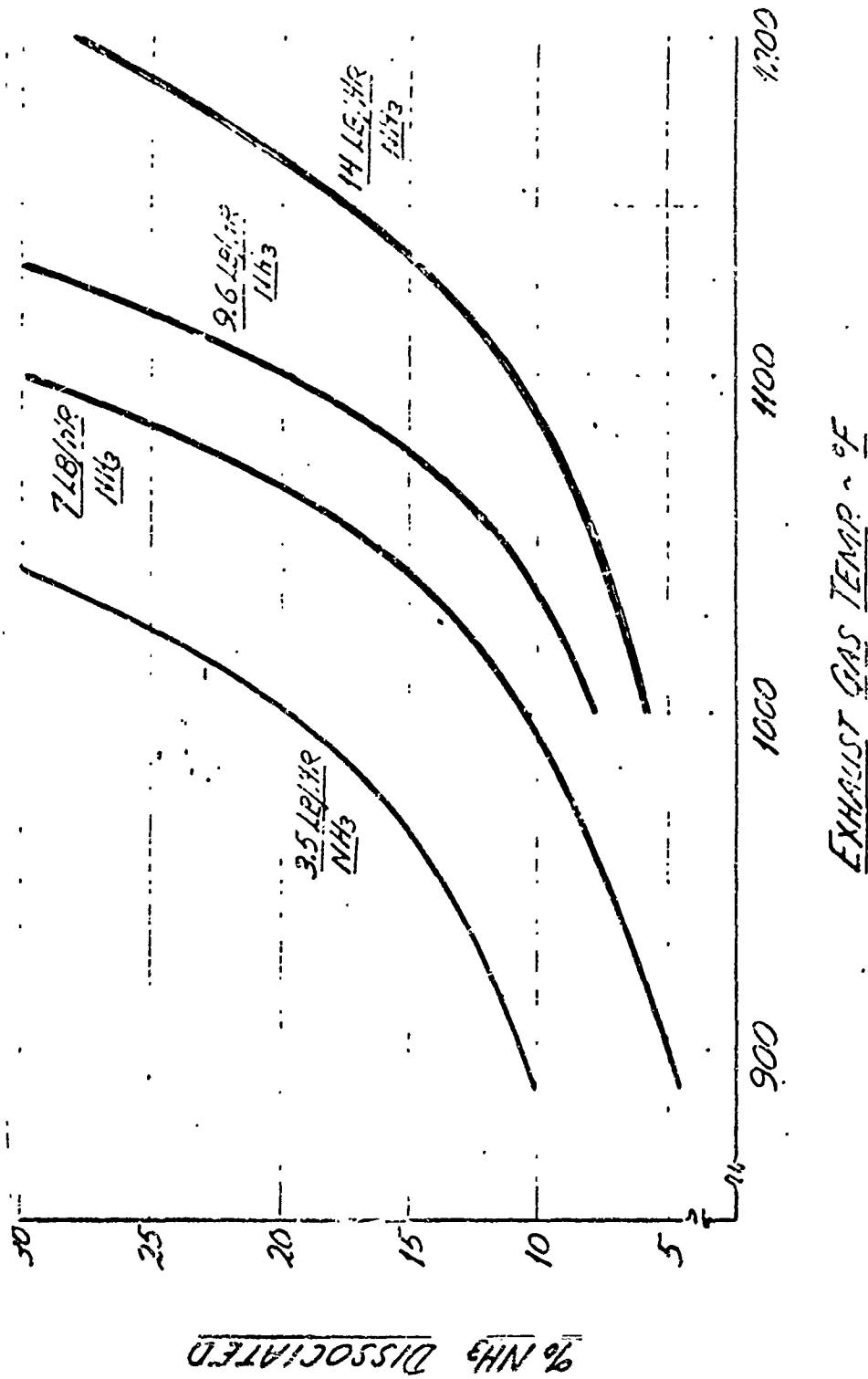
Fig. 2. Subscale Dissociator, Dissociation Versus Exhaust Temperature
0.724 Pound ICI35-4 Catalyst.

T A B L E   I

Dissociator Design Parameters at Selected L-141 Engine Condition

Engine speed	2400 r.p.m.
Manifold pressure	18" hg. a.b.s.
Ammonia flow rate	40.35 lb./hr.
Air flow rate	245 lb./hr.
Exhaust gas temperature	1275^c F.
Ammonia inlet temperature	32° F.
Ammonia pressure	58.5 p.s.i.a.
Dissociator products temperature at cooler inlet	820° F.

products from 820°F to 80°F. was sufficient to vaporize about 63% of
the incoming liquid ammonia. The overall size of the disseciation
products cooler-ammonia vaporizer was 3½-inch diameter by 16 inches
in length. Design details are shown in Figure 3, Allison drawing
FX-73993, Continental drawing 595713.

Preheater-Dissociator

The dissociator unit for the L-141 engine was designed to be attached
to the engine exhaust manifold and to utilize exhaust waste heat to
preheat and dissociate the ammonia. The preheater section consisted of
two helical coils of ½-inch stainless steel tubing wound in opposite
directions and joined by a reverse bend to minimize thermal distortion.
A catalyst bed, fabricated of 2 3/8-inch stainless steel tube, was
positioned inside the preheater coil. Eight longitudinal fins on the
catalyst and supporting the preheater coil. Five pounds of triply-pro-
moted iron oxide catalyst (ICI 35-4) were packed in the catalyst tube.
The catalyst was retained by cones of 20-mesh stainless steel wire
cloth. The preheater coil and catalyst tube were encased in a 4½-inch
steel shell, 19 inches long. Diametrically opposed exhaust ports were
located at opposite ends of the shell. The exhaust gas flowed axially
through the shell, across the preheater coils and parallel to the
catalyst tube.

The dissociator was designed to complete vaporization of the ammonia, to
heat the ammonia vapor to dissociation temperature, and to dissociate
14.2 percent of the ammonia (providing 2.5 percent hydrogen by weight).
During the single pass through the preheater-dissociator, the exhaust
gas was cooled from 1275° to 975°F. Design details of the preheater-
dissociator are shown in Figure 4, Allison drawing SK-15363, Continental
drawing 595711.
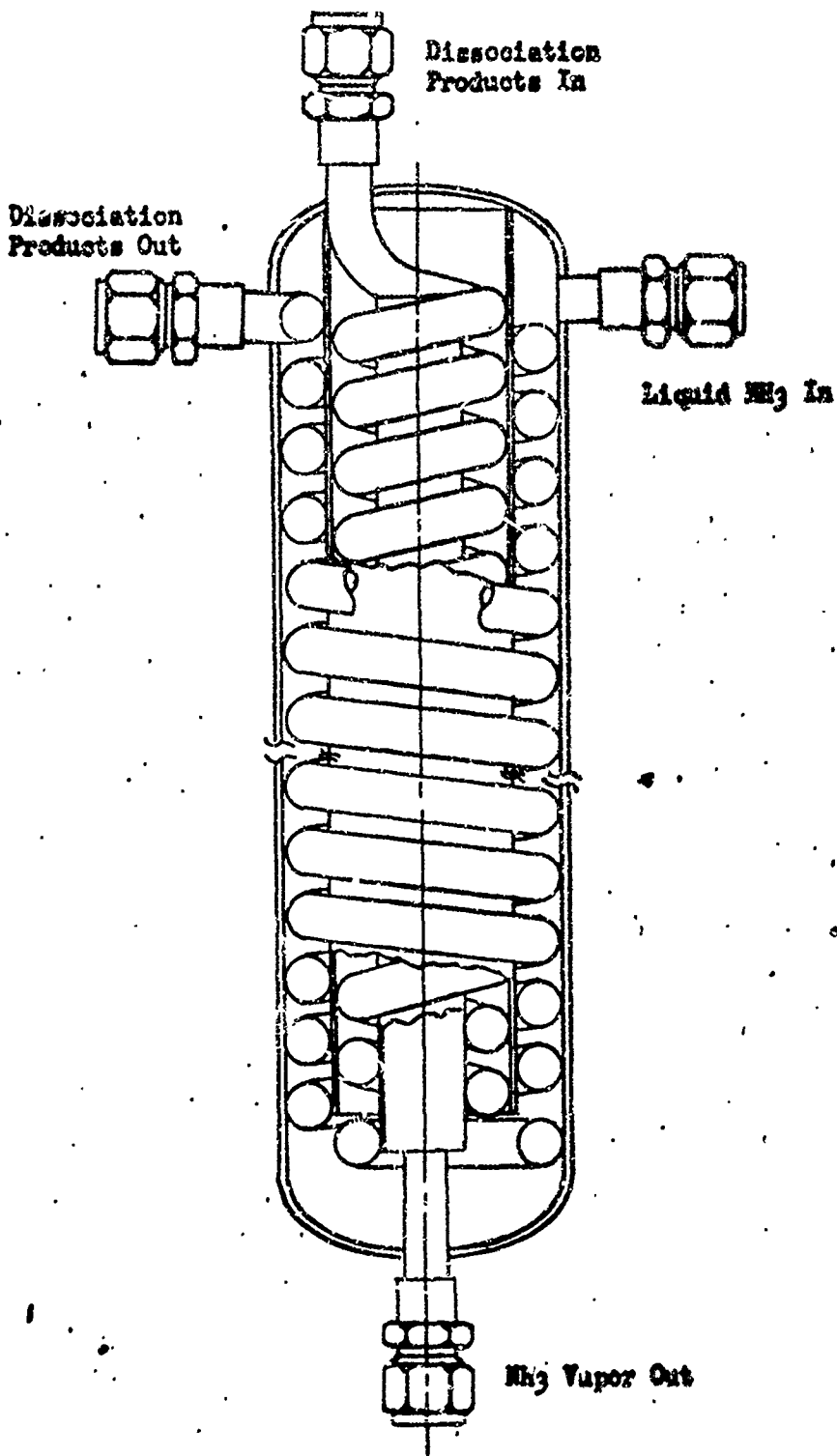
Fig. 3. EX-73993 Dissociation Products Cooler.
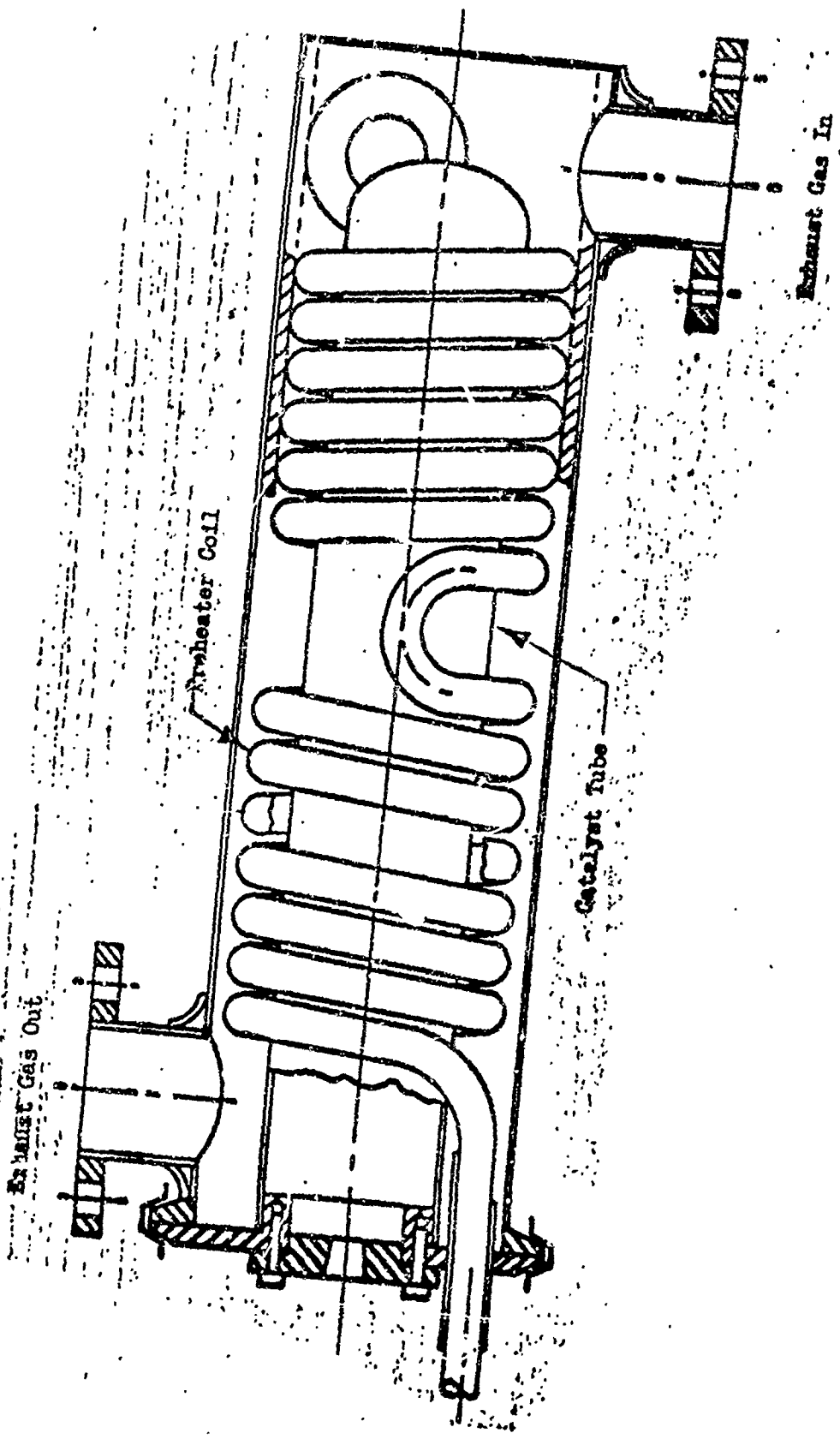
Fig. 4. SK-15363 Preheater-Dissociator

Two dissociator systems were fabricated; one for bench testing at
Allison, and one for engine testing at Continental.

Preliminary Testing of L-141 Dissociator

The L-141 dissociator system consisting of the EX-73993 cooler-
vaporizer and SK-15363 preheater-dissociator, was installed in the
Allison burner test rig. Liquid ammonia was available in the test cell
at room temperature and at 225 p.s.i.g. pressure. Hot exhaust gas was
furnished by a JP-4 (hydrocarbon) fueled combustor. Instrumentation was
provided to measure pressures, temperatures and flows at all critical
locations.

Performance data obtained at temperature and flow conditions
corresponding to engine operation at speeds from 800 to 3600 r.p.m. and
at manifold pressures from 12 to 30 inches of mercury are shown in
Table II. The fuel enrichment provided by the dissociator at various
simulated engine conditions is shown in Figure 5.

The excessively high cooler outlet temperatures shown in Table II
were due to liquid ammonia being thrown to the outside of the coiled
passages and a large amount of the heat transfer surface was not being
effectively used. This situation was corrected by replumbing the
cooler so that the liquid ammonia was inside the tubes and the hot
products were on the shell side.

Table 2

L-141 Dissociator System Test Data
Simulated Engine Conditions

Equiv. RPM	Manifold Pressure "hg	Exhaust Temp. °F	NH3 Flow Lb/hr	Air Flow Lb/hr	Catalyst Outlet Temp.-°F	Cooler Outlet Temp.-°F	% H2 By Wt.
800	12	725	9.05	54.8	433	83	.05
1800		1060	20.30	123.0	725	175	.95
2000		1126	22.60	137.0	728	262	1.10
2400		1215	27.00	164.0	765	325	1.30
800	18	875	13.50	81.8	560	150	.06
1400		1050	23.60	143.0	695	230	.94
2400		1275	40.35	245.0	815	415	2.10
800	24	1000	17.95	109.0	665	210	.46
1300		1140	29.20	177.0	750	335	1.25
2400		1360	53.60	326.0	870	450	2.40
700	30	1055	19.65	119.0	725	175	.90
1700		1280	47.65	289.0	835	430	1.70
2400		1350	67.40	408.0	880	510	2.00
3600		1450	98.40	600.0	920	580	2.10
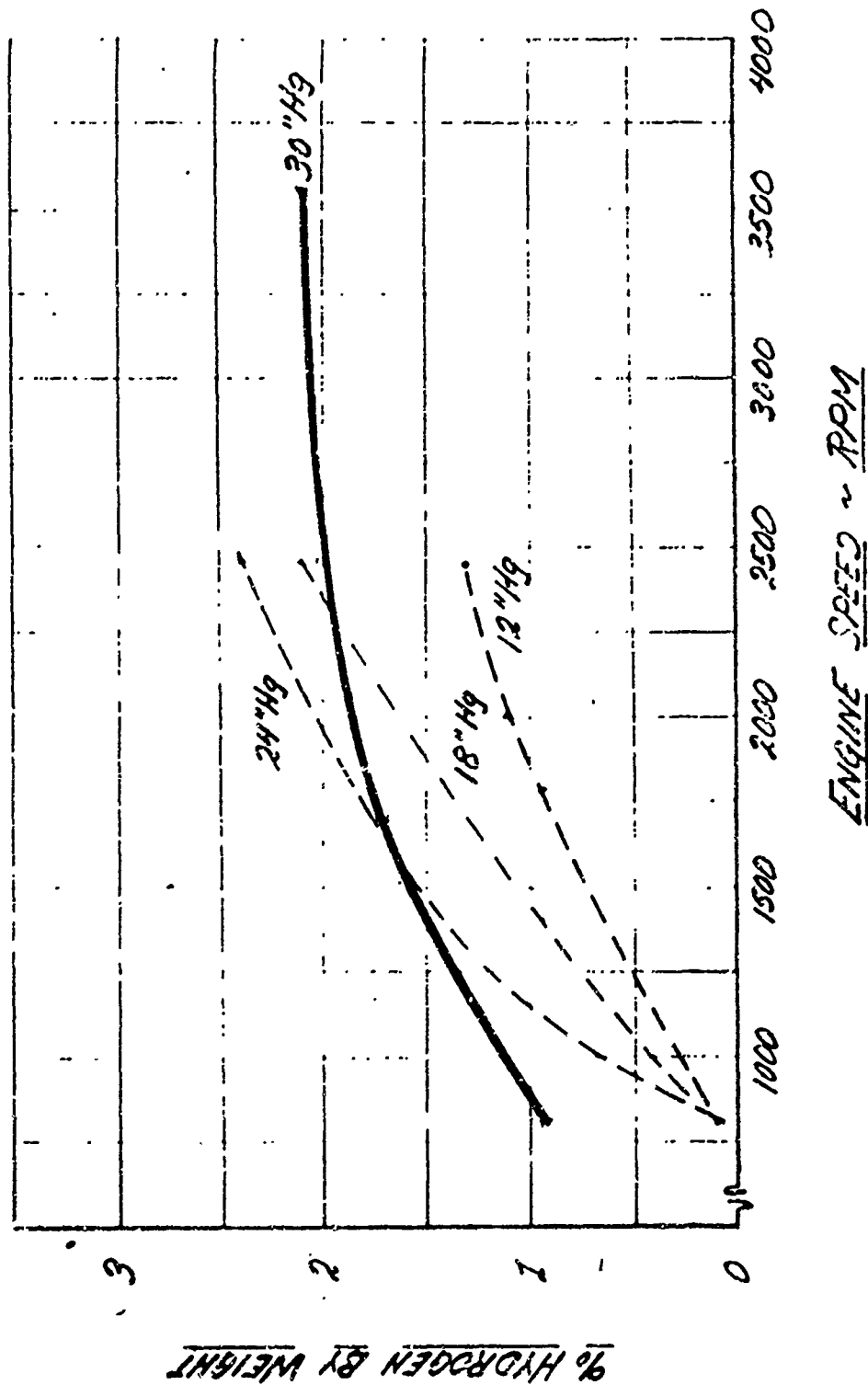
Fig. 5. L-141 Dissociator Performance At Simulated Engine Conditions

Preliminary engine testing of the dissociator system was terminated

at an early date because of ICI 35-4 catalyst disintegrated into a fine

powder that could not be retained in the catalyst bed.

Modified L-141 Dissociator System

The tendency of the granules of ICI 35-4 triply promoted iron catalyst

to disintegrate under temperature and vibration conditions encountered

in engine operation rendered it clearly unsuitable. Several attempts were

made to use this catalyst in another form, such as sintering into a

solid plug and plasma spraying on stainless steel mesh. These

approaches were all unsatisfactory.

A number of other catalysts were investigated as substitutes for

ICI 35-4. Among these were promoted iron (KM1R), stainless stell,

Incomel and nickel. Porous nickel in the form of "Foametel" was

finally selected due to the large active surface area and high mechanical

strength. The relatively low activity of the nickel catalyst necessitated

a complete redesign of the preheater-dissociator unit. A new set of

design criterian, based on actual engine test results, were established

as follows:

Fuel enrichment   1.25 percent hydrogen by weight
                                at 1000 r.p.m. full throttle to
                                3.15 percent hydrogen by weight
                                at 4000 r.p.m. full throttle.

Fuel temperature   The partially dissociated ammonia
                                fuel to be delivered to the carburetor
                                at a temperature of 50 - 100° F.

Design parameters

Based on 2400 r.p.m., full throttle
operation of the L-141 engine on
hydrogen enriched ammonia fuel
(see Table III).

T A B L E   I I I

Revised Design Parameters for L-141 Engine Dissociator

Engine Speed	2400 r.p.m.
Manifold pressure	29" hg a.b.s.
Ammonia flow rate	37 lb./hr.
Air flow rate	220 lb./hr.
Exhaust gas temperature	1235° F.
Ammonia inlet temperature	32° F.
Ammonia pressure	58.5 p.s.i.a.
Dissociation products temperature at catalyst outlet	1025° F.

The preheater-dissociator was redesigned with an automatic bypass
arrangement so that only part of the ammonia vapor would flow over the
catalyst bed. In order to obtain a low pressure drop across the catalyst,
the Foametel nickel was machined into 16 discs, each 29/32 inch thick and
3.275 inches in diameter. The discs were separated in the catalyst tube
by 3/32 inch spacers, and internal manifolding was provided so that ammonia
flowed through the 16 discs in parallel. The catalyst bed was installed
in a stainless steel tube 16-1/2 inches long, having 32 longitudinal fins
to increase heat transfer. Two double helicol coils of 5/16 inch
stainless steel tubing were wound concentric with the catalyst tube,
providing four parallel flow paths for the ammonia vapor. A thin
cylindrical shield was placed around the catalyst tube to direct the

exhaust gas flow. The preheater coils and catalyst tube were encased in

a 6 inch stainless steel shell. A split 3-1/2 inch tube, extending

the length of the preheater-dissociator shell, contained a 70 inch length

of 1/2 inch tubing which served as an auxiliary evaporator.

Exhaust gas from the engine enters through the center of one end

of the preheater-dissociator shell, flows along the catalyst tube, back

across the preheater coils, out the side of the shell into the auxiliary

vaporizer section, axially through the auxiliary vaporizer and exits into

the vehicle exhaust system. Design details of the modified preheater-

dissociator are shown in Figure 6, Allison drawing EX-79016, CAE

drawing 595712.

Electrically Heated Auxiliary Dissociator

When the L-141 engine is operating under part throttle conditions with

ammonia vapor alone as the fuel, the exhaust temperatures are below

1000° F. Under these conditions, the nickel catalyst is relatively

ineffective. It was, therefore, decided to design and fabricate an

electrically heated auxiliary dissociator for use during starting and

low load operation.

The size and geometry of the auxiliary dissociator was determined

primarily by available heater and tubing sizes. The auxiliary dissociator

consists of a concentric tube heat exchanger with a Foametal nickel

cylindrical catalyst and an electric cartridge heating element. A 5/8

inch diameter by 6 inch long, 28 volt, 450 watt Firerod cartridge,

manufactured by Watlow Electric Manufacturing Company, was selected for use.
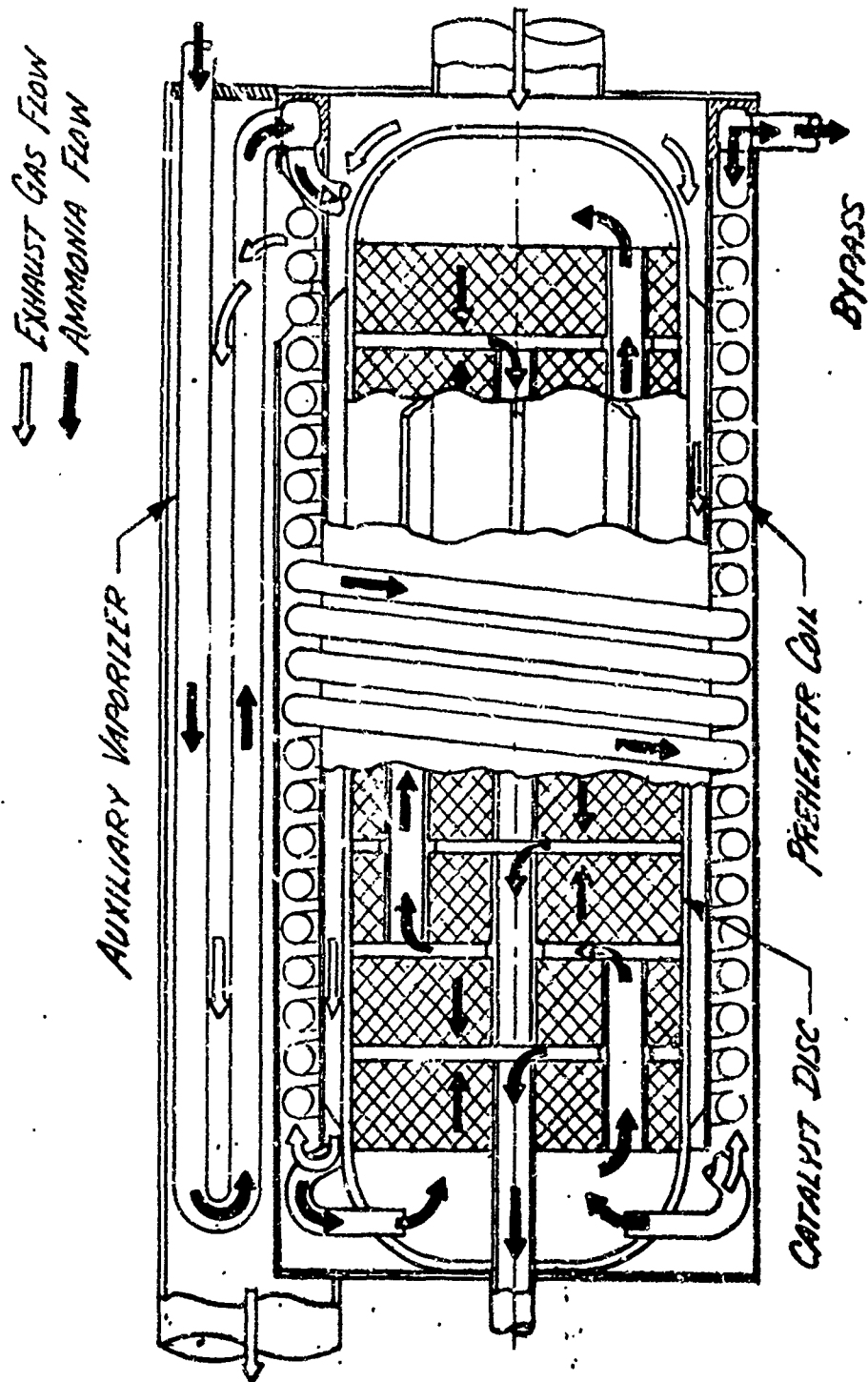
Fig. 6. EX79016 Preheater-Dissociator.

The porous nickel catalyst cylinder which surrounded the heating element was 1.5 inches in diameter by 5/16 inch wall by 7 inches long and weighed approximately 1 pound. This was encased in a 2-1/4 inch tube by 8 inches long.

Preheated ammonia vapor from the dissociator outlet enters the outer annulus of the auxiliary dissociator. Approximately 2/3 of the entering ammonia is bypassed directly to the auxiliary dissociator outlet through a hole drilled in the inner tube. The remaining ammonia flows axially through the c .er annulus, back along the heating element, then radially through the catalyst cylinder. From the auxiliary dissociator, the dissociation products are routed into the cooler side of the EX-73993 vaporizor cooler. A cross-sectional sketch of the auxiliary dissociator is shown in Figure 7.

Burner Rig Testing of the Redesigned L-141 Dissociator System

The redesigned L-141 dissociator system, consisting of the EX-73993 cooler-vaporizor, the EX-79016 redesigned preheater-dissociator and the electrically heated auxiliary dissociator, together with the necessary plumbing and instrumentation, was installed in the burner test rig. A schematic of the test setup is shown in Figure 8. Performance data obtained at temperature and flow conditions corresponding to engine operation at speeds from 200 to 4000 r.p.m. and at manifold pressures of 15 and 29 inches of mercury are shown in Table IV. The fuel enrichment provided by the dissociator at various simulated engine conditions with the auxiliary dissociator off is compared to the desired and predicted enrichment in Figure 9.
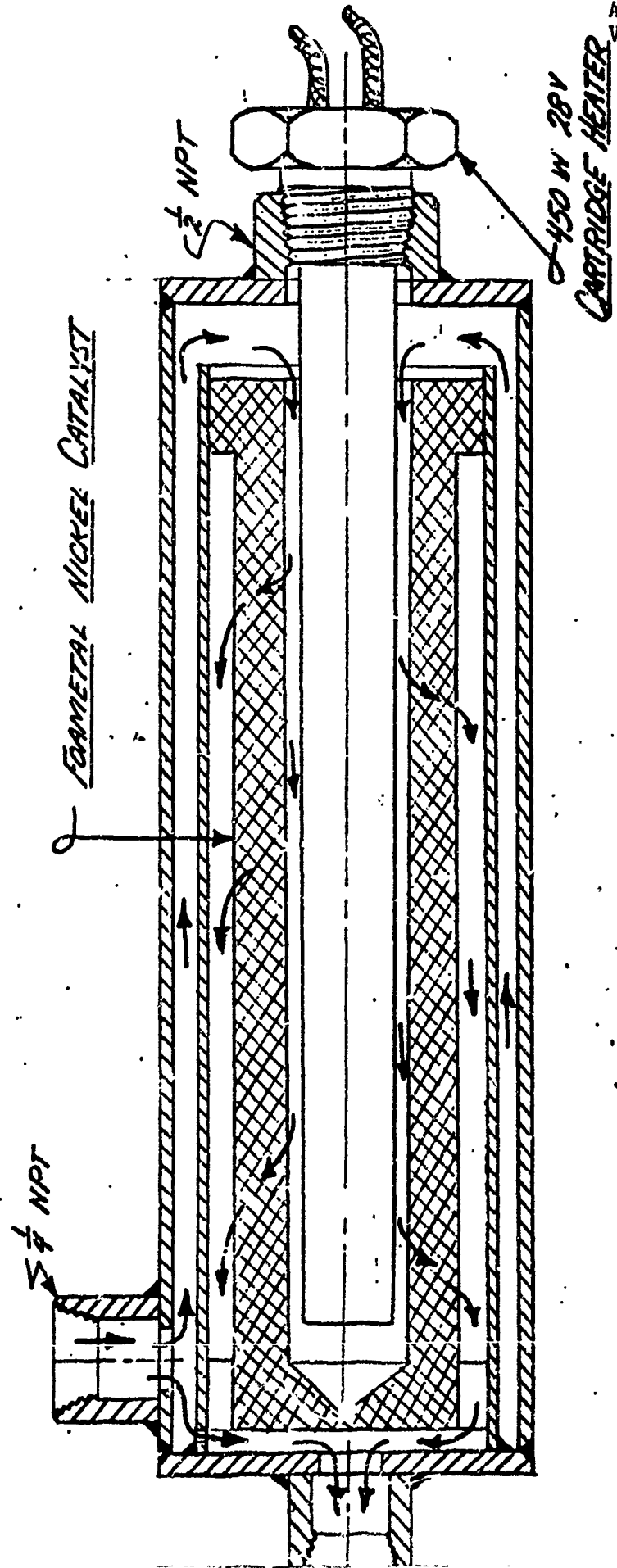
Fig. 7. Auxiliary Dissociator.
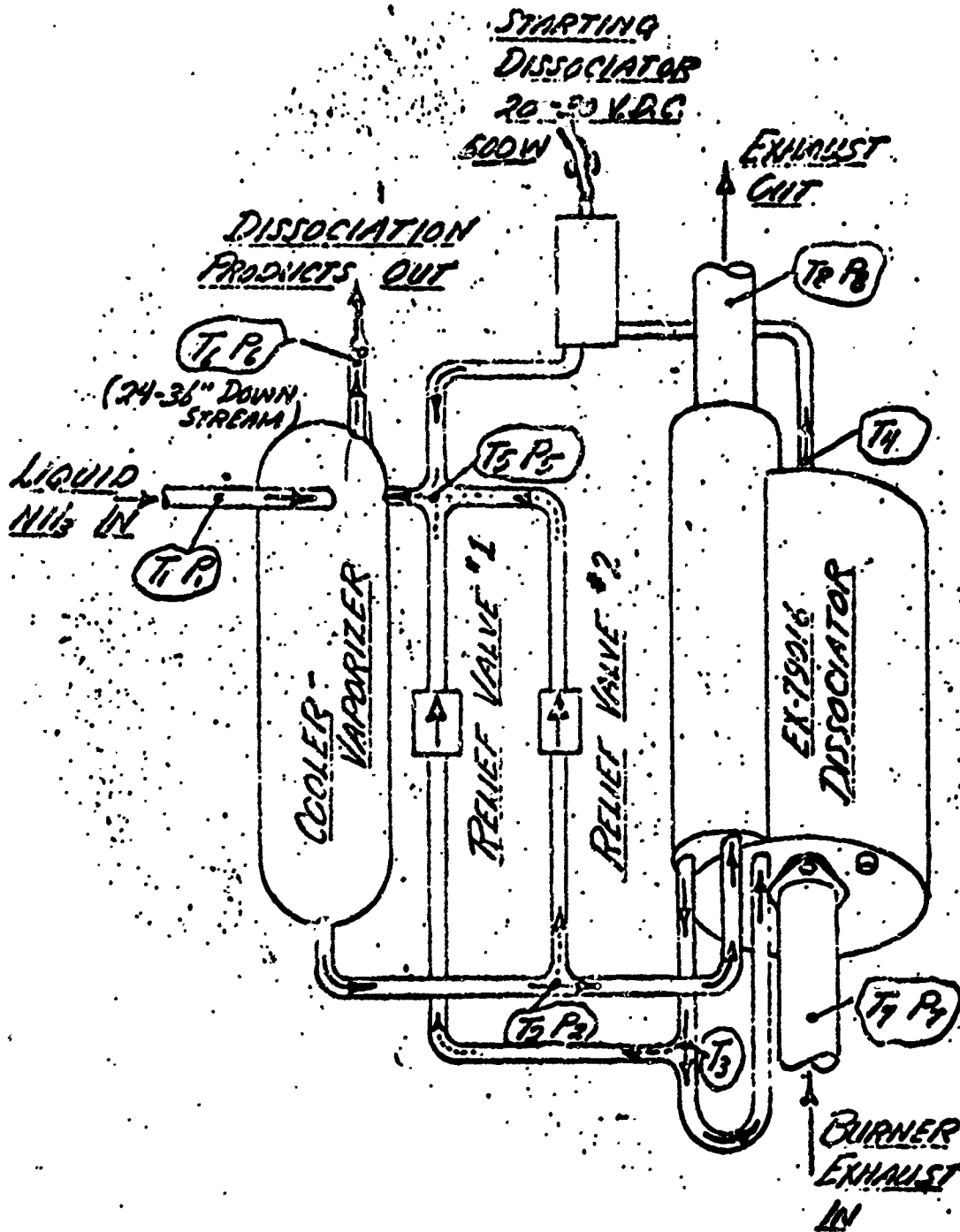
Fig. 8. Burner Test Rig Setup for Redesigned L-141 Dissociator.

Table 4

Redesigned L-141 Dissociator System Burner Test Rig Data

Simulated Engine Conditions

Equiv. RPM	Manifold Pressure "hg	Exhaust Temperature °F	NH3 Flow lb/hr	Air Flow lb/hr	Power to Auxiliary Dissociator watts	Cooler Outlet Temperature °F	%H2 By Weight
200	29	-	4.2	-	750	50	1.15
1000	29	940	14.9	105	750	75	0.9
1200	29	1010	17.75	128	750	75	0.8
1200	29	1020	16.7	128	0	55	0.31
1600	15	960	13.0	90	750	75	1.02
1600	29	1125	24.75	169	0	50	1.06
2000	15	1060	15.8	112	750	90	1.15
2000	29	1170	30.2	222	0	50	1.33
2400	29	1240	37.0	257	0	60	1.76
2800	29	1285	43.2	300	0	60	2.12
3200	29	1340	48.7	344	0	65	2.15
3600	29	1365	55.4	385	0	65	2.73
4000	29	1375	61.0	428	0	65	2.74

Predicted Performance

CAE Desired Limits

⊙ Observed Data Points

Percent hydrogen by weight

Engine speed - RPM
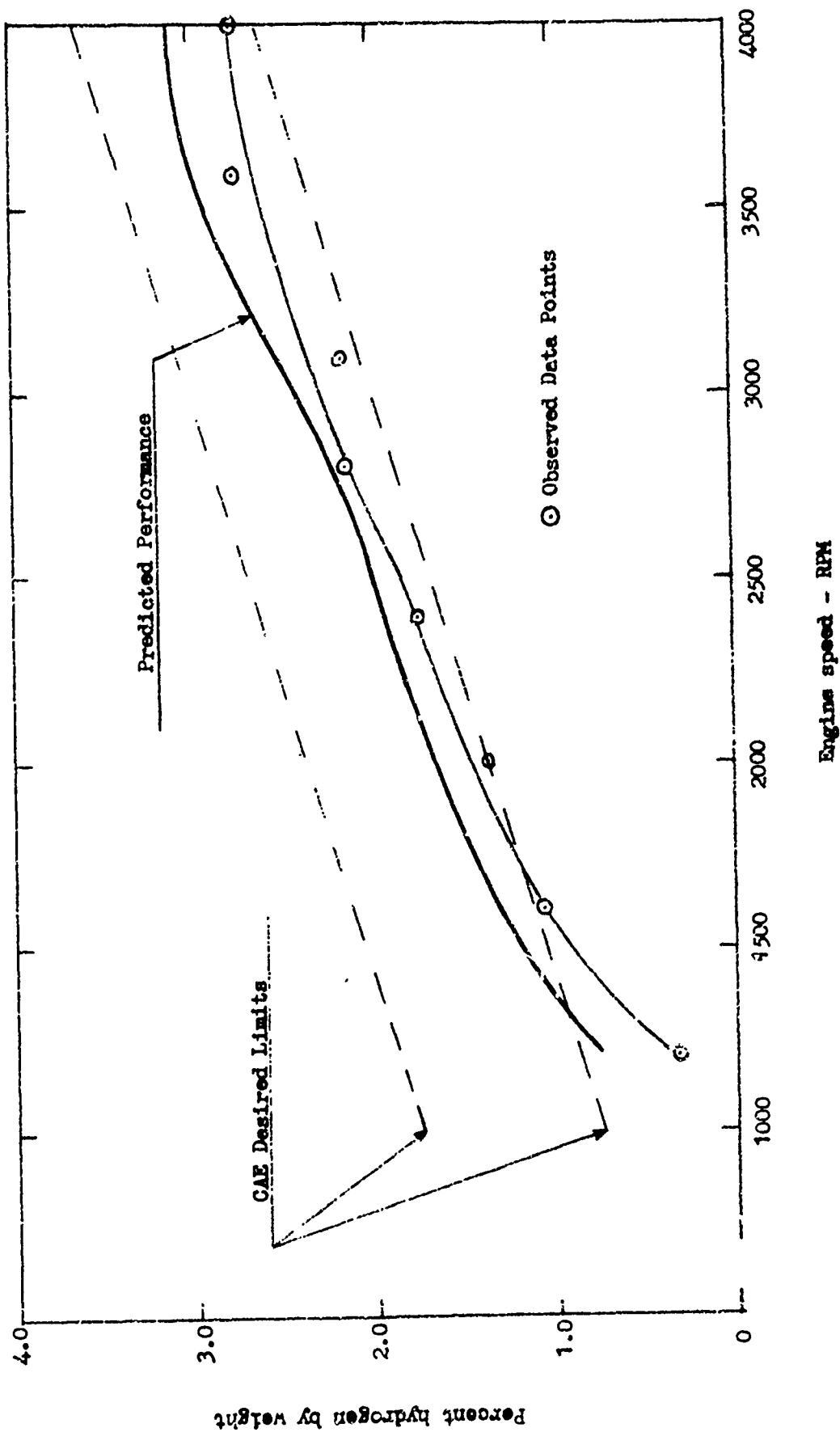
Fig. 9. Redesigned L-141 Burner Test Rig Performance Data Simulated Full Throtle Engine Conditions With Auxiliary Dissociator "OFF".

Engine testing of the redesigned L-141 dissociator system is discussed in the main body of the report.

Design calculations for the original L-141 engine dissociator system, the redesigned system using nickel catalyst, and the electrically heated auxiliary dissociator are included as Appendices A, B and C.

Appendix III-A

Design Calculations for L-141 Engine Dissociator System

Calculated air and fuel flows for L-141 engine

Engine displacement -- 141 in^3

Swept volume per revolution = $\dfrac{141}{2 \times 1728}$ = .0408 ft^3/rev

Density of air: $\rho \approx \dfrac{1.325\,P}{T}$

$$(\text{assume } T = 110^\circ F = 570^\circ R)$$

$$\rho = \frac{1.325}{570}\, P = .00232\, P$$

Density of air at various manifold pressures:

$$12" \,hg \qquad \rho = .00232 \times 12 \qquad = .0278 \text{ lb/ft}^3$$

$$18" \,hg \qquad .00232 \times 18 \qquad = .0417 \text{ "}$$

$$24" \,hg \qquad .00232 \times 24 \qquad = .0557 \text{ "}$$

$$30" \,hg \qquad .00232 \times 30 \qquad = .0696 \text{ "}$$

Air weight flow per revolution at various manifold pressures. (Assume 100% volumetric efficiency):

$$12" \,hg \qquad W_g = .0408 \times .0278 \qquad = .00114 \text{ lb/rev}$$

$$18" \,hg \qquad .0408 \times .0417 \qquad = .00170 \text{ lb/rev}$$

$$24" \,hg \qquad .0408 \times .0557 \qquad = .00227 \text{ lb/rev}$$

$$30" \,hg \qquad .0408 \times .0696 \qquad = .00284 \text{ lb/rev}$$

Assume air-fuel ratio 6.07:1.

Engine Conditions Selected for Design Point

RPM	2400
Manifold pressure	18" hg
Fuel flow	40.35 lbs/hr
Air flow	245 lbs/hr
Exhaust mass flow	285.35 lbs/hr
Exhaust gas temperature	1275°F
Ammonia temperature	32°F
Ammonia pressure	58.5 psia
Dissociation products temperature at cooler inlet	820°F
(for 2.5% hydrogen enrichment and 5 lbs ICI 35-4 catalyst)	

Figure A-1

Dissociation Products Out Temperature at 14.2% Dissociation

⊙ Burner rig test data

$$\frac{NH_3 \ flow}{Catalyst \ weight} - \frac{lbs/hr}{lb}$$
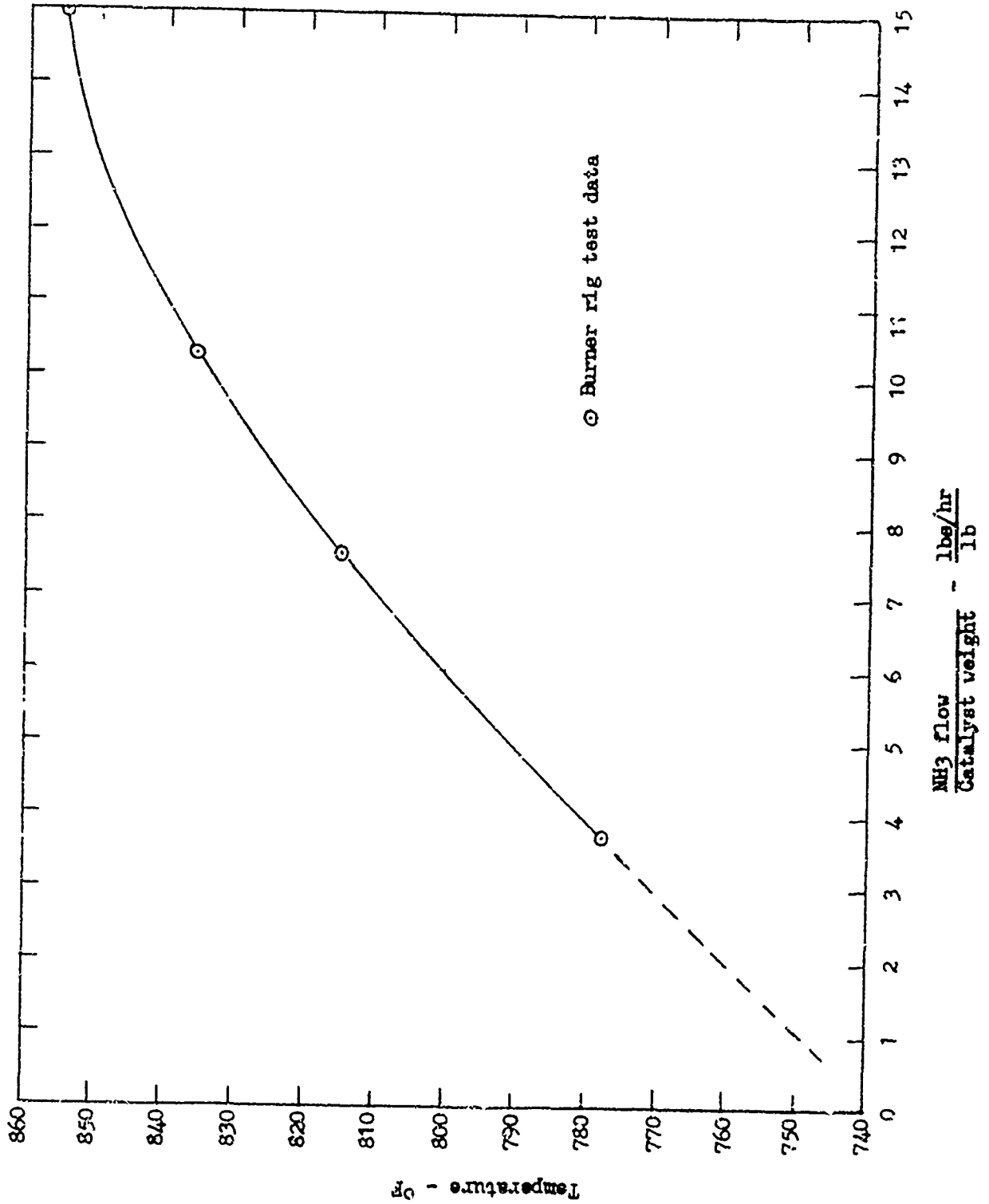
Temperature - °F

Figure A-2

Estimated Exhaust Temperatures for L-141 Engine
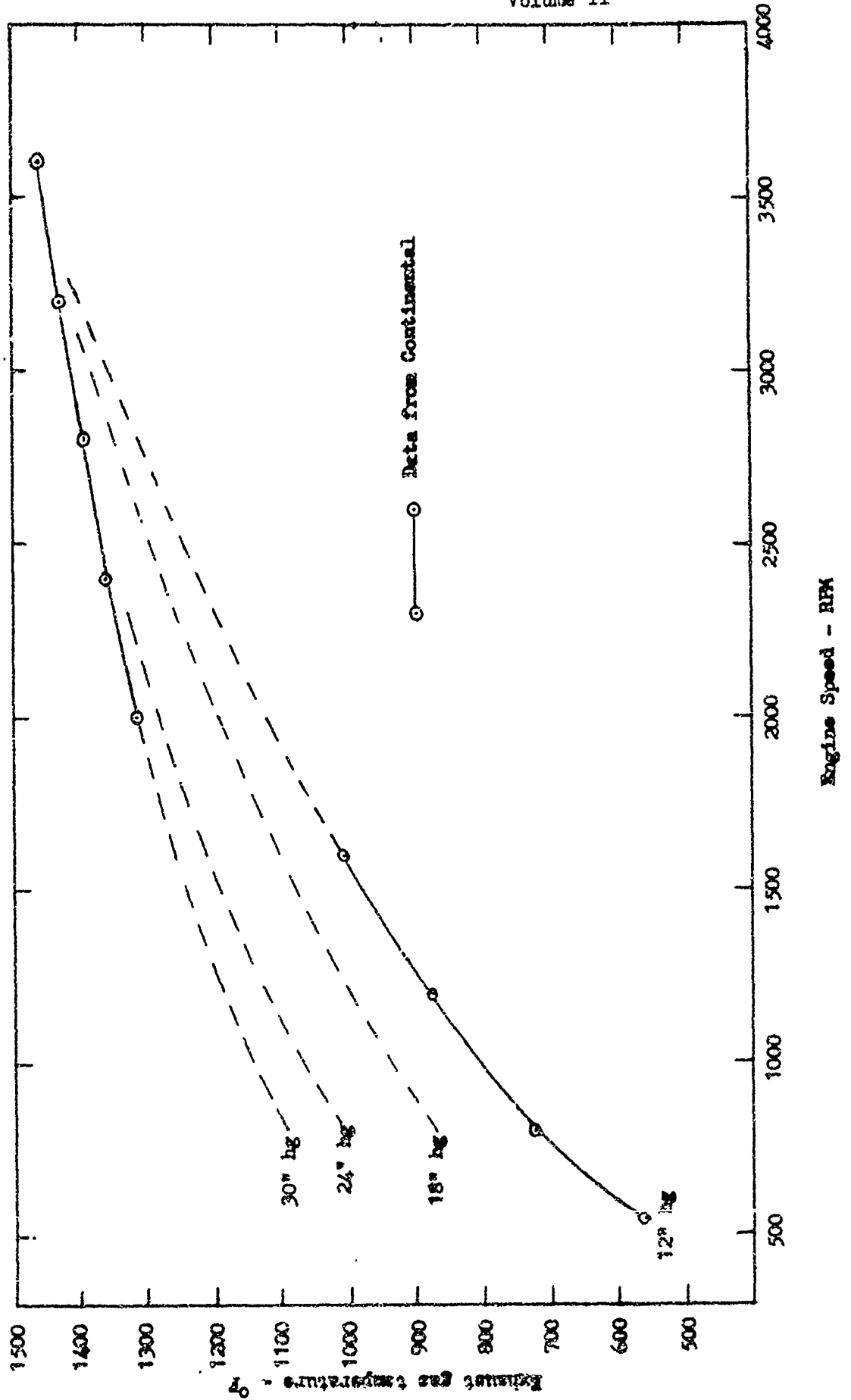
Dissociation Products Cooler

Configuration: Double helix heat exchanger
                Liquid NH_3 on outside of coil
                Dissociation products inside coil

Assume 18 turns $\frac{1}{2}$ OD x .032 wall tubing each helix length of tubing

$(2.76 \, \pi \times 18) + (1.6 \, \pi \times 18) = 248$ in

Surface area $.5 \, \pi \times 248 = 390 \, in^2 = 2.7 \, ft^2$

Cold side conditions: NH_3 flow rate   40.35 lbs/hr
                        Pressure   58.5 psia
                        Inlet temperature   32°F
                        Outlet temperature   32°F

Hot side conditions: Gas flow rate   40.35 lbs/hr
                        Pressure   58.5 psia
                        Inlet temperature   820°F

Cooler - hot side:

$$D_i = .500 - .064 = .436 \, in = .0363 \, ft$$

$$\text{Flow Area} = \pi \frac{(.0363)^2}{4} = .001035 \, ft^2$$

$$G_i = \frac{40.35 \, lb/hr}{.001035 \, ft^2} = 39,000 \, lb/hr \, ft^2$$

$$N_R = \frac{4 r_i \, G_i}{\mu} = \frac{.0363 \times 39000}{.035} = 40,500$$

$$N_R^{.8} = 4851$$

$$N_{PR} = \frac{C_p \mu}{k} = \frac{.61 \times .035}{.034} = .63$$

$$N_{PR}^{.33} = .857$$

$$h_i = .023 \frac{k}{D_i} N_R^{.8} N_{PR}^{.33}$$

$$= .023 \frac{.034}{.0363} \times 4851 \times .857 = 89 \, Btu/hr \, ft^2 \, °F$$

Vaporizer - cold side:

assume film boiling

$$\bar{h}_b = .62 \left[\frac{k_N^3 \rho_N (\rho_S - \rho_N) g \lambda'}{D_o \mu_N \Delta T_x} \right]^{\frac{1}{4}}$$ (Kreith pp 146)

where: $\lambda' = h_N \left(1 + \frac{.4 \Delta T_x C_{pN}}{h_N} \right)$

k_N = Thermal conductivity, vapor .013 Btu/hr ft °F
ρ_N = density, vapor .216 lb/ft³
ρ_S = density, liquid 39.9 lb/ft³
g = 4.17 × 10⁸ ft/hr²
μ_N = viscosity, vapor .023 lb/ft hr
C_{pN} = specific heat, vapor .52 Btu/lb °F
h_N = heat of vaporization 543 Btu/lb
ΔT_x = surface temp minus saturation temp
D_o = tube OD = .0417 ft

at hot end:

Temp inside tube	820°F
Temp outside tube	32°F
surface temp	426°F
ΔT_x	394°F

$\lambda' = 543 \left(1 + \frac{.4 \times 394 \times .52}{543} \right) = 625$

$$\bar{h}_b = .62 \left[\frac{2.2 \times 10^{-6} \times .216 (39.9 - .216) \, 4.17 \times 10^8 \, \lambda'}{.0417 \times .023 \times \Delta T_x} \right]^{\frac{1}{4}}$$

$$= .62 \left[8.2 \times 10^6 \frac{\lambda'}{\Delta T_x} \right]^{\frac{1}{4}}$$

$$= .62 \left[8.2 \times 10^6 \frac{625}{394} \right]^{\frac{1}{4}} = 37.2 \text{ Btu/hr ft}^2 \text{ °F}$$

$\frac{Q}{A} = 37.2 \times 788 = 29,300 \text{ Btu/hr ft}^2$

near cold end: temp inside tube   150°F (assumed)
                temp outside tube   32°F
                surface temp   91°F
                ΔT_x 59°F

$$i' = 543 \left(1 + \frac{.4 \times 59 \times .52}{543}\right) = 555$$

$$\bar{h_b} = .62 \left[8.2 \times 10^6 \; \frac{555}{59}\right]^{\frac{1}{4}} = 58 \; Btu/hr\,ft^2\,°F$$

$$\frac{Q}{A} = 58 \times 118 = 6850 \; Btu/hr\,ft^2$$

near mid point: temp inside tube   485°F
                 temp outside tube   32°F
                 Surface temp   258°F
                 ΔT_x 226°F

$$\lambda' = 543 \left(1 + \frac{.4 \times 226 \times .52}{543}\right) = 590$$

$$\bar{h_b} = .62 \left[8.2 \times 10^6 \; \frac{590}{226}\right]^{\frac{1}{4}} = 42 \; Btu/hr\,ft^2\,°F$$

$$\frac{Q}{A} = 42 \times 453 = 19000 \; Btu/hr\,ft^2$$

Approx average $\frac{Q}{A} = \dfrac{29\,300 + 6850 + 19000}{3} = 18,380 \; Btu/hr\,ft^2$

Average $\Delta T \approx \left(\dfrac{820 + 150}{2}\right) - 32 = 453°F$

Average $h_b \approx \dfrac{18380}{453} = 40.5 \; Btu/hr\,ft^2\,°F$

$$U = \frac{1}{\frac{A_o}{A_i}\frac{1}{h_i} + \frac{1}{h_b}} = \frac{1}{\frac{.500}{.436} \times \frac{1}{89} + \frac{1}{40.5}} = \frac{1}{.0128 + .0243} = \frac{1}{.0371}$$

$$= 27 \; Btu/hr\,ft^2\,°F$$

hot side capacity rate $\quad C_h = W_h C_p = 40.35 \times .61 = 25$

cold side capacity rate $\quad C_c \approx W_c h_{fg} = 40.35 \times 543 = 21900$

$$\frac{C_{min.}}{C_{max}} = \frac{25}{21900} \approx .001$$

Heat transfer units $\quad NTU = \frac{AU}{C_{min}} = \frac{2.7 \times 27}{25} = 2.9$

$\mathcal{E} \approx .94 \quad$ (Kays & London. Fig 2).

$$t_{h_2} = t_{h_1} - \frac{C_{min}}{C_h} \mathcal{E} (t_{h_1} - t_{c_1})$$

$$= 820 - \frac{25}{25} .94 (820 - 32)$$

$$= 80°F$$

Heat transfer required for complete vaporization

$Q_r = 40.35 \text{ lb/hr} \times 543 \text{ Btu/lb} = 21,910 \text{ Btu/hr}$

Calculated heat transfer

$Q = W_f C_p \Delta T = 40.35 \text{ lb/hr} \times .61 \text{ Btu/lb °F} \times 740°F = 18,214 \text{ Btu/hr}$

% vaporization performed in vaporizer

$$\frac{18214}{21910} = 83\%$$

Preheater-Dissociator

Preheater heat transfer surface:

$$A_p = .5\pi \times 20 \times 3.375\pi = 333 \, in^2 = 2.31 \, ft^2$$

Dissociator (catalyst tube) heat transfer surface

(tube) $A_t = 2.375\pi \times 14.75 + \frac{(2.375 + 1.57)\pi}{2} \times 2 = 122 \, in^3$

(fins) $A_f = 8 \times 2 \times \frac{3}{4} \times 12\frac{1}{4} = 49 \, in^2$

total $= 171 \, in^2 = 1.18 \, ft^2$

Volume of Catalyst

$$V = \pi \frac{(2.245)^2}{4} \times 14.75 = 58.5 \, in^3$$

(minus screen) $\frac{2}{3}\pi \frac{(2.245)^2}{4} \times 1.5 = 4.0 \, in^3$

total $= 54.5 \, in^3$

Catalyst weight $= 54.5 \, in^3 \times .092 \, lb/in^3 = 5 \, lb$

Cold side conditions : NH_3 flow rate   40.35 lb/hr
                        Pressure   58.5 psia
                        Inlet Temp   32°F
                        Outlet Temp   820°F

Heat transfer required
Vaporization 21,910 - 18214 =   3696 Btu/hr
Heating gas 40.35 × .59 (820-32) = 18700
Dissociation 40.35 × .142 × $\frac{2272.5}{17.032}$ =   7650

                                  ─────────────
                                    30,046 Btu/hr

Hot Side Conditions : Exhaust gas flow rate   285 lb/hr

           Pressure $\approx$ 14.7 psia

           Inlet temp   1275 °F

$$\text{Outlet temp} = 1275 - \frac{30046}{285 \times .35} = 1275 - 300 = 975\,°F$$

Preheater Section

Configuration : Helical coil with cross flow

        $\frac{1}{2}$ OD X .032 wall tubing

        coil diameter $2\frac{7}{8}$ ID , $3\frac{1}{8}$ OD

        pitch .625 "

NH_3 flow inside tubing

$$D_i = .500 - .064 = .436 \text{ in} = .0363 \text{ ft.}$$

$$\text{Flow Area} = \pi \frac{(.0363)^2}{4} = .001035 \text{ ft}^2$$

$$G_i = \frac{40.35 \text{ lb/hr}}{.001035 \text{ ft}^2} = 39000 \text{ lb/hr ft}^2$$

$$N_R = \frac{4 \dot{m}}{\mu} G = \frac{.0363 \times 39000}{.035} = 40500$$

$$N_R^{.8} = 4851$$

$$N_{PR} = \frac{C_p \mu}{k} = \frac{.59 \times .035}{.034} = .608$$

$$N_{PR}^{.33} = .847$$

$$\bar{h_i} = .023 \frac{k}{D_i} N_{PR}^{.33} N_R^{.8}$$

$$= .023 \frac{.034}{.0363} .847 \times 4851$$

$$= 88.5 \text{ Btu/hr ft}^2 \,°F$$

For exhaust gas flow over outside of tube:
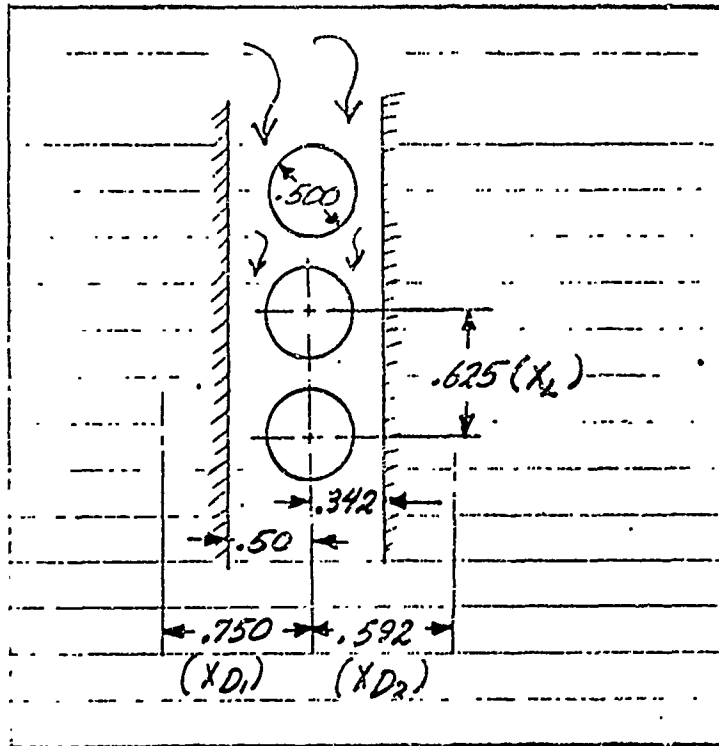
Flow area = cross section of outer shell (inside) - cross section of catalyst
tube (outside) - area of preheater tube (end view)

$$= \pi \frac{(4.060)^2}{4} - \pi \frac{(2.375)^2}{4} - \left[\pi \frac{(3.875)^2}{4} - \pi \frac{(2.875)^2}{4} \right]$$

$$= 12.95 - 4.430 - \left[11.79 - 6.492 \right]$$

$$= 3.222 \, in^2 \quad = \, .0224 \, ft^2$$

$$G_0 = \frac{285 \; lb/hr}{.0224 \; ft^2} = 12700 \; lb/hr \, ft^2$$

$$N_{Re} = \frac{D \, G_0}{\mu} = \frac{12700 \times .0417}{.097} = 5500$$

$$N_R{}^{.6} = 176$$

$$N_{PR} = .74 \quad (Kern)$$

$$N_{PR}{}^{.3} = .905$$

$$\bar{h}_0 = .26 \, \frac{k}{D_0} \, N_{PR}{}^{.3} \, N_R{}^{.6}$$

$$= .26 \frac{.036}{.0417} \times .905 \times 176 = 35.7 \; Btu/hr \, ft^2 \, °F$$

the overall conductance

$$U = \frac{1}{\frac{1}{35.7} + \frac{.500}{.436} \frac{1}{885}} = \frac{1}{.0280 + .01295} = \frac{1}{.04695}$$

$$= 21.4 \; Btu/hr \, ft^2 \, °F$$

Dissociator Section

2.375 OD $\times$ .065 wall tube

8 fins $\frac{1}{4} \times \frac{1}{16} \times 12\frac{1}{4}$

tube packed with promoted iron granules

Mass Velocity $\dfrac{40.35\ lb/hr}{\pi\ \dfrac{(2.245)^2}{144\times 4}\ ft^2} = 1465\ lb/hr\,ft^2$

$= .407\ lb/sec\,ft^2$

from Jakob, Fig 42-15 $\quad h_i = 12.5\ Btu/hr\,ft^2\,°F$

for exhaust gas flow over exterior of tube

$G = \dfrac{285\ lb/hr}{.0224\ ft^2} = 12700\ lb/hr\,ft^2$

$D_e = \dfrac{4A}{wp} = \dfrac{4 \times 2.062}{7.45 + 4} = \dfrac{8.248}{11.45} = .72\,in = .06\,ft$

$N_R = \dfrac{D_e G}{\mu} = \dfrac{.06 \times 12700}{.097} = 7850$

$J_i \approx 31 \qquad (Kern)$

$\bar{h}_o = J \dfrac{k}{D_e} N_{PR}^{\frac{1}{3}} = 31 \cdot \dfrac{.036}{.06} \cdot .905 = 16.8\ Btu/hr\,ft^2\,°F$

say fin effectiveness $\eta_f \approx .93$ (Kays & London)

overall effectiveness $\eta_o = 1 - \dfrac{A_f}{A_o}(1 - \eta_f) = 1 - \dfrac{49}{171}(1 - .93) = .98$

$U = \dfrac{1}{\dfrac{1}{\eta_o h_o} + \dfrac{d_i}{d_o} \dfrac{1}{h_i}} = \dfrac{1}{\dfrac{1}{.98 \times 16.8} + \dfrac{1}{\dfrac{121}{171} \times 12.5}} = \dfrac{1}{.065 + .112} = \dfrac{1}{.1725}$

$= 5.8\ Btu/hr\,ft^2\,°F$
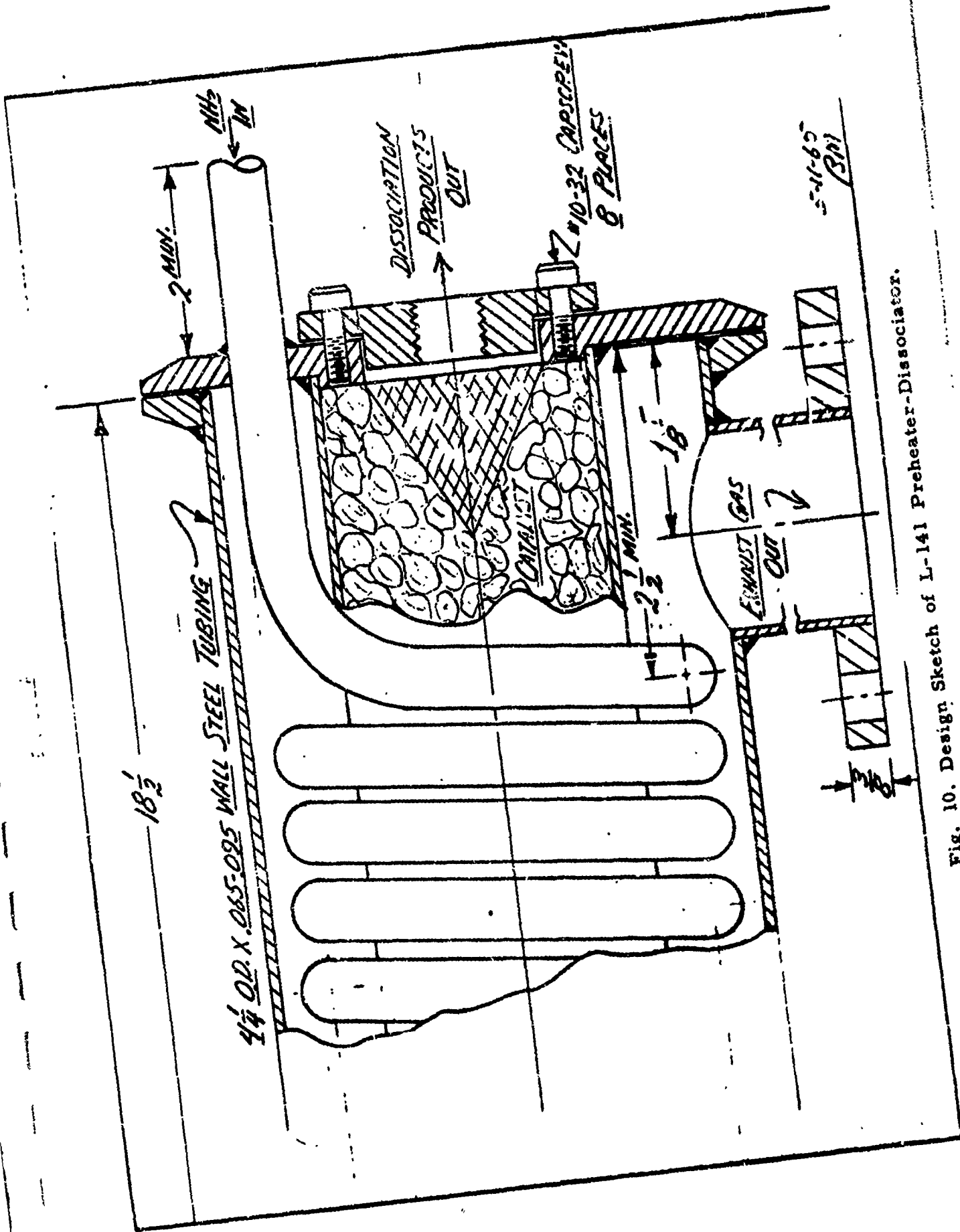
Fig. 10. Design Sketch of L-141 Preheater-Dissociator.
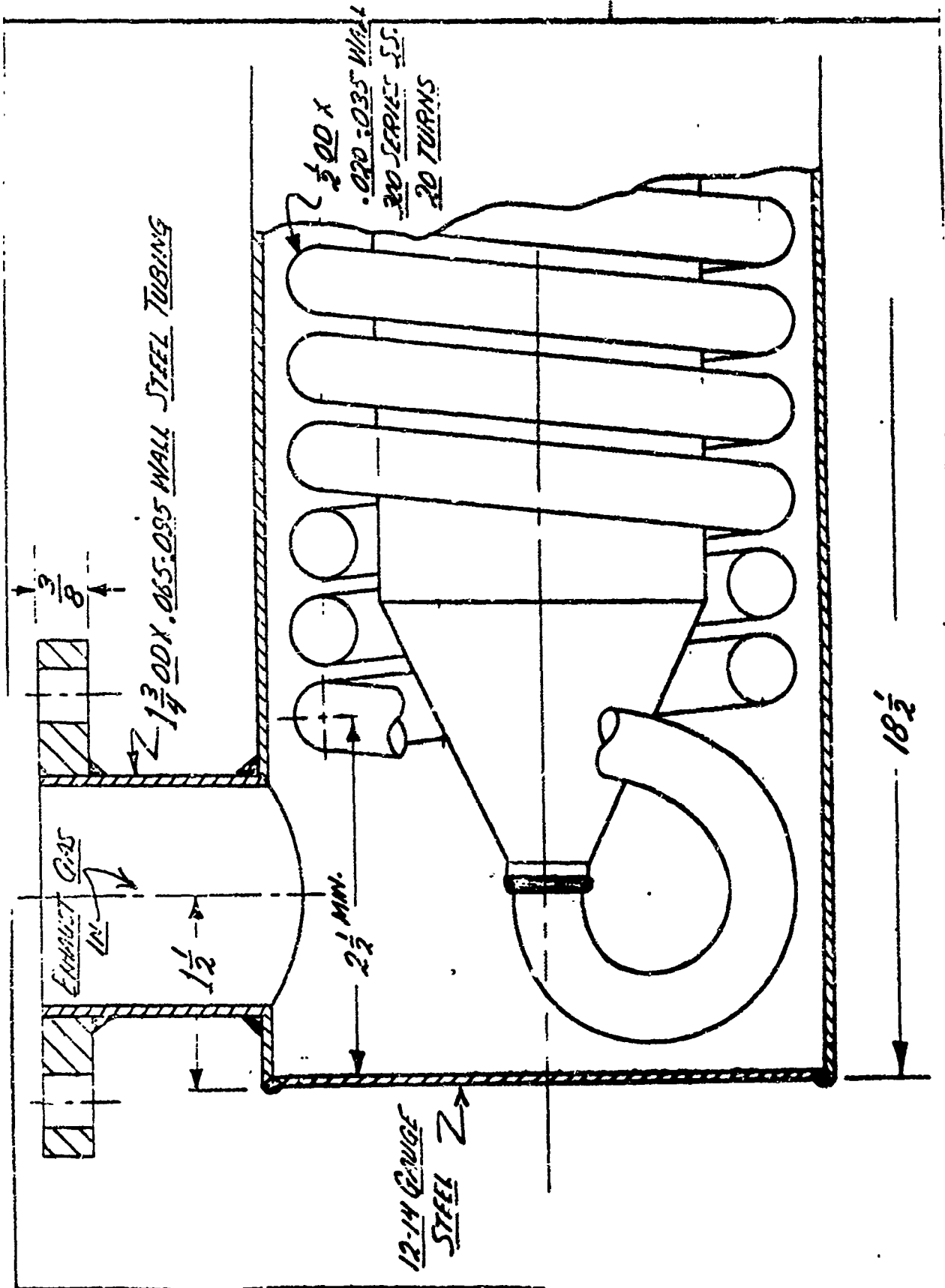
Fig. 11. Design Sketch of L-141 Preheater-Dissociator.

Preheater Section Heat Balance

$$1275°F \xrightarrow{\hspace{3cm}} 975°F$$

$$1255°F \xleftarrow{\hspace{3cm}} 32°F$$

$$LMTD = \frac{943-220}{\ln\frac{943}{220}} = \frac{723}{1.459} = 497°F$$

$$Q_h = (1055°-32)°F \times 40.35\ \text{lb/hr} \times .59\ \text{Btu/lb}°F = 24400\ \text{Btu/hr}$$
$$Q_N = \underline{\hspace{2cm}3696}$$
$$Q_t = \overline{28096\ \text{Btu/hr}}$$

check

$$Q_t = AU\Delta T = 2.31\ ft^2 \times 24.4\ \text{Btu/hr ft}^2°F \times 497°F = 28,000\ \text{Btu/hr}$$

Dissociator Section Heat Balance

$$1275°F \xrightarrow{\hspace{3cm}} 975°F$$

$$1055°F \xrightarrow{\hspace{3cm}} 820°F$$

$$LMTD = \frac{220-155}{ln\frac{220}{155}} = \frac{65}{.336} = 193°F$$

Q_s (sensible heat from gas)
$= (1055 - 820)°F \times 40.35 \text{ lb/hr} \times .61 \text{ Btu/lb°F} = 5790 \text{ Btu/hr}$

Q_i (heat influx
$= AU\Delta T = 1.18 ft^2 \times 5.8 \text{ Btu/hr ft}^2°F \times 193°F = 1320$

Total heat available for dissociation
$Q_d = 5790 + 1320 = 7110 \text{ Btu/hr}$

Calculated % dissociation

$$\frac{7110 \text{ Btu/hr}}{1354 \text{ Btu/lb} \times 40.35 \text{ lb/hr}} = 13\%$$

Percent H_2 by Weight

$$\frac{3}{17} \times 13 = 2.3\%$$

Appendix IIJ-B

Design Calculations for Redesigned L-141 Dissociator
(EX-79016 with Nickel Catalyst)

Auxiliary Evaporator Section

(a) $\frac{1}{2}$ OD X .035 wall X 70 in long SS tubing

Heat exchanger surface = .5π X 70 = 110 in² = .76 ft²

(b) $\frac{5}{8}$ X $\frac{9}{16}$ X 5 dia manifold

Heat exchanger surface 5π X 2(.625 + .5625) = 37.1 in² = .26 ft²

total auxiliary evaporator surface = .76 + .26 = 1.02 ft²

Preheater Section

$\frac{5}{16}$ OD X .035 wall SS tubing
40 turns 5.4375 PD + 40 turns 4.6875 PD

length of tubing π(5.4375 + 4.6875) X 40 = 1270 in = 105.5 ft

Heat exchanger surface .3125 π X 1270 = 1245 in² = 8.62 ft²

Catalyst Section

3.42 OD X .075 wall X 16½ long SS tube with 32 fins
.29 X .070 X 15¾

Tube surface area 3.42 π X 16.5 = 177 in² = 1.23 ft²

Fin surface area 32 X 2 X .29 X 15.75 = 292 in² = 2.03 ft²

Total surface 1.23 + 2.03 = 3.26 ft²

Catalyst

Nickel Foametal (GE) 45% density
16 discs, 3.275 dia x .906 thick

Volume of catalyst

$$.906\left[15\left(\pi\frac{(3.275)^2}{4}-2\pi\frac{(.375)^2}{4}-\pi\frac{(.5)^2}{4}\right)+\left(\pi\frac{(3.275)^2}{4}-2\pi\frac{(.375)^2}{4}\right)\right]=117.2\ in^3$$

Weight of Catalyst

$$117.2\ in^3 \times .322\ lb/in^3 \times .45 = 16.9\ lb.$$

Cross Section of Catalyst exposed to NH_3 flow

$$\frac{117.2\ in^3}{.906\ in} = 128.3\ in^2 = .89\ ft^2$$

Calculated Pressure Drop in Catalyst Foametal Nickel, 45% Density 29" hg.
4000 RPM Engine Conditions

For pressure drop thru porous media (Perry's)

$$\frac{P_1^2 - P_2^2}{L} = \frac{2\alpha \, RT \mu G}{M g_c} + \left(\beta + \frac{L}{L} \ln \frac{P_1}{P_2}\right)\left(\frac{2 RT G^2}{M g_c}\right)$$

P_1 = upstream pressure ..... 60 psia ..... = 8640 lb/ft² abs

P_2 = downstream pressure

L = length ..... .906 in ..... = .0755 ft

G = superficial mass velocity $\frac{169 \, lb/hr}{.89 \, ft^2 \times 3600 \, sec/hr}$ = .00527 lb/sec ft²

μ = viscosity ..... = 18 × 10⁻⁶ lb/ft sec

g_c = dimensional constant ..... = 32.17 ft/sec²

M = molecular weight ..... = 17 lb/lb mole

R = gas constant ..... = 1546 ft lb/lb mole

T = temperature ..... 1240°F ..... = 1700°R

from Green & Duwez (J. Applied Mechanics 1951)

α = 2 × 10⁸ in⁻² × 144 $\frac{in^2}{ft^2}$ = 2.88 × 10¹⁰ ft⁻²

β = 1.5 × 10⁴ in⁻¹ × 12 $\frac{in}{ft}$ = 1.80 × 10⁶ ft⁻¹

$$\frac{P_1^2 - P_2^2}{L} = \frac{(8640)^2 - P_2^2}{.0755} = \frac{74.65 \times 10^6 - P_2^2}{.0755}$$

$$\frac{2 \alpha \, RT \mu \, G}{M g_c} = \frac{2 \times 2.88 \times 10^{10} \times 1546 \times 1700 \times 18 \div 10^{-6} \times .00527}{17 \times 32.17} = 26.3 \times 10^6$$

$$\beta + \frac{1}{L} \ln \frac{P_1}{P_2} = 1.80 \times 10^6 + \frac{1}{.0755} \ln \frac{P_1}{P_2} \approx 1.80 \times 10^6$$

$$\frac{2 RT G^2}{M g_c} = \frac{2 \times 1546 \times 1700 \times (.00527)^2}{17 \times 32.17} = .2675$$

substituting:

$$\frac{74.65 \times 10^6 - P_2^2}{.0755} = 26.3 \times 10^6 + \left(1.80 \times 10^6 \times .2675 \right)$$

$$P_2^2 = 74.65 \times 10^6 - 2.03 \times 10^{-6} = 72.62 \times 10^6$$

$$P_2 = 8520 \ lb/ft^2 = 59 \ psia$$

Pressure drop $\approx$ 1 psi

Calculated Pressure Drop in Preheater Coil 29" hg, 4000 RPM Engine Conditions

Dia of tubing (inside) $.3125 - .070 = .2425$ in $= .0202$ ft

Free Flow Cross Section (per coil) $\pi \frac{(.0202)^2}{4} = .00032$ ft^2

$$G = \frac{16.9 \text{ lb/hr}}{4 \times .00032 \text{ ft}^2} = 13,200 \text{ lb/hr ft}^2$$

$$N_R = \frac{4 r_h \, G}{\mu} = \frac{.0202 \text{ ft} \times 13200 \text{ lb/hr ft}^2}{.035 \text{ lb/hr ft}} = 7620$$

$$w_f = \frac{16.9 \text{ lb/hr}}{4} = 4.22 \text{ lb/hr} = .00117 \text{ lb/sec}$$

$$v = \frac{RT}{P} = \frac{88.5 \text{ ft lb/lb °R} \times 1700 °R}{60 \text{ lb/in}^2 \times 144 \text{ in}^2/\text{ft}^2} = 17.4 \text{ ft}^3/\text{lb}$$

$$L = \frac{105.5 \text{ ft}}{4} = 26.4 \text{ ft}$$

For pressure drop thru a pipe (Marks)

$$\Delta P = 174.2 \; f \; w_f^2 \; v \; L \, / \, d^5$$

$$f = .042 \quad (\text{Marks})$$

$$\Delta P = 174.2 \times .042 \times (.00117)^2 \times 17.4 \times 26.4 \times \frac{1}{(.2425)^5}$$

$$= 174.2 \times .042 \times 13.69 \times 10^{-7} \times 17.4 \times 26.4 \times 1195$$

$$= 5.5 \text{ psi}$$

Stress in Catalyst Tube at 60 psia
(Operating pressure)　　　　45 psig

$$\frac{45 \text{ lb/in}^2 \times 3.27 \text{ in}}{2 \times .0775 \text{ in}} = 945 \text{ psi}$$

at max vapor pressure 2.0 psig

$$\frac{260 \text{ psig}}{45 \text{ psig}} \times 945 \text{ psi} = 5450 \text{ psi}$$

Exhaust Gas Flow Cross Section Area

Exhaust Manifold (reference)

$D_i = 1.5625$ in

$A = \pi \dfrac{(1.5625)^2}{4} = 1.93 \text{ in}^2 = .0133 \text{ ft}^2$

$V = \dfrac{v \, W_g}{A} = \dfrac{RT W_g}{PA} = \dfrac{55.16 \text{ lb ft/lb}° \times 1840° \times .118 \text{ lb/sec}}{15 \text{ lb/in}^2 \times 144 \text{ in}^2/\text{ft}^2 \times .0133 \text{ ft}^2} = 415 \text{ ft/sec}$

(at 29" hg 4000 RPM)

Catalyst Section

$A = \pi \dfrac{(4)^2}{4} - \pi \dfrac{(3.425)^2}{4} - (32 \times .070 \times .287)$

$= 12.56 - 9.22 - .64 = 2.7 \text{ in}^2 = .01875 \text{ ft}^2$

Preheater Section

$A = \pi \dfrac{(5.93)^2}{4} - \pi \dfrac{(4.064)^2}{4} - 4.6875 \pi \times .3125 - 5.4375 \pi \times .3125$

$= 27.00 - 12.95 - 4.60 - 5.32 = 4.13 \text{ in}^2 = .0281 \text{ ft}^2$

Auxiliary Evaporator Section

$A \approx \dfrac{\pi}{2} \dfrac{(3.43)^2}{4} - 4\pi \dfrac{(.5)^2}{4}$

$= 4.60 - .78 = 3.82 \text{ in}^2 = .0265 \text{ ft}^2$

Figure B-1

Dissociated Ammonia Temperature Versus Percent Dissociated
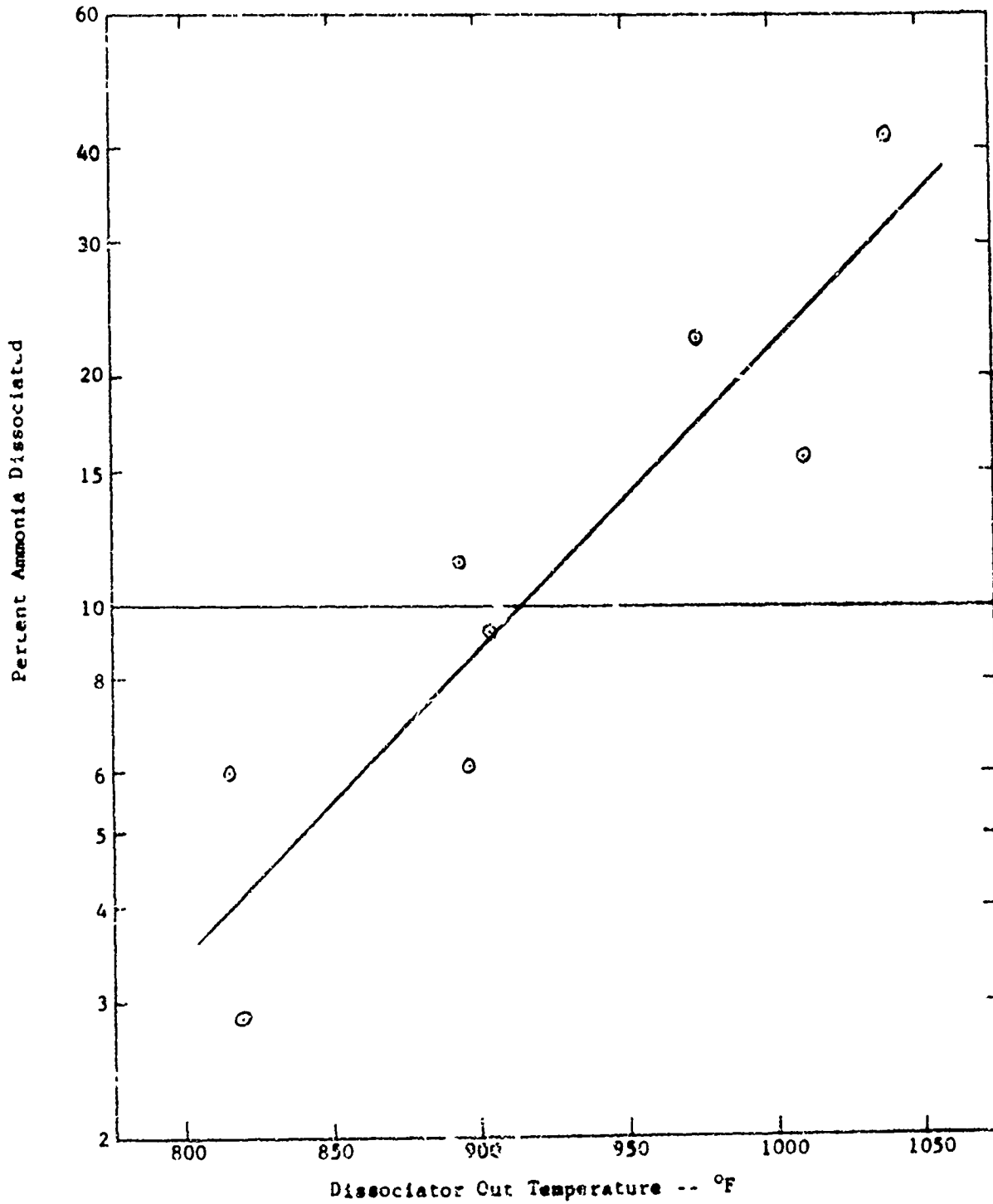
Design Point: 2400 RPM
                 29 " hg Manifold Pressure
                 37 lb/hr NH₃ Flow
                 257 lb/hr Exhaust Mass Flow
                 1235 °F Exhaust Gas Temperature

NH₃ Flow thru dissociator 14.75 lb/hr

Dissociation Products Temp (out of catalyst) ≈ 1025 °F
(from Test data, assume 1.92 % H₂ effective enrichment
                         4.8 % H₂ at catalyst outlet
                         27.2 % dissociation in catalyst.)

Dissociation Products Temp (out of cooler) = 100 °F
(assumed)

Vaporization performed in cooler:

$$Q = 14.75 \text{ lb/hr} \times .62 \text{ Btu/lb°F} (1025-100)°F = 8450 \text{ Btu/hr}$$

which will vaporize

$$\frac{8450 \text{ Btu/hr}}{553 \text{ Btu/lb}} = 15.3 \text{ lb/hr}$$

or $\frac{15.4 \text{ lb/hr}}{37 \text{ lb/hr}} = 41.4 \%$ of total NH₃ flow

Quality of Vapor at Auxiliary Evaporator Inlet

          58.6 % Liquid ,   41.4 % Vapor

Figure B-2

Calculated U Versus G for Auxiliary Evaporator

G -- lb/sec ft²

U -- Btu/hr ft² °F
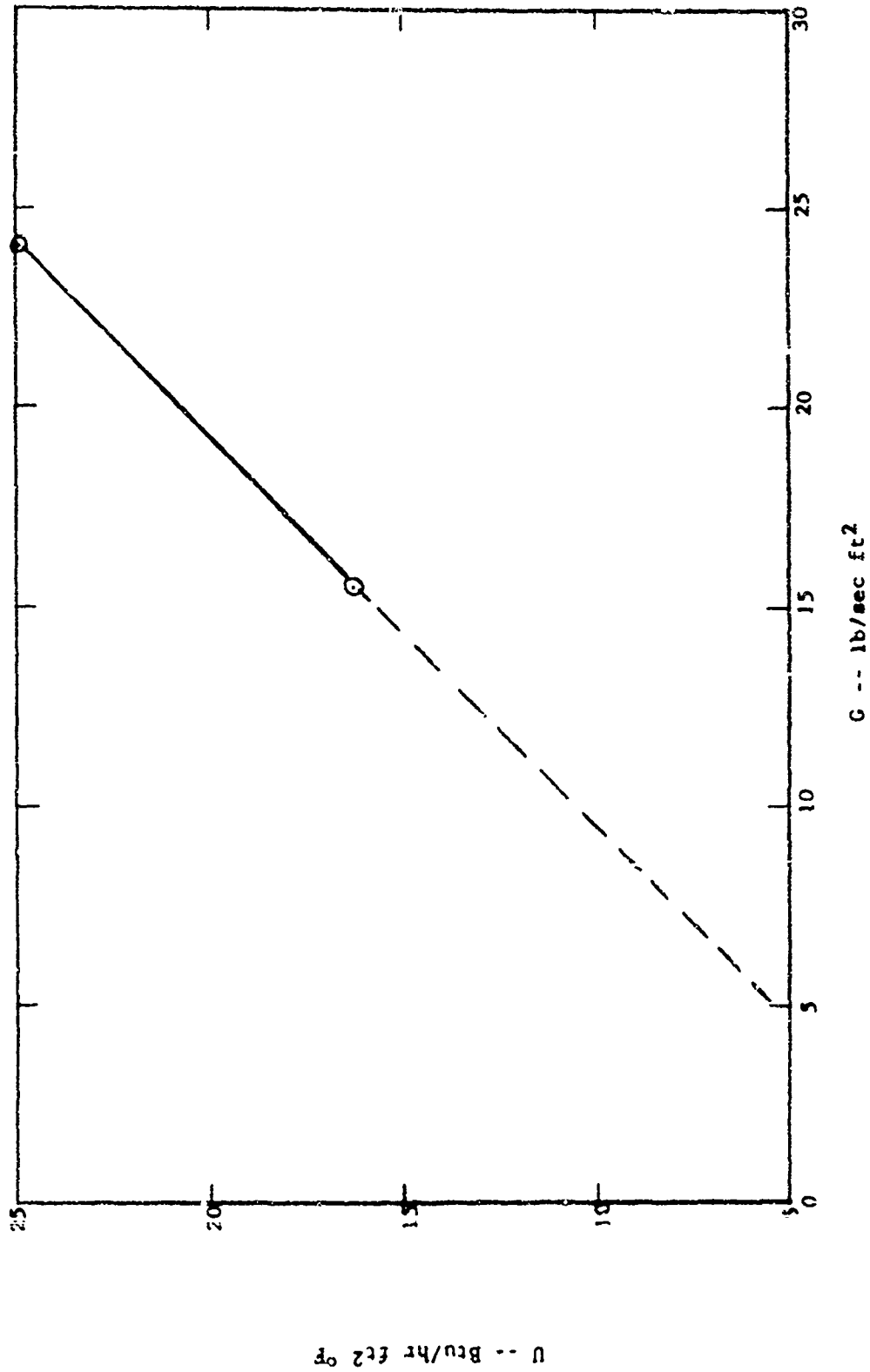
Auxiliary Evaporator

Inlet Conditions :   37 Lb/hr NH_3 (58.6% liquid) 60 psia
                      257 Lb/hr Exhaust Mass Flow
                      32 °F NH_3 Temp

$\frac{1}{2}$ OD X .035 wall X 70 in long SS Tubing

D_i = .500 - .070 = .430 in = .0358 ft

Flow Area = $\pi \frac{(.0358)^2}{4}$ = .001005 ft²

$G = \frac{37 \, Lb/hr}{.001005 \, ft^2}$ = 36,800 Lb/hr ft² = 10.2 Lb/sec ft²

$U \approx$ 11 Btu/hr ft² °F   (from curve)

Required heat transfer to complete vaporization

Q_N = .586 X 37 Lb/hr X 553 Btu/lb = 12000 Btu/hr

Assume 1.92 % H_2 at design point (test data)

Q_d = .0192 X 37 Lb/hr X 7673 Btu/lb = 5450 Btu/hr

Assume 14.75 Lb/hr NH_3 preheated from 32° to 1025°F

Q_h = 14.75 Lb/hr X .62 Btu/lb°F X (1025-32)°F = 9100 Btu/hr

Temp of exhaust gas at aux evaporator inlet

$1235 = \frac{(5450 + 9100) \, Btu/hr}{257 \, Lb/hr \, X \, .24 \, Btu/lb°F}$ = 999 °F

$$999°F \xrightarrow{\quad 252 \, lb/hr \quad} \text{Exhaust Gas}$$

$$A = 1.02 \, ft^2$$
$$U = 11 \, Btu/hr \, ft^2 °F$$

$$32°F \xrightarrow{\quad \wedge\wedge\wedge \quad} NH_3$$

The capacity rates   (Kays & London)

$$C_h = W_h \cdot C_{p_h} = 257 \, lb/hr \times .24 \, Btu/lb°F = 61.7$$

$$C_c \approx W_{c} \, h_{fg} = .582 \times 37 \, lb/hr \times 553 \, Btu/lb = 11,900$$

$$\frac{C_{min}}{C_{max}} = \frac{61.7}{11,900} \approx .005$$

Heat transfer units $NTU = \dfrac{AU}{C_{min}} = \dfrac{1.02 \, ft^2 \times 11 \, Btu/hr \, ft^2 °F}{61.7} = .2$

$\varepsilon \approx 20\%$ (Fig 3, Kays & London)

$$t_{h_2} = t_{h_1} - \frac{C_{min}}{C_h} \varepsilon (t_{h_1} - t_{c_1})$$

$$= 999 - \frac{61.7}{61.7} .20 (999 - 32) = 806°F$$

Heat transfer in aux evaporator

$$Q = 257 \, lb/hr \times .24 \, Btu/lb°F (999 - 806)°F = 11,900 \, Btu/hr$$

Temp of NH_3 at aux evaporator outlet

$$32 + \frac{(11,900 - 11,250) \, Btu/hr}{37 \, lb/hr \times .62 \, Btu/lb°F} = 60°F$$

Preheater Section

Inlet Conditions: 14.75 lb/hr NH_3 at 60 psia
257 lb/hr Exhaust Mass Flow
60 °F NH_3 Temp

Assume 1.92% H_2 enrichment (Test data)

$Qd = .0192 \times 37 \, lb/hr \times 7613 \, Btu/lb = 5450 \, Btu/hr$

Temp of exhaust gas at preheater inlet

$1235 - \dfrac{5450 \, Btu/hr}{257 \, lb/hr \times .24 \, Btu/lb°F} = 1146°F$

For NH_3 Flow inside preheater coils

Free Flow Area $= 4\pi \dfrac{(.2425)^2}{4} = .185 \, in^2 = .001285 \, ft^2$

$G = \dfrac{14.75 \, lb/hr}{.001285 \, ft^2} = 11500 \, lb/hr \, ft^2$

$N_R = \dfrac{4rh}{\mu} G = \dfrac{.0202 \, ft \times 11500 \, lb/hr \, ft^2}{.035 \, lb/ft \, hr} = 6540$

$N_R^{.8} = 1142$

$N_{PR} = \dfrac{C_p \mu}{k} = \dfrac{.61 \, Btu/lb°F \times .035 \, lb/ft \, hr}{.034 \, Btu/hr \, ft°F} = .63 \quad (at \, 500°F)$

$N_{PR}^{.33} = .857$

$h_i = .023 \dfrac{k}{D_i} N_{PR}^{.33} N_R^{.8}$

$= .023 \dfrac{.034 \, Btu/hr \, ft°F}{.0202 \, ft} \times .857 \times 1142$

$= 37.8 \, Btu/hr \, ft^2 \, °F$

For Exhaust Gas Flow over outside of Coils

Free Flow Area .0287 ft^2

$$G = \frac{257 \ lb/hr}{.0287 \ ft^2} = 8950 \ lb/hr \ ft^2$$

$$N_R = \frac{G \ D_o}{\mu} = \frac{8950 \ lb/hr \ ft^2 \times .026 \ ft}{.081 \ lb/hr \ ft} = 2880$$

$$N_R^{.6} = 119.$$

$$N_{PR} = .74 \qquad (Marks)$$

$$N_{PR}^{.3} = .905$$

$$h_o = .26 \ \frac{k}{D_o} \ N_{PR}^{.3} \ N_R^{.6}$$

$$= .26 \ \frac{.036 \ Btu/hr \ ft \ °F}{.026 \ ft} \times .905 \times 119$$

$$= 38.8 \ Btu/hr \ ft^2 \ °F$$

$$U = \frac{1}{\frac{1}{38.8} + \frac{.3125}{.2425} \times \frac{1}{37.8}} = \frac{1}{.026 + .034} = \frac{1}{.060} = 16.6 \ Btu/hr \ ft^2 \ °F$$

$$C_h = W_h \ C_{ph} = 257 \ lb/hr \times .24 \ Btu/lb° = 61.7$$

$$C_c = W_c \ C_{pc} = 14.75 \ lb/hr \times .62 \ Btu/lb° = 9.1$$

$$\frac{C_{min}}{C_{max}} = \frac{9.1}{61.7} = .148 \qquad NTU = \frac{AU}{C_{min}} = \frac{8.62 \times 16.6}{9.1} = 15.7$$

$$\varepsilon \approx .98 \qquad (Kays \ \& \ London)$$

$$\therefore t_{c_2} = t_{c_1} + \frac{C_{min}}{C_c} \ \varepsilon \ (t_{h_1} - t_{c_1}) = 60 + \frac{9.1}{9.1} \ .98 \ (1146 - 60) = 1124 \ °F$$

Dissociator Section

For exhaust gas flow over catalyst tube

$$G = \frac{257 \; lb/hr}{.01875 \; ft^2} = 13700 \; lb/hr \, ft^2$$

$$De = \frac{4A}{wp} = \frac{4 \times 2.7 \, in^2}{\pi \times 3.425 in + (32 \times .58) in} = .368 in = .0307 \, ft$$

$$NR = \frac{De \, G}{\mu} = \frac{.0307 \, ft \times 13700 \; lb/hr \, ft^2}{.081 \; lb/hr \, ft} = 5190$$

$$NPR^{.3} = .905$$

$$J \approx 21 \qquad (\text{Kern "Process Heat Transfer"})$$

$$h_0 = J \frac{k}{De} NPR^{.3} = 21 \frac{.036 \, Btu/ft \, °F \, hr}{.0307 \, ft} \times .905 = 22.3 \; Btu/hr \, ft^2 \, °F$$

for fin effectiveness   (Kays & London)

$$ml = \sqrt{\frac{2h}{k\delta}} \, l = \sqrt{\frac{2 \times 22.3}{12 \times .07}} \, .29 = 2.1$$

$$\eta_f = .46 \qquad (\text{Fig 1 Kays & London})$$

Overall effectiveness

$$\eta_0 = 1 - \frac{A_f}{A} (1 - \eta_f) = 1 - \frac{2.03}{3.26} (1 - .46) = 1 - .358 = .642$$

$$h_0 A_0 = .642 \times 22.3 \; Btu/hr \, ft^2 \, °F \times 3.26 \, ft^2 = 45.4 \; Btu/hr \, °F$$

For NH_3 flow thru catalyst

(use Kays & London data for 60x60x.011 screen matrix)
for estimate of h_i for porous nickel catalyst

$$A_c = \rho \, A_{fr} = .55 \times .055 \, ft^2 \times 16 = .484 \, ft^2$$

$$G = \frac{14.75 \, lb/hr}{.484 \, ft^2} = 30.5 \, lb/hr \, ft^2$$

$$N_R = \frac{4 r_h \, G}{\mu} = \frac{.001328 \, ft \times 30.5 \, lb/hr \, ft^2}{.035 \, lb/hr \, ft} = 1.16$$

$$N_{ST} \cdot N_{PR} = .46 (N_R)^{-.4} = .46 \times (1.16)^{-.4} = .46 \times .945 = .435$$

$$N_{PR} = .63$$

$$N_{ST} = \frac{.435}{.63} = .69$$

$$h_i = N_{ST} \, G \cdot c_p = .69 \times 30.5 \times .62 = 13. \, Btu/hr \, ft^2 \, °F$$

$$A_i = a V = 1820 \, ft^2/ft^3 \times .0202 \, ft^3 = 36.76 \, ft^2$$

$$h_i A_i = 13 \, Btu/hr \, ft^2 \, °F \times 36.76 \, ft^2 = 478 \, Btu/hr \, °F$$

$$UA = \frac{1}{\frac{1}{45.4} + \frac{1}{478}} = \frac{1}{.022 + .002} = \frac{1}{.024} = 41.5 \, Btu/hr \, °F$$

Catalyst Section

$$1235° \xrightarrow{\text{EXHAUST GAS}} 1146°$$

$$1124° \xrightarrow{\text{NH}_3} 1025°$$

$$LMTD = \frac{121-111}{\ln\frac{121}{111}} = \frac{10}{.086} = 116°$$

The heat transfer

$$Q = UA\Delta T = 41.5 \text{ Btu/hr °F} \times 116°F = 4810 \text{ Btu/hr}$$

Sensible heat available for dissociation

$$Q = W C_p \, dT = 14.75 \text{ lb/hr} \times .62 \text{ Btu/lb °F} \times (1124-1025)°F = 890 \text{ Btu/hr}$$

Total heat available for dissociation

$$4810 + 890 = 5900 \text{ Btu/hr}$$

which would provide a hydrogen enrichment of

$$\frac{5900 \text{ Btu/hr}}{37 \text{ lb/hr} \times 1673 \text{ Btu/lb}} = 2.08\%$$

Figure B-3

L-141 Dissociation Products Cooler Performance
with Liquid Ammonia Inside Tubes

Calculated Value (132°F)

58 psig

70 psig

85 psig

150°

U -- Btu/hr Ft² °F

Ammonia Flow -- lb/hr
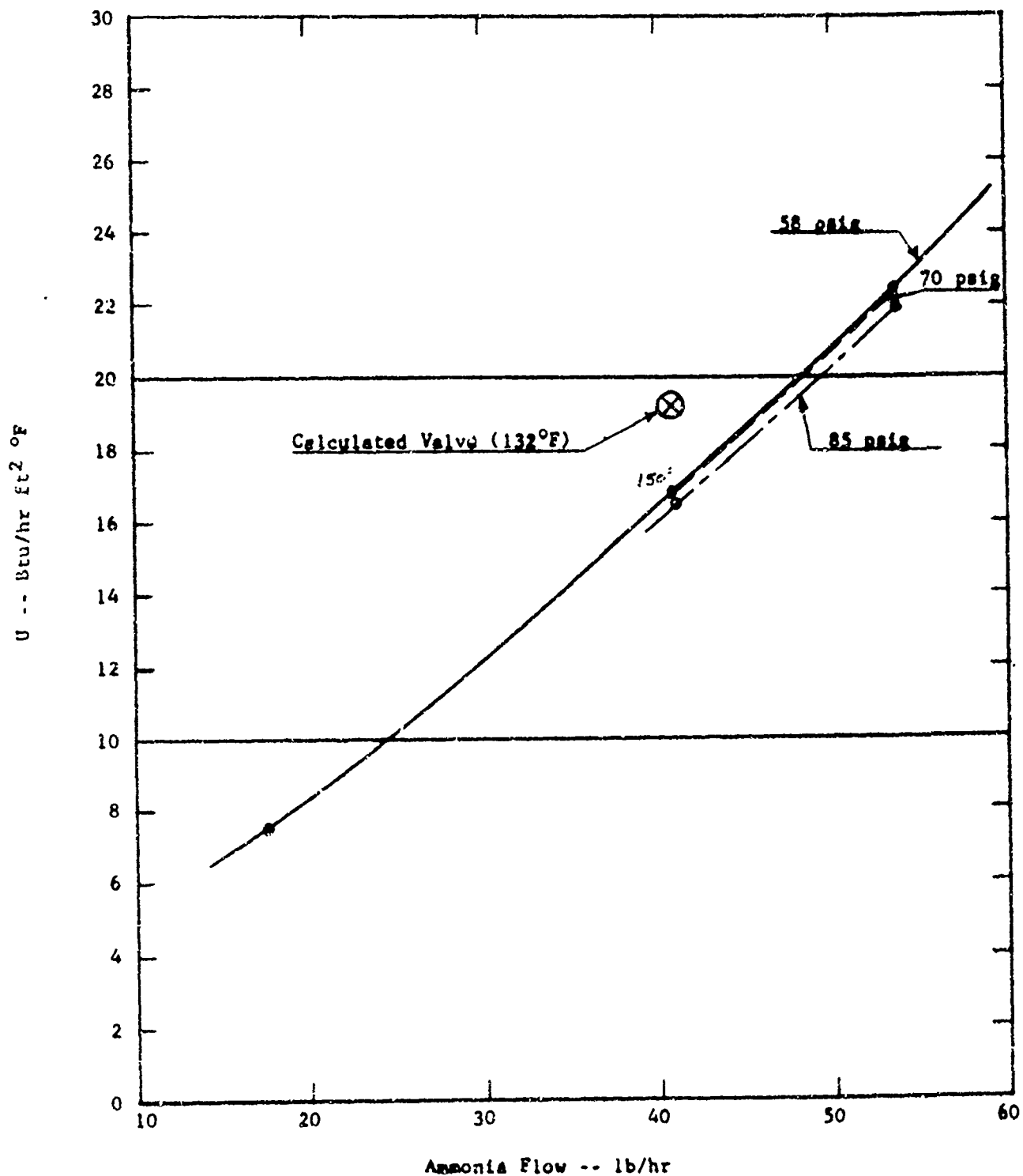
Calculated Temp of Dissociation Products Out of Cooler (Using Existing Cooler)
2400 RPM

Bypass Flow   22.25 lb/hr   at   60°F

Dissociator Flow   14.75 lb/hr   at   1025°F

Temp of mixed NH_3 to Cooler

$$60° + \frac{(1025-60) \times 14.75 \text{ lb/hr} \times .62 \text{ Btu/lb °F}}{37 \text{ lb/hr} \times .62 \text{ Btu/lb °F}} = 455°F$$

Assume Liquid NH_3 Temp = 32°F

Heat exchanger surface in cooler = 2.7 ft²

U (from test data) = 15 Btu/hr ft² °F

$$C_h = Wf_h \; C_{p_h} = 37 \text{ lb/hr} \times .62 \text{ Btu/lb}° = 23$$

$$C_c = Wf_c \; h_{fg} = 37 \text{ lb/hr} \times 553 \text{ Btu/lb} = 20250$$

$$\frac{C_{min}}{C_{max}} = \frac{23}{20250} \approx .001$$

$$NTU = \frac{AU}{C_{min}} = \frac{2.7 \text{ ft}^2 \times 15 \text{ Btu/hr ft}^2 °F}{23} = 1.76$$

$$\varepsilon \approx .84$$

$$t_{h_e} = 455 - \frac{23}{23} \times .84 (455 - 32) = 100°F$$

Design Point: 1200 RPM
29" hg Manifold Pressure
18.5 lb/hr NH₃ Flow
128.5 lb/hr Exhaust Mass Flow
1000°F Exhaust Gas Temperature

NH₃ Flow thru Dissociator   13.2 lb/hr

Dissociation Products Temp (out of catalyst) = 900°F
(from test data, assume 1.1% effective H₂ enrichment
1.55% H₂ at catalyst outlet
8.8% dissociation in catalyst

Dissociation Products Temp (out of cooler) = 100°F
(assumed)

Vaporization performed in cooler:

$Q = 13.2 \text{ lb/hr} \times .62 \text{ Btu/lb°F} (900-100)°F = 6550 \text{ Btu/hr}$

which will vaporize

$$\frac{6550 \text{ Btu/hr}}{553 \text{ Btu/lb}} = 11.85 \text{ lb/hr}$$

or $\frac{11.85 \text{ lb/hr}}{18.5 \text{ lb/hr}} = 64.2\%$ of total NH₃ flow

Quality of Vapor at Auxiliary Evaporator Inlet

35.8 % liquid , 64.2 % vapor

Auxiliary Evaporator

Inlet Conditions : 18.5 lb/hr NH_3 (35.8% Liquid)
128.5 lb/hr Exhaust Mass Flow
32°F NH_3 Temp

$G = \dfrac{18.5 \text{ lb/hr}}{.001005 \text{ ft}^2} = 18400 \text{ lb/hr ft}^2 = 5.1 \text{ lb/sec ft}^2$

$U \approx 5.5 \text{ Btu/hr ft}^2 °F$ (from curve)

Required Heat transfer to complete vaporization

$Q_v = .358 \times 18.5 \text{ lb/hr} \times 553 \text{ Btu/lb} = 3660 \text{ Btu/hr}$

Assume 1.1% H_2 at this design point

$Q_d = .011 \times 18.5 \text{ lb/hr} \times 7673 \text{ Btu/lb} = 1560 \text{ Btu/hr}$

Assume 13.2 lb/hr NH_3 preheated from 32°F to 900 °F

$Q_h = 13.2 \text{ lb/hr} \times .62 \text{ Btu/lb °F} \times (900-32)°F = 7100 \text{ Btu/hr}$

Temp of exhaust gas at aux. evaporator inlet

$1000 - \dfrac{(1560 + 7100) \text{ Btu/hr}}{128.5 \text{ lb/hr} \times .24 \text{ Btu/lb °F}} = 719 °F$

$719°$ $\xrightarrow{\quad 128.5 \ \text{lb/hr} \quad}$ Exhaust Gas

$$A = 1.02 \ ft^2$$
$$U = 5.5 \ Btu/hr\,ft^2\,°F$$

$32°$ $\xrightarrow{\quad \wedge\!\wedge\!\wedge\!\wedge\!\wedge \quad}$ NH_3
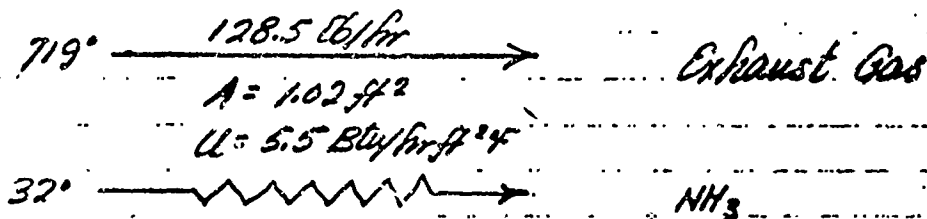
$$C_h = W_h\, C_{p_h} = 128.5 \times .24 = 30.8$$

$$C_c = W_c\, h_v = .40 \times 18.5 \times 553 = 4100$$

$$\frac{C_{min}}{C_{max}} = \frac{30.8}{4100} \approx .0075$$

$$NTU = \frac{AU}{C_{min}} = \frac{1.02 \times 5.5}{30.8} \approx .2$$

$$\mathcal{E} \approx 20\%$$

$$t_{h_2} = t_{h_1} - \frac{C_{min}}{C_h}\, \mathcal{E}\,(t_{h_1} - t_{c_1})$$

$$= 719 - \frac{30.8}{30.8} \cdot .20\,(719 - 32) = 582°F$$

Heat transfer in aux evaporator

$$Q = 128.5 \ \text{lb/hr} \times .24 \ Btu/lb°F\,(719 - 582)°F = 4,220 \ Btu/hr$$

Temp of NH_3 at aux evaporator outlet

$$32 + \frac{(4220 - 3660)\ Btu/hr}{18.5 \ \text{lb/hr} \times .62 \ Btu/lb°F} = 81 °F$$

Preheater Section

Inlet Conditions: 13.2 lb/hr NH_3

128.5 lb/hr Exhaust Mass Flow

81 °F NH_3 Temp

Assume 1.1% H_2 enrichment

Q_d = .011 X 18.5 lb/hr X 7673 Btu/lb = 1560 Btu/hr

Temp of exhaust gas at preheater inlet

$$1000° - \frac{1560 \ Btu/hr}{128.5 \ lb/hr \times .24 \ Btu/lb°F} = 949 °F$$

For NH_3 flow inside preheater coils

$$G = \frac{13.2 \ lb/hr}{.001285 \ ft^2} = 10250 \ lb/hr \ ft^2$$

$$N_R = \frac{4 r_h}{\mu} G = \frac{.0202 \ ft \times 10250 \ lb/hr \ ft^2}{.035 \ lb/ft \ hr} = 5900$$

$N_R^{.8} = 1039$

$N_{PR}^{.33} = .857$

$h_i = .023 \frac{k}{D_i} N_{PR}^{.33} N_R^{.8}$

$$= .023 \frac{.034}{.020} \times .857 \times 1039$$

$$= 34.5 \ Btu/hr \ ft^2 °F$$

For exhaust gas flow over outside of coils

$$G = \frac{128.5 \ lb/hr}{.0287 \ ft^2} = 4475 \ lb/hr \cdot ft^2$$

$$N_R = \frac{G D_0}{\mu} = \frac{4475 \ lb/hr \cdot ft^2 \times .026 \ ft}{.081 \ lb/hr \cdot ft} = 1435$$

$$N_R^{.6} = 78.25$$

$$N_{PR}^{.3} = .905$$

$$h_0 = .26 \frac{k}{D_0} N_{PR}^{.3} N_R^{.6}$$

$$= .26 \frac{.036 \ Btu/hr \cdot ft \cdot °F}{.026} \times .905 \times 78.25$$

$$= 25.5 \ Btu/hr \cdot ft^2 \cdot °F$$

$$U = \frac{1}{\frac{1}{25.5} + \frac{.3125}{.2425} \times \frac{1}{34.5}} = \frac{1}{.0392 + .0375} = \frac{1}{.0767} = 13 \ Btu/hr \cdot ft^2 \cdot °F$$

$$C_f = W_f \ Cp_H = 128.5 \times .24 = 30.8$$

$$C_c = W_c \ Cp_c = 13.2 \times .62 = 8.2$$

$$\frac{Cmin}{Cmax} = \frac{8.2}{30.8} = .266$$

$$NTU = \frac{AU}{Cmin} = \frac{8.62 \times 13}{8.2} = 13.7$$

$$\mathcal{E} \approx .98$$

$$t_{c_2} = t_{c_1} + \frac{Cmin}{C_c} \mathcal{E} (t_{f_1} - t_{c_1})$$

$$= 81° + \frac{8.2}{8.2} .98 (949 - 81)°$$

$$= 931 °F$$

Dissociator Section

For exhaust gas flow over catalyst tube

$$G = \frac{128.5 \text{ lb/hr}}{.01875 \text{ ft}^2} = 6860 \text{ lb/hr ft}^2$$

$$N_R = \frac{D_o G}{u} = \frac{.0307 \times 6860}{.081} = 2600$$

$$N_{PR}^{\,.3} = .905$$

$$J = 10.5$$

$$h_o = J \frac{k}{D_o} N_{PR}^{\,.3} = 10.5 \frac{.036}{.0307} \times .905 = 11.1 \text{ Btu/hr ft}^2\,°F$$

$$\eta_o = .642$$

$$h_o A = .642 \times 11.1 \text{ Btu/hr ft}^2\,°F \times 3.26 \text{ ft}^2 = 23.2 \text{ Btu/hr }°F$$

For NH$_3$ flow thru catalyst

$$G = \frac{13.2 \text{ lb/hr}}{.484 \text{ ft}^2} = 27.3 \text{ lb/hr ft}^2$$

$$N_R = \frac{4 r_H}{u} G = \frac{.001328 \text{ ft} \times 27.3 \text{ lb/hr ft}^2}{.035 \text{ lb/hr ft}} = 1.035$$

$$N_{ST} N_{PR} = .46 (N_R)^{-.4} = .46 \times .95 = .437$$

$$N_{PR} = .63$$

$$N_{ST} = \frac{.437}{.63} = .692$$

$$h_i = N_{ST} G C_p = .692 \times 27.3 \times .62 = 11.7 \text{ Btu/hr ft}^2\,°F$$

$$h_i A_i = 11.7 \text{ Btu/hr ft}^2\,°F \times 36.76 \text{ ft}^2 = 430 \text{ Btu/hr }°F$$

$$UA = \frac{1}{\frac{1}{23.2} + \frac{1}{430}} = \frac{1}{.043 + .0023} = \frac{1}{.0453} = 22 \text{ Btu/hr }°F$$

Catalyst Section

$1000°$ ⟶ EXHAUST GAS ⟶ $949°$

$931°$ ⟶ NH_3 ⟶ $900°$
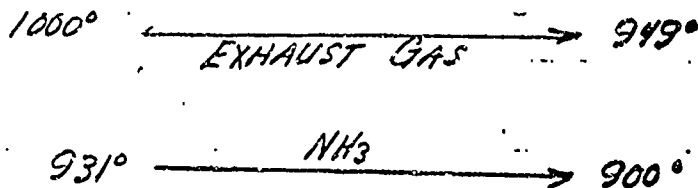
$$LMTD = \frac{69-49}{\ln\frac{69}{49}} = \frac{20}{.336} = 60°$$

$Q = UA\Delta T = 22 \; Btu/hr \;°F \times 60°F = 1320 \; Btu/hr$

sensible heat available for dissociation

$Q = W_f \; C_p \; dT = 13.2 \; lb/hr \times .62 \; Btu/lb° \; (931-900) = 254 \; Btu/hr$

Total heat available for dissociation

$$1320 + 254 = 1574 \; Btu/hr$$

which would provide a hydrogen enrichment of

$$\frac{1574 \; Btu/hr}{18.5 \; lb/hr \times 7623 \; Btu/lb} = 1.1 \%$$

Calculated Temp of Dissociation Products Out of Cooler

Bypass flow   5.3 lb/hr at 81°F

Dissociator flow   13.2 lb/hr at 900°F

Temp of mixed NH_3 to cooler

$$81° + \frac{(900-81)° \times 13.2 \, lb/hr \times .62 \, Btu/lb°}{18.5 \, lb/hr \times .62 \, Btu/lb°} = 666 °F$$

Assume liquid NH_3 temp = 32°F

U (from test data) = 8 $Btu/hr\,ft^2\,°F$

$$C_h = 18.5 \times .62 = 11.5$$
$$C_c = 18.5 \times 553 = 10200$$

$$\frac{C_{min}}{C_{max}} \approx .001$$

$$NTU = \frac{AU}{C_{min}} = \frac{2.7 \times 8}{11.5} = 1.9$$

$$\mathcal{E} \approx .86$$

$$t_{h_2} = 666 - .86(666-32) = 121 °F$$

Appendix III-C

Design Calculations for Electrically Heated Auxiliary Dissociator

Design Point: 1200 RPM

                          15" hg. Manifold Pressure

                          810°F Exhaust Temperature (Fig. C-1)

                          10 lb/hr NH_3 Flow (Fig. C-2)

Assume desired enrichment   =   1% H_2 by weight

                            =   5.65% NH_3 dissociated

Assume NH_3 vaporized and preheated to 700°F in existing dissociator.
(Figure C-3)

From catalyst performance curve (Figure C-5), 16% dissociation may be obtained at
a catalyst bed temperature of 1000°F with a flow of 1.4 lbs/hr through .05 lb nickel
on alumina catalyst.

Required flow thru dissociator $\frac{5.65}{16}$ = 35.2%

or   .352 x 10 lb/hr   =   3.52 lb/hr

Q_h required to heat 35.2% of W_f from 700°F to 1000°F

     Q_h = 3.52 lb/hr x .61 Btu/lb°F x 300°F = 644 Btu/hr

Q_d required to dissociate 5.65% of W_f

     Q_d = 1354 Btu/lb x 10 lb/hr x .0565 = 765 Btu/hr

Total Q = 644 + 765 = 1409 Btu/hr

     1409 Btu/hr x .2931 watts/Btu/hr = 413 watts

Assume 24 volt source, $\frac{413 \text{ watts}}{24 \text{ volts}}$ = 17.2 amps

Figure C-1

Estimated L-141 Exhaust Temperature During Normal Start

29" hg

15" hg

Engine Speed - RPM

Exhaust Gas Temperature--°F
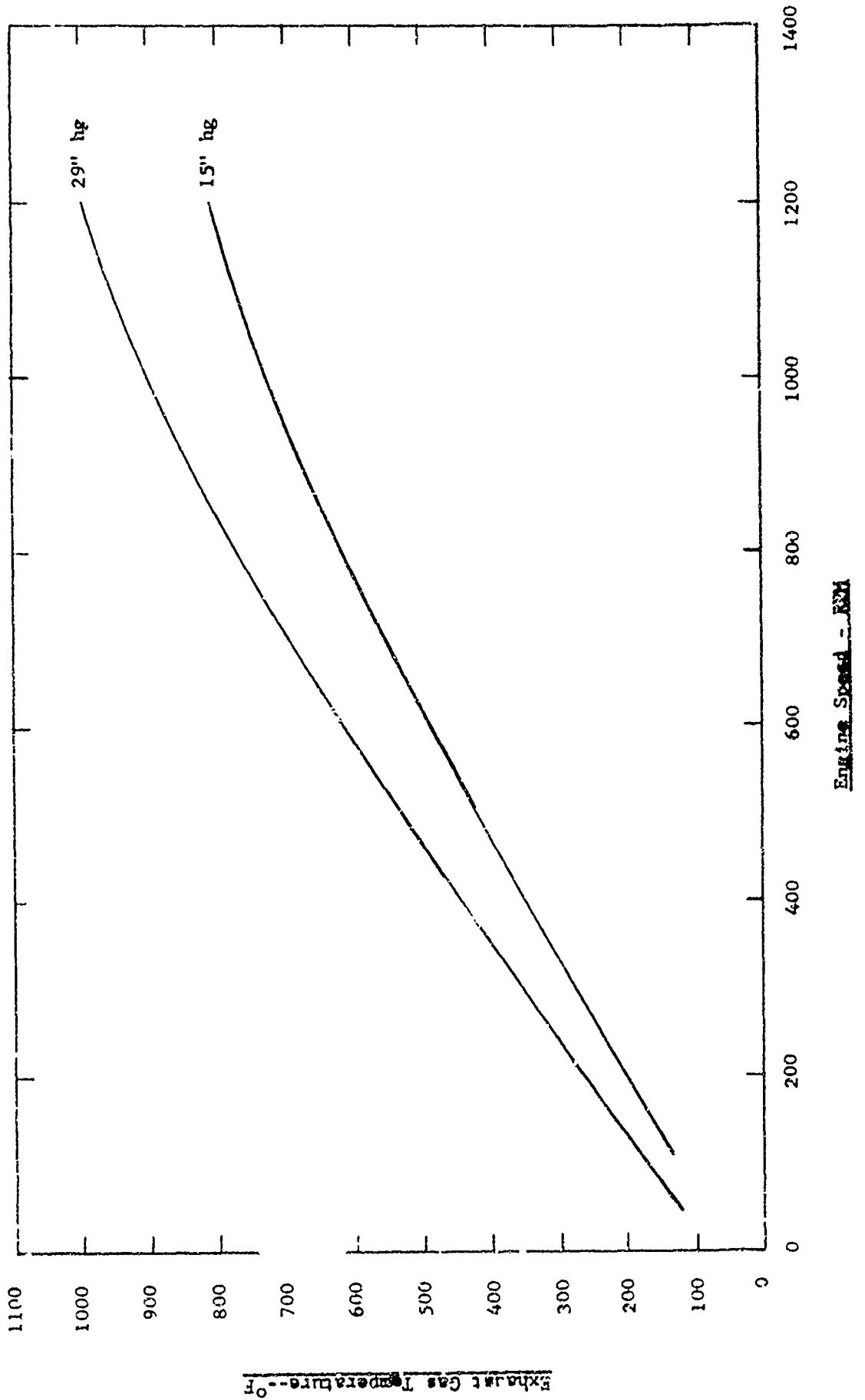
Figure C-2

Estimated Ammonia Fuel Flow Versus Engine Speed For L-141 Starting Range
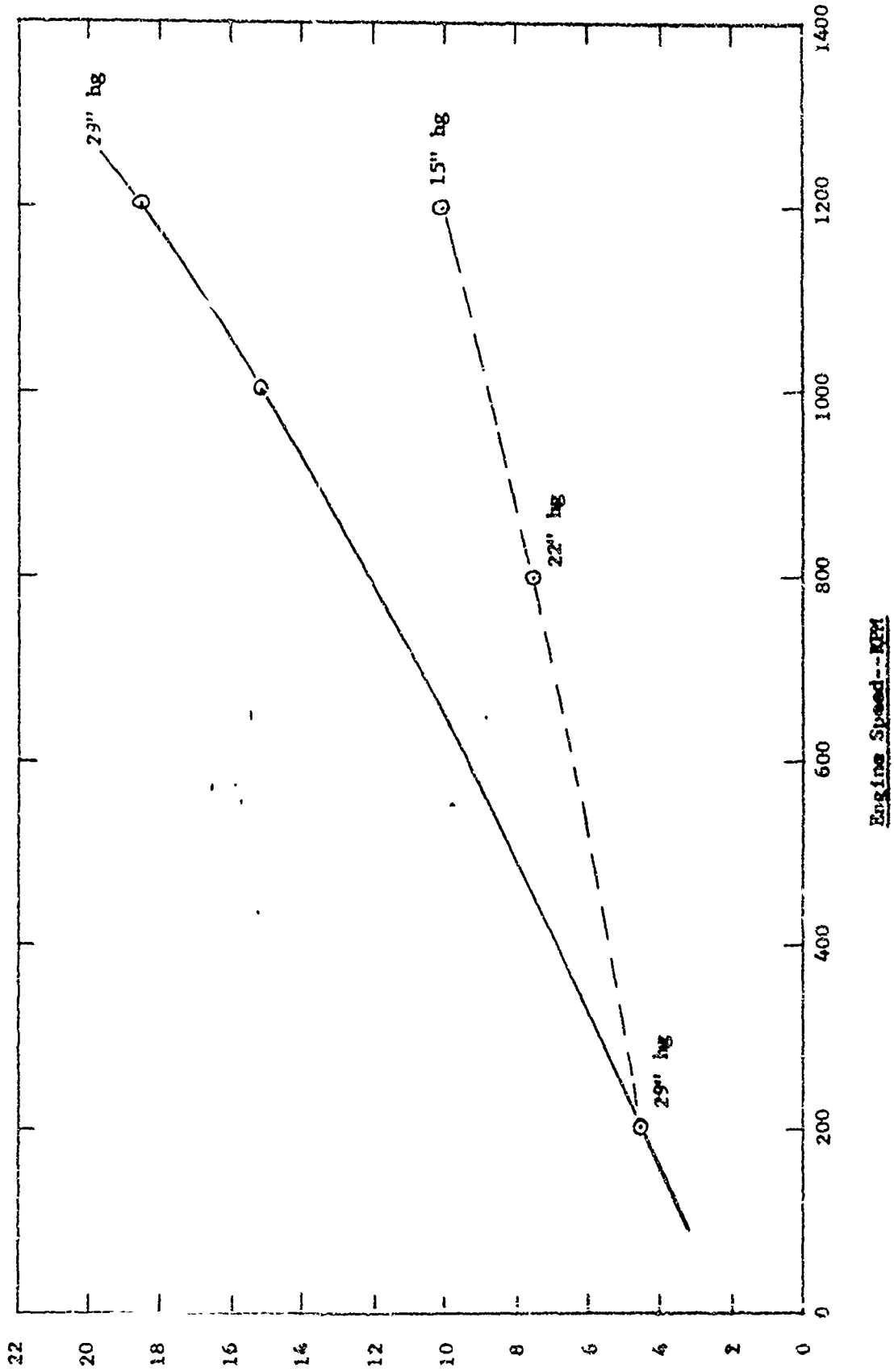
Figure C-3

Estimated Preheated Ammonia Temperature During Normal Engine Start

Engine Speed--RPM

Estimated Preheat Ammonia Temperature--°F
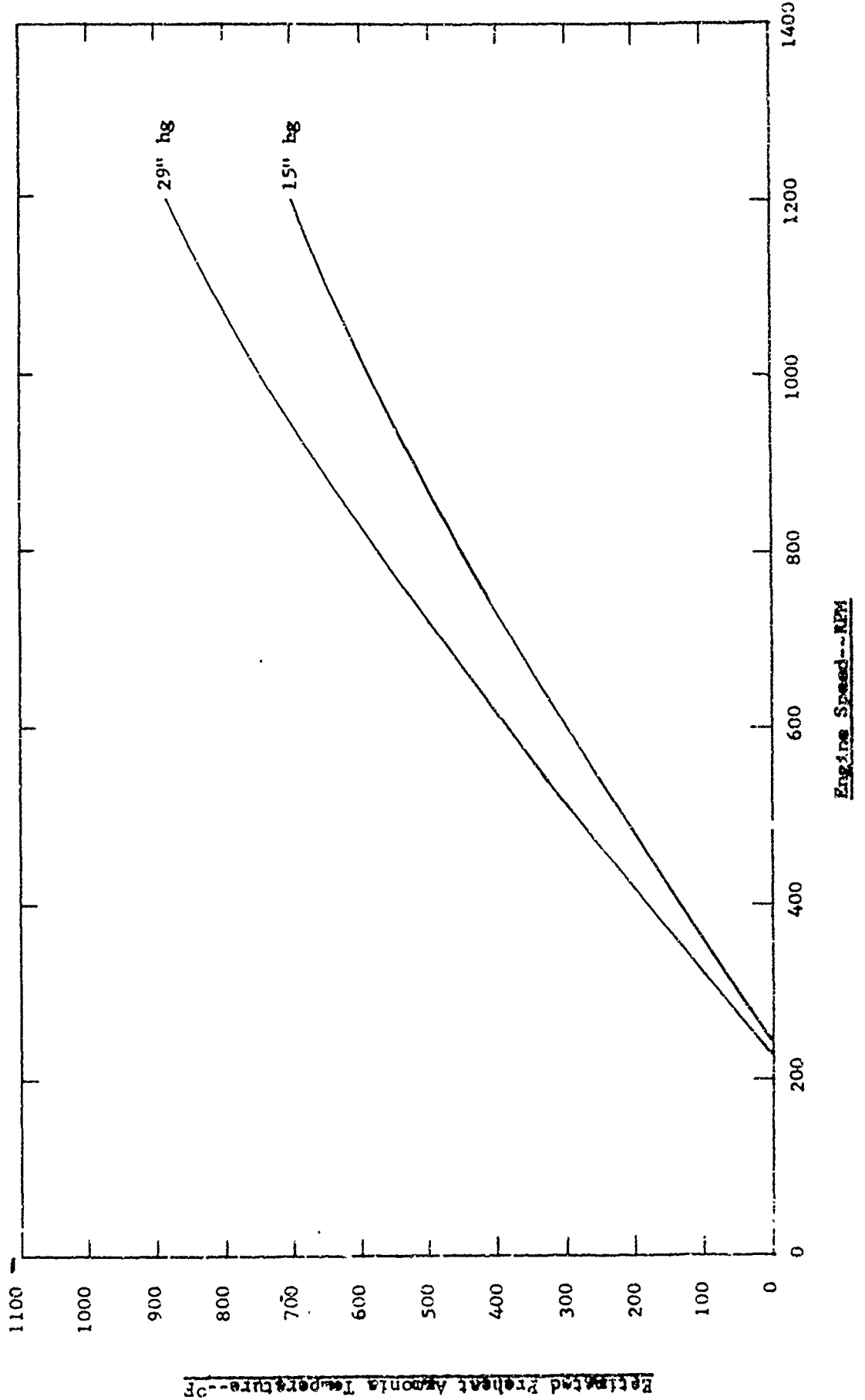
At 700°F inlet temperature, assume 15 psia pressure

$$v = \frac{.63T}{p} = \frac{.63 \times 1160}{15} = 48.8 \ ft^3/lb$$

At 3.52 lb/hr flow thru dissociator

$$V = 3.52 \ lb/hr \times 48.8 \ ft^3/lb = 172 \ ft^3/hr$$

$$= 2.9 \ ft^3/min$$

From catalyst performance curve (Figure 3) dissociator with nickel on alumina catalyst will be 1.5 in. long x 1.25 in. diameter with .05 lb. catalyst, 1.4 lb/hr NH_3 flow.

Resizing for 3.52 lb/hr flow:

$$\frac{3.52}{1.4} = 2.5 \times size$$

Area of 1.25 in. diameter catalyst bed = 1.227 in.^{2}

$$1.227 \ in.^2 \times 2.5 = 3.06 \ in.^2 = 2" \ diameter$$

Required catalyst bed size 1.5 in. long x 2 in. diameter

Catalyst weight = 2.5 x .05 lb. = .125 lbs.

Starting conditions (at 59°F Ambient temperature)

    200 RPM cranking speed

    29" hg. manifold pressure (14.2 psia)

Assume NH_3 vapor temperature = 59°F (to carb.)

Density of air

$$\rho = \frac{P}{RT} = \frac{14.2 \ psia \times 144 \ in.^2/ft^2}{53.3 \ ft.lb./lb°R \times 519°R} = .074 \ lb/ft^3$$

Density of NH_3

$$\rho = \frac{P}{RT} = \frac{14.2 \ psia \times 144 \ in.^2/ft^2}{90.77 \ ft.lb/lb°R \ r \ 519°R} = .0435 \ lb/ft^3$$

A/F Ratio (stoch.)   =   6.05.1

Assume Q   =   .95

A/F Ratio (by weight $=$ $\frac{6.05}{.95}$:1 $=$ 6.37:1

A/F Ratio (by volume) $=$ 6.37:$\frac{.074}{.0435}$ $=$ 6.37:1.7 $=$ 3.75:1

Engine Displacement $=$ 141 in.^{3}

Swept Volume per revolution $=$ $\frac{141 \text{ in}^3}{2 \times 1728 \text{ in}^3/\text{ft}^3}$ $=$ .0408 ft^3/rev.

Air flow at 200 RPM

   200 rev/min   x   .0408 ft^3/rev.   x $\frac{3.75}{4.75}$ $=$ 6.43 ft^3/min

   $=$ 386 ft^3/hr

W_a $=$ 386 ft^3/hr   x   .074 lb/ft^3 $=$ 28.6 lb/hr

NH_3 flow at 200 RPM

   200 rev/min   x   .0408 ft^3/rev   x $\frac{1}{4.75}$ $=$ 1.72 ft^3/min

   $=$ 103.2 ft^3/hr

W_f $=$ 103.2 ft^3/hr   x   .0435 lb/ft^3 $=$ 4.48 lb/hr

Assume 35.2% of W_f thru dissociator

   .352   x   4.48 lb/hr   =   1.59 lb/hr

Assume min. NH_3 vapor temperature to dissociator   =   -5°F

   (corresponding to vapor pressure of 10 psig)

Q_h required to heat 1.59 lb/hr from -5°F to 1000°F

   Q_h $=$ 1.59 lb/hr   x   .61 Btu/lb°F   x   1005°F $=$ 975 Btu/hr

Using the 1409 Btu/hr input, the remaining Q available for dissociation

   Q_d $=$ 1409 - 975 $=$ 434 Btu/hr

Estimated dissociation level of NH_3 out of dissociator

   $\frac{434 \text{ Btu/hr}}{1354 \text{ Btu/lb} \times 1.58 \text{ lb/hr}}$ $=$ 20.2%

Estimated effective dissociation

   $\frac{.202 \times 1.59 \text{ lb/hr}}{4.48 \text{ lb/hr}}$ $=$ 7.2%

% H_2 by weight $= \frac{3}{17}$ x .072 $\approx$ .012 = 1.2%

Cold start condition (Assume -40°F Ambient Temperature)

   200 RPM cranking speed

   29" hg. manifold pressure

   4.48 lb/hr NH_3 Flow

Q_h required to raise temperature of 4.48 lbs/hr liquid from -40°F to -5°F

Q_h = 4.48 lb/hr x 1.065 Btu/lb°F x 35°F = 167 Btu/hr

Q_v required to vaporize 4.48 lb/hr

Q_v = 4.48 lb/hr x 589.3 Btu/lb = 2640 Btu/hr

Total Q = 2640 + 167 = 2807 Btu/hr

Assume regenerative system to cool NH_3 out of dissociator from 1000°F to 100°F

Q available from regenerator

Q_r = 1.59 lb/hr x .61 Btu/lb°F x 900°F = 872 Btu/hr

Net Q requirement   2807 - 872 = 1935 Btu/hr

   1935 Btu/hr x .2931 watts/Btu/hr = 566 watts

   $\frac{566 \text{ watts}}{24 \text{ volts}}$ = 23.6 amps

Total power requirement during cold start (-40°F) vaporizer plus dissociator

   413 + 533 = 946 watts

   17.2 + 22.2 + 39.4 amps (at 24V)

Weight of 24V Battery with capacity of 54 amps for 5 minutes = 34 lbs.

(Exide #53033)

Check Point: 800 RPM

22" hg. Manifold Pressure

675°F Exhaust Temperature

7.5 lb/hr NH_3 Flow

Flow thru dissociator = .352 x 7.5 lb/hr = 2.64 lb/hr

From Figure C-3, NH_3 is preheated to 500°F

Q available   1409 Btu/hr

Assume (for trial) 5.65% dissociation of 7.5 lb/hr

    (or 16% dissociation of 2.64 lb/hr)

    (or 1% H_2 by weight)

Q_d = 1354 Btu/lb   x 7.5 lb/hr x .0565 = 573 Btu/hr

leaving 1409 - 573   =   836 Btu/hr for heating NH_3

Temperature in catalyst

$$500 + \frac{836 \text{ Btu/hr}}{2.64 \text{ lb/hr} \times .61 \text{ Btu/lb}^\circ\text{F}} = 1020^\circ\text{F}$$

which is the correct temperature for this dissociation level (Figure C-5).

Auxiliary Dissociator

Figure C-4

Calculated Enrichment During Start Using Electric Auxiliary Dissociator

59°F Ambient Temperature

413 Watts Power Input
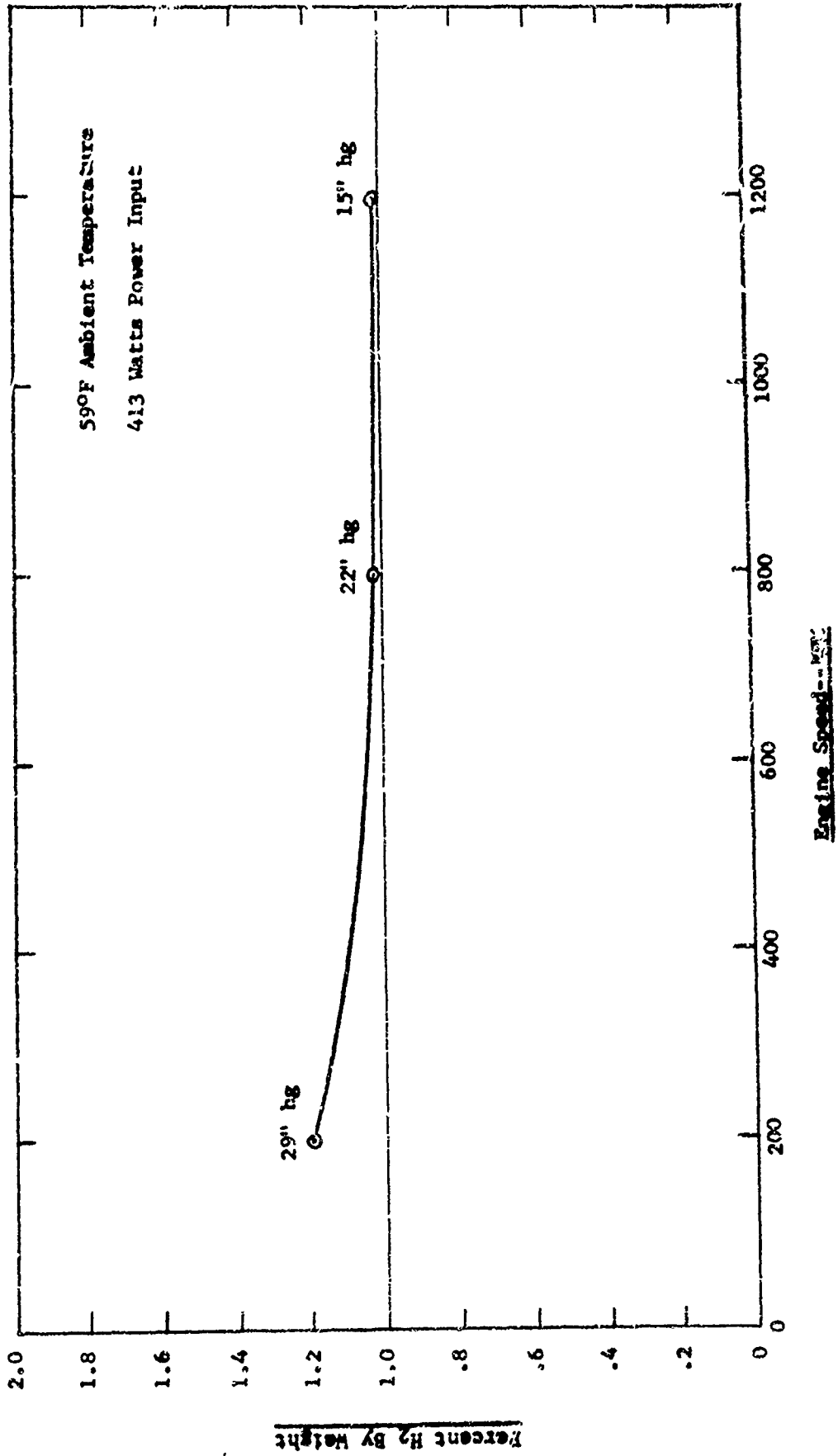
Figure P-5
Appendix III, Volume II
Percent Dissociated Versus Ammonia Temperature
for Nickel on Alumina Catalyst - Reference 1
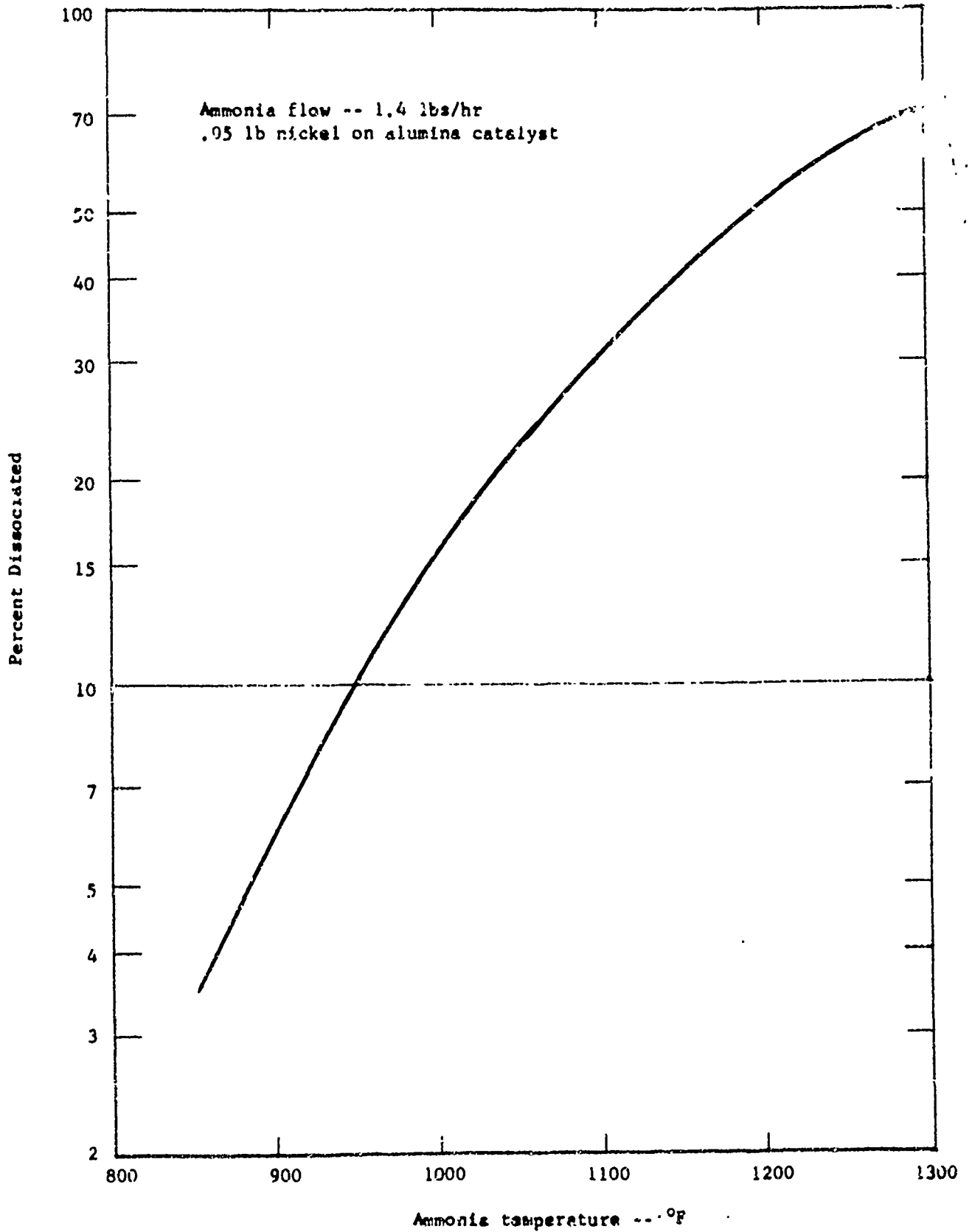
APPENDIX IV

Ammonia Combustion Aids

AMMONIA COMBUSTION AIDS

Two Approaches for Improving the Performance of Ammonia
As a Fuel for Reciprocating Engines

High-Energy Discharge Study

by

K. B. Schinke & C. T. Lunghard

Radio-Frequency Dissociation Study

by

S. J. Lukasik & P. H. Rank, Jr.

Approved

37 pages
3 tables, 22 figures
1 appendix (11 pages)

IRMIN O. KAMM
Assistant Manager
Transportation Research Group

FOREWORD

ABSTRACT

A study was conducted to determine the feasibility of using two
known sources of high energy to overcome some of the difficulties in-
volved in using ammonia as a reciprocating-engine fuel. The two approaches
were: (a) The employment of a high voltage, high-energy, spark discharge
across as large a gap as possible in the combustion chamber. "Bomb"
tests indicated that the desirable combustion characteristics could be
realized and that combustion of the mixture was reliable under conditions
of temperature and pressure which would cause a standard ignition system
to fail completely. (b) The dissociation of inlet air (nitrogen) by a
strong local radio-frequency field, adding the recombination energy to
the cylinder-trapped gases. Differential equations of reaction rates
were solved by using computer subroutine PRECOR. Product lifetimes were
less than desired, but temperature dependent.

KEY WORDS

Fuel
Energy Depot
Ignition
Ammonia
Dissociation
Engines (Reciprocating)

TABLE OF CONTENTS

LIST OF FIGURES

BACKGROUND

As a result of the Energy Depot Concept, calling for in-the-field production of internal-combustion-engine fuel, the feasibility of using anhydrous ammonia as a fuel has become of interest.

The suitability of ammonia as a fuel for the internal combustion engine depends on the answers to a number of questions. Some of these involve the cost and feasibility of producing ammonia in the field; others relate to the characteristics of an ammonia-fueled engine, such as ease of starting, power output, stability of operation, etc.; still others concern the modifications that might be required to enable the engine to use ammonia as a fuel, engine corrosion resulting from the combustion products, and so on.

Two peculiarities of the combustion of this gas, as compared with combustion of normal hydrocarbon fuels, are of particular importance. The first is the relatively large amount of energy necessary to ignite the reactants, and the second is the relatively slow speed of flame propagation.

It was therefore proposed to dissociate or ionize either the intake gases or the cylinder-trapped gases, to aid and accelerate the oxidation process in the combustion chamber; and this program was undertaken to examine the feasibility of using two known high-energy sources to achieve these ends without major modifications to present engines. Methods similar to those selected had already been used on a larger scale, to produce high energy for mobile radar equipment and high-temperature fusing equipment.

The present work was divided into two basic tasks: (a) the investigation of an arc discharge of much higher energy than is customary in spark-ignition applications, and (b) the dissociation of molecular nitrogen by passing the intake air through an intense local radio-frequency (RF) field.

HIGH-ENERGY DISCHARGE STUDY

It has been shown in previous work that the combustion of ammonia can be initiated through spark devices. However, ordinary spark devices operating on pure ammonia and air mixtures have left much to be desired, since the energy they make available is marginal for ignition. When supplied at a point source, the energy does not compensate for the extraordinarily low flame speed of ammonia fuel.

The purpose of this study was to learn whether or not a high-energy line discharge by the longest possible path could alleviate these problems.

It was first assumed that, if many times the minimum ignition energy were available, ammonia decomposition would (on a sufficiently large scale) result in the realization of better burning properties. Secondly, it was assumed that, if much of the volume of the chamber were to be affected by ionization due to the discharge rather than by the point source presented by a spark plug, the low flame speed would not have to be critical.

The investigation was conducted by means of a laboratory pulse generator which discharges its high energy by means of electrodes mounted in a "bomb" chamber containing controlled mixtures of ammonia and air at various pressures and temperatures.

APPARATUS

A "bomb" chamber with internal configuration approximating the combustion chamber at TDC of the LDS-465 engine was designed and built by using the upper portion of a piston from that engine and a flat plate to simulate the cylinder head (see Fig. 5). Several variants of this head were built, to allow for testing of different electrode configurations. The mixtures were introduced into the "bomb" from high-pressure tanks by means of pressure-regulation devices and valve arrangements, as shown in Figure 1.

The initial plan called for in-house design and construction of the high-energy pulse generator. It was found, however, that the Tobe-Deutschmann Company had just begun to manufacture a unit representing the forefront of the state of the art. Their unit is capable of producing up to 10 joules at up to 200-kV output pulse, with a duration of 10^{-7} seconds. The unit requires only a 10-kV, low current supply. In physical size (exclusive of power supply) it measures approximately 8 inches in diameter by 4 inches in height.

A standard coil and breaker ignition system was used for comparison. A Delco-Remy 328 coil was used. By increasing the primary voltage, output energy up to about 60 millijoules was made available. Spark-plug gaps ranged from 0.020 to 0.060 inches.

Dynamic pressure measurements were taken with a Kistler natural-quartz piezoelectric transducer, an amplifier calibrator, and a Tektronix oscilloscope. Pressure-time recordings were made by means of an oscilloscope camera (see Fig. 4 for typical example).

TEST PROGRAM

In order to test the pulser, atmospheric discharges with varying arc length were tried. Spectacular arcs up to 10 inches in length were drawn (see Fig. 2). When of any length in excess of about 4 inches, the arc is not confined to a single main bolt, but rather is spread to many fine tendrils following the lines of the electric field.

Automotive spark plugs, suitably modified, were selected for use as electrodes. Modification entailed the cutting away of the ground electrode and a portion of the thread, in order to provide spacing adequate for prevention of flash-over.

A series of "open air" observations was made, with the electrode mounted in the head plates to determine the path of the arc. A strong tendency to "short-cut" through the head plate was noted. A considerable measure of care had to be exercised in locating the electrodes, in order to centralize the discharge in the combustion chamber and provide a long discharge path without causing the arc to short-cut either to the head or piston crown (see Fig. 3).

After a few firings in the pressurized chamber, the performance of the system deteriorated rapidly. It was found that the ceramic insulation at the spark-plug nose had been punched through by the discharge, reducing the arc's length and severely masking it. After some trial and error, it was found that certain series of Autolite plugs have significantly thicker insulation at the nose. These performed satisfactorily throughout the remainder of the test program.

An effort was made to use hydrocarbon fuel, in the form of gasoline, for reference and calibration. Since the test equipment was designed for gaseous fuel, difficulty in controlling the air-fuel ratio and the degree of vaporization rendered this approach impractical. The obvious recourse was to use a gaseous fuel, thereby permitting familiarization with the gas-handling equipment for air-fuel ratio control (see Fig. 1). Thus, even though hydrocarbon fuel would have provided better reference data, hydrogen had to be used for check-out and calibration.

The optimum air-fuel ratio with hydrogen was determined experimentally. A determination was made of the effects on total combustion time of total chamber pressure and of total discharge energy at lean air-fuel ratios.

Ammonia combustion was then attempted. Again the optimum air-fuel ratio was experimentally determined. The difference in total combustion time between hydrogen and ammonia fuel was very clearly evidenced, not only by the oscillograph record, but by observations through a quartz window in the combustion chamber. Reliable ammonia combustion was achieved with the high-energy system, for all pressures in the range from 200 to 600 psig.

The effect of discharge energy at constant total pressure was investigated next, for air-fuel ratios at or near stoichiometric. It was found that combustion time did not increase significantly even at the lowest energy of which the pulse generator was capable (about 5 joules).

For the sake of convenience, these first tests were performed with the bomb and gases at room temperature. It was felt that these conditions (and the lack of turbulence and swirl), although not realistic, were very much more severe than those in an actual engine. Chamber temperature was then elevated by insertion into an oven -- with a practical limit of $710^{o}R$ set to prevent damage to equipment. The temperature dependence of combustion time and pressure rise was thus determined.

Up to this time, all tests had been performed with a head plate which provided a 3/16-inch gap 3/8-inch below the head (see Figs. 5, 6, and 7). Now a second head plate was installed in which the arc was placed deeper in the chamber ($\frac{1}{2}$ inch) and lengthened to 3/8 inch; and the tests were repeated.

RESULTS

Experimental results are plotted in Figures 8 through 15. Figures 8, 9, and 10 show the results of calibration runs with hydrogen.

Figure 11 indicates the determination of best fuel-air ratio, on the basis of minimized combustion time. This was found to be slightly in excess of 18-percent ammonia by pressure.

The effect of total initial pressure on the total combustion time is relatively small in the region tested (see Fig. 12). The variation is on the order of ±10 milliseconds about the average of about 100 msec, showing no specific trend.

The effect of discharge energy on total combustion time, shown in Figure 13, is also small in the range provided by the pulse generator. The energy provided by a coil and breaker ignition system, however, was insufficient to initiate combustion at all. This seems to indicate that the pulse generator is much more productive than necessary to obtain reliable, rapid combustion. Perhaps the most interesting feature of Figure 13, however, is the large difference in total combustion time, at all energy values, between the small- and large-gap electrode configurations. The combustion time with small gap is nearly halved in going to the larger gap. This supports the initial premise that increasing the amount of gas affected by the discharge (by increasing arc length) would tend to counteract the slow flame speed of ammonia.

The effect of temperature on combustion time is plotted in Figure 14. Combustion time decreases significantly with temperature, for both large and small discharge paths. Of more interest than the actual values in the range tested is the trend indicated by the curves. Polytropic compression (k=1.35) with compression ratios of 10 and 20 yields compression end temperatures of about 1200° and $1460^{\circ}R$ respectively. A conservative extrapolation of the curves in Figure 14 yields results on the order of a few milliseconds -- i.e., the practical range for an engine.

Perhaps the most interesting combustion characteristic is the rate of pressure rise. In Figure 15, pressure rise per millisecond is plotted against temperature, with the initial pressure and discharge length as

the parameters. The pressure rate is very strongly affected by the discharge length, the longer path yielding between two and three times the rate of the shorter path. Also, the increase in rate with temperature is quite strong. These results can be interpreted in terms of an engine by relating pressure rise per millisecond to crank-angle degrees of an engine. At 2,000 rpm, one millisecond is equivalent to 1.2 degrees of rotation. In a diesel engine, pressure rates of 3 to 6 atm (44 to 88 psi) per degree are normal. An engine with 10:1 compression ratio will have compression end conditions of $1200^{\circ}R$ and 330 psig. Likewise, the 20:1 engine will have $1460^{\circ}R$ and 840 psig. Extrapolating the experimental data conservatively, and dividing by 1.2 to convert to crank angle at 2,000 rpm, we obtain 6 and 10 atm (88 and 147 psi) per degree crankshaft, respectively, for the two compression ratios.

In summary, the high-energy system produced reliable combustion under much less favorable conditions than one would expect in an engine even under adverse conditions such as cold starting, and -- in fact -- even under circumstances in which a standard ignition system failed to produce ignition at all. Extrapolation of results of tests indicates that a high-energy system can reduce total combustion time to appropriate values. If this energy is released through a large portion of the mixture, pressure rates can be raised sufficiently for engine operation, even in a test chamber without turbulence, and at low temperatures.

CONCLUSIONS

It has been demonstrated to our satisfaction that the initial assumptions (with regard to the effect of a high-energy line discharge) hold -- and that ammonia-combustion characteristics are enhanced by the use of a high-energy line discharge.

It is highly significant that the high-energy system ignited the mixture at conditions under which the coil and breaker system failed completely. It is also very significant that increasing the arc length reduced combustion time drastically.

To arguments against the extrapolation to engine temperatures, from test temperatures, it may be pointed out that these extrapolations were made very conservatively. (Furthermore, even at the temperature of $710^{o}R$ the pressure rate is on the order of 3 atm per millisecond, and the results show a safety margin.)

There are strong indications that the energy needed to yield the improvement in combustion is less than that produced by the laboratory pulse generator, and that a unit for engine use could be smaller. In preliminary discussions, representatives of the Tobe-Deutschmann Company have indicated that a unit of reduced energy capacity can be built with repetition rates commensurate with engine requirements, without encounter with any great technical difficulty. Furthermore, other manufacturers of high-energy pulse systems are developing units which may be applicable, and available, soon.

RECOMMENDATION

In the light of the promising results of these tests, it is recommended that a pulse generator with attendant equipment, suitable for engine operation, be assembled and tested. Several engines should be selected for the purpose and modified to incorporate electrode location and spacing which will enhance, to the maximum possible extent, the properties found desirable in this study.

RADIO-FREQUENCY DISSOCIATION STUDY

During early discussions of the problems presented by ammonia-fueled internal combustion engines, attention was centered on the question of ignition. The larger ignition energy and the slower flame speed for ammonia-air as compared with hydrocarbon-air mixtures suggested consideration of alternatives to the conventional spark ignition. One scheme that appeared to be attractive was that of dissociating a part of the incoming nitrogen in a manifold by means of an electrodeless RF discharge. The atomic nitrogen would then be distributed to the engine cylinders along with the ammonia-air mixture. Upon recombining, the nitrogen dissociation energy would be recovered and would be available for ignition of the ammonia. In this way large amounts of ignition energy could be added to the air-fuel mixture and, most importantly, the energy would be distributed over the entire volume of reactants, instead of being concentrated in a small region of space around the spark discharge.

Experience with RF dissociation of pure nitrogen indicated that the RF energy source was not particularly difficult to construct, that the atomic nitrogen has a sufficiently long lifetime, and that the recombination can be easily stimulated by interposing a refractory surface into the dissociated nitrogen stream. However, it is important to note that in the RF discharge-region relatively high temperatures exist; and this has the effect of prolonging the atomic nitrogen lifetime. In view of the differences between the RF dissociation of pure nitrogen and the use contemplated here as an aid to the ignition of an ammonia-air mixture, it was felt that theoretical calculations should be undertaken before even consideration of any practical implementation of the idea.

Within the limitations imposed, a modest program was undertaken focusing on two basic problems:

    a. The time scale of the nitrogen recombination as a function of temperature and initial atomic nitrogen density

    b. Significant effect of the presence of oxygen on the time scale of the recombination

These questions have been examined by solving appropriate sets of differential equations that express the rates at which the various chemical reactions proceed. By carrying out such calculations parametrically, in terms of the degree of dissociation and temperature, considerable insight can be obtained into the processes taking place. In Section A the kinetics of the dissociated-nitrogen air system are discussed. This includes all of the possibly important reactions and their rate coefficients. In Section B a number of numerical results are presented for a series of increasingly sophisticated models used to describe the time behavior of the dissociated-nitrogen air system. Conclusions and recommendations are contained in Section C. Finally, in the Appendix of this report, some of the numerical techniques employed are briefly summarized.

KINETICS OF THE DISSOCIATED-NITROGEN AIR SYSTEM

It is assumed that, by means of an RF discharge operating in air, N_2 is dissociated to atomic nitrogen.

$$N_2 \rightarrow N + N \tag{1}$$

Furthermore, it is assumed that the corresponding oxygen dissociation does not proceed significantly until all of the molecular nitrogen is dissociated. In addition, we neglect the following:

a. Mass diffusion from the manifold-reactor region

b. Wall effects

c. Heat addition due to chemical reactions

Thus, we have as the initial state of the manifold a mixture of N_2, O_2, and N. The pressure is likely to be atmospheric and the temperature $\geq 300°K$ ($540°R$) depending on the degree of heating resulting from the RF discharge.

Primary Reactions

The lifetime of the atomic nitrogen is of major interest. We can approach this problem most simply if we restrict ourselves to considera-tion of the reactions that can be supported by the initial mixture only. One class of such reactions is nitrogen recombination which usually proceeds via the three-body process

$$N + N + M \rightarrow N_2 + M \tag{2}$$

where M can be N, N_2, or O_2. A very complete review of the reaction-rate literature relating to this process can be found in Cary.[8] Reaction rates when the third body is N or N_2 are well known; the reac-tion rate when the third body is O_2 has not been specifically investi-gated, but one can assume that it is similar to the rate when the third body is N_2. The rate of the radiative recombination process

R-1122

$$N + N \rightarrow N_2 + h\nu \qquad (3)$$

is negligible.[4]

Atomic nitrogen can be lost not only by nitrogen recombination but also by oxidation. This proceeds either to NO with atomic oxygen as a product,

$$N + O_2 \rightarrow NO + O \qquad (4)$$

or radiatively to NO_2,

$$N + O_2 \rightarrow NO_2 + h\nu \qquad (5)$$

The rate for (4) has been investigated by a number of workers and can be considered to be reasonably well known.[24, 25,28,32] The rate for the radiative process (5) has been estimated by Bortner.[4]

Secondary Reactions

Note that (4) and (5) form O, NO, and NO_2. If the degree of nitrogen dissociation is small and/or the net effect of (2)-(5) does not result in a significant loss of N then the formation of O, NO, and NO_2 can be ignored. However, if significant amounts of O, NO, and NO_2 are formed, then their reactions must be considered also. This involves a large number of reactions, potentially, although one expects to find only a few that are actually dominant. The secondary reactions can be divided into these classes:

a. Reactions of O_2 or N_2 (which are expected to be present in substantial amounts) with O, NO, or NO_2

b. Reactions requiring N (which may not be present in a substantial amount) and O, NO, or NO_2

c. Reactions requiring O, NO, and NO_2 only

d. Reactions requiring O_3 and N_2O, which are formed as products of reactions in classes a and b

13

These are now considered in detail.

a. Reactions of O_2 or N_2 with O, NO, or NO_2

The three-body reaction

$$NO + NO + O_2 \rightarrow NO_2 + NO_2 \tag{6}$$
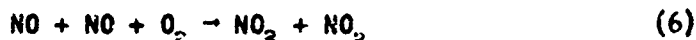
has been investigated by Harteck and Dondes.[18] Ozone formation proceeds either by the three-body process

$$O + O_2 + M \rightarrow O_3 + M \tag{7}$$

or radiatively,

$$O + O_2 \rightarrow O_3 + h\nu \tag{8}$$

The former has been studied by Axworthy and Benson,[1] Zaslowsky et al,[39] and Campbell and Nudelman.[7] The reaction rate for the radiative process has been estimated by Bortner.[4] Finally, there are the oxidation processes.

$$O + N_2 \rightarrow NO + N \tag{9}$$

$$O + N_2 \rightarrow N_2O + h\nu \tag{10}$$

$$O + N_2 + M \rightarrow N_2O + M \tag{11}$$

The two-body rearrangement reaction (9) has been extensively studied by Kaufman and Kelso,[24] Kistiakowsky and Volpi,[26] Wray and Teare,[37] Clyne and Thrush,[9] Phillips and Schiff.[33] The two-body radiative rate for (10) has been estimated by Bortner.[4] The three-body process (11) has been studied by Harteck and Dondes.[16]

b. Reactions of N with O, NO, or NO_2

The reaction of N and O to NO can take place either by a three-body process,

$$N + O + M \rightarrow NO + M \tag{12}$$

or radiatively,

$$N + O \rightarrow NO + h\nu \tag{13}$$

The rate of (12) has been studied by Harteck, Reeves, and Mannella,[17] Barth,[2] and Kaplan and Barth[21] while the rate of (13) has been estimated by Bortner.[4]

The reaction of N and NO can take place either by the rearrangement process

$$N + NO \rightarrow N_2 + O \tag{14}$$

studied by Kistiakowsky and Volpi,[26] Nicolet and Aikin,[32] Kaufman and Kelso,[24] Herron,[19] Clyne and Thrush,[9] and Phillips and Schiff[33] — or radiatively,

$$N + NO \rightarrow N_2O + h\nu \tag{15}$$

for which the rate has been estimated by Bortner.[4]

The reaction of N and NO_2 can proceed to a variety of products:

$$N + NO_2 \rightarrow NO + NO \tag{16}$$

$$N + NO_2 \rightarrow N_2O + O \tag{17}$$

$$N + NO_2 \rightarrow N_2 + O + O \tag{18}$$

$$N + NO_2 \rightarrow N_2 + O_2 \tag{19}$$

Reactions (16)-(18) have been studied by Harteck and Dondes[44,18] while the rate of (19) has been estimated by Bortner.[4]

c. Reactions requiring O , NO , NO_2 only

Oxygen recombination can take place either by a three-body process,

$$O + O + M \rightarrow O_2 + M \tag{20}$$

or radiatively,

$$0 + 0 \rightarrow O_2 + h\nu \qquad (21)$$

The three-body process has been studied by Golden and Myerson,[14] Kaufman and Kelso,[47] Reeves, Mannella, and Harteck,[34] Morgan, Elias, and Schiff,[29] and Kaplan and Barth.[21] The radiative process has been considered by Nicolet[30] and Nicolet and Mange.[31]

O and NO react in these three different ways:

$$0 + NO + M \rightarrow NO_2 + M \qquad (22)$$

$$0 + NO \rightarrow NO_2 + h\nu \qquad (23)$$

$$0 + NO \rightarrow O_2 + N \qquad (24)$$

The three-body reaction (22) has been studied by Kaufman and Kelso,[24] Kaufman,[23] and Ford, Doyle and Endow.[12] The radiative path to NO_2 , (23), has been treated by Clyne and Thrush,[10] while the rearrangement reaction (24) has been examined by Kaufman and Kelso,[24] Wray and Teare,[37] and Kistiakowsky and Volpi.[25]

Finally, 0 and NO_2 can react by

$$NO_2 + 0 \rightarrow NO + O_2 \qquad (25)$$

Reaction rates have been reported by Ford, Doyle, and Endow,[12] Harteck and Dondes,[18] Kaufman and Kelso,[24] and Phillips and Schiff.[33]

d. Reactions requiring O_3 and N O

The two reactions of interest that consume O_3 are

$$0 + O_3 \rightarrow O_2 + O_2 \qquad (26)$$

$$NO + O_3 \rightarrow NO_2 + O_2 \qquad (27)$$
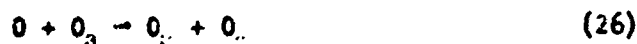
The first of these, (26), has been studied by Benson and Axworthy,[3] Zarlowsky et al,[39] Phillips and Schiff,[33] and Campbell and Nudelman.[7]

The second reaction, (27), has been examined by Johnston and Crosby,[20] and by Greaves and Garvin.[15]

Finally, N_2O can react with O in the following two possible ways:

$$O + N_2O \to O_2 + N_2 \tag{28}$$

$$O + N_2O \to NO + NO \tag{29}$$

The first of these, (28), has been studied by Bradley and Kistiakowsky,[5] Fenimore,[11] and Kaufman, Gerri, and Bowman.[22] The second reaction, (29), has been considered by Wray and Teare[37] and by Kaufman, Gerri, and Bowman.[22]

Other Reactions

There are a number of other possible reactions that are not believed to be important at normal temperatures and pressures. While it is conceivable that they may occur during the high-temperature and high-pressure conditions attendant upon the ammonia combustion, the low concentrations of the reactants probably still justifies their neglect. These reactions are

$$NO + M \to N + O + M \tag{30}$$

$$NO_2 + M \to O + NO + M \tag{31}$$

$$O_3 + M \to O + O_2 + M \tag{32}$$

$$N_2O + M \to O + N + M \tag{33}$$

Wray and Teare[37] and Freedman and Daiber[13] have considered (30) while Bradley and Kistiakowsky[5] and Fenimore[11] have considered (31). Bortner[4] has commented on (32) and (33).

Finally, while collisional dissociation of N_2 and O_2,

$$N_2 + M \to N + N + M \tag{34}$$

$$O_2 + M \to O + O + M \tag{35}$$

obviously does not proceed rapidly at normal temperature and pressure, these reactions may play a role during combustion. The work of Cary[8]

R-1122

In connection with (34) has already been mentioned. Studies of the collisional dissociation of O_2 have been made by Rink, Knight, and Duff,[35] Byron,[6] Matthews,[27] Schexnayder and Evans,[36] and Wray.[38]

Reaction Rates

Before quantitative calculations can be made of the nitrogen recombination times resulting from the preceding reactions, one must have numerical values for the reaction rates. These have been obtained from several secondary sources such as published review papers and unpublished industrial reports. These in turn reference the primary publication of the data. The reaction rates are presented below in tabular form, along with references to both the primary and the secondary source of the information. In some cases the information is available as a function of temperature, while in others a single value for a specific temperature is given. In some cases rather considerable differences in the reaction rates may be observed. These differences serve to emphasize the uncertainty attached to this type of information, sometimes of the order of several orders of magnitude. The physical origin of these differences lies in the difficulty of ascertaining in a given experiment the degree of electronic excitation of the reactants and their velocity distribution. Thus different experimental measurements of what is presumed to be the same physical quantity sometimes yield rather dissimilar results. In such a case, however, it is often possible — by judicious choice of values for a calculation — to set upper or lower limits for a particular reaction rate and thereby establish its importance or unimportance.

Reaction-rate tables follow.

TABLE 1

REACTION RATES FOR THE DISSOCIATED-NITROGEN AIR SYSTEM
(Primary Reactions)

Reaction		Equation Number	Rate	Temp.	Primary Reference	Secondary Reference
N+N+M→N₂+M	(M-N₂)	2	$5 \times 10^{-30 \pm 0.5} T^{-1} cm^6/sec$	—	45,17,42	4
	(M-N)		$5 \times 10^{-30 \pm 0.5} T^{-1}$	—	—	4
	(M/N,N₂)		$3 \times 10^{-30 \pm 0.5} T^{-1}$	—	—	4
			1.4×10^{-32}	300°K (540°R)	46,21	7
			2×10^{-33}	300°K (540°R)	45	43
N+N→N₂+hν		3	—	—	—	4
N+O₂→NO+O		4	$3.3 \times 10^{-12} e^{-3100/T} cm^3/sec$	—	25	2
			$1.5 \times 10^{-13} e^{-6200/RT}$	—	25,32	43
			$4 \times 10^{-13 \pm 0.5} T^{1/2} e^{-6600/RT}$	—	24,28	4
N+O₂→NO₂+hν		5	$10^{-20 \pm 2} cm^3/sec$	—	—	4

TABLE 2

REACTION RATES FOR THE DISSOCIATED-NITROGEN AIR SYSTEM
(Secondary Reactions - Type a)

Reaction	Equation Number	Rate	Temp.	Primary Reference	Secondary Reference
$NO+NO+O_2 \rightarrow NO_2+NO_2$	6	$10^{-37\pm0.2}$ cm^6/sec	$300^\circ K$ $(540^\circ R)$	18	43
$O+O_2+M \rightarrow O_3+M$	7	$10^{-34.5\pm0.5}$ cm^6/sec	$300^\circ K$ $(540^\circ R)$	1	43
		6.8×10^{-34} $e^{300/T}$	—	3	2
		3×10^{-34}	—	3,29,7	4
$O+O_2 \rightarrow O_3+h\nu$	8	$10^{-20\pm2}$ cm^3/sec	—	—	4
$O+N_2 \rightarrow NO+N$	9	$10^{-10\pm0.5}$ $e^{-37500/T}$ cm^3/sec	—	24,26,37,9,33	4
$O+N_2 \rightarrow N_2O+h\nu$	10	$10^{-20\pm2}$ cm^3/sec	—	—	4
$O+N_2+M \rightarrow N_2O+M$	11	2×10^{-33} $e^{-1200/RT}$ cm^6/sec	—	16	4

TABLE 2 (Cont'd)

REACTION RATES FOR THE DISSOCIATED-NITROGEN AIR SYSTEM

(Secondary Reactions - Type b)

Reaction	Equation Number	Rate	Temp.	Primary Reference	Secondary Reference
$N+O+M \rightarrow NO+M$	12	$5 \times 10^{-31 \pm 0.5} \, T^{-1/2} \, cm^6/sec$	—	17	4,2
		1.5×10^{-32}	$300°K$ $(540°R)$	21	2
$N+O \rightarrow NO+h\nu$	13	$10^{-23 \pm 2} \, cm^3/sec$	—	—	4
$N+NO \rightarrow N_2+O$	14	$2.2 \times 10^{-11 \pm 0.5} \, cm^3/sec$	—	24,19,9,33	4
		8.3×10^{-11}	$300°K$ $(540°R)$	26	2
		$1.5 \times 10^{-11} \, T^{1/2}$	—	26,32	43
$N+NO \rightarrow N_2O+h\nu$	15	$10^{-20 \pm 2} \, cm^3/sec$	—	—	4
$N+NO_2 \rightarrow NO+NO$	16	$5 \times 10^{-14 \pm 0.5} \, cm^3/sec$	$300°K$ $(540°R)$	18	43
$N+NO_2 \rightarrow N_2O+O$	17	$3.2 \times 10^{-14 \pm 0.5} \, cm^3/sec$	$300°K$ $(540°R)$	18	43
$N+NO \rightarrow N_2+O+O$	18	$2 \times 10^{-14 \pm 0.5} \, cm^3/sec$	$300°K$ $(540°R)$	18	43
$N+NO_2 \rightarrow N_2+O_2$	19	$2 \times 10^{-14 \pm 1} \, cm^3/sec$	—	—	4

TABLE 2 (Cont'd)

REACTION RATES FOR THE DISSOCIATED-NITROGEN AIR SYSTEM
(Secondary Reactions - Type c)

Reaction	Equation Number	Rate	Temp.	Primary Reference	Secondary Reference
$O+O+M \cdot O_2+M$ (M-O_2)	20	$6 \times 10^{-32 \pm 0.5} T^{-1/2}$ cm^6/sec	—	14,47,34,79	4
(M-O)		$2 \times 10^{-31 \pm 0.5} T^{-1/2}$	—	—	4
(M/O,O_2)		$10^{-32 \pm 0.5} T^{-1/2}$	—	—	4
		1.6×10^{-32}	300°K (540°R)	29,21	2
		3×10^{-33}	300°K (540°R)	14	43
$O+O \cdot O_2+h\nu$	21	$10^{-22 \pm 2}$ cm^3/sec	—	31,30,48	4,43
$O+NO+M \cdot NO_2+M$ (M-N_2,A)	22	5.5×10^{-32} cm^6/sec	300°K (540°R)	23	43
		5×10^{-32}	—	24	4
		5.2×10^{-32}	300°K (540°R)	12	2
$O+NO \cdot NO_2+h\nu$	23	$10^{-20 \pm 2}$ cm^3/sec	—	10	4
$O+NO \cdot O_2+N$	24	$10^{-13 \pm 0.5} T^{1/2} e^{-38600/RT}$ cm^3/sec	—	24,37,25	4
$NO_2+O \cdot NO+O_2$	25	10^{-12} cm^3/sec	300°K (540°R)	18	43
		3.5×10^{-12}	300°K (540°R)	12	2
		$2.5 \times 10^{-12 \pm 0.5}$	—	24,33	4

TABLE 2 (Cont'd)

REACTION RATES FOR THE DISSOCIATED-NITROGEN AIR SYSTEM

(Secondary Reactions – Type d)

Reaction	Equation Number	Rate	Temp.	Primary Reference	Secondary Reference
$O+O_3 \cdot O_2+O_2$	26	$5.0 \times 10^{-11} e^{-3000/T} \ cm^3/sec$	–	3	2
		$7.1 \times 10^{-12 \pm 0.5} e^{-1600/T}$	–	3,39,33,7	4
$NO+O_3 \cdot NO_2+O_2$	27	$8 \times 10^{-13} T^{1/2} e^{-2500/RT} \ cm^3/sec$	198-230°K (356-414°R)	20,15	43
$O+N_2O \cdot O_2+N_2$	28	$5 \times 10^{-11 \pm 1} e^{-27000/RT} \ cm^3/sec$	–	5,22,11	4
$O+N_2O \cdot NO+NO$	29	$1.7 \times 10^{-10 \pm 1} e^{-28000/RT} \ cm^3/sec$	–	37,22	4

TABLE 3

UNIMPORTANT REACTIONS FOR THE DISSOCIATED-NITROGEN AIR SYSTEM

Reaction	Equation Number	Primary Reference	Secondary Reference
$NO+M \rightarrow N+O+M$	30	37,13	4
$NO_2+M \rightarrow O+NO+M$	31	5,11	4
$O_2+M \rightarrow O+O_2+M$	32	--	4
$N_2O+M \rightarrow O+N_2+M$	33	—	4
$N_2+M \rightarrow N+N+M$	34	40,41,42,8	4
$O_2+M \rightarrow O+O+M$	35	35,6,27,36,38	4

CALCULATION OF NITROGEN RECOMBINATION TIMES

We have considered four models for the chemical reactions occurring after a given amount of nitrogen is dissociated. The first two models lend themselves to analytic solutions; the last two were solved numerically.

Model 1

In Model 1 we consider the recombination of N to N_2 by a three-body reaction where the third body M may be O_2, N_2, or N. Furthermore, we assume that the concentration of the third body is constant.

The chemical equation is

$$N + N + M \rightarrow N_2 + M \tag{36}$$

and the associated rate equation is

$$\frac{dn[N]}{dt} = k\, n[M]\; \{n[N]\}^2 \tag{37}$$

where $n[X]$ is the concentration of X, $(X = N, N_2$ or $O_2)$ and k is the rate constant for this reaction.

If we dissociate f percent of the N_2, then the initial amount of N is given by $2f/100$ times the initial concentration of N_2. The initial concentration of N_2 can be computed by noting that at STP there are 6.02×10^{23} molecules of air per 22.4 liters. Hence the concentration of air is given by

$$\frac{6.02 \times 10^{23}}{22.4 \times 10^3} = 2.69 \times 10^{19} \text{ molecules of air per cm}^3$$

If we assume air consists of 20-percent O_2 and 80-percent N_2, the initial concentration of N, $n_o[N]$, is given by

$$n_o[N] = 4.3f \times 10^{17} \text{ cm}^{-3}$$

Here we have assumed standard temperature, $T = 300^\circ K$. If we assume

the concentration is inversely proportional to the temperature, then $n_o[N]$ is given by

$$n_o[N] = 4.3 \ f \times 10^{17} \ (300/T)$$

If we assume $n[M]$ is a constant, then

$$n[M] = (2.69 \times 10^{19}) \ \left(\frac{300}{T}\right)$$

The rate constant k is given by[4]

$$k = 5.0 \times 10^{-30}/T \ cm^6/sec$$

Solving equation (37) we have

$$n[N] = \frac{n_o[N]}{1 + n_o[N] \ n[M] \ k \ t} \tag{38}$$

Inserting numerical values,

$$n[N] = T^2 \left[\frac{1.29 \times 10^{20}}{\frac{T^2}{f} + (5.2 \times 10^{12}) \ t} \right]$$

Therefore, for large values of time $\left(t \gg \frac{T^3}{5.2f} \times 10^{-12}\right)$ we have

$$n[N] = T^2 \ (2.48 \times 10^7)/t$$

Hence the amount N, in this approximation, is essentially independent of the initial amount of N, decreases as $1/t$, and is proportional to the square of the temperature (the temperature once set, is assumed constant).

Model 2

In Model 1 we assumed that the concentration of the third body remained fixed; in fact this is not the case, for each time you form an

N_2 molecule you lose two atoms for each molecule gained. Also, there is a small difference between the rate constant when the third body is N_2 or N, and O_2. Model 2 takes these effects into consideration.

The chemical equation is the same as before, but the rate equation is

$$\frac{dM[N]}{dt} = (k_n n[N] + k_n n[N_2] + k_o n[O_2]) \, n[N] \tag{39}$$

where k_n is the rate constant for N_2 or N as the third body and k_o is the rate constant for O_2 as the third body.

The solution for (39) is

$$n[N] = \frac{n_o[N]}{1 + n_o[N]B K_n t} \left[1 + \frac{n[N]}{n_o[N]} \log \left\{ \frac{n[N]}{n_o[N]} \left(\frac{n_o[N]+B}{n[N]+B} \right) \right\} \right] \tag{40}$$

where $B = n_o[N_2] + \frac{1}{2} n_o[N] + \frac{k_o}{k_n} n_o[O_2]$ and

$$k_n = 5 \times 10^{-30}/T \quad cm^6/sec$$

$$k_o = 3 \times 10^{-30}/T \quad cm^6/sec$$

Therefore as the concentration decreases we have

$$\frac{n[N]}{n_o[N]} \log \left\{ \frac{n[N]}{n_o[N]} \left(\frac{n_o[N] + B}{n[N] + B} \right) \right\} \ll 1$$

and hence the solution takes the same form as (38) with $n[M]$ replaced by B.

If we plotted the Model 1 or Model 2 solution on a logarithmic scale, we would expect asymptotically to have a straight line with slope -1. Figures 16 and 17 show the results for Models 1 and 2 for 10-percent dissociation at $T = 300^\circ K$ and at $T = 600^\circ K$. Several points are apparent from these figures. First, the time scale for the recombination is short. At about 0.1 msec the atomic nitrogen concentration has decreased by two

orders of magnitude. By this time the asymptotic behavior has been achieved so that $n[N] \sim 1/t$; hence the atomic nitrogen concentration decreases by another order of magnitude by 1 msec. To put the time scale into proper perspective, one can assume an average linear flow velocity from the manifold into the cylinder of about 100 m/sec. If the distance from the atomic nitrogen source to the cylinder is 5 cm, then the transit time is about 0.5 msec and so a sufficient amount of atomic nitrogen must survive to times of this order of magnitude if it is to assist in the ammonia combustion.

The second major point is that high temperatures lead to higher concentrations at late times. This is due to the $1/T$ dependence of the recombination constant. At higher temperatures k decreases and so the recombination proceeds more slowly. The manifold temperature will be of the order of room temperature ($300°K$) while the cylinder temperature at peak compression may be of $700-800°K$. It was with these temperatures in mind that $300°K$ and a conservative $600°K$ was assumed. However, the major significance of the $600°K$ calculations is to demonstrate the direction of the temperature dependence of the reaction rates, since it is the lower temperature manifold conditions that are expected to control the atomic nitrogen recombination.

The third point is that aside from some minor differences for times less than 0.1 msec, Models 1 and 2 give identical results at both $300°$ and $600°K$. This similarity is what one expects when the degree of dissociation is small. If $n_o[N]$ is not large, the third-body concentration is almost constant. Regardless of the initial dissociation, there will always be some late time when $n[N]$ has decreased sufficiently to a point where the third-body concentration is no longer changing significantly.

Model 3

Up to now we have neglected any reactions involving O_2 with N. The two most significant are

$$N + O_2 \rightarrow NO + O \qquad k_1 = (3.3 \times 10^{-12}) e^{-3100/T} \text{ cm}^3/\text{sec} \qquad (41)$$

$$N + O_2 \rightarrow NO_2 + h\nu \qquad k_2 = 10^{-20} \text{ cm}^3/\text{sec} \qquad (42)$$

R--12.
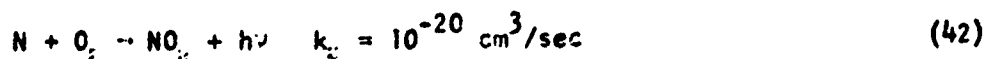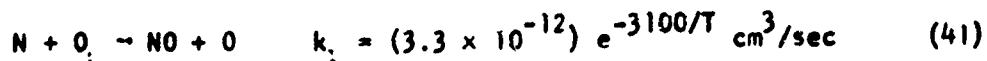
Combining these reactions with (36) we are led to the following set of differential equations:

$$\frac{dn[N]}{dt} = - \left\{ k_n n[N] + k_n n[N_2] + k_o M' \right\} n[N]^2 \tag{43}$$

$$- (k_1 + k_2) n[N] n[O_2]$$

$$\frac{dn[O_2]}{dt} = - (k_1 + k_2) n[N] n[O_2] \tag{44}$$

$$\frac{dn[N_2]}{dt} = \left\{ k_n n[N] + k_n n[N_2] + k_o M' \right\} n[N]^2 \tag{45}$$

where

$$M' = n[O_2] + n[N_2] + n[O] + n[NO_2]$$

$$M' = n[O_2] + \frac{2k_1 + k_2}{k_1 + k_2} \left[2(n_o[N_2] - n[N]) + n_o[N] - n[N] \right]$$

Equations (43) to (45) form a set of nonlinear coupled differential equations. With the aid of a subroutine PRECOR that uses a predictor-corrector technique to solve differential equations (discussed in the appendix), numerical solutions for this model were obtained.

Figures 18 through 20 show solutions plotted on a logarithmic scale for $T = 300^{\circ}K$ and $600^{\circ}K$ with initial nitrogen dissociation of 1, 5, and 10 percent. Note that there is an appreciable change in the behavior of the solutions for different values of temperature. This is explained by the increase in the rate constant for reaction (41) as the temperature increases. At $T = 300^{\circ}K$, $k_1 = 1.07 \times 10^{-16}$, while at $T = 600^{\circ}K$, $k_1 = 1.88 \times 10^{-14}$.

If one assumes that $n[O_2]$ is roughly constant and that the only reaction of any consequence is (41), then

$$n[N] = n_o[N] e^{-k n[O_2] t}$$

Taking the logarithm of both sides we have

$$\log \frac{n[N]}{n_o[N]} = - k_1 n[O_2] \, t$$

Therefore, if in fact equation (41) does dominate the reaction, the plot of $n[N]$ vs. t on semi-log paper should be a straight line with slope $-(k_1 n[O_2])^{-1}$. Figure 21 is such a plot for 1-percent dissociation. Its slope is -4.8×10^4 while $-k_1 n[O_2]$ is approximately -4.78×10^4. Hence we conclude that at higher temperatures the oxidation reaction (41) dominates. At the lower temperature the three-body nitrogen recombination reaction continues to dominate, as is indicated by the nearly straight line on the logarithmic plot that is identical to the Model 2 result in Figure 17 for $t \geq 0.1$ msec. Reaction (42) has a rate constant that is too small to be of any significance. The essentially new fact revealed by these calculations is the rapid decrease in the atomic nitrogen concentration for $t < 0.1$ msec at higher temperatures due to the oxidation reaction (41).

Model 4

Model 3 took into account the major reactions concerning N, O_2, and N_2; in Model 4 we take into account reactions of these gases with the molecules formed by the reactions of Model 3. The chemical equations are the three from Model 3 plus six reactions involving NO, O, NO_2. They are

$$N+N+M \rightarrow N_2+M \qquad k_n = 5.0 \times 10^{-30}/T$$

$$\qquad\qquad\qquad\qquad\qquad k_o = 3.0 \times 10^{-30}/T$$

$$N+O_2 \rightarrow NO+O \qquad k_1 = 3.3 \times 10^{-12}\, e^{-3100/T}$$

$$N+O_2 \rightarrow NO_2+h\nu \qquad k_2 = 10^{-20}$$

$$N_2+O+M \rightarrow N_2O+M \qquad k_3 = 2.0 \times 10^{-33}\, e^{-6060/T}$$

$$N_2+O \rightarrow NO+N \qquad k_4 = 10^{-10}\, e^{-37500/T}$$

R-122

$$N_2 + O \rightarrow N_2O + h\nu \qquad\qquad k_5 = 10^{-20}$$

$$O_2 + O + M \rightarrow O_3 + M \qquad\qquad k_6 = 3.162 \times 10^{-35}$$

$$O_2 + O \rightarrow O_3 + h\nu \qquad\qquad k_7 = 10^{-20}$$

$$O_2 + NO + NO \rightarrow NO_2 + NO_2 \qquad\qquad k_8 = 10^{-37}$$
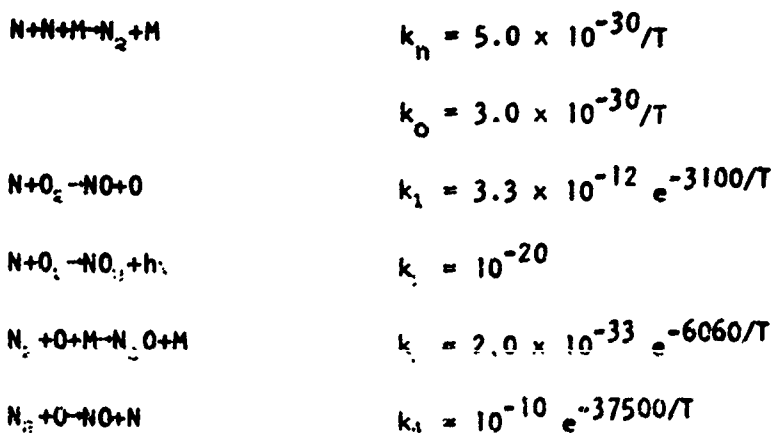
The associated rate equations are

$$\frac{dn[N]}{dt} = -A_0 - A_1 - A_2 + A_3$$

$$\frac{dn[N_2]}{dt} = A_0 - A_3 - A_4 - A_5$$

$$\frac{dn[O_2]}{dt} = -A_1 - A_2 - A_6 - A_7 - A_8$$

$$\frac{dn[NO]}{dt} = A_2 + A_4 - A_8$$

$$\frac{dn[NO_2]}{dt} = A_1 + 2A_8$$

$$\frac{dn[O]}{dt} = A_3 - A_2 - A_4 - A_5 - A_6 - A_7$$

$$\frac{dn[N_2O]}{dt} = A_4 + A_5$$

$$\frac{dn[O_3]}{dt} = A_6 + A_7$$

where

$$A_0 = \left\{ k_n (n[N] + n[N_2]) + k_0 (M - n[N] - n[N_2]) \right\} (n[N])^2$$

$$A_1 = k_1 n[N] \, n[O_2]$$

$$A_2 = k_2 n[N] \, n[O_2]$$

$$A_3 = k_3 \cdot M \cdot n[N_2] \cdot n[O]$$

$$A_4 = k_4 n[N_2] \cdot n[O]$$

$$A_5 = k_5 n[N_2] \, n[O]$$

$$A_6 = k_6 n[O_2] \, n[O]M$$

$$A_7 = k_7 n[O_2] \, n[O]$$

$$A_8 = k_8 n[O_2] \, (n[NO])^2$$

and M = summation of the concentrations of all the constituents.

This set of differential equations was solved numerically using PRECOR. Figure 22 compares Model 3 and Model 4 at $T = 300^{\circ}$ and $600^{\circ}K$ and 10-percent dissociation. Here one sees that, at both 300° and $600^{\circ}K$, Models 3 and 4 give substantially equivalent results. The small difference between the two results at $300^{\circ}K$ where the three-body recombination reaction dominates is due to the more exact calculation of the three-body concentration that is possible in the more elaborate Model 4. There is no significant effect of the atomic nitrogen regeneration provided by one of the Type (a) secondary reactions included in Model 4.

CONCLUSIONS AND RECOMMENDATIONS

1. Considering the simplest case of recombination in pure nitrogen, one finds that the process is controlled by a three-body reaction. Its rate thus increases with pressure. The rate coefficient is inversely proportional to temperature, however, so that the lifetime of dissociated nitrogen increases with increasing temperature. As long as one is interested in the asymptotic time behavior, it is not necessary to consider the variation in the third-body concentration with time. In this period $n[N] \sim time^{-1}$ and is independent of the initial atomic nitrogen concentration.

2. Under typical conditions (STP, 10-percent dissociation) the asymptotic time period is reached in about 0.1 msec, at which time the atomic nitrogen has decreased by two orders of magnitude from its initial value.

3. The effect of oxygen on the nitrogen recombination depends on temperature. At $300^{0}K$ all oxygen reactions are unimportant and the oxygen serves simply as a third-body for the nitrogen recombination. In this case the remarks in (1) and (2) above apply. By $600^{0}K$, one oxygen reaction has become sufficiently important to completely replace the three-body recombination as the most important atomic nitrogen loss mechanism. The reaction is

$$N + O \rightarrow NO + O$$

This reaction will dominate the atomic nitrogen loss in the asymptotic time period $t > 0.1$ msec and it will result in a much greater loss rate than would be the case for three-body recombination.

4. Although detailed calculation of the energetics of the ammonia-ignition process has not been undertaken, it would not appear feasible to rely completely on nitrogen dissociation for this function, because the major part of the recombination will occur before the dissociated nitrogen reaches an engine cylinder.

5. This work does suggest, however, that RF dissociation of ammonia may be of interest, since it is known that thermal dissociation

of ammonia prior to ignition is effective in improving the operation of ammonia-fueled engines. The RF dissociator can be expected to be considerably easier to control than a thermal dissociator, and should not require a warm-up period.

REFERENCES

1. AXWORTHY, A. E., Jr., and BENSON, S. W., Ozone Chemistry and Technology, Am. Chem. Soc., 1959.

2. BARTH, C. A., JPL Tech. Report 32-63, April 1961.

3. BENSON, S. W. and AXWORTHY, A. E., Jr., J. Chem. Phys. 26, 1718 (1957).

4. BORTNER, M. H., G. E. Missile and Space Division Report R63SD34, September 1963.

5. BRADLEY, J. N. and KISTIAKOWSKY, G. B., J. Chem. Phys. 35, 256 (1961).

6. BYRON, S., J. Chem. Phys. 30, 1380 (1959).

7. CAMPBELL, E. S. and NUDELMAN, C., AFOSR TN-60-502 (1960).

8. CARY, B. Phys. Fluids 8, 26 (1965).

9. CLYNE, M. A. and THRUSH, B. A., Nature 189, 56 (1961).

10. CLYNE, M. A. and THRUSH, B. A., 9th Intl. Symp. on Combustion ??.

11. FENIMORE, C. P., J. Chem. Phys. 35, 2243 (1961).

12. FORD, H. W., DOYLE, G. J., and ENDOW, N., J. Chem. Phys. 26, 1336 (1957).

13. FREEDMAN, E. and DAIBER, J. W., J. Chem. Phys. 34, 1271 (1961).

14. GOLDEN, J. A. and MYERSON, A. L., Proc., Conf. on Physical Chemistry in Aerodynamics and Space Flight, Pergamon Press, 1961.

15. GREAVES and GARVIN, J. Chem. Phys. 30, 348 (1958).

16. HARTECK, P. and DONES, S., J. Chem. Phys. 22, 758 (1954).

17. HARTECK, P., REEVES, R. R., and MANNELLA, G., J. Chem. Phys. 29, 608 (1958).

18. HARTECK, P. and DONDES, S., J. Phys. Chem. 63, 956 (1959).

19. HERRON, J. T., J. Chem. Phys. 35, 1138 (1961).

20. JOHNSTON and CROSBY, J. Chem. Phys. 22, 689 (1954).

21. KAPLAN, J. and BARTH, C. A., Proc., Natl. Acad. Sci. 44, 105 (1958).

22. KAUFMAN, F., GERRI, N., and BOWMAN, R., J. Chem. Phys. 25, 106 (1956).

23. KAUFMAN, F., J. Chem. Phys. 22, 352 (1958).

24. KAUFMAN, F. and KELSO, J. R., Proc., 7th Intl. Symp. on Combustion
    (Butterworth), 1959.

25. KISTIAKOWSKY, G. B. and VOLPI, G. G., J. Chem. Phys. 27, 1141 (1957).

26. KISTIAKOWSKY. G. B. and VOLPI, G. G., J. Chem. Phys. 28, 665 (1958).

27. MATTHEWS, D. L., Phys. Fluids 2, 170 (1959).

28. MAVROYANNIS, C. and WINKLER, C. A., Proc., Intl. Symp. of Chemical
    Reactions in the Lower and Upper Atmosphere, International
    Publishers, Inc., New York, 1961.

29. MORGAN, J. E. ELIAS, L., and SCHIFF, H. I., J. Chem. Phys. 33, 930
    (1960).

30. NICOLET, M., Inst. R. Met. Belgique, Mem. 19, 74 (1945).

31. NICOLET, M., and MANGE, P., J. Geophys. Res. 59, 15 (1954).

32. NICOLET and AIKEN, J. Geophys. Res. 65, 1469 (1960).

33. PHILLIPS, L. F. and SCHIFF, H. I., J. Chem. Phys. 36, 1509 (1962).

34. REEVES, R. R., MANNELLA, G., and HARTECK, P., J. Chem. Phys. 32, 632 (1960).

35. RINK, J. P., KNIGHT, H. I., and DUFF, R. E., J. Chem. Phys. 34, 1942 (1961).

36. SCHEXNAYDER, C. J. and EVANS, J. S., NASA Tech. Report R-108 (1961).

37. WRAY, K. L. and TEARE, J. D., J. Chem. Phys. 36, 2582 (1962).

38. WRAY, K. L., J. Chem. Phys. 37, 1254 (1962).

39. ZASLOWSKY, J. A., URBACK, H. B., LEIGHTON, F., WNUK, R. J., and
    WOJTOWICZ, J. A., J. Am. Chem. Soc. 82, 2082 (1960).

40. BYRON, S., 9th General Assembly of AGARD, NATO, Aachen, September 1959.

41. CAMM, J. C. and KECH, J. C., AVCO Res Note 140, June 1959.

42. CARY, B., G. E. MSVD TIS R62SD32 (1962).

43. HAALAND, C. M., Armour Research Foundation ARFDA-28, August 1960.

44. HARTECK, P. and DONDES, S., J. Chem. Phys. 29, 234 (1958).

45. HERRON, J. T., FRANKLIN, J. L., BRANDT, P., and DIBELER, V. H.,
J. Chem. Phys. 29, 230 (1958).

46. HERRON, J. T., FRANKLIN, J. L., BRANDT, P., and DIBELER, V. H.,
J. Chem. Phys. 30, 879 (1959).

47. KAUFMAN, F. and KELSO, J. R., Proc., Intl. Symp. on Chemical
Reactions in the Lower and Upper Atmosphere, Interscience
Publishers, Inc., New York, 1961.

48. KUIPER, G. P., The Earth as a Plant, University of Chicago Press, 1954.

49. RALSTON, A. and WILF, H. S., Mathematical Methods for Digital Computers,
John Wiley and Sons, New York, 1960, pp. 95-109.

50. HAMMING, R. W., "Stable Predictor Corrector Methods for Ordinary
Differential Equations," J. Assoc. Comp. Mach. 6 (1959), pp. 37-47.

51. RALSTON, A., "Runge-Kutta Methods with Mimimum Error Bounds,"
Mathematics of Computation 16, 431 (1962).

52. RANK, P. H., JR., "PRECOR, a Kingston Fortran II Subroutine for
Solving Sets of Ordinary Differential Equations by a Predictor-
Corrector Technique," Davidson Laboratory TM-142, June 1965.
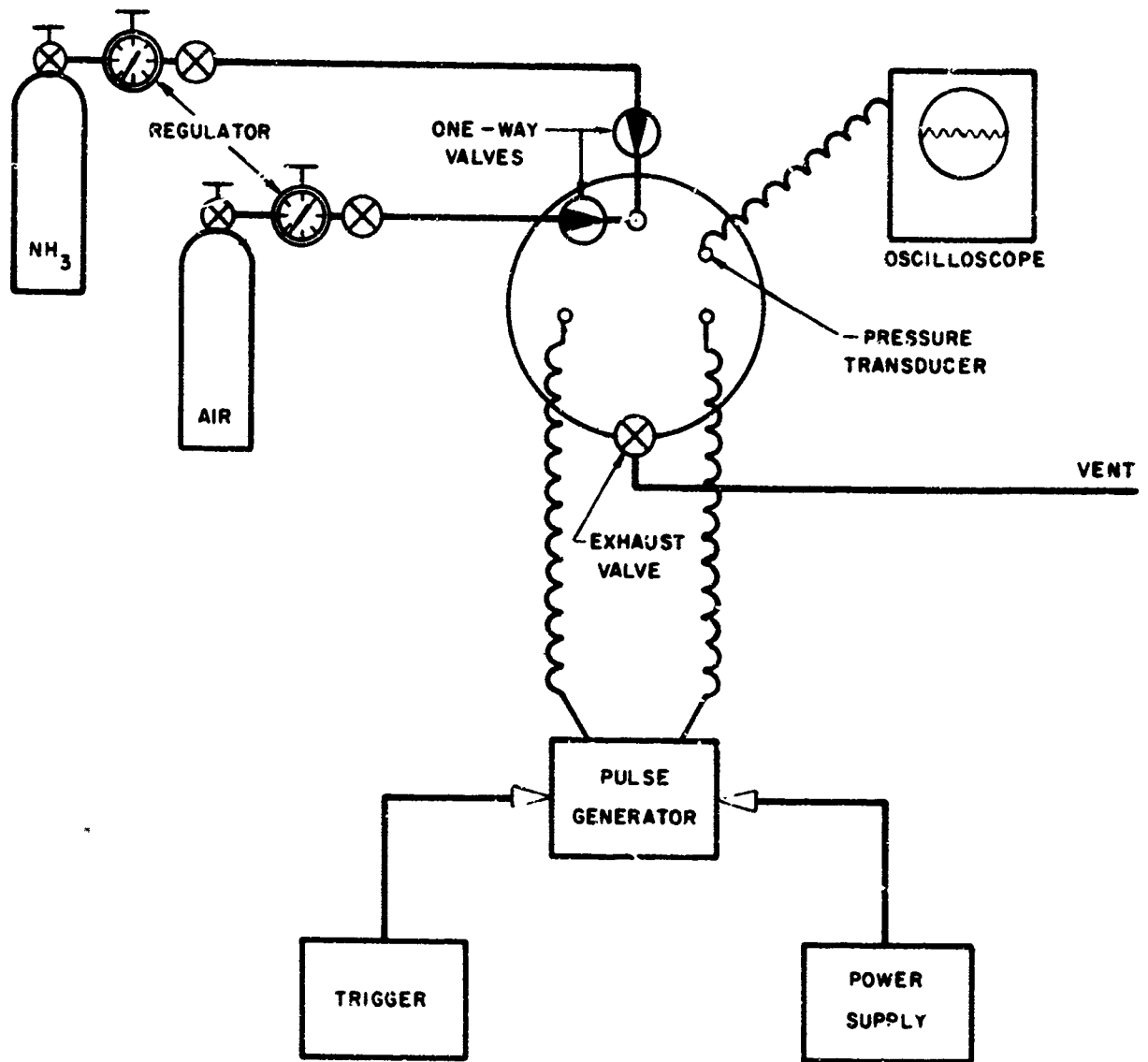
FIGURES

FIGURE I. DIAGRAM OF TEST SET-UP, HIGH ENERGY DISCHARGE

R-1122
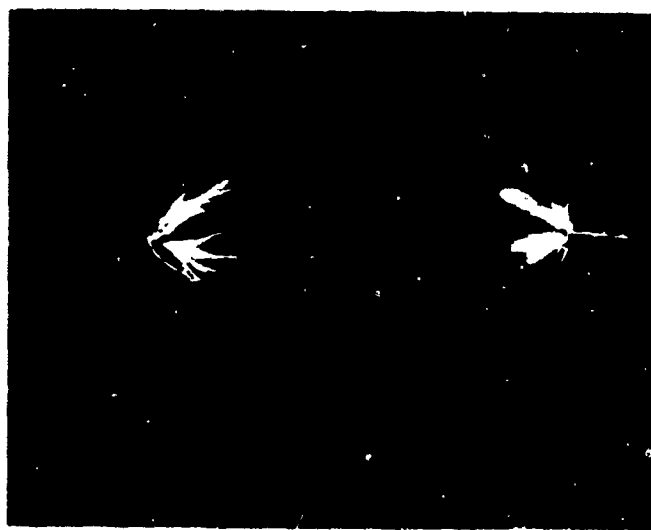
FIGURE 2.   HIGH-ENERGY PULSER DISCHARGING IN AIR
200,000 VOLTS   10 JOULES
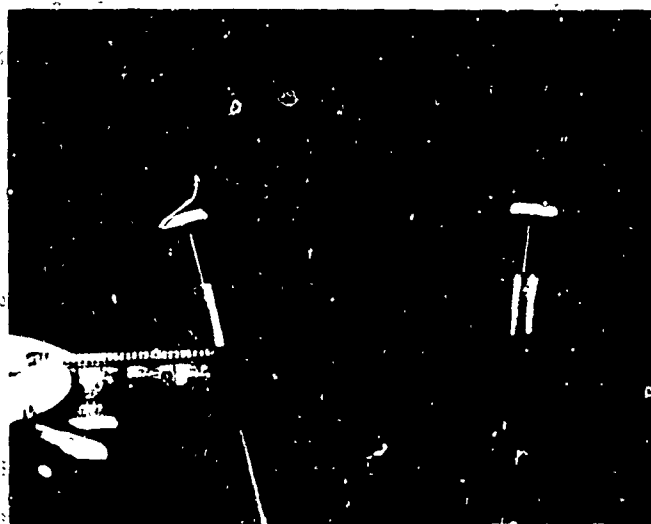
R-1122

FIGURE 2.   HIGH-ENERGY PULSER DISCHARGING IN AIR
200,000 VOLTS   10 JOULES
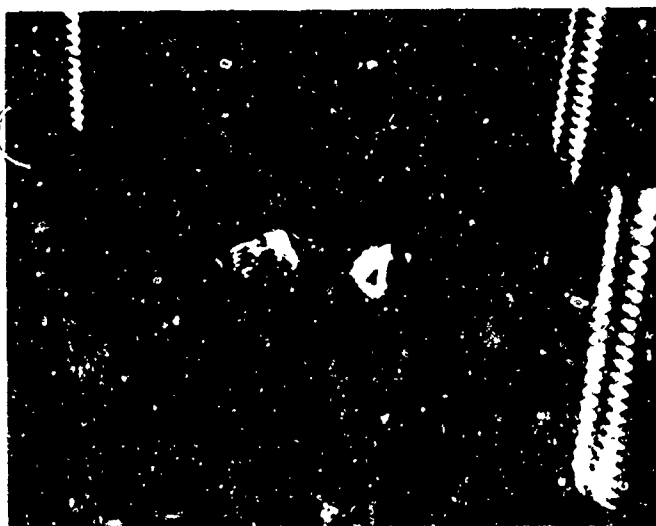
R-1122

FIGURE 3.   TWO ELECTRODE CONFIGURATIONS, SHOWING THE TENDENCY
TO ARC TO THE CYLINDER HEAD. THIS WAS SOLVED BY EXTENDING
THE ELECTRODES DEEPER INTO THE CHAMBER AND POLISHING
THE ROUGH EDGES OFF

R-1122

$\frac{3}{4}$ —10 ST 'D, 7$\frac{1}{2}$" LG
8 REQ'D
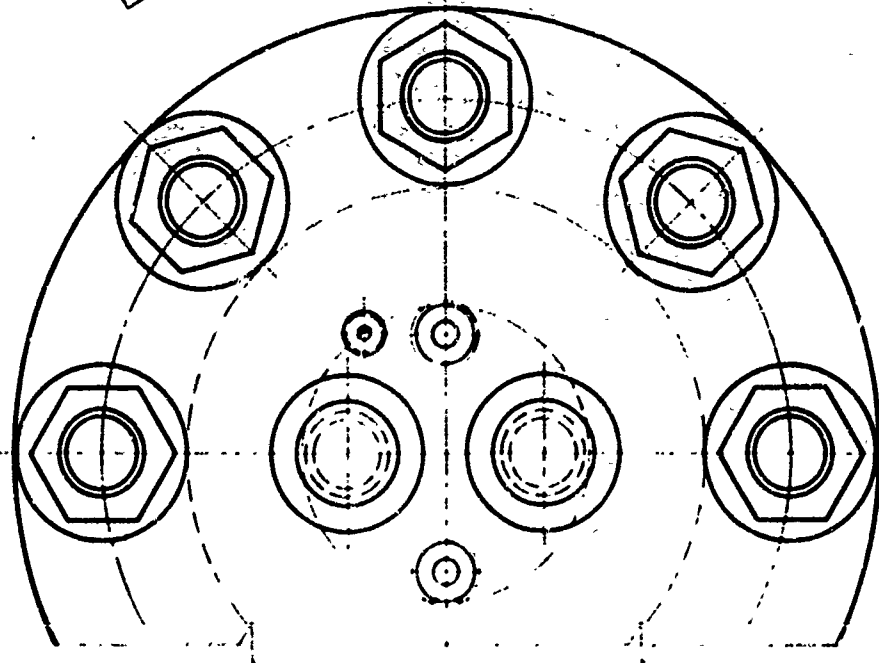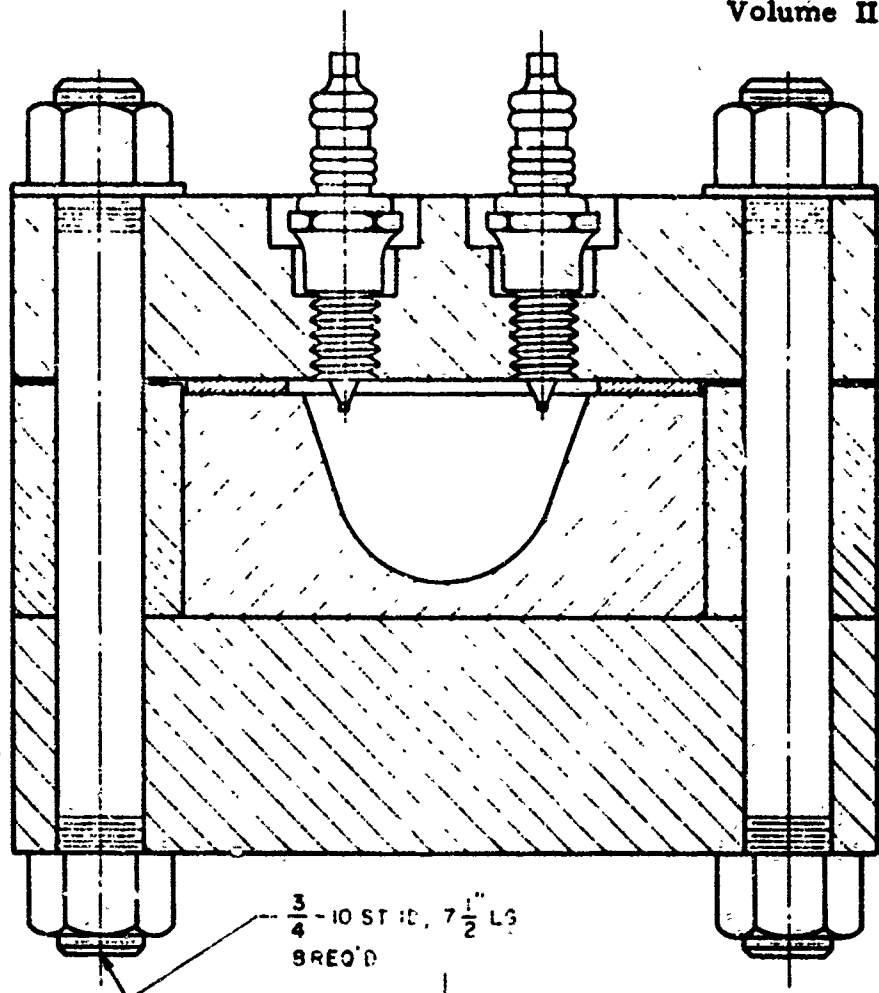
FIGURE 5. CHAMBER ASSEMBLY DRAWING
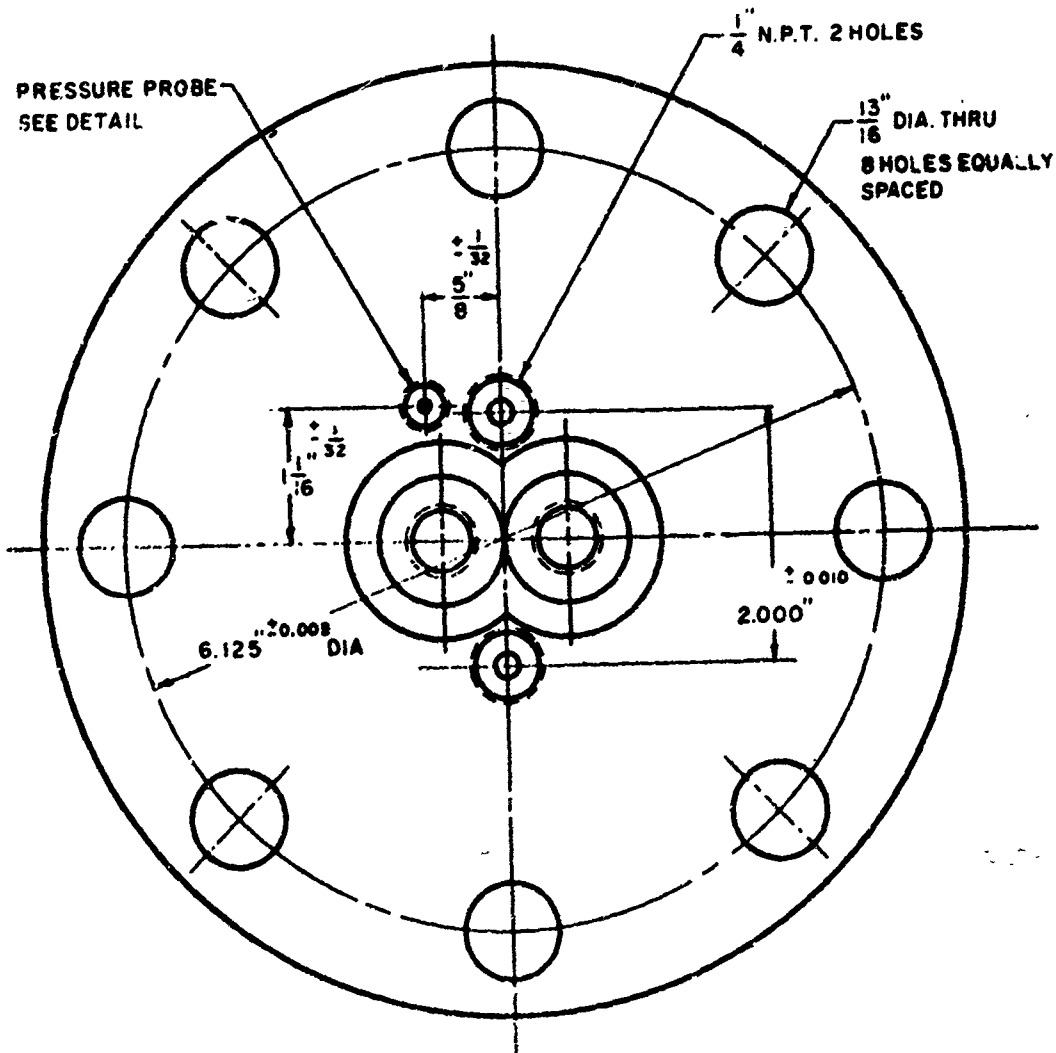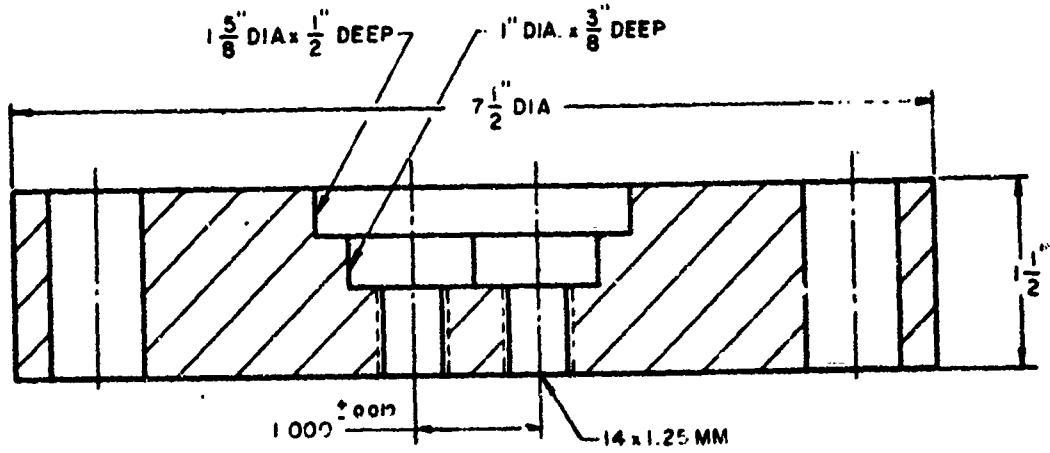
FIGURE 6.   TOP PLATE, TYPE I
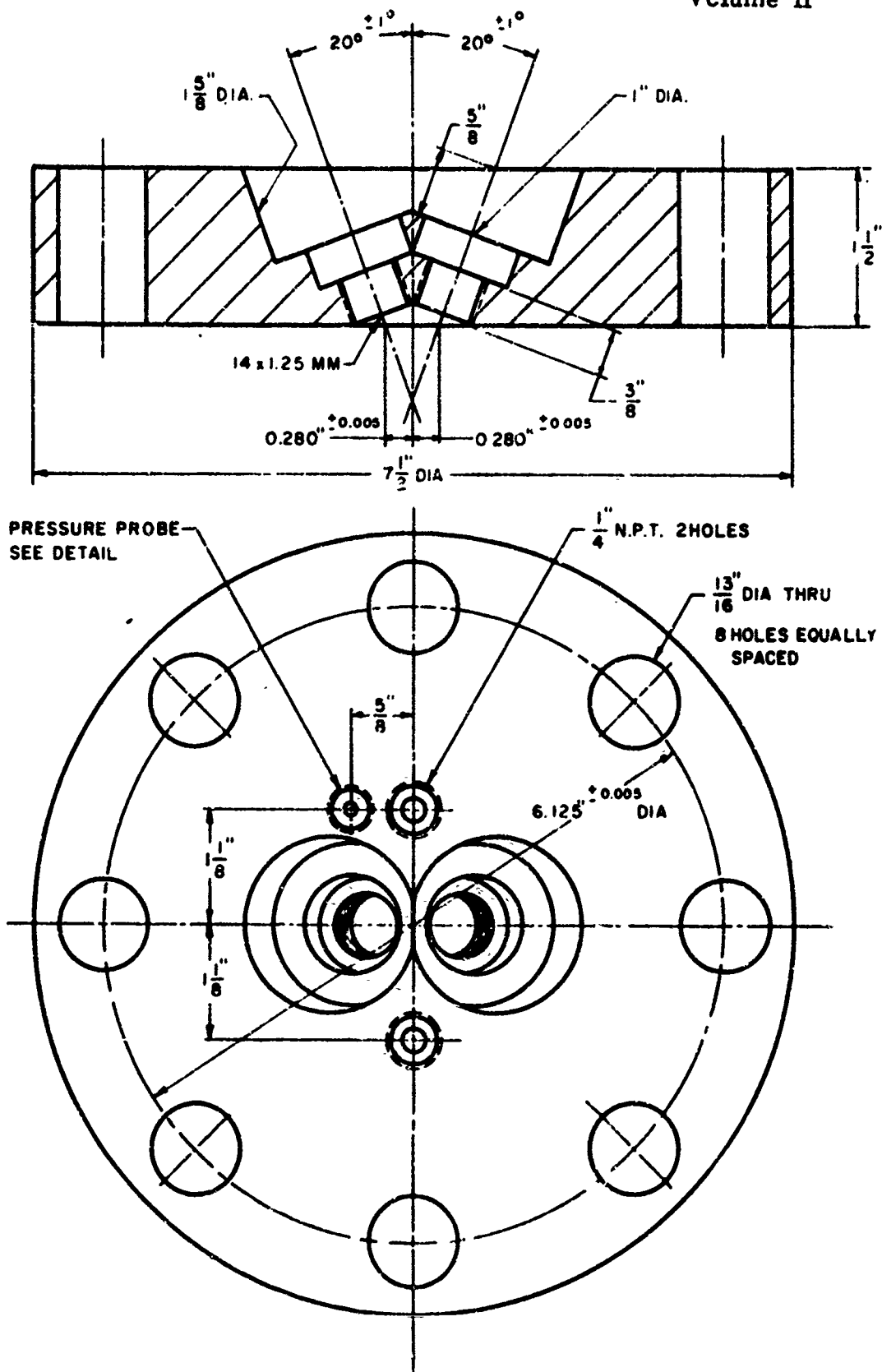
FIGURE 7.   TOP PLATE, TYPE 2
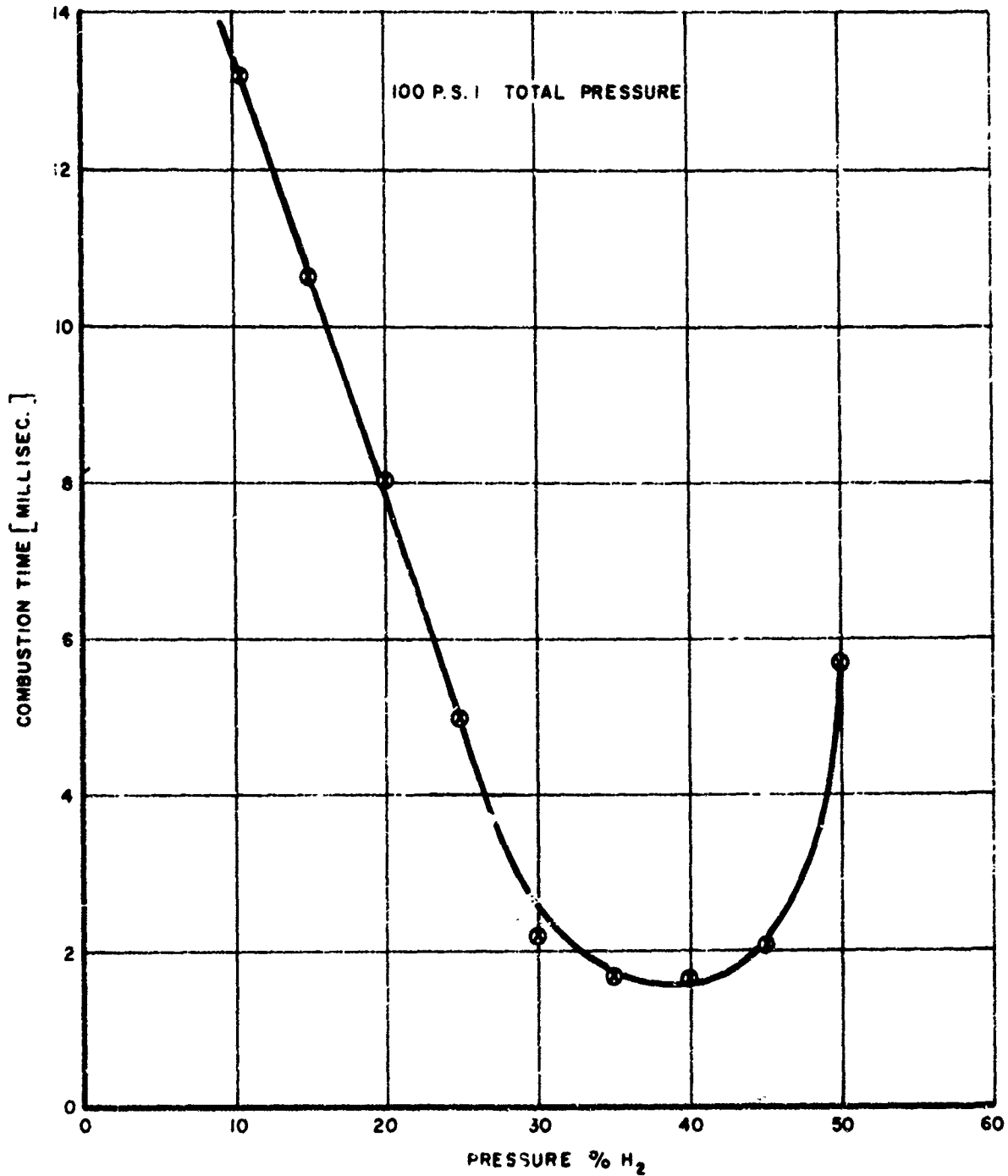
FIGURE 8. COMBUSTION TIME VERSUS PRESSURE PERCENT OF HYDROGEN
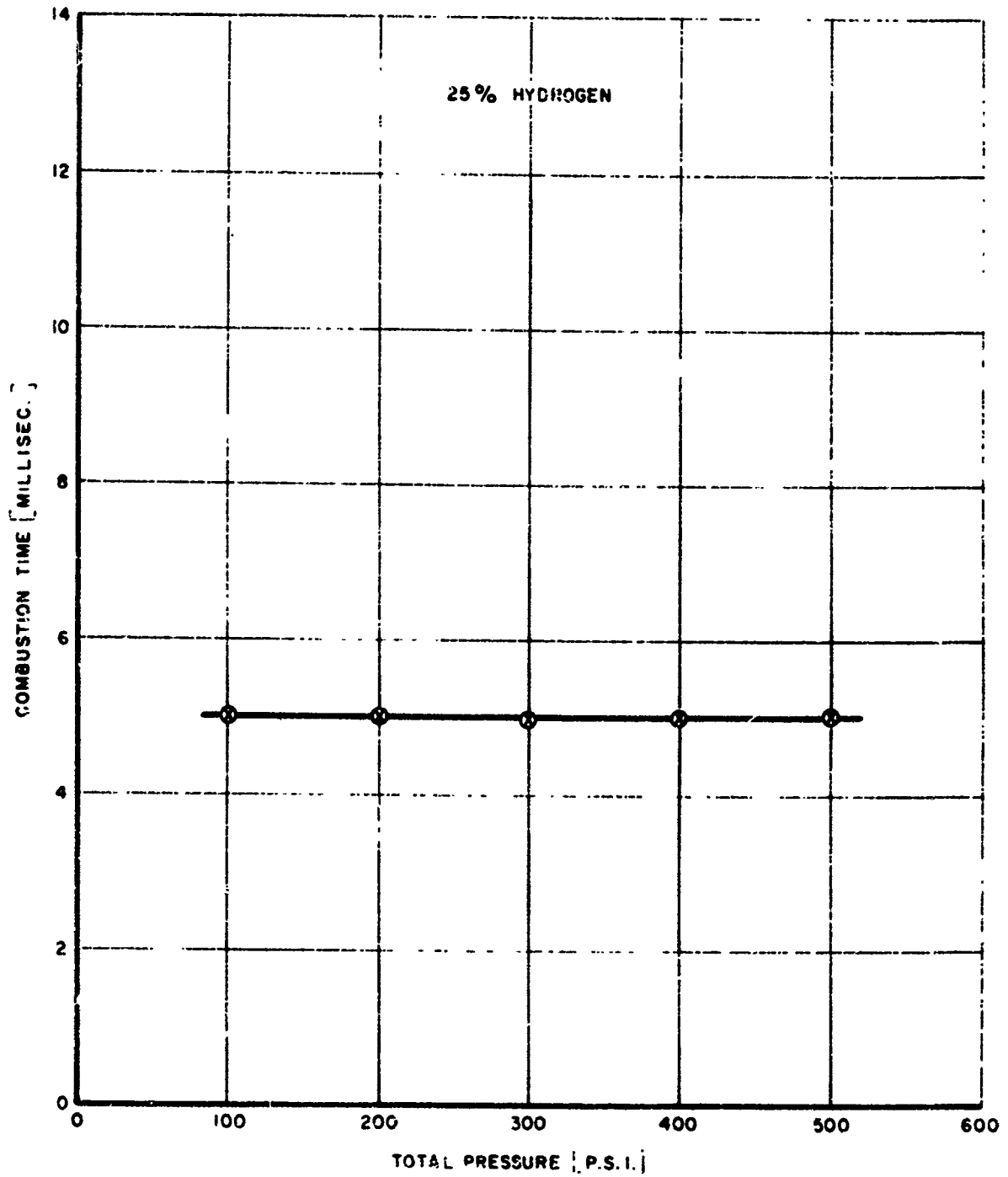
FIGURE 9. COMBUSTION TIME VERSUS TOTAL PRESSURE FOR HYDROGEN
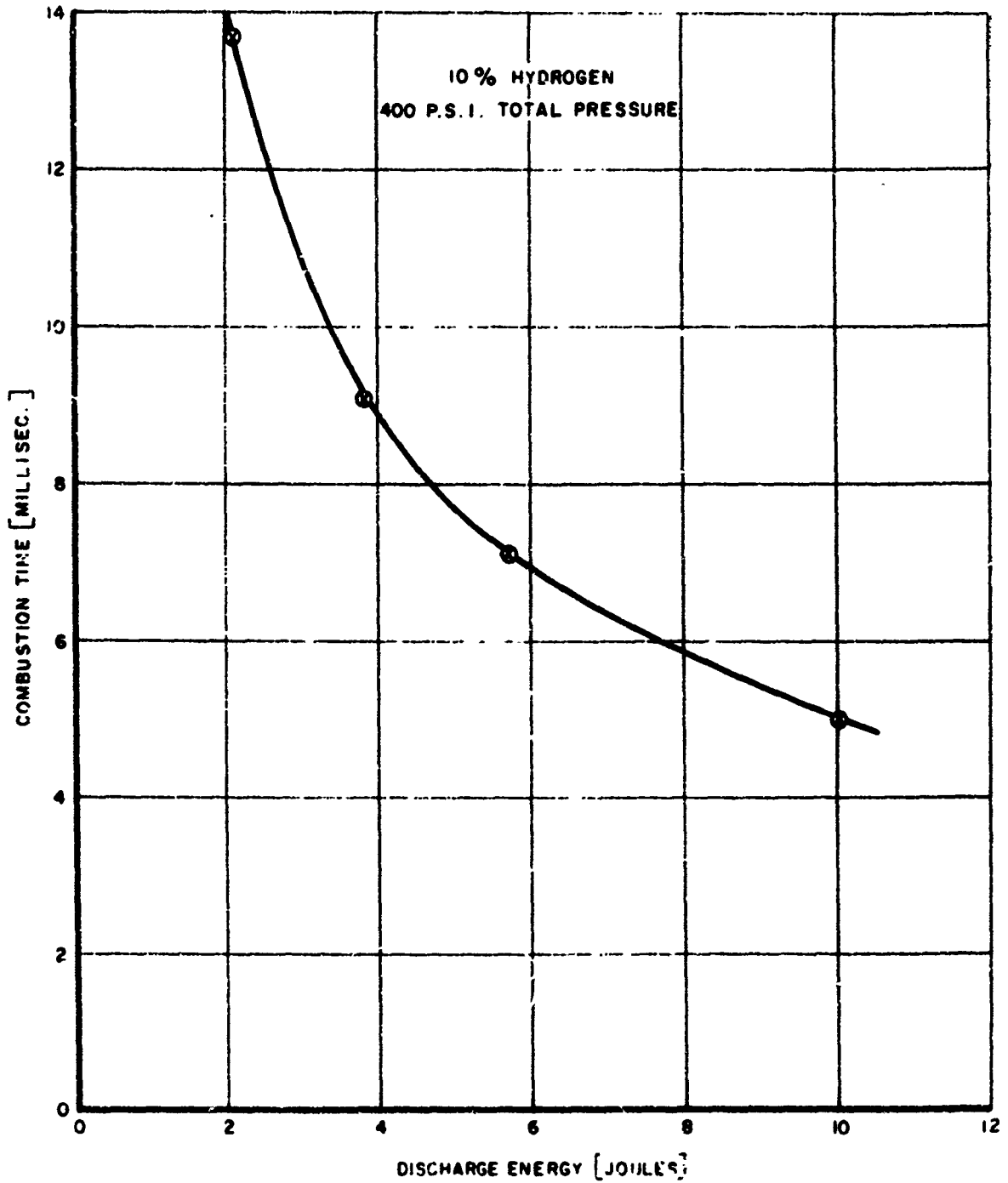
FIGURE 10.   COMBUSTION TIME VERSUS DISCHARGE ENERGY FOR HYDROGEN
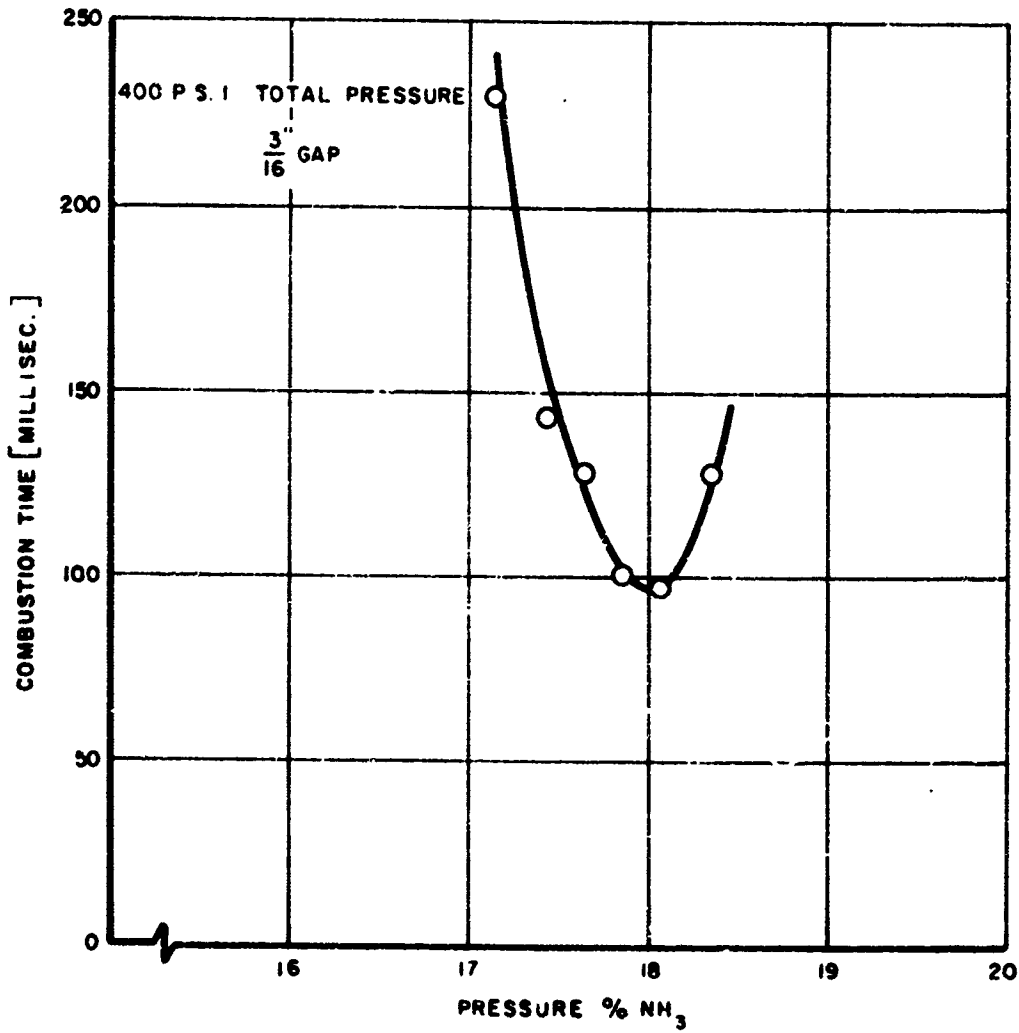
FIGURE II. COMBUSTION TIME VERSUS PRESSURE PERCENT AMMONIA
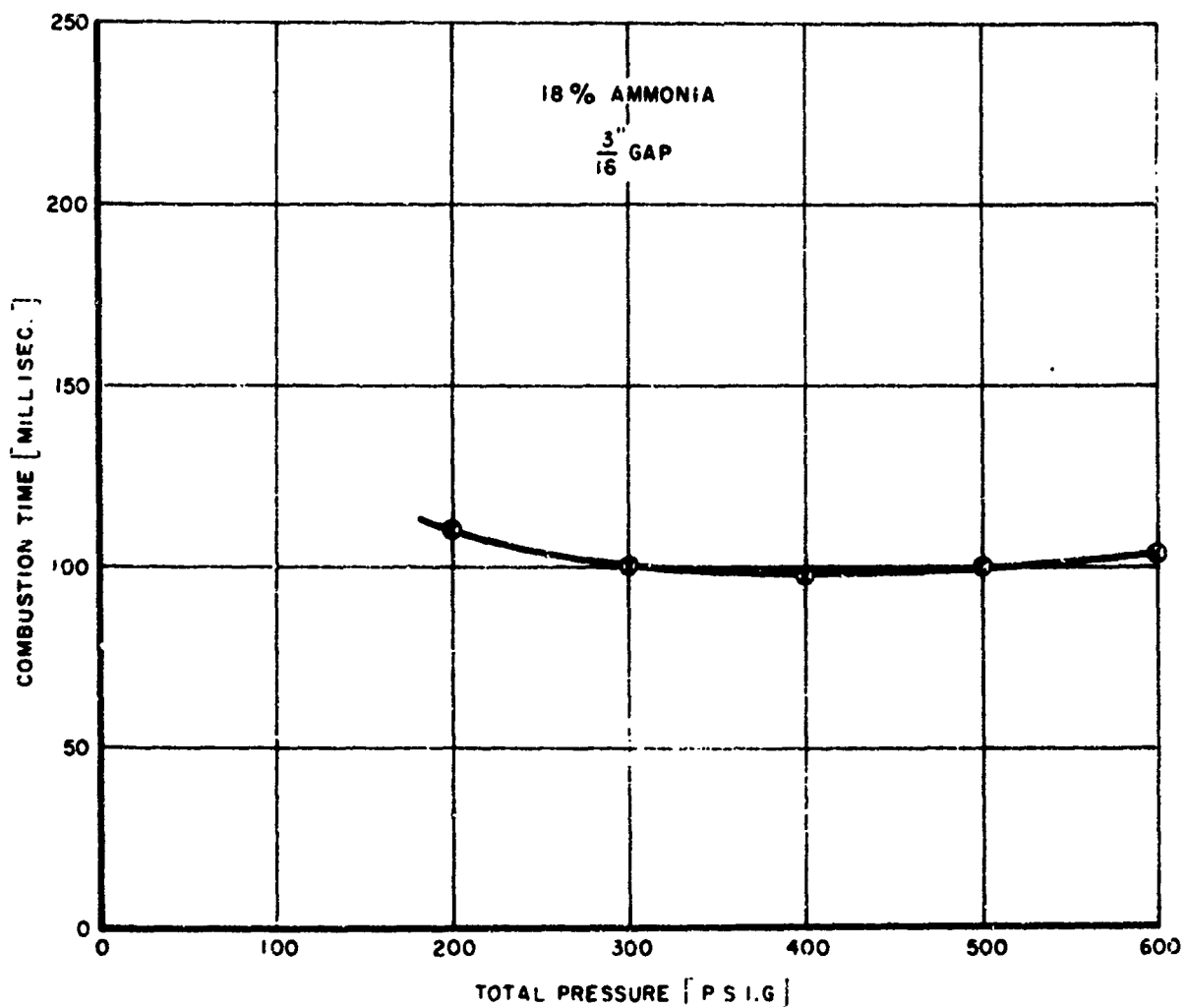
FIGURE 12. COMBUSTION TIME VERSUS TOTAL PRESSURE FOR AMMONIA
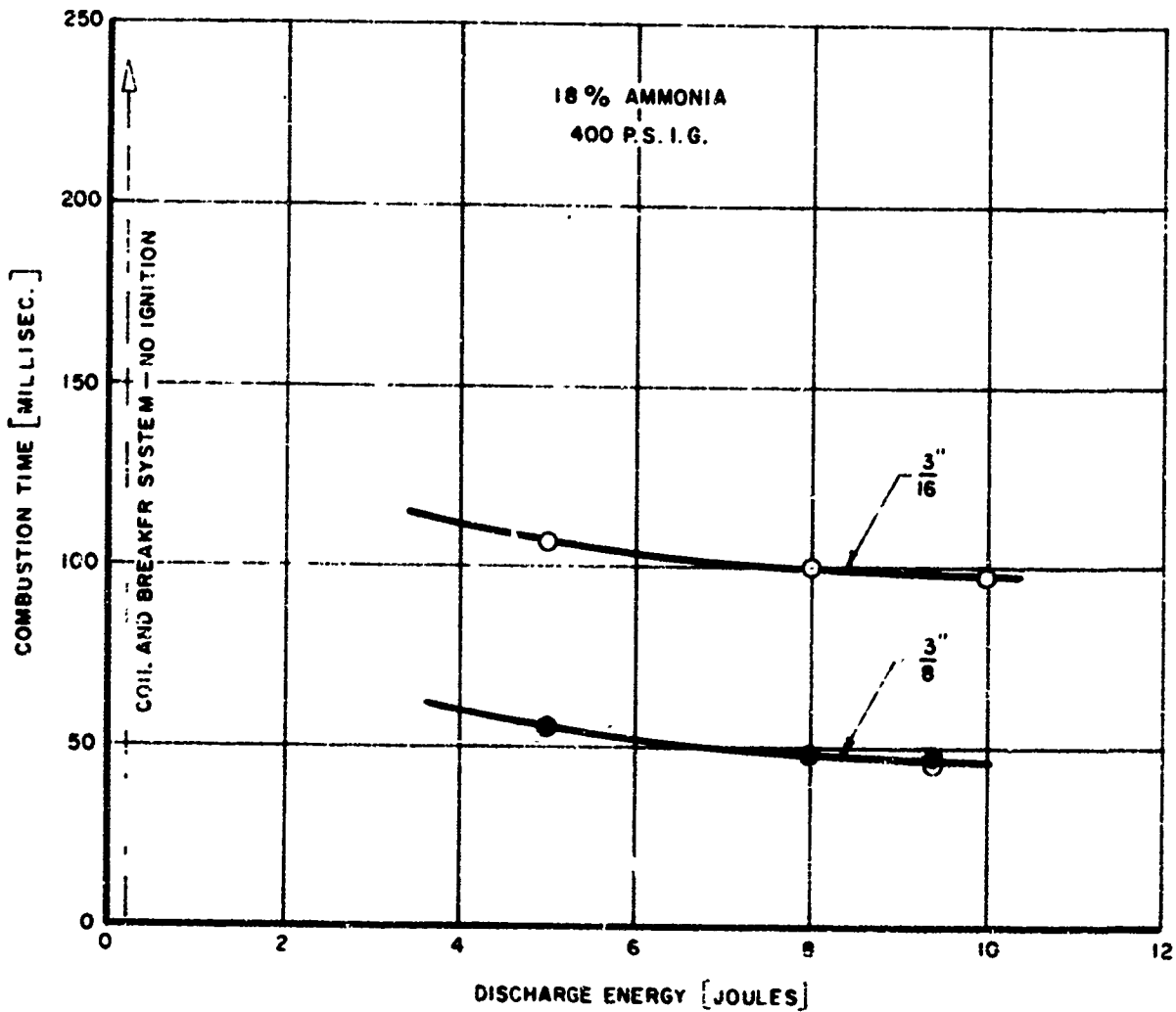
FIGURE 13. COMBUSTION TIME VERSUS DISCHARGE ENERGY FOR AMMONIA
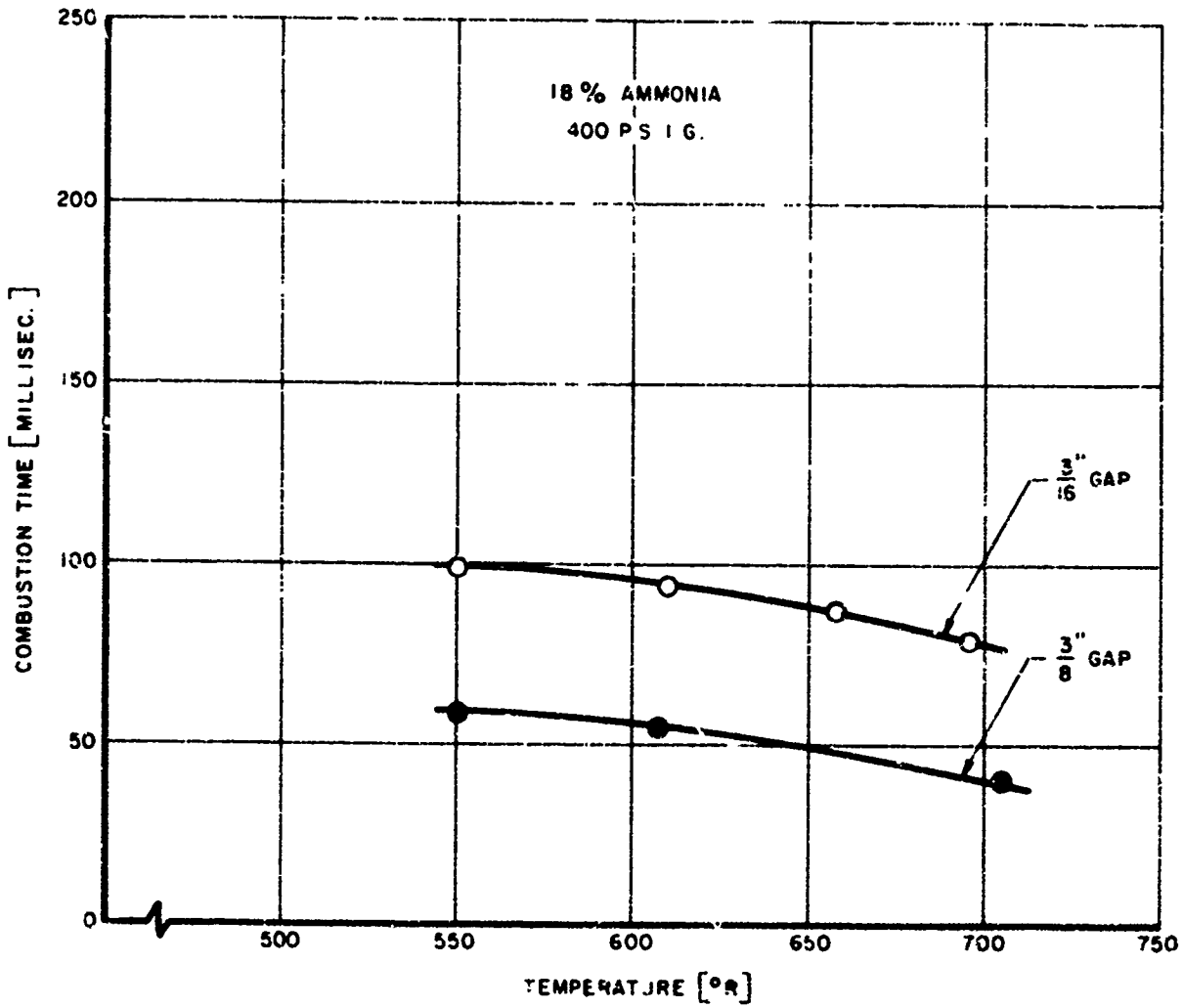
FIGURE 14.   COMBUSTION TIME VERSUS TEMPERATURE FOR AMMONIA
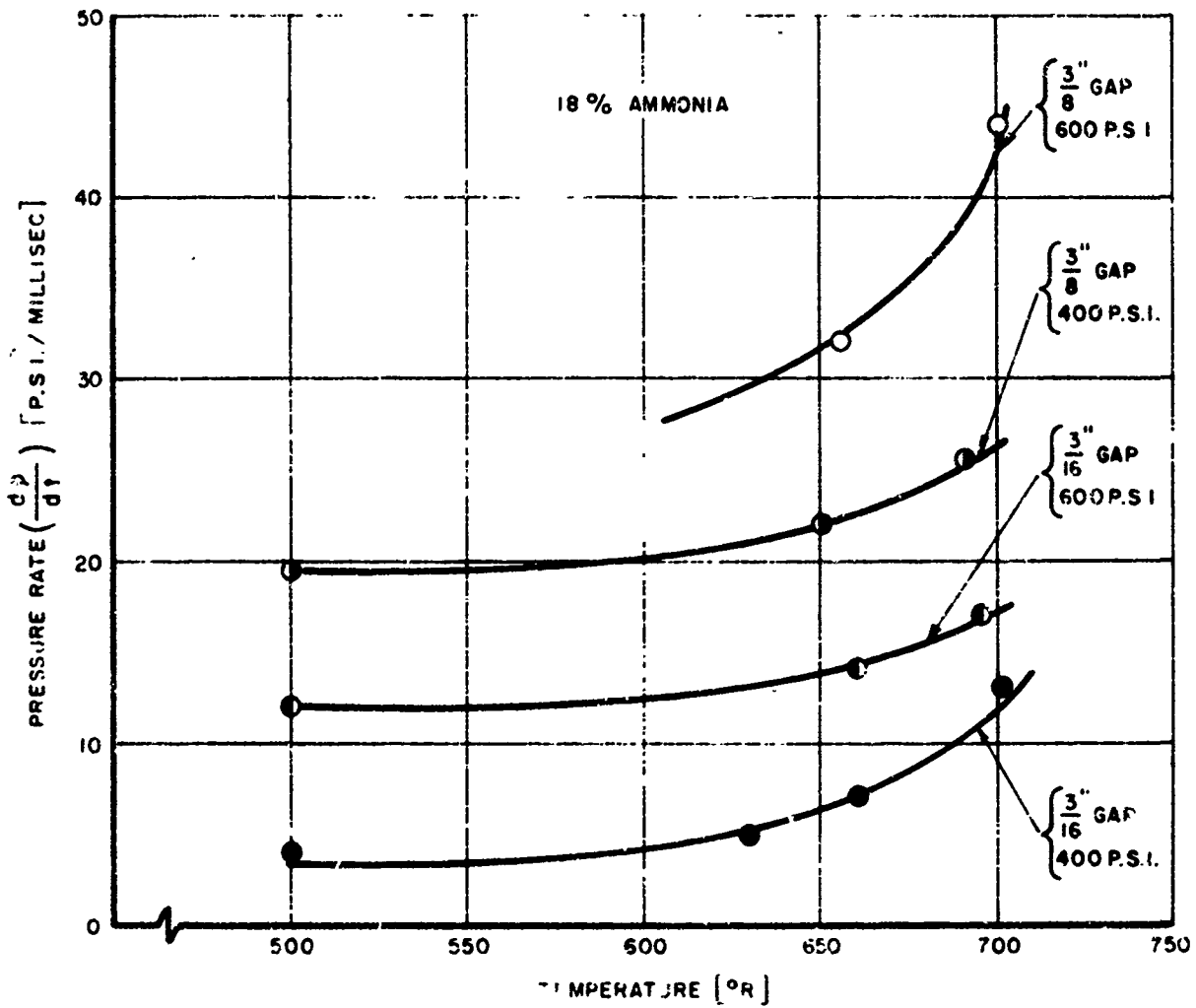
FIGURE 15. PRESSURE RATE VERSUS TEMPERATURE FOR AMMONIA
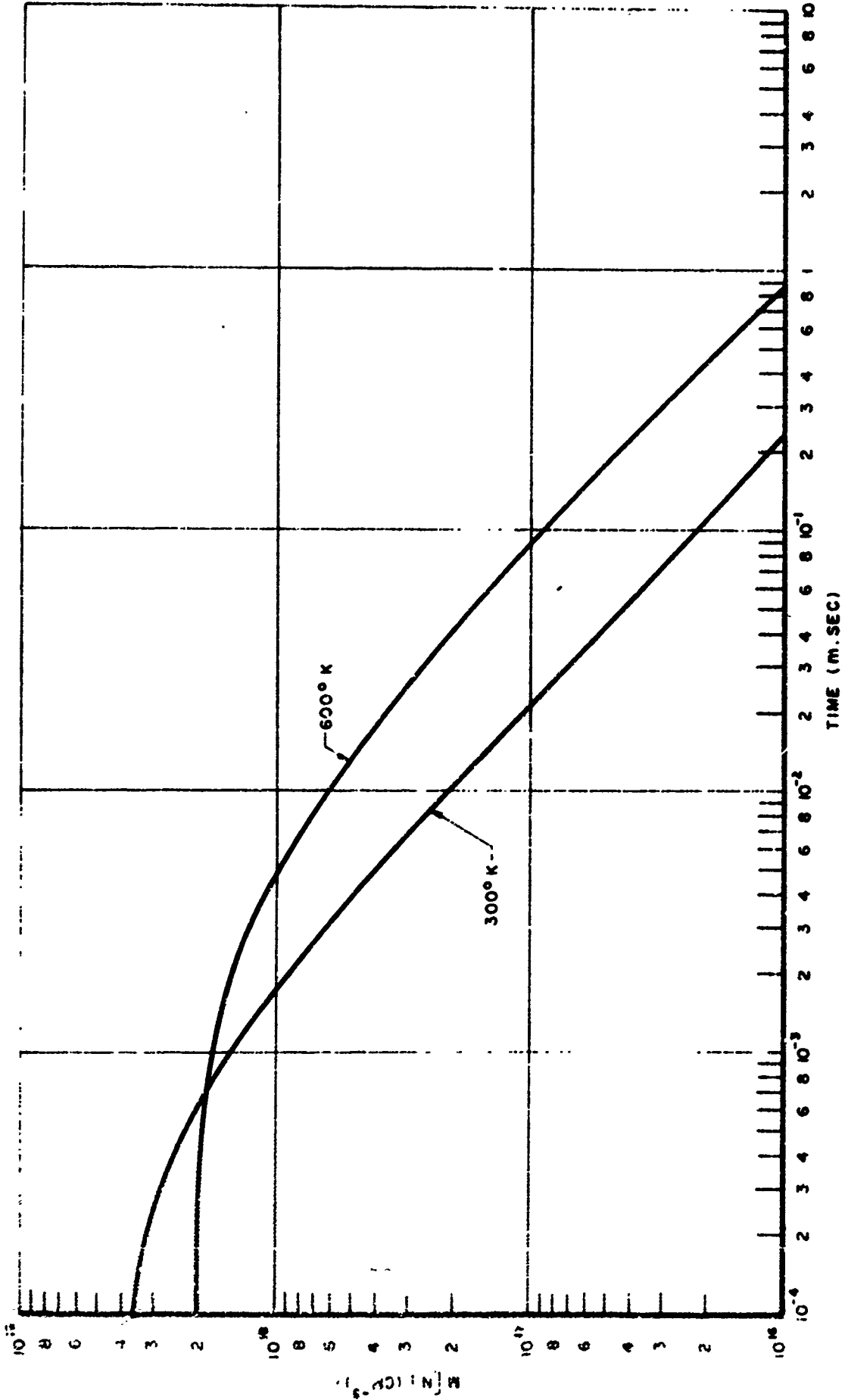
FIGURE 16. MODEL 1, 10% INITIAL N_2 DISSOCIATION
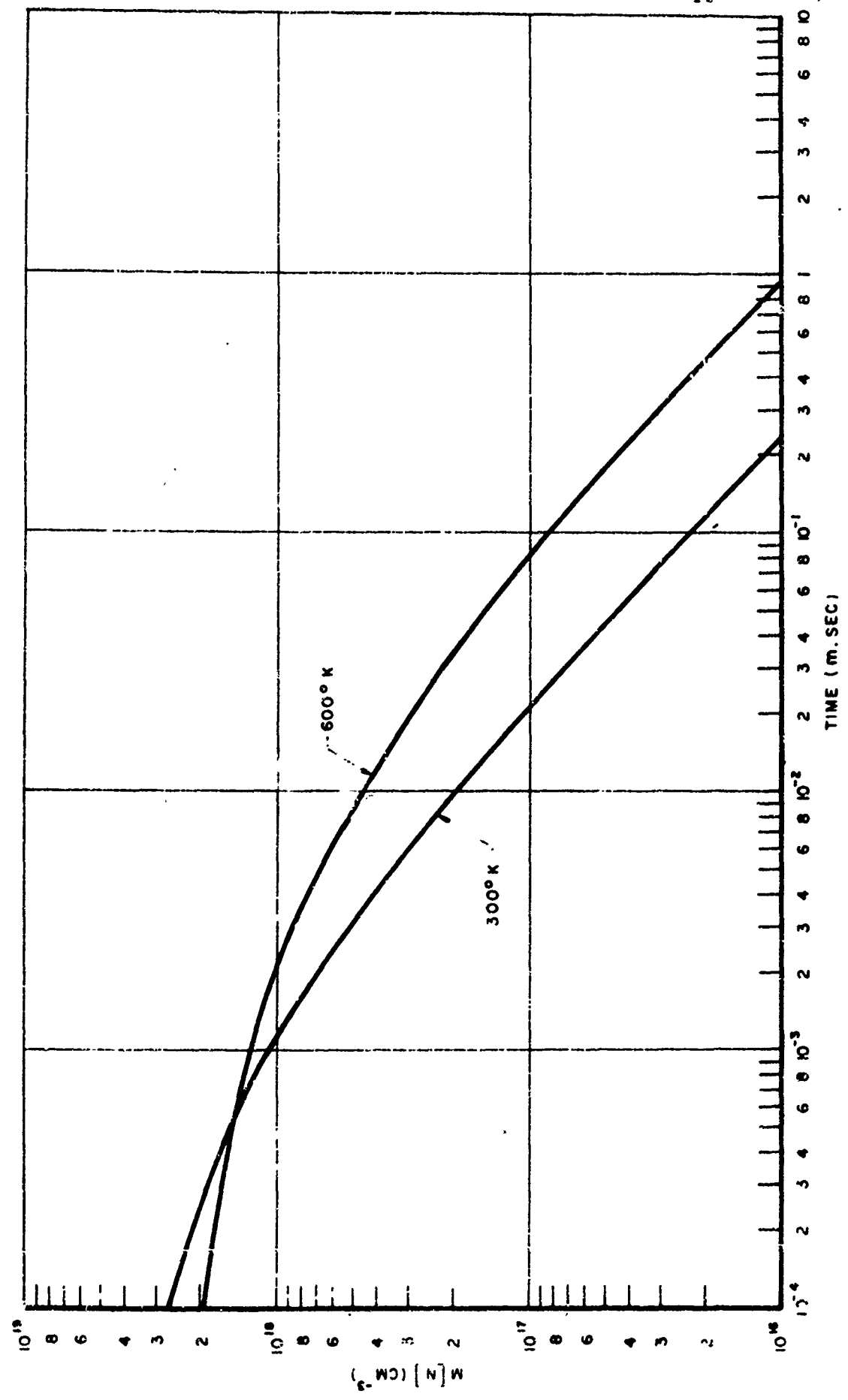
FIGURE 17. MODEL 2, 10% INITIAL N_2 DISSOCIATION
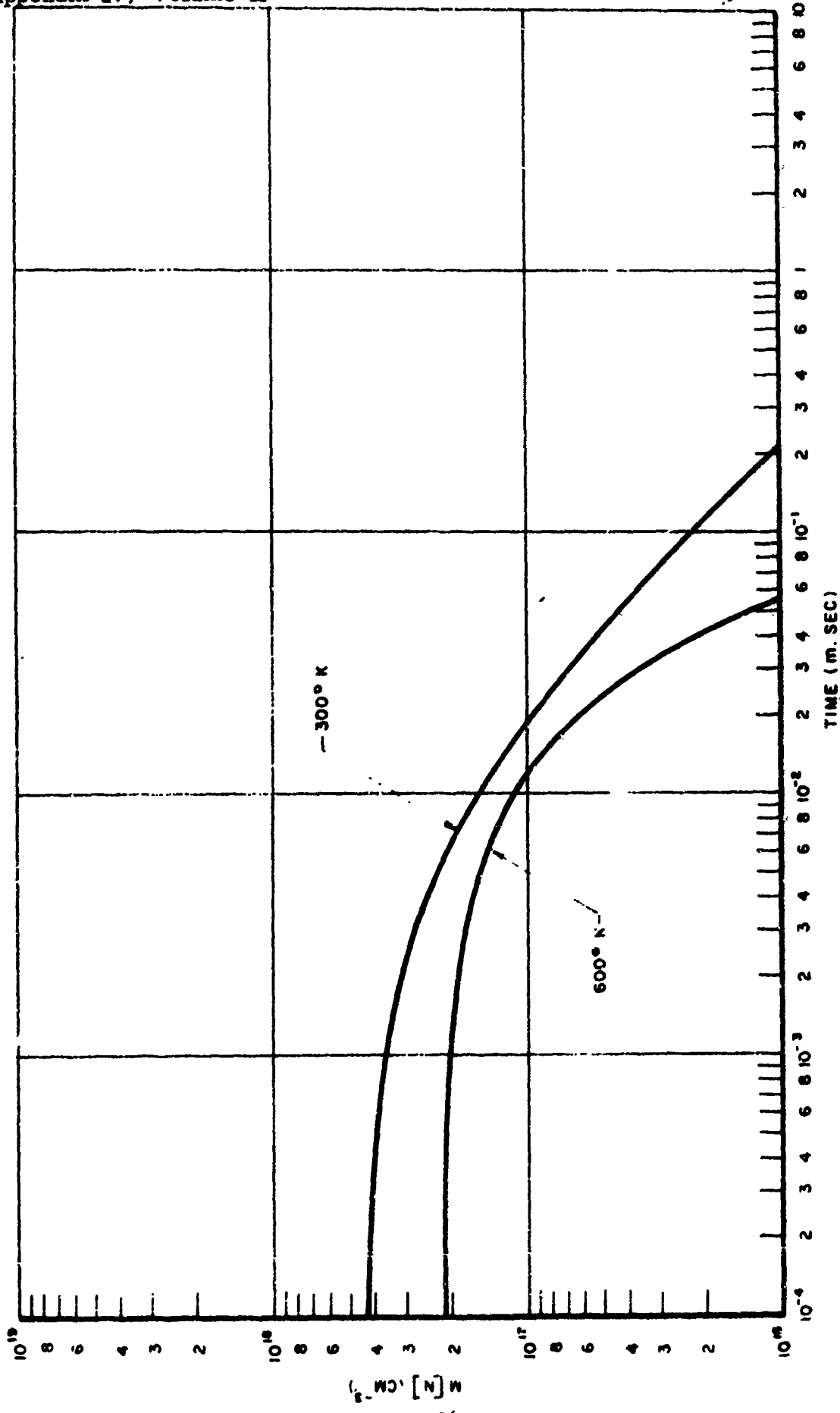
FIGURE 18.   MODEL 3,   1 % INITIAL N_2 DISSOCIATION
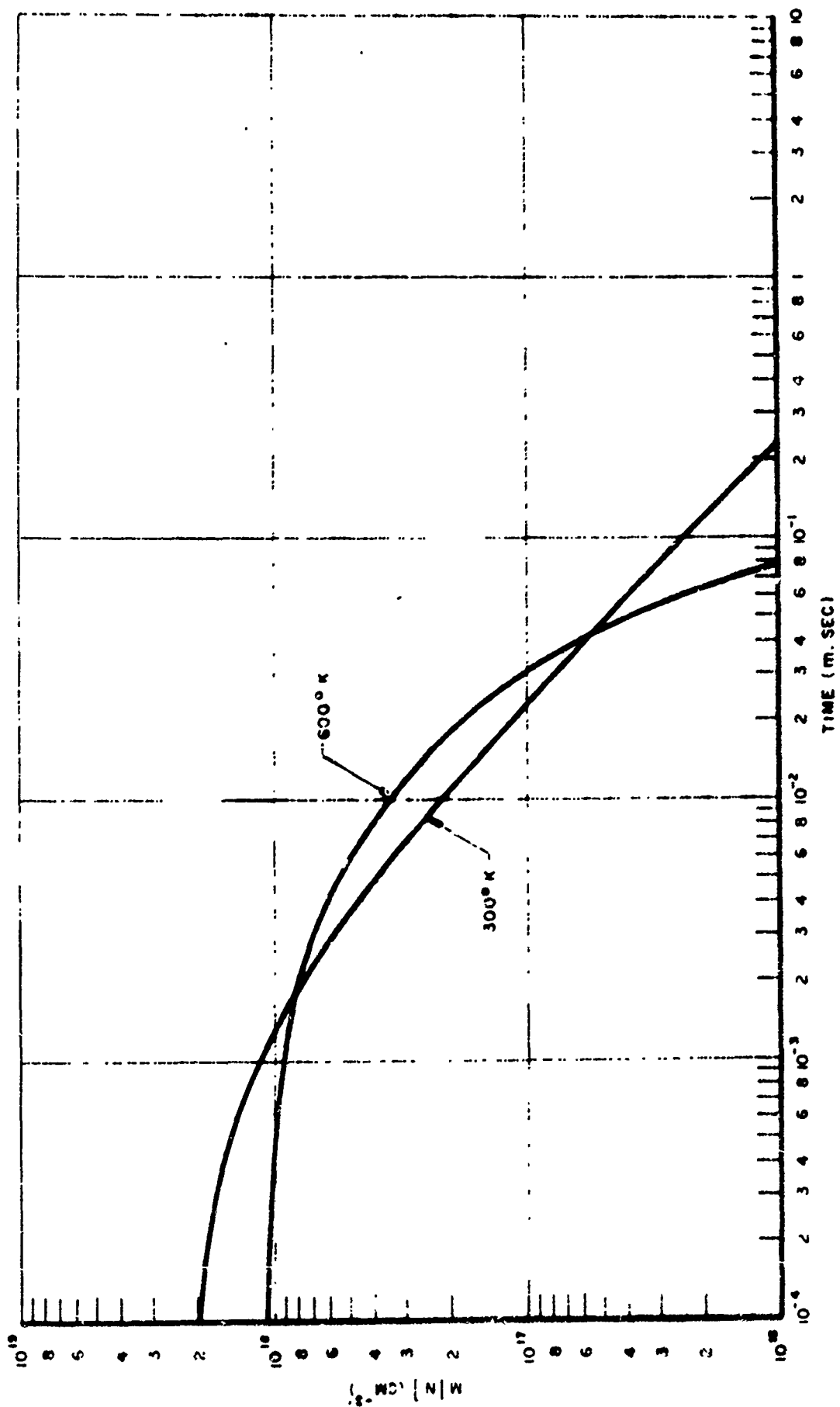
FIGURE 19. MODEL 3, 5% INITIAL N_2 DISSOCIATION
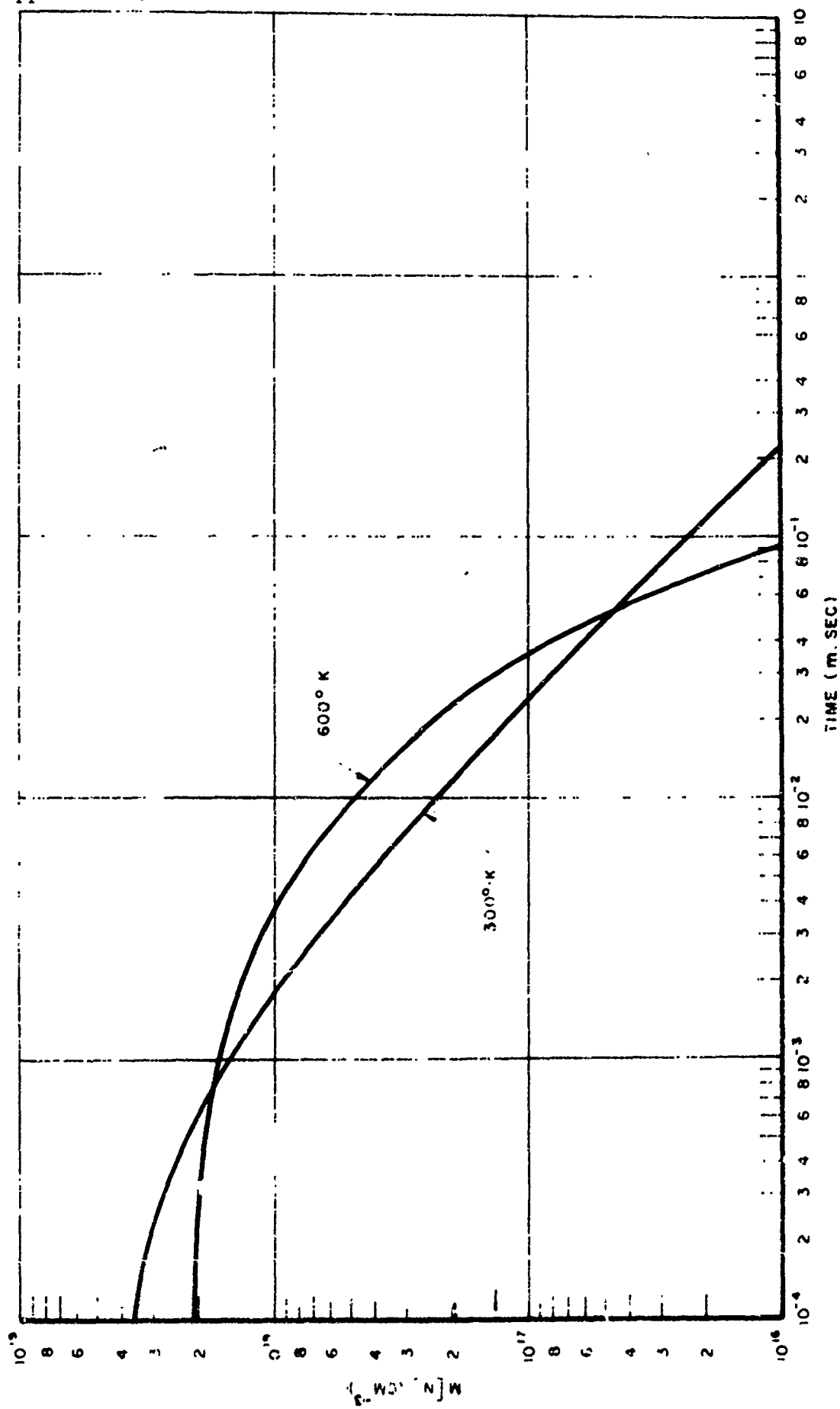
FIGURE 20 MODEL 3, 10% INITIAL N_2 DISSOCIATION
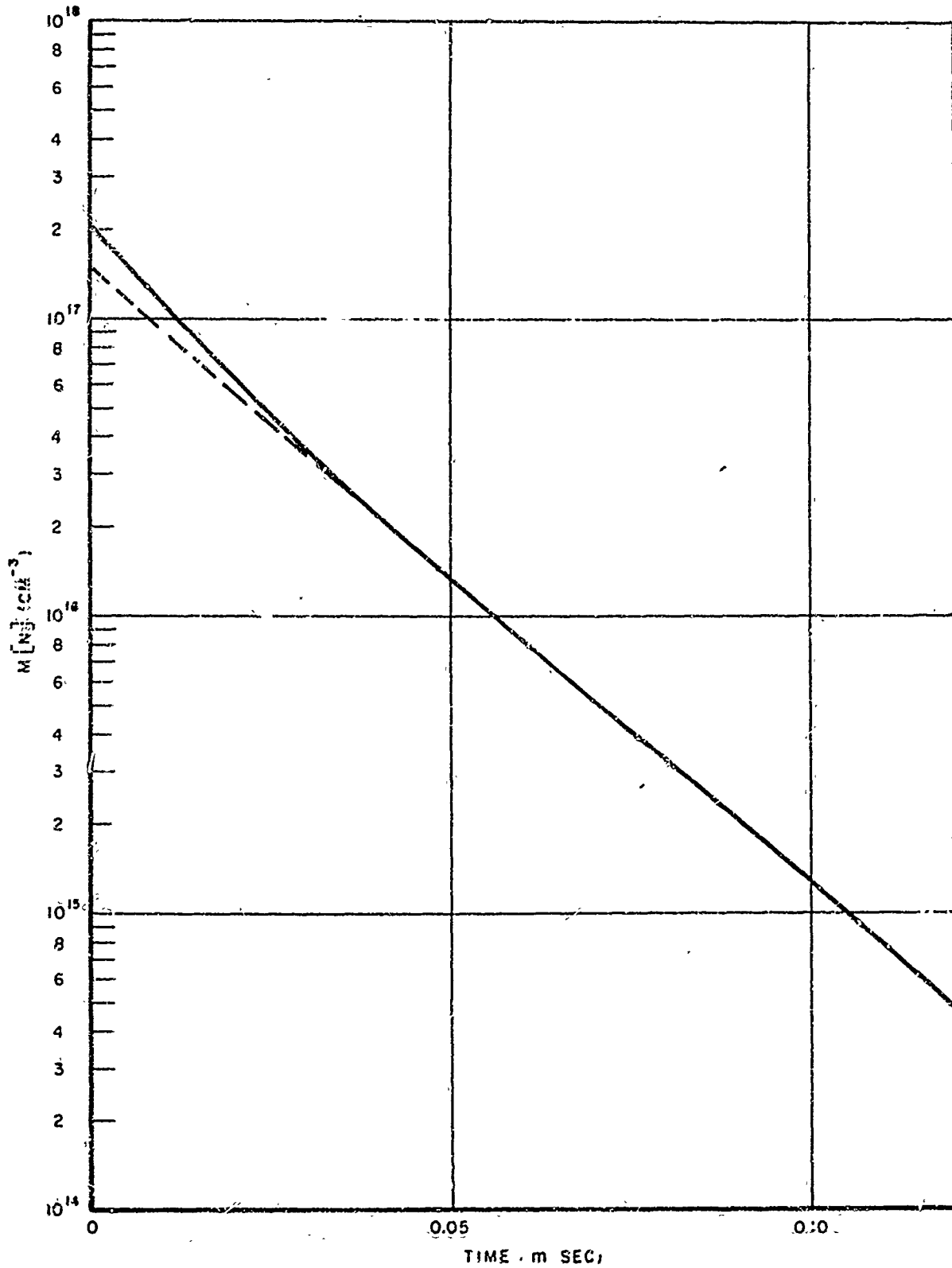
FIGURE 21   MODEL 3,   1% INITIAL N_2 DISSOCIATION 800° K
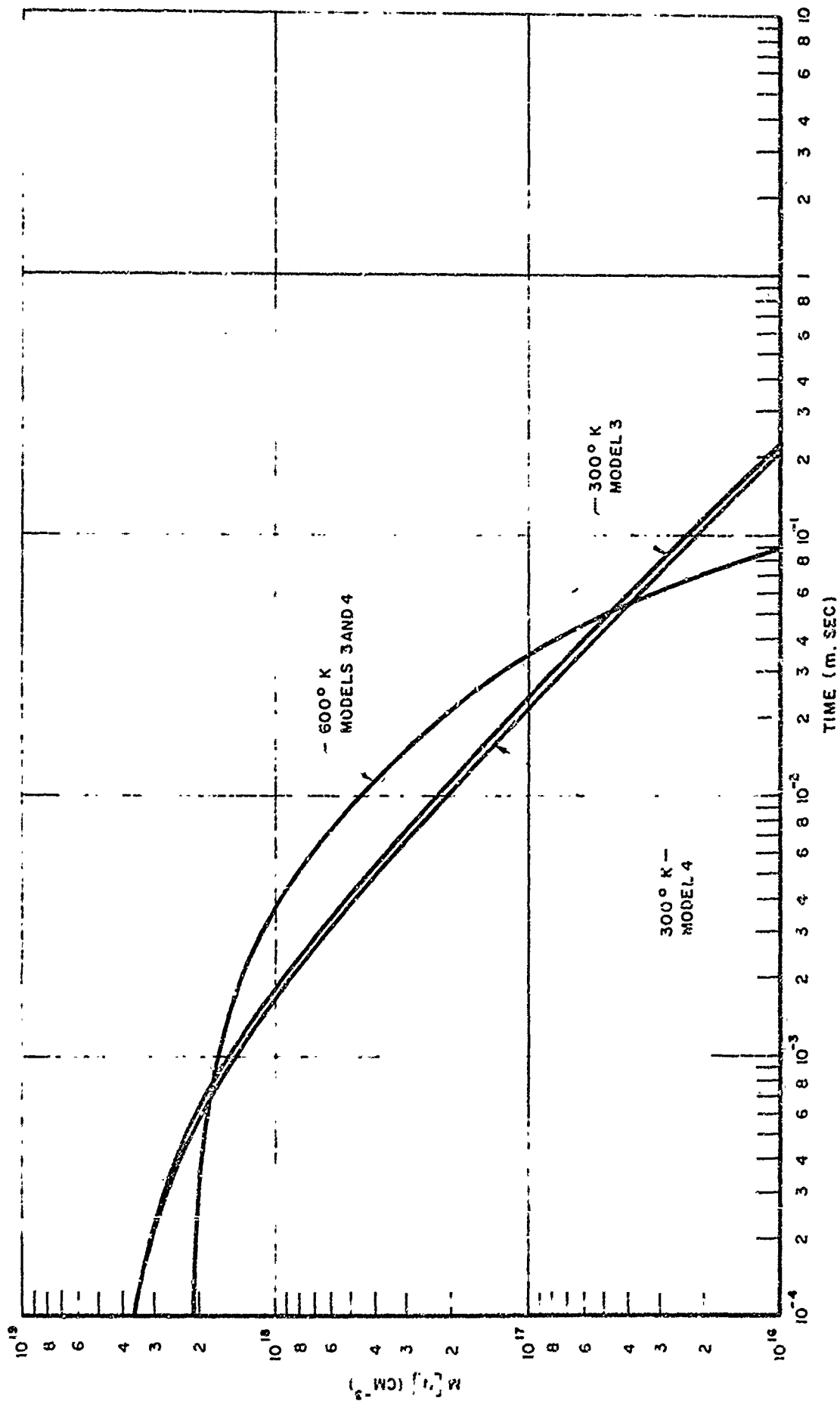
FIGURE 22. MODELS 3 AND 4, 10% INITIAL N_2 DISSOCIATION

APPENDIX IV-A

Subroutine PRECOR

The subroutine PRECOR used for some of the numerical calculations presented here is particularly well suited for the sets of coupled non-linear ordinary differential equations encountered in this type of study. Because of its general utility, the following discussion of the subroutine and a listing of the subroutine is presented here. This material is abstracted from the memorandum of Rank.[52]

INTRODUCTION

A fourth-order stable predictor-corrector technique is used to solve any differential equation of the form

$$\frac{dy}{dx} = \vec{f}\,(x\,,\,\vec{y})$$

with initial conditions

$$\vec{y}(x_o) = \vec{y}_o$$

THEORY

In order to simplify what follows, y and f will be taken to be scalars; the extension to N dimensions is obvious. Hamming has devised a predictor-corrector scheme which is stable and has the advantage that only two values of f are computed at each step (see Ralston and Wilf,[49] and Hamming[50]).

Using the notation $y_n = y\,(x_n)$, and $x_n = x_o + nh$, the equations for Hamming's method are

Predictor $\quad P_{n+1} = y_{n-3} + \dfrac{4h}{3}\,(2y_n{}' - y_{n-1}{}' + 2y_{n-2}{}')$

Modifier $\quad m_{n+1} = P_{n+1} - \dfrac{112}{121}\,(P_n - C_n)$

$$m_{n+1}{}' = f\,(x_{n+1}\,,\,m_{n+1})$$

Corrector $\quad C_{n+1} = \dfrac{1}{8}\,[9y_n - y_{n-2} + 3h\,(m_{n+1}{}' + 2y_n{}' - y_{n-1}{}')]$

Final value $\quad y_{n+1} = C_{n+1} + \dfrac{9}{121}\,(P_{n+1} - C_{n+1})$

$$y_{n+1}{}' = f\,(x_{n+1}\,,\,y_{n+1})$$

An estimate of the truncation error is given by

$$C_{n+1} - P_{n+1} = \frac{121}{360} h^5 y^V (\xi) \qquad\qquad x_{n-1} < \xi < x_{n+1}$$

Note that this method is not self-starting, for it requires the four previous values of y and y'. Therefore, in order to start the calculation, y_1, y_2, and y_3 must be computed (y_0 is given). A fourth-order Runge-Kutta technique devised by A Ralston[51] is used to compute these values.

If the truncation error becomes too large, the interval h can be halved by using the following sixth-order interpolation formulas for the needed values of y.

$$y_{n-\frac{1}{2}} = \frac{1}{256} (80y_n + 135y_{n-1} + 40y_{n-2} + y_{n-3})$$

$$+ \frac{h}{256} (-15y_n' + 90y_{n-1}' + 15y_{n-2}')$$

$$y_{n-\frac{3}{2}} = \frac{1}{256} (12y_n + 135y_{n-1} + 108y_{n-2} + y_{n-3})$$

$$+ \frac{h}{256} (-3y_n' - 54y_{n-1}' + 27y_{n-2}')$$

If the truncation error becomes smaller than required, the interval may be doubled if enough of the previous values of y and y' are known.

FORTRAN PROGRAM

FLOW CHART

Figure A-1 is a flow chart for PRECOR. A brief description of each subroutine which appears on this chart follows:

STRTUP   The first three values of $\dot{y}$ and $\ddot{y}'$ needed to start the predictor-corrector scheme are computed by a Runge-Kutta

technique. If the truncation error is too large, the spacing h is halved and the calculation repeated.

DIFF This subroutine is called by STRTUP to compute an estimate of the truncation error after the first three calculations.

CALC This calculates the next value of y and y′, and estimates the truncation error.

HALF h is halved.

DOUBLE h is doubled.

ADJUST This is essentially a bookkeeping subroutine; it rearranges the values of y and y′, to prepare for the next calculation.

The control variable JJ is used for testing to find out if there are enough previous values of y and y′ stored in memory in order to double h.

The results of the integration are punched on cards with the following format:

$$X \qquad 1 \qquad y^1(x)$$
$$2 \qquad y^2(x)$$
$$\cdot$$
$$\cdot$$
$$\cdot$$
$$n \qquad y^n(x)$$

The estimate of the truncation error, SUM, is given by a weighted sum of the absolute value of the difference between the components of the predictor and corrector.

$$S1 = \sum_{i}^{n} c_i \left| p^i - c^i \right|$$

where n $=$ the dimension of $\vec{y}$

a_i $=$ weights

p^i $=$ the ith component of the predictor

c^i $=$ the ith component of the corrector

Two conditions are provided in PRECOR for return to the mainline program. The first is smallness of the spacing, relative to the input parameter HMIN; singular behavior of the solution will usually be the cause of this exit. The other exit occurs if the ratio X/XF becomes greater than 1, where XF is the final value of X for which the integration is to be carried out. If the programmer desires other criteria for exiting, e.g. when the second component of $\vec{y}$ exceeds 5, these conditions should be inserted into PRECOR, and the existing test removed. Note that in general these changes will affect the arguments of PRECOR, but will not affect the COMMON statement.

Irrespective of the truncation error, it may be desirable that the spacing h never exceed a certain value. This value is given by HMAX.

EXPLICIT ARGUMENTS OF PRECOR

XO x_o , initial value of x

YO $\vec{y}_o$, initial value of $\vec{y}$

SMAX If the estimation of truncation error is greater than SMAX, spacing is halved.

SMIN If the estimation of truncation error is less than SMIN, spacing is doubled. The difference between SMAX and SMIN should be at least one order of magnitude.

HMAX Maximum value of the spacing allowed

HMIN Minimum value of the spacing allowed

XF Final value of x

FUNC Dummy name of subroutine to compute $f(x, \vec{y})$; the actual name used in the argument of PRECOR in the mainline may be anything except FUNC, PRECOR, STRTUP, DIFF, CALC, HALF, DOUBLE, or ADJUST. This name must appear in an EXTERNAL

statement in the mainline program and must be a subroutine
subprogram; i.e. a CALL statement must be used to call it.
The arguments for this function must be of the form (X, W,
WD, CI), where

X   is a non-dimensioned variable;

W   is a dimensioned variable with the same dimension as Y :

WD   is a dimensioned variable with the same dimension as Y :

CI   is a dimensioned variable whose elements may be used as

           parameters in defining $\vec{f}$;

           and

X, W, and WD must be related by

$$WD (I) = \vec{f} (X, W(I))$$

IMPLICIT ARGUMENTS OF PRECOR
(CALLED THROUGH COMMON)

H   h, initial value of the spacing

N   Dimension of $\ddot{y}$ and $\vec{f}$, i.e. number of components

A   Weights needed in computing SUM

CI   Parameters required to define $\vec{f}$

OTHER REQUIREMENTS

A COMMON statement of the type appearing in PRECOR must appear in the
mainline but not in the subroutine used for calculating $\vec{f}(x, \vec{y})$.

The program as written restricts the maximum dimension of $\vec{y}$ to
eight. To remove this restriction, change all eight's in the dimensioning
information to the dimension of $\vec{y}$ required. Do not change the seven's.

This program must be used with the Kingston Fortran II compiler. The
restriction is imposed because the IBM 1620 Fortran II compiler lacks the
EXTERNAL and REAL statements. A listing of the program follows.

statement in the mainline program and must be a subroutine
subprogram; i.e. a CALL statement must be used to call it.
The arguments for this function must be of the form (X, W,
WD, CI), where

X   is a non-dimensioned variable;

W   is a dimensioned variable with the same dimension as Y ;

WD   is a dimensioned variable with the same dimension as Y ;

CI   is a dimensioned variable whose elements may be used as

parameters in defining $\bar{f}$;

and

X, W, and WD must be related by

$$WD (I) = \bar{f} (X, W(I))$$

IMPLICIT ARGUMENTS OF PRECOR
(CALLED THROUGH COMMON)

H   h, initial value of the spacing
N   Dimension of $\ddot{y}$ and $\ddot{f}$, i.e. number of components
A   Weights needed in computing SUM
CI   Parameters required to define $\ddot{f}$

OTHER REQUIREMENTS

A COMMON statement of the type appearing in PRECOR must appear in the
mainline but not in the subroutine used for calculating $\bar{f}(x, \ddot{y})$.

The program as written restricts the maximum dimension of $\ddot{y}$ to
eight. To remove this restriction, change all eight's in the dimensioning
information to the dimension of y required. Do not change the seven's.

This program must be used with the Kingston Fortran II compiler. The
restriction is imposed because the IBM 1620 Fortran II compiler lacks the
EXTERNAL and REAL statements. A listing of the program follows,

PROGRAM LISTING

```
      SUBROUTINE PRECOR(XO,YO,SMAX,SMIN,HMAX,HMIN,XF,FUNC)
      COMMON X,Y(7,8),YD(7,8),H,N,D(8),DS(8),A(8),SUM,JJ,CI(50)
      DIMENSION YO(8)
100   FORMAT (//7X,1HX,12X,1HI,7X,4HY(I)/)
 99   FORMAT(E15.8,I6,E17.8)
 98   FORMAT(  15X,I6,E17.8)
      PUNCH 100
      JJ=3
      CALL STRTUP(XO,YO,FUNC,SMAX)
      X=XO
      DO 4 J=1,4
      I=1
      PUNCH 99,X,I,Y(J+2,I)
      IF(N-1)4,4,1
  1   DO 2 I=2,N
  2   PUNCH 98,I,Y(J+2,I)
  4   X=X+H
  5   CALL CALC(FUNC)
      IF(SUM-SMAX)7,6,6
  6   CALL HALF(FUNC)
      IF(HMIN/H-1.0)5,5,17
  7   I=1
      PUNCH 99,X,I,Y(7,I)
      IF(N-1)10,10,8
  8   DO 9 I=2,N
  9   PUNCH 98,I,Y(7,I)
 10   IF(X/XF-1.0) 11,17,17
 11   IF(JJ-1) 13,13,12
 12   JJ=JJ-1
      GO TO 14
 13   IF(SUM-SMIN) 15,15,14
 14   CALL ADJUST
      GO TO 5
 15   IF(2.0*H/HMAX-1.0) 16,16,14
 16   CALL DOUBLE
      GO TO 5
 17   RETURN
      END
```

```
C   STRTUP-   USES RUNGE-KUTTA METHOD TO COMPUTE THE FIRST 4 VALUES OF Y
      SUBROUTINE STRTUP(XO,YO,FUNC,SMAX)                         AND F
      COMMON X,Y(7,8),YD(7,8),H,N,D(8),DS(8),A(8),SUM,JJ,C1(50)
      DIMENSION YO(8),W(8),WD(8),YDO(8),K1(8),K2(8),K3(8),K4(8)
      REAL K1,K2,K3,K4
      CALL FUNC(XO,YO,YDO,C1)
      DO 1 I=1,N
      Y(3,I)=YO(I)
    1 YD(3,I)=YDO(I)
    7 X=XO
      DO 6 J=1,3
      DO 2 I=1,N
      K1(I)=YD(J+2,I)*H
    2 W(I)=Y(J+2,I)+0.4*K1(I)
      X=X+0.4*H
      CALL FUNC(X,W,WD,C1)
      DO 3 I=1,N
      K2(I)=H*WD(I)
    3 W(I)=W(I)-.10302239*K1(I)+.15875964*K2(I)
      X=X+.05573725*H
      CALL FUNC(X,W,WD,C1)
      DO 4 I=1,N
      K3(I)=H*WD(I)
    4 W(I)=W(I)-.07887721*K1(I)-3.2097248*K2(I)+3.8328648*K3(I)
      X=X+.54426275*H
      CALL FUNC(X,W,WD,C1)
      DO 5 I=1,N
      K4(I)=H*WD(I)
    5 W(I)=Y(J+2,I)+.17476028*K1(I)-.55148066*K2(I)+1.2055356*K3(I)+.171
     118478*K4(I)
      CALL FUNC(X,W,WD,C1)
      DO 6 I=1,N
      Y(J+3,I)=W(I)
    6 YD(J+3,I)=WD(I)
      CALL DIFF
      IF(SUM-SMAX) 8,9,9
    9 H=H*0.5
      GO TO 7
    8 RETURN
      END


C   DIFF-   COMPUTES PRED. COR. DIFFERENCES AND THEIR WEIGHTED SUM
      SUBROUTINE DIFF
      COMMON X,Y(7,8),YD(7,8),H,N,D(8),DS(8),A(8),SUM,JJ,C1(50)
      CONS1=8.962963
      CONS2=0.375*H
      SUM=0.0
      DO 1 I=1,N
      DS(I)=CONS1*(Y(6,I)-Y(3,I)-CONS2*(YD(6,I)+3.0*YD(5,I)+3.0*YD(4,I)+
     1YD(3,I)))
    1 SUM=SUM+A(I)*ABSF(DS(I))
      RETURN
      END
```

63

```
C    CALC- COMPUTES NEW VALUES OF Y AND F(X,Y)
     SUBROUTINE CALC(FUNC)
     COMMON X,Y(7,8),YD(7,8),H,N,D(8),DS(8),A(8),SUM,JJ,C1(50)
     DIMENSION M(8),MD(8),P(8),C(8),W(8),WD(8)
     REAL M,MD
     CONS1=1.333333*H
     CONS2=.9256198J
     CONS3=1.0-CONS2
     SUM=0.0
     DO 1 I=1,N
     P(I)=Y(3,I)+CONS1*(2.0*YD(6,I)-YD(5,I)+2.0*YD(4,I))
   1 M(I)=P(I)-CONS2*DS(I)
     CALL FUNC(X,M,MD,C1)
     DO 2 I=1,N
     C(I)=0.125*(9.0*Y(6,I)-Y(4,I)+3.0*H*(MD(I)+2.0*YD(6,I)-YD(5,I)))
     D(I)=P(I)-C(I)
     SUM=SUM+A(I)*ABSF(D(I))
   2 W(I)=C(I)+CONS3*D(I)
     CALL FUNC(X,W,WD,C1)
     DO 3 I=1,N
     Y(7,I)=W(I)
   3 YD(7,I)=WD(I)
     RETURN
     END


C    HALF-   HALVES THE SPACING
     SUBROUTINE HALF(FUNC)
     COMMON X,Y(7,8),YD(7,8),H,N,D(8),DS(8),A(8),SUM,JJ,C1(50)
     DIMENSION W(8),WD(8)
     CONS1=.00390625
     DO 1 I=1,N
     YA=CONS1*(80.0*Y(6,I)+135.0*Y(5,I)+40.0*Y(4,I)+Y(3,I)+H*(-15.0*YD(
    16,I)+90.0*YD(5,I)+15.0*YD(4,I)))
     YB=CONS1*(12.0*Y(6,I)+135.0*Y(5,I)+108.0*Y(4,I)+Y(3,I)+H*(-3.0*YD(
    16,I)-54.0*YD(5,I)+27.0*YD(4,I)))
     YD(2,I)=YD(4,I)
     YD(4,I)=YD(5,I)
     Y(2,I)=Y(4,I)
     Y(4,I)=Y(5,I)
     Y(5,I)=YA
   1 Y(3,I)=YB
     H=0.5*H
     FA=3.0
     DO 3 J=5,3,-2
     DO 2 I=1,N
   2 W(I)=Y(J,I)
     XC=X-FA*H
     CALL FUNC(XC,W,WD,C1)
     FA=5.0
     DO 3 I=1,N
```

```
    3 YD(J,I)=WD(I)
      X=X-H
      JJ=2
      RETURN
      END



C    DOUBLE- DOUBLES THE SPACING
      SUBROUTINE DOUBLE
      COMMON X,Y(7,8),YD(7,8),H,N,D(8),DS(8),A(8),SUM,JJ,C1(50)
      DO 1 I=1,N
      Y(6,I)=Y(7,I)
      Y(4,I)=Y(3,I)
      Y(3,I)=Y(1,I)
      YD(6,I)=YD(7,I)
      YD(4,I)=YD(3,I)
      YD(3,I)=YD(1,I)
    1 DS(I)=D(I)
      H=2.0*H
      JJ=3
      X=X+H
      RETURN
      END



C   ADJUST-  REARRANGES Y AND F(X,Y) ARRAYS TO PREPARE FOR NEXT PASS
      SUBROUTINE ADJUST
      COMMON X,Y(7,8),YD(7,8),H,N,D(8),DS(8),A(8),SUM,JJ,C1(50)
      DO 1 I=1,N
      DS(I)=D(I)
      DO 1 J=JJ,6
      YD(J,I)=YD(J+1,I)
    1 Y(J,I)=Y(J+1,I)
      X=X+H
      RETURN
      END
```
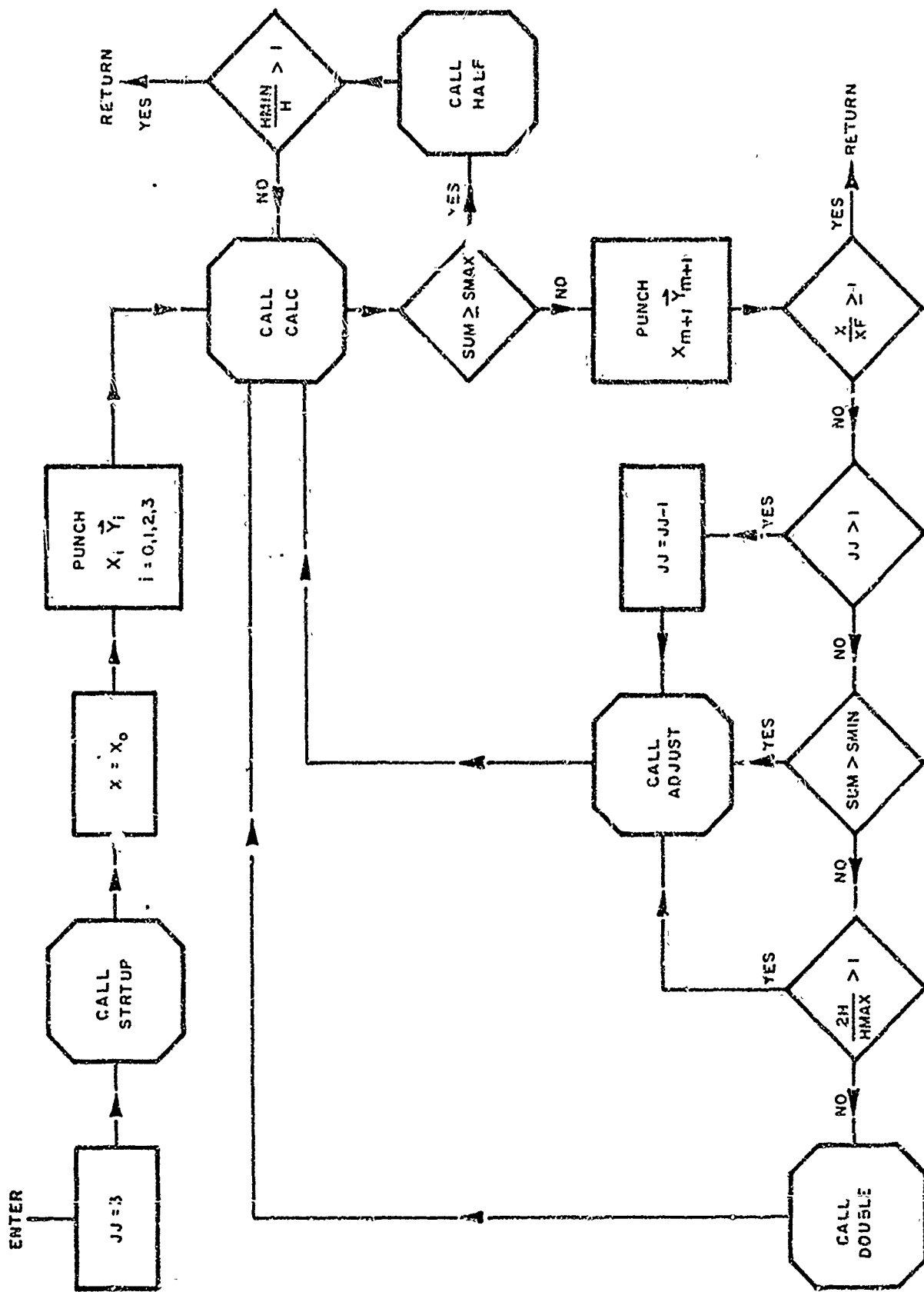
FIGURE 4-1

APPENDIX V

Ammonia Dissociation By
Radio-Frequency Energy

STEVENS INSTITUTE OF TECHNOLOGY

DAVIDSON LABORATORY
CASTLE POINT STATION
HOBOKEN, NEW JERSEY

April 1967

REPORT 1210

AMMONIA DISSOCIATION BY RADIO-FREQUENCY ENERGY

by

K.D. Schinke
and
F. Jones

Prepared for
Continental Aviation and Engineering Corporation
P.O. RD-113509
DL 3200/441

15 Pages

13 Figures

Approved

I.O. Komm
Assistant Manager
Transportation Research
Group

TABLE OF CONTENTS

FIGURES (1 - 13)

ABSTRACT

This study is to determine the feasibility of obtaining hydrogen for improving combustion of ammonia in internal combustion engines.

Important recombination react'ons and their rate constants were obtained from the literature, and the combined rate equations solved numerically with a digital computer.

Steady-state concentrations of hydrogen and hydrazine were found with initial disassociation from 1% to 10% and temperatures from 0° to 100°C.

Yields were found to be too low for practical use in an ammonia engine.

STEVENS INSTITUTE OF TECHNOLOGY
DAVIDSON LABORATORY
CASTLE POINT STATION
HOBOKEN, NEW JERSEY

AMMONIA DISSOCIATION BY RADIO-FREQUENCY ENERGY

INTRODUCTION

Background

Within the framework of a program to determine the suitability of
ammonia as an engine fuel, CAE conducted, along with other work, spark-
ignition engine tests in which a thermal dissociator produces free
hydrogen. Stevens Institute has investigated the use of high-energy
spark discharge, and radio-frequency ionization of the nitrogen in
the intake air, as means of increasing ignition energy.

Experience with the thermal dissociator has shown that operation is
satisfactory when sufficient hydrogen is generated. But during starting
and certain transient conditions the hydrogen produced is insufficient
for operation. Also, there is evidence of limitations on catalyst
lifetime.

Therefore, a look at means other than thermal, for the dissociation
of ammonia, is in order. The primary concern of this work is to
determine whether an RF dissociator can substitute for or operate in
conjunction with the current thermal unit, to alleviate present shortcomings.

Character of Work

Although in the final analysis the merits of this scheme must rest
upon an experimental demonstration, analytical studies at the first stage
will be useful in establishing the feasibility of the approach, and
helpful in defining the general nature of any experimental work to be
undertaken.

The purpose of this work is to establish, analytically, the feasi-
bility of ammonia dissociation by the use of RF or other energy and to
estimate the size and power requirements of a suitable device.

ANALYSIS

In recent years, radio-frequency discharges have been used as ion sources in plasma physics, as high-temperature torches for the welding of refractory materials, and as detectors of ionizing radiations.[1]

The oscillatory field may be produced in the gas by electrodes to which the high-frequency potential is applied, or by induction from a coil carrying an oscillatory current; or the gas could be contained in a wave guide or resonant cavity.

The mechanism of radio-frequency dissociation operates, in general, in the following way. Initially, a small amount of the gas is ionized, producing free electrons; these electrons are accelerated by the oscilla-ting electromagnetic field and collide with the molecules of the gas; the energy of collision, if sufficient, will cause dissociation of the molecules of the gas; and the dissociated products will then seek to recombine, the eventual state of the gas being dependent on the kinds of recombination reactions possible, on the relative probabilities of the recombinations, and on the stability of the recombination products.

The amount of dissociation is dependent on the RF power available, the efficiency with which the RF is coupled into the gas, and the above recombination considerations. The coupling efficiency depends on among other things, the frequency of the RF source. If the electrons are accelerated to their maximum velocity in about one mean free path, their collisional energy will be highest. Unfortunately, at atmospheric pressure, this corresponds to an impossibly high frequency.

The primary objective of this study is to establish the yield of free hydrogen in the mixture, as a function of the temperature and the density of the reactants. From the system of recombination reactions that can occur, sets of coupled ordinary non-linear differential equations are constructed; these govern the time and temperature dependence of the con-centrations of the various chemical species. The equations will then be solved by the use of a high-speed digital computer, to determine what

environmental and initial conditions must be satisfied if an adequate
concentration of hydrogen is to be maintained in the ammonia-air mixture.

In addition to hydrogen, hydrazine (N_2H_4) evolves. Although not
of primary interest, the hydrazine concentration will also be examined,
to determine whether or not the effects of this component are significant.

PROCEDURE

The work of this project was divided into the five major phases listed below:

(1) Assemble data on the reaction kinetics and rate coefficients of the ammonia system. The literature search on these kinetics was performed by Dr. Frank Jones.

(2) Set up mathematical models of the reaction system, based on the rate equations obtained in phase (1) above.

(3) Solve the sets of equations on a high-speed digital computer, using subroutine PRECOR.[2]

(4) Interpret the results as they apply to the physical problem.

(5) Perform a check on the accuracy with which the mathematical analysis describes the physical system

RESULTS

Reaction Mechanism

The collision between ammonia molecules and electrons accelerated in an electric field produces excited ammonia molecules which may ultimately decompose when the excitation energy is sufficiently high. Anderson et al[3] have shown that the energy required for dissociation in an RF discharge is very close to the N-H bond energy in NH_3 (4.5 eV), implying that the primary products and H and NH_2 radicals in their ground states; thus

$$NH_3 \; \text{-----} \; NH_2 + H \qquad\qquad (0)$$
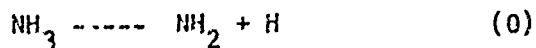
Other decomposition modes such as $NH_3 \; \text{---} \; NH + H_2$ require higher energies and can therefore occur only to an insignificant extent. Reaction (0) is also the sole mode of decomposition in the photochemistry of ammonia for light of wavelengths above 1500 Å.[4,5].

The primary decomposition products, H and NH_2, may interreact in three different ways:

$$H + H + M \; \text{-----} \; H_2 + M \qquad\qquad (1)$$

$$H + NH_2 + M \; \text{----} \; NH_3 + M \qquad\qquad (2)$$

$$NH_2 + NH_2 + M \; \text{----} \; N_2H_4 + M \qquad\qquad (3)$$
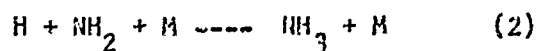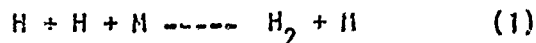
where M is any third body.

Reaction (1) is exothermic by an amount equal to the H-H bond energy, so the H_2 molecules thus formed have a high probability of splitting up again unless the energy can be dissipated to other molecules in the system. The rate of reaction (1) therefore depends not only on the concentration of H atoms[21] but also on the total gas pressure: Rate $= k_1(H)^2(M)$. Similar arguments hold for reactions (2) and (3); however, in these two

cases the respective products NH_3 and N_2H_4 are complex enough to allow for storage of some of the released energy, in other bonds within the molecule - hence the molecule can exist for a finite length of time before decomposing . The rates of these reactions should depend on total pressure only at low pressures and should reach a limiting value as the pressure is increased. Both reactions (2) and (3) are therefore independent of total gas pressure at pressures above 200-400 mm Hg. For 1 atm. the rates are given in Table 1a.[6]

If a third body is not present when two NH_2 radicals collide, the reaction below may occur,[7] with a rate constant[8] $k_{3a} = 0.46 \times 10^9$ Mole^{-1} sec^{-1} (cf. $k_3 = 2.5 \times 10^9$[9]).

$$NH_2 + NH_2 \text{-----} NH_3 + NH \qquad (3a)$$
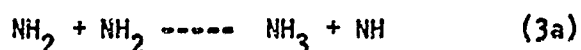
However, the reaction of NH with NH_3 to form hydrazine is fast,[9] so that the net result is stoichiometrically equivalent to reaction (3).

$$NH + NH_3 \text{------} N_2H_4$$

The temperature dependence of reaction-rate constants generally obeys the Arrhenius equation $k = A\, e^{-E_a/RT}$, where k is the rate constant at obsolute temperature T, E_a is the Arrhenius activation energy, and A is a temperature-independent pre-exponential factor. Reactions between free radicals are always found to have very low or zero activation energies, and therefore the rate constants for reactions (1), (2), and (3) are independent of temperature.

H and NH_2 radicals undergo many collisions with ammonia molecules at 1 atm. The reaction of NH_2 with ammonia,

$$NH_2 + NH_3 \text{-----} NH_3 + NH_2$$

is thermoneutral and can be disregarded since it does not lead to chemical change. The reaction of N with ammonia has been the subject of a great

deal of discussion; it is

$$H + NH_3 \longrightarrow H_2 + NH_2 \qquad (4)$$
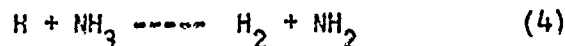
Dixon[10] and Taylor and Jungers[11] found no evidence for reaction (4) over the temperature range 25 - 260°C and placed a lower limit on the activation energy of $E_a \gtrsim 8.5$ k-cal/mole. But Jones in the radiation chemistry[12] and Takamuku and Back in the mercury-sensitized photolysis[13] explained increased yields at temperatures up to 350°C on the basis of reaction (4). Using H atoms generated in a high-frequency discharge in H_2, Volpi[14] estimated an activation energy of 10 - 15 k-cal/mole and pre-exponential factor of between 10^{12} and 10^{13} cc/mole sec; Oganesyan[15] determined an activation energy of 13.7 k-cal/mole but did not measure the pre-exponential factor. Probably the best determinations were made by Farkas and Melville[16] for the D_2-NH_3 exchange reaction ($E_a = 11 \pm 1$ k-cal/mole and $A = 2 \times 10^{13}$ cc/mole-sec). In contrast to these values, very low activation energies[18] of 1-2 k-cal/mole have often been erroneously assigned to reaction (4), but these values must refer to the over-all process of hydrogen-formation in ammonia and not to reaction (4).

$$H_2 + NH_2 \longrightarrow H + NH_3 \qquad (4a)$$
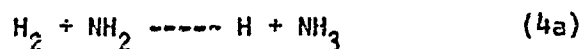
If reaction, (4) is important, then (4a), the reverse reaction, must also be considered. The equilibrium constant for the exchange of the hydrogen atom between H_2 and NH_3, as measured for example with the deuterium isotope $D_2 + NH_3 \longrightarrow HD + NH_2D$, has been determined to be $K = 3.0$, independent of temperature[19]. Since $K = K_4/K_{4a}$, the rate constant for (4a) is $K_{4a} = \frac{1}{3} k_4$.

Secondary Reactions

Hydrazine formed in (3) and (3a) may be destroyed by H and NH_2 radicals:

$$H + N_2H_4 \text{ -----} \; H_2 + N_2H_3 \qquad (5)$$

$$NH_2 + N_2H_4 \text{ -----} \; NH_3 + N_2H_3 \qquad (6)$$
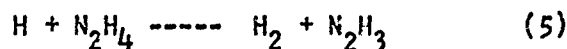
The rate constant for (5) has been measured by Volpi,[14] but it has not
yet been possible to measure the rate constant for (6), although it is
expected that $k_6 \approx k_5$. However, the results indicate that (6) can be
neglected in pure ammonia, because of the rapid disappearance of NH_2
radicals by reaction (3).

The unstable N_2H_3 radical formed in (5) or (6) may be further
degraded by reaction sequence (A),[12]

$$H + N_2H_3 \text{ -----} \; H_2 + N_2H_2$$

$$H + N_2H_2 \text{ -----} \; H_2 + N_2H$$

$$H + N_2H \text{ -----} \; H_2 + N_2$$

although Sequence B has also been suggested,[14] with $k_B \geq 3.0 \times 10^9$
$Mole^{-1} \; sec^{-1}$, so that

$$N_2H_3 + N_2H_3 \text{ -----} \; N_2 + 2NH_3$$

Sequence B must itself be the net result of a series of steps for which
k_B is the rate constant for the slowest reaction. In either case,
reaction (5) is the rate-determining step whether N_2H_3 decomposes by
A or B, and K_5 much greater than K_A or K_B; but the rate of H_2 production
by the sequence (5)-(A) will be four times that for the sequence (5)-(B).

Kinetic Rate Equations

The reaction mechanism discussed above is summarized in Table 1,
and the appropriate rate constants are compiled in Table 1a. The
appropriate differential-rate equations were formulated and are presented
in Table 2.

These coupled differential equations, with initial conditions specifying the level of first dissociation products, were then solved on a Univac 1105 computer with subroutine PRECOR.

An assumption inherent in the method is that the dissociation reaction is separated from the recombination reactions--that is, no effort has been made to examine the effects of simultaneous dissociation and recombination. It is felt that this assumption is of negligible consequence.

At first glance, the reaction mechanisms would lead one to believe that the Model A system would yield a considerably greater quantity of hydrogen than Model B. Actual computation, however, shows that the difference in hydrogen yield between the systems is insignificant.

Since the reactions are temperature dependent, solutions were obtained at 0°, 20°, 50°, and 100° C (32°, 68°, 122° and 212°F).

It was not feasible to solve for initial dissociation concentration in terms of the final products, and it was therefore necessary to assume a set of initial conditions such that the range of the resulting steady-state hydrogen concentration spanned the region of interest.

Steady-state concentration of H_2, N_2H_4 and NH_3 is presented in terms of gram-moles per liter in Table 3, mole (volume) percent in Table 4, and weight percent in Table 5. The column labeled H_2^1 is explained in the section entitled "Discussion".

Figure 1 shows typical concentration vs. time behavior on a linear scale. This is shown for reference only, since the crowding on the left of the diagram does not permit accurate observation of differences in behavior.

A more useful presentation is a log-log plot of concentration against time, as in Figures 2 through 13.

PRECISION

In order to correlate the analytical study with the actual physical phenomena, and to ensure that the mechanism selected is in fact the one followed by the reaction in this temperature-density domain, the initial conditions and temperatures employed in an experimental study[12] of ammonia dissociation by radiation were inserted in the computer program.

At temperatures of 23° and $300^{\circ}C$, with initial concentrations of H and NH_2 of 3×10^{-3} <u>percent</u>, Jones obtained 1.0 and 1.9×10^{-6} gram moles per liter of N_2H_4 respectively, and an increase in hydrogen concentration by a factor of 3.7.

Analytically, at those same points, we obtained 0.65 and 0.86×10^{-6} gram moles per liter of N_2H_4 and an increase in H_2 by 3.79.

DISCUSSION

References to Tables 3 through 5 show that hydrazine (N_2H_4) production is quite significant. In fact, the reaction efficiency with respect to hydrogen lies in the vicinity of 10%, and about 16% for hydrazine.

Since no conclusive data on the effect in engine operation of a mixture of ammonia, hydrogen, and hydrazine is available, it is not possible to make very strong direct statements regarding such a mixture.

The steady-state concentrations calculated in Tables 3 through 5 are based on a homogeneous gas-phase mechanism. Heterogeneous and surface-catalyzed reactions have not been consdiered. Although H_2 is a stable product and is not expected to be influenced by metal surfaces. N_2H_4 is known to be readily decomposed by metals even at low temperatures. The thermo- dynamically favored mode for hydrazine decomposition on a surface is

$$3N_2H_4 \text{ ------ } N_2 + 4NH_3$$

but this stoichiometry is achieved only in aqueous solutions or on quartz surfaces at high temperatures. On metal surfaces, H_2 is usually produced in addition to N_2 and NH_3. There is no agreement on the stoichiometry of the metal-catalyzed decomposition in the gas phase, and results on the same surface are often found to vary with the number of times the experiment has been carried out.[20] The maximum H_2 yield from the decomposition of hydrazine corresponds to

$$N_2H_4 \text{ ------ } N_2 + 2H_2$$

and the H_2^1 yields in column 5 of Table 5 were calculated on this basis.

A straightforward calculation proceeding from the 4.5 eV first dissociation energy of ammonia yields the information that 3.21 kilowatts are necessary to dissociate on pound per hour of ammonia.

Assuming a brake specific ammonia consumption of 0.75 lb/Bhp hr, a 40-hp engine would consume 30 lb/hr. If 10% dissociation were sufficient, (H_2^1 = 0.56% by weight) then we would require

$$33 \ NH_3 \ \text{-----} \ 30 \ NH_3 + 3 \ NH_3^*$$

$$3 \ \#/hr. \ . \ 3.21 \ Kw \ H/\# = 9.65 \ Kw$$
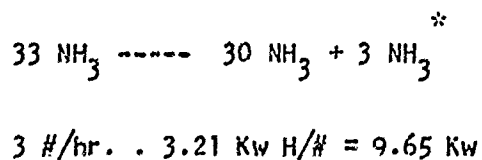
coupled to the gas.

Cobine and Wilbur[22] of G.E. Research constructed an RF torch and found efficiencies in coupling to polyatomic gases of 70%, nearly all the energy going into dissociation.

Thus, an over-all efficiency of 55% should not be difficult to realize.

The power requirement of 17.6 Kw leads to the untenable result that approximately 50% of the total engine output is required to generate the hydrogen.

As for physical size, the 1 Kw torch of Cobin and Wilbut had an rf generator 8 5/8 inches in diameter and a wave-guide-coupler 20-inches long.

CONCLUSIONS AND RECOMMENDATIONS

Due to the very small yield, this scheme would not be practical as the sole source of hydrogen for an engine. It is possible that this scheme may find use as a starting and warm-up aid, but the complexity of a source of high frequency is discouraging.

Therefore, it is recommended that this approach be abandonned.

REFERENCES

Primary Sources of Data

1. Llewellyn-Jones, F., _Ionization and Breakdown in Gases_, John Wiley & Sons, 1957, p. 153.

2. Rank, P. H.,Jr., _PRECOR, A Kingston Fortran II Subroutine for Solving Sets of Ordinary Differential Equations by a Predictor-Corrector Technique_. Davidson Laboratory Technical Memorandum 142 (1965).

3. Anderson, W. H., Zwolinski, B.J. and Parlin, R. B., Ind. Eng. Chem. 51, 527, 1959.

4. Noyes, W. A. and Leighton, F. A., _Photochemistry of Gases_, Reinhold, N.Y.

5. McNesby, J. R., Tanaka, I and Okabe, H., J. Chem. Phys. 36, 605 (1962).

6. Hanes, M. H. and Bair, E. J., J. Chem. Phys. 38, 672 (1963).

7. Diesen, R. W., J. Chem. Phys. 39, 2121 (1963).

8. Salzman, J. D. and Bair, E. J., J. Chem. Phys. 41, 3654 (1964).

9. Wannagat, U. and Kohnen, H., Z. anorg. allgem. Chemie, 304, 276 (1960).

10. Dixon, J. K., J. Am. Chem. Soc. 54, 4262 (1932).

11. Taylor, H. S. and Jungers, J. C., J. Chem. Phys. 2, 452 (1934).

12. Jones, F. T. and Sworski, T. J., Trans. Faraday Soc. 62, 000 (1967).

13. Takamuku, S. and Back, R. A., Can. J. Chem. 42, 1426 (1964).

14. Schiavello, M. and Vol;I, G. G., J. Chem. Phys. 37, 1510 (1962).

15. Oganesyan, K. T. and Nalbandyan, A. B., Dokl Akad. Nauk. S.S.S.R. 160, 162 (1965).

16. Farkas, L. and Melville, H. W., Proc. Roy. Soc. A 157, 625 (1936).

17. Melville, H. W. and Boland, R., Proc. Roy. Soc. A 160, 384 (1937).

18. Sorokin, Yu A. and Pshezhetskii, S. Ya, Russ. J. Phys. Chem. 38, 434 (1964).

19. Dainton, F. S. Smithies, D. Skwarski, T., and Wezranowski, E., Trans. Faraday Soc. 60, 1068 (1964).

14

20. Audrieth, L. F. and Ogg, B. A., _The Chemistry of Hydrazine_, John Wiley and Sons, New York, (1951).

21. Steiner, W., Trans. Faraday Soc. 31, 623 (1935).

22. Cobine, J. D. and Wilbur, D. A., Appl. Phys. $\underline{22}$, 835 (1951).

TABLE 1

System of Chemical Reactions Which Govern the Recombination

0. $NH_3 \xrightarrow{RF} NH_2 + H$

1. $H + H + M \longrightarrow H_2 + M$

2. $H + NH_2 + M \longrightarrow NH_3 + M$

3. $NH_2 + NH_2 + M \longrightarrow N_2H_4 + M$

3a. $NH_2 + NH_2 \longrightarrow NH_3 + NH$; $\qquad NH + NH_3 \longrightarrow N_2H_4$

4. $H + NH_3 \longrightarrow H_2 + NH_2$

4a. $H_2 + NH_2 \longrightarrow H + NH_3$

5. $H + N_2H_4 \longrightarrow H_2 + N_2H_3$

<u>A</u>	<u>B</u>
$H + N_2H_3 \longrightarrow H_2 + N_2H_2$	$N_2H_3 + N_2H_3 \longrightarrow 2 NH_3 + N_2$
$H + N_2H_2 \longrightarrow H_2 + N_2H$	
$H + N_2H \longrightarrow H_2 + N_2$	
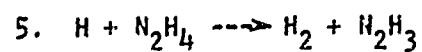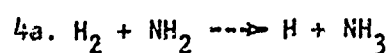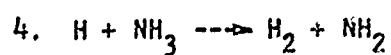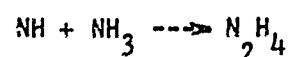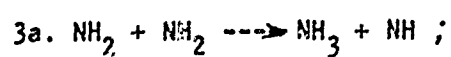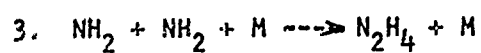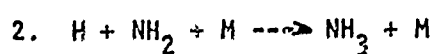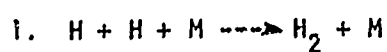
TABLE 1a

Rate Constants of the Reactions in Table 1

1. $13. \pm 2. \times 10^3$ $mole^{-2} sec^{-1}$ (room temperature) (Ea = 0)

2. $12. \pm 1. \times 10^9$ $mole^{-1} sec^{-1}$ (room temperature limit) (Ea = 0)

3. $2.5 \pm .2 \times 10^9$ $mole^{-1} sec^{-1}$ (room temperature limit) (Ea = 0)

3a. 0.46×10^9 $mole^{-1} sec^{-1}$

4. $2 \times 10^{10} e^{-10.7 \, k\text{-cal}/RT}$ $mole^{-1} sec^{-1}$

4a. $\frac{1}{3} k_4$

5. $3.5 \times 10^8 e^{-2.0 \, k\text{-cal}/RT}$ $mole^{-1} sec^{-1}$

A. $3.5 \cdot 10^8 e^{-2.0 \, k\text{-cal}/RT}$ $mole^{-1} sec^{-1}$

B. $3.0 \cdot 10^9$ $mole^{-1} sec^{-1}$

TABLE 2

Differential Rate Equations of the Recombination

Model A

1. $\dfrac{d(H)}{dt} = -k_1 (H)^2 (M) -k_2 (H)(NH_2) -k_4 (H)(NH_3) + k_{4a}(NH_2)(H_2) -4k_5(H)(N_2H_4)$

2. $\dfrac{d(NH_2)}{dt} = -k_2 (H)(NH_2) - k_3(NH_2)^2 + k_4(H)(NH_3) -k_{3a}(NH_2)^2 -k_{4a}(NH_2)(H_2)$

3. $\dfrac{d(N_2H_4)}{dt} = k_3(NH_2)^2 + k_{3a}(NH_2)^2 -k_5(N_2H_4)(H)$

4. $\dfrac{d(H_2)}{dt} = \dfrac{1}{2} k_1 (H)^2 (M) + k_4 (H)(NH_3) -k_{4a}(H_2)(NH_2) + 4k_5(H_2)(N_2H_4)$

Model B

1. $\dfrac{d(H)}{dt} = -k_1 (H)^2 (M) -k_2 (H)(NH_2) -k_4(H)(NH_3) -k_5(H)(N_2H_4) + k_{4a}(NH_2)(H_2)$

2. $\dfrac{d(NH_2)}{dt} = -k_2 (H)(NH_2) -k_3(NH_2)^2 + k_4(H)(NH_3) -k_{3a}(NH_2)^2 -k_{4a}(NH_2)(H_2)$

3. $\dfrac{d(N_2H_4)}{dt} = k_3(NH_2)^2 = k_{3a}(NH_2)^2 -k_5(N_2H_4)(H)$

4. $\dfrac{d(H_2)}{dt} = \dfrac{1}{2} k_1 (H)^2 (M) + k_4(H)(NH_3) -k_{4a}(H_2)(NH_2) +k_5(H)(N_2H_4)$

TABLE 3

Concentration in Gram-Mol/Liter

Condition		NH_3	H_2	N_2H_4
0°	1%	4.415×10^{-2}	3.8×10^{-5}	7.2×10^{-5}
	5%	4.237×10^{-2}	2.25×10^{-4}	3.75×10^{-4}
	10%	4.014×10^{-2}	3.85×10^{-4}	6.99×10^{-4}
20°	1%	4.118×10^{-2}	4.0×10^{-5}	6.8×10^{-5}
	5%	3.952×10^{-2}	2.0×10^{-4}	3.4×10^{-4}
	10%	3.744×10^{-2}	4.1×10^{-4}	$6.6 \cdot 10^{-4}$
50°	1%	3.732×10^{-2}	3.80×10^{-5}	6.7×10^{-5}
	5%	3.581×10^{-2}	2.0×10^{-4}	3.1×10^{-4}
	10%	3.393×10^{-2}	3.95×10^{-4}	6.0×10^{-4}
100°	1%	3.237×10^{-2}	4.0×10^{-5}	7.5×10^{-5}
	5%	3.106×10^{-2}	1.7×10^{-4}	2.8×10^{-4}
	10%	2.943×10^{-2}	3.78×10^{-4}	5.4×10^{-4}

TABLE 4

Concentration in Volume Percent

Condition		H_2	N_2H_4
0°	1%	0.085	0.161
	5%	0.505	0.84
	10%	0.865	1.56
20°	1%	0.096	0.163
	5%	0.48	0.82
	10%	0.98	1.58
50°	1%	0.101	0.18
	5%	0.53	0.82
	10%	1.05	1.59
100°	1%	0.122	0.23
	5%	0.52	0.86
	10%	1.15	1.65

TABLE 5

Weight in Percent Relative to Ammonia

Condition		$x = H_2$	$x = N_2H_4$	H_2^1
0°	1%	0.0101	0.306	
	5%	0.0625	1.66	
	10%	0.113	3.27	0.52
20°	1%	0.0115	0.31	
	5%	0.0595	1.62	
	10%	.129	3.31	0.54
50°	1%	0. 2	0.337	
	5%	0.065	1.625	
	10%	0.137	3.32	0.554
100°	1%	0.0145	0.436	
	5%	0.0645	1.695	
	10%	0.152	3.45	0.584

NOTE: $\% = \dfrac{wt \ x}{wt \ NH_3} \times 100$

Figure 1
Concentration vs. Time From Start
Linear Plot
1% Initial
20°C

Figure 2
Concentration vs. Time From Start
10% Initial
0°C.

Figure 3
Concentration vs. Time From Start
10% Initial
20°C.

FIGURE 4
Concentration vs. Time From Start
10% Initial
50°C

Figure 5 —
Concentration vs. Time From Start
10% Initial
100°C.

Figure 6 — Concentration vs. Time From Start
5% Initial
0°C.

Figure 7
Concentration vs. Time From Start
5% Initial
2?° C.

$N_2\bar{H}_4$

$\bar{H}_2$

H

$\bar{N}H_2$

Time Sec.

10^{-9} 10^{-8} 10^{-7} 10^{-6} 10^{-5} 10^{-4}

10^{-2} 10^{-3} 10^{-4} 10^{-5}

Concentration, $\dfrac{GM - MOL,}{Liter}$

Figure 8
Concentration vs. Time From Start
5% Initial
50°C.

Figure 9
Concentration vs. Time From Start
5% Initial
100°C.

Figure 10
Concentration vs. Time From Start
1% Initial
0°C.

N₂H₄

H₂

H

NH₂'

Time Sec.

Concentration — GM - MOL. / Liter

Figure 11
Concentration vs. Time From Start
1% Initial
20°C.

Figure 12
Concentration vs. Time From Start
1% Initial
50°C.

Figure 13
Concentration vs. Time From Start
1% Initial
100°C.